

Essays on Risk Appetite and Uncertainty

Ran (Nancy) Xu

Submitted in partial fulfillment of the
requirements for the degree of
Doctor of Philosophy
under the Executive Committee
of the Graduate School of Arts and Sciences

COLUMBIA UNIVERSITY

2018

© 2018
Ran (Nancy) Xu
All rights reserved

ABSTRACT

Essays on Risk Appetite and Uncertainty

Ran (Nancy) Xu

This dissertation focuses on the identification of the dynamics of risk aversion (price of risk) and economic uncertainties (amount of risk) and their effects on both domestic and international asset markets. In the first essay, I study the differences between global equity return comovements and global bond return comovements and use a consistent and flexible asset pricing framework to motivate and quantify the role of various economic determinants in explaining the comovement difference. This study contributes to the recent debate on how shocks transmit across countries, and documents that the “risk compensation” channel plays a major role in affecting international comovements.

In the second essay, I find that fundamental shocks (consumption growth) and cash flow shocks (dividend growth) comove procyclically. This new stylized fact helps explain the “Duffee Puzzle” (Duffee, 2005): stock returns and consumption growth covary procyclically, whereas the conventional wisdom and extant consumption-based asset pricing models suggest that returns respond to fundamental shocks more significantly in a bad economic environment. This research contributes to an under-explored area in the consumption-based asset pricing literature: the dynamics of the “amount of risk”. I then explore the asset pricing implications of this procyclical source of amount of risk in a consumption-based workhorse model that allows for time-varying risk aversion.

In my joint paper with Geert Bekaert and Eric Engstrom, we develop a new measure of time-varying risk aversion that is consistent with a dynamic no-arbitrage asset pricing model, using a wide range of observed asset moments, macro and option data. In addition, our findings formally support the close relationship between variance risk premium and risk aversion (as suggested in the literature), and propose a financial proxy to economic uncertainty, which is a more significant predictor of future economic growth than VIX and true economic uncertainty.

CONTENTS

LIST OF TABLES	iv
LIST OF FIGURES	vii
1 GLOBAL RISK AVERSION AND INTERNATIONAL RETURN COMOVEMENTS	1
1.1 Introduction	2
1.2 Stylized Facts of Global Comovements	6
1.2.1 Setup	6
1.2.2 A New Econometric Model for Global Comovements	7
1.2.3 Estimation Procedure	13
1.2.4 Data	15
1.2.5 Estimation Results	15
1.2.6 Model Fit	19
1.3 Economic Determinants	23
1.3.1 An Asset Pricing Model	23
1.3.2 The Identification of the Economic Determinants	31
1.4 A Theory-Motivated Factor Model	35
1.4.1 Dynamic Equity and Bond Return Factor Model	35
1.4.2 Estimation	37
1.4.3 Model Fit	38
1.4.4 Global Conditional Comovement Decomposition	40
1.4.5 Economic Significance of Risk Aversion	44
1.5 Countercyclical Divergence of Bond Risk Characteristics	45
1.6 Conclusion	47
Appendices	49

2	PROCYCLICALITY OF THE COMOVEMENT BETWEEN DIVIDEND GROWTH AND CONSUMPTION GROWTH	88
2.1	Introduction	88
2.2	The Duffee Puzzle Revisited, Econometrically	93
2.2.1	The Model	93
2.2.2	Data	97
2.2.3	Estimation Methodology and Cyclicity Inferences	98
2.2.4	Empirical Analysis	100
2.2.5	Summary of the Empirical Part of the Paper	105
2.3	A New DGP for the Joint Consumption-Dividend Dynamics	106
2.3.1	The New DGP	108
2.3.2	DGP Estimation Results	111
2.4	An External Habit Model	117
2.4.1	Habit-Based Preferences	118
2.4.2	Asset Prices	118
2.4.3	Numerical Solutions and Results	127
2.5	The Cross Section of Expected Returns	135
2.6	Conclusion	137
	Appendices	138
3	THE TIME VARIATION IN RISK APPETITE AND UNCERTAINTY	164
3.1	Introduction	165
3.2	Modeling Risk Appetite and Uncertainty	167
3.2.1	General Strategy	168
3.2.2	Economic Environment: State Variables	171
3.2.3	Asset Pricing	178
3.3	The Identification and Estimation of Risk Aversion and Uncertainty	184
3.3.1	General Estimation Philosophy	184
3.3.2	Identifying Economic Uncertainty	186

3.3.3	Identifying Risk Aversion	186
3.4	Data	191
3.4.1	State variables	192
3.4.2	Financial Variables	193
3.5	Estimation Results	194
3.5.1	State Variable Dynamics	194
3.5.2	Risk Aversion	197
3.6	Risk Aversion, Uncertainty and Asset Prices	199
3.6.1	Risk Aversion, Macro-Economic Uncertainty and the First and Second Moments of Asset Returns	199
3.6.2	An Uncertainty Index	203
3.6.3	Correlations with Extant Measures	204
3.7	The Curious Case of Treasury Bond Markets	207
3.8	Conclusion	208
	Appendices	209

LIST OF TABLES

1.1	Summary Statistics.	64
1.2	Estimation Results of Global Bond Comovement.	65
1.3	Estimation Results of Global Equity Comovement.	66
1.4	Model Fit: (In)Equality between Global Equity Comovement and Global Bond Comovement.	67
1.5	Model Fit: (A)symmetry in Global Comovements.	68
1.6	Model Fit: Cyclicalities of Global Equity Comovement and Global Bond Comovement.	69
1.7	Dynamic Factor Model Fit & Economic Significance of Risk Aversion	70
1.8	Global Return Covariance Decomposition.	71
1.9	Global Return Correlation Decomposition.	72
1.10	Dynamic Factor Model Fit & Economic Significance of Other State Variables	73
1.11	Conditional Variance Decomposition.	74
1.12	Conditional Volatility Models for Asset Returns.	83
1.13	Model Fit: Flight-to-Safety Channel, Given Best Model in Table 1.3	84
1.14	Estimation Results of Global Equity Comovement: $x_{i,t}$ =Standardized Country Output Growth.	84
1.15	Estimation Results of Global Equity Comovement: DECO Estimates, No Domestic Comovement Part.	85
1.16	Factor Exposures of Global Asset Returns in a Seemingly Unrelated Regression (SUR) Frameworks; Constant Beta.	86
1.17	Factor Exposures of Global Asset Returns in Seemingly Unrelated Regression (SUR) Framework; USD; Time-Varying Beta.	87
2.1	Models of the Univariate Conditional Variances.	146

2.2	Parameter Estimates for the Best Univariate Conditional Variance Models.	148
2.3	Cyclicity of the Conditional Comovements between Consumption Growth and Market Return Components: Decomposing the Duffee Puzzle.	149
2.4	Seven extant consumption-based asset pricing models, and their implications on the cyclicity of the exogenous component, $Cov_t(\Delta d_{t+1}, \Delta c_{t+1})$, and the endogenous component, $Cov_t(r_{t+1}^m - \Delta d_{t+1}, \Delta c_{t+1})$, of the amount of risk.	150
2.5	The New DGP for the Joint Consumption-Dividend Dynamics.	151
2.6	Theoretical Models: Resolving the Exogenous Part of the Duffee Puzzle.	152
2.7	Theoretical Models: Unconditional Moments of the Duffee Puzzle Components.	153
2.8	Non-DGP Model Parameter Choices (*=annualized).	154
2.9	Theoretical Models: Unconditional Asset Price Statistics (*=annualized).	154
2.10	Theoretical Models: Resolving the Endogenous Part of the Duffee Puzzle.	155
2.11	Price Dividend Ratio Variance Decomposition.	156
2.12	The Pricing of b_t in Cross Section: Factor Loadings and Prices of Risk.	157
3.1	The Dynamics of the Macro Factors	224
3.2	The Dynamics of the Corporate Loss Rate	225
3.3	Cash Flow Dynamics	226
3.4	Shock Correlations	226
3.5	Financial Instruments Spanning Risk Aversion	227
3.6	Reduced-Form Risk Aversion Parameters	228
3.7	Structural Risk Aversion Parameters.	229
3.8	Fit of Moments.	229
3.9	Asset Prices and the State Variables.	230
3.10	Predicting Realized Excess Returns and Variances.	230
3.11	Out-Of-Sample Exercise.	231
3.12	Uncertainty Index.	231
3.13	On the Predictive Power of Risk Aversion Index and Uncertainty Index on Future Output Growth.	232

3.14 Alternative Risk Aversion and Uncertainty Measures.	233
3.15 Market Integration Test.	233

LIST OF FIGURES

1.1	Global Dynamic Comovement Estimates.	75
1.2	Global Exceedance Correlations of Asset Returns Denominated in USD.	76
1.3	Dynamics of the Seven Economic Determinants.	77
1.4	Data-Implied (Empirical Benchmark) and Model-Implied (Dynamic Factor Model) Global Equity Return Comovements.	78
1.5	Data-Implied (Empirical Benchmark) and Model-Implied (Dynamic Factor Model) Global Bond Return Comovements.	79
1.6	Time Variation in Shares of Economic Determinants in Explaining the Fitted Conditional Covariance Decomposition.	80
1.7	Fit of Equity and Bond Comovement Differences. Global Return Comovements When Omitting One Factor.	81
1.8	Global Dynamic Comovement Estimates, Omitting Certain Countries	82
2.1	The Decomposition of the Duffee Puzzle from the Empirical Analyses.	158
2.2	Annualized Conditional Volatility of the Two Consumption Shocks from the DGP Estimation.	159
2.3	Annualized Conditional Volatility of the Two Dividend Shock Components from the DGP Estimation.	160
2.4	Economic Interpretations for the Fundamental Shock and the Event Shock.	161
2.5	Dependence of the Price Dividend Ratio on the State Variables s and n	162
2.6	Dependence of the Price Dividend Ratio on the State Variable b	163
3.1	Filtered state variables extracted from industrial production growth.	234
3.2	Model-implied conditional moments for industrial production growth.	235

3.3	Conditional moments of the loss rate.	236
3.4	Decomposition of the conditional variance of the loss rate.	237
3.5	Model-implied and empirical risk-neutral conditional variances of equity market returns.	238
3.6	The Time Variation in the Risk Aversion. Risk aversion is $\gamma \exp(q_t)$	239
3.7	Risk aversion index (solid blue/left y-axis) and Uncertainty index (dashed red/right y-axis).	240
3.8	q_t and Uncertainty Index at Daily Frequency Around the Bear Stearns and Lehman Brothers Collapses in 2008.	241

ACKNOWLEDGMENTS

In this adventure, I have been fortunate to learn and grow under the guidance of great minds. My committee members—Geert Bekaert, Bob Hodrick, Eric Engstrom, Xiaoyan Zhang, Simona Abis—are my role models forever.

I am deeply indebted to my advisor, Geert Bekaert. He *raised* me in the strictest yet warmest way possible and believed in me unconditionally. His work ethics and grit have inspired me to persevere. Thanks to him, I learned how to write my first single-authored paper, how to respond to referees, how to develop a seminar talk, and how to lead a discussion. I cannot ask for a better mentor.

Bob Hodrick is the person who recruited me to Columbia. I worked as the teaching assistant for his PhD class for three consecutive years, during which I practiced presenting and teaching. To me, he exemplifies both broad and deep scholarship. I am always amazed by how thoughtful and insightful he is.

I am thankful to have Eric Engstrom and Xiaoyan Zhang as my external committee members. Eric encouraged me to explore cutting-edge econometrics models, which greatly strengthened the technicality of my dissertation. Xiaoyan is always so caring and generous despite her incredibly busy schedule. They are just great mentors and coauthor(s).

This journey would not have started without Stephan Siegel and Thomas Gilbert. When I was feeling lost in the final year of college, the experiences of being Stephan's research assistant and taking Thomas' PhD-level courses altered the course of my life.

This journey would not have been this delightful without my encounter with Simona Abis in the Fall of 2017. She took me to lunch, to coffee and spent numerous hours preparing me for the job market. Deep down, I view her as my academic sister.

I am thankful to receive supports and guidance from many talented and insightful people at Columbia: Tania Babina, Charles Calomiris, Kent Daniel, Oliver Darmouni, Xavier Giroud,

Matthieu Gomez, Laurie Hodrick, Gur Huberman, Wei Jiang, Charles Jones, Anton Lines, Harry Mamaysky, Michaela Pagel, Giorgia Piacentino, Tomasz Piskorski, Tano Santos, Suresh Sundaresan, Paul Tetlock, Neng Wang and Kairong Xiao. There are also too many friends, inside or outside academia, to thank individually.

Last but not least, I am indebted to my parents and my family back in Hangzhou, China. I have been “under review” for 27 years—Thank you for everything.

To my dearest family – who inspire, support, and protect

慈母手中线，游子身上衣。
临行密密缝，意恐迟迟归。
谁言寸草心，报得三春晖。
《游子吟》唐·孟郊

1

GLOBAL RISK AVERSION AND INTERNATIONAL RETURN COMOVEMENTS

This article addresses the ongoing debate about the relative importance of fundamental sources of risk that transmit across countries, and provides evidence for the role of “global” risk aversion. I first compare international equity and bond return comovements, and establish three new stylized facts: (1) bond return correlations are smaller in magnitude than equity return correlations, (2) equity returns have downside correlations that are significantly higher than upside correlations, while bond return correlations are symmetric, and (3) equity return correlations are countercyclical, while bond return correlations are weakly procyclical. I then interpret the stylized facts in the context of a linear dynamic factor model, which is motivated using a dynamic no-arbitrage asset pricing model. The theoretical model features time-varying global economic uncertainties (of output growth, inflation, and real interest rates) and time-varying risk aversion (of a global investor) and consistently prices international equities and Treasury bonds. I find that all three stylized facts above can be explained by the different sensitivities of equity returns (strongly negative) and bond returns (weakly positive or negative) to the global risk aversion shock. In addition, global risk aversion explains 90 percent of the fitted global equity conditional comovements and 40 percent of the fitted global bond conditional comovements, after controlling for a wide set of global economic uncertainties. Inflation upside uncertainty is the other key driver for global bond comovement.

1.1 Introduction

Since the global financial crisis, there is renewed interest in understanding how asset returns comove across countries, for both risky and safe asset classes. A large empirical literature has focused on quantifying the evolution of international equity return comovements (see e.g. Bekaert, Hodrick, and Zhang (2009), and Christoffersen, Errunza, Jacobs, and Langlois (2012), among many others). However, given the important role of safe assets in both domestic and international markets, there is surprisingly little research on how government bond returns comove across countries (see Cappiello, Engle, and Sheppard (2006) for an exception). These correlations are important inputs when evaluating the benefits of international diversification for bond and equity investments. In addition, studying why the comovements among equities versus bonds are different contributes to the ongoing debate about the relative importance of fundamental sources of risk that transmit across borders. My paper formally contrasts global equity return comovements and global bond return comovements, both unconditionally and dynamically, and interprets the comovement differences in the context of a dynamic no-arbitrage asset pricing model with time-varying global economic uncertainties (of output growth, inflation, and the real interest rate) and risk aversion of a global investor.

In the first part of the paper, I formulate a new model of multi-dimensional dynamic dependence to estimate the global equity and bond comovements of 8 developed countries from March 1987 – December 2016. A parametric model helps reveal substantive time variation in global correlation, and provides testable empirical benchmarks in evaluating an asset pricing model (later). The model belongs to the class of Dynamic Equicorrelation models (Engle and Kelly, 2012) but with modifications to accommodate correlation asymmetry, and to ensure the simultaneous fit of domestic equity-bond comovement. In addition, I conduct three tests within the model to identify the differences between equity and bond comovements from three perspectives: magnitude, tail behavior, and cyclicity. Three new stylized facts are established and tested against unconditional moments:

1. Bond return correlations are smaller in magnitude than equity return correlations;

2. Equity returns have downside correlations that are significantly higher than upside correlations, while bond return correlations are symmetric;
3. Equity return correlations are countercyclical, while bond return correlations are weakly procyclical.

As prices are the sums of discounted cash flows, asset return innovations can be explained by cash flow (CF) shocks or discount rate (DR) shocks. Commonalities in asset returns across countries come from a collection of “common” shocks, CF or DR, that are priced in individual country assets. In particular, there has been growing interest regarding the role of global risk aversion as a DR source of international comovements. For instance, Miranda-Agrippino and Rey (2015) suggest that global risk aversion is a key transmission mechanism for exporting U.S. monetary policy to countries worldwide, thus driving the global financial cycle of risky assets. Jotikasthira, Le, and Lundblad (2015) suggest that around 70 percent of long-term bond yield comovement derives from the commonality of term premia. While these studies have indicated potential economic determinants of global comovements within either risky or safe asset classes, no research has formally explained global equity and bond return comovements in a unified framework. Having a unified framework is helpful for identifying the relative importance of common shocks.

In the second part of the paper, I formulate and solve a U.S.-centric dynamic no-arbitrage asset pricing model, featuring time-varying global macroeconomic uncertainties and time-varying risk aversion of a global (U.S.) investor, that prices *both* international equities and government bonds. The state variable capturing risk aversion is motivated from a general HARA utility function; as in Bekaert, Engstrom, and Xu (2017; henceforth, BEX), it represents the non-fundamental variable (in contrast to the macroeconomic variables) in the real pricing kernel. In BEX, a risk aversion index is filtered using moments of risky assets, whereas in the current paper I also focus on government bond markets. Therefore, I consider a broader set of market-wide economic uncertainties in order to price nominal bonds: adding to the real output growth uncertainties as in BEX, inflation uncertainties and real short rate uncertainties. Furthermore, because the asset moment of interest in this paper is comovement, my model admits (1) heteroskedasticity and (2)

conditional non-Gaussianity in the shock assumptions, which has the potential to capture (1) substantive time variation and (2) asymmetric properties as established in the first part of my paper using the parametric model. In particular, I acknowledge left- and right-tail sources of macroeconomic uncertainties, given the recent growing literature discovering their different asset pricing implications (see e.g. Bekaert and Engstrom (2017) in a habit formation framework). Hence, I adapt a realistic and tractable “Bad Environment–Good Environment” shock structure consisting of two centered heteroskedastic non-Gaussian shocks to model the dynamics of upside and downside uncertainties of the three macroeconomic variables. I estimate them using approximate maximum likelihood methods.

Despite the non-Gaussian shock structure, the theoretical model still fits in the affine class of asset pricing models with a closed-form solution. I use the model solution to motivate a dynamic factor model of asset returns where the factors are *shocks* of the aforementioned market-wide economic determinants (global risk aversion and economic uncertainties); I refer to them as “global shocks” in this paper. The dynamics of both global equity and bond return comovements are driven by the second moments of these global shocks, and the difference between the two comovements in my model is explained by the different sensitivities of asset returns to these shocks. In the last part of the paper, I estimate the dynamic factor model with asset returns of the 8 countries to interpret the three stylized facts.

The core finding is that different sensitivities of equity returns (strongly negative) and bond returns (weakly positive or negative) to the *global risk aversion shock* dominantly drive all three stylized facts. Regarding the first stylized fact, because not every country’s government bonds are considered safe (i.e., some bond prices increase with risk aversion while others decrease) but all equities are considered highly risky (i.e., asset prices decrease with risk aversion), bond return comovements are smaller in magnitude than equity return comovements. Second, the fact that bond returns do not respond to the global risk aversion shock with the same sign weakens the role of strongly positively-skewed risk aversion in driving global bond comovements. Third, the finding that all bonds are safe in a good economic environment while only a few bonds remain safe in a bad economic environment results in higher comovement among international

bond returns in these good environments, explaining a (weakly) procyclical global bond comovement.

In addition, factor models with time-varying betas spanned by economic uncertainties increase the correlation between the model-implied conditional correlations and conditional correlations implied by the flexible parametric model from the first part of the paper. The fit increases from 55% to 69% for global equity comovement, and from 0% to 17% for global bond comovement. Global risk aversion accounts for 90% (40%) of the fitted global equity (bond) comovement. As to the economic significance of economic uncertainties, real uncertainties (inflation uncertainties) explain 7% (47%) of the fitted global equity (bond) comovement.

The paper contributes to the finance and economics literature in three ways.

First, the core finding in the paper stresses the importance of the “non-cash flow channel” of international return comovements: risk aversion of the global investor. Risk aversion has featured as a source of capital flow waves (Forbes and Warnock, 2012), monetary policy shock transmission to foreign stock markets (Miranda-Agrippino and Rey, 2015), interest rate correlations (Jotikasthira, Le, and Lundblad, 2015). My contribution is to quantify the “price of risk” or “risk compensation” channel simultaneously with the “cash flow” channel for explaining global equity and bond return comovements.

Second, as documenting stylized facts of global equity and bond comovements, my empirical contribution is oriented toward global bond comovements. For example, the asymmetry of global equity return comovement is a widely-recognized fact and has been tested using different econometric approaches, such as exceedance correlation (Longin and Solnik, 2001), bivariate GARCH models (Cappiello, Engle and Sheppard, 2006), and asymmetric copula models (Christoffersen et al., 2012). The countercyclical behavior of global equity correlation is also well-known (see e.g. Longin and Solnik, 1995; De Santis and Gerard, 1997; Riberio and Veronesi, 2002). However, there is little formal research on these properties for global bond comovement. Most importantly, the first stylized fact is a new and surprising finding because the existing literature documents that 10-year Government bond yields are highly correlated at around 92% (Jotikasthira, Le, and Lundblad, 2015).

Third, from a modeling standpoint, the new econometric model contains two innovations. It allows for the possibility of asymmetric correlations in a multi-dimensional space. In addition, it offers a parsimonious way to ensure the simultaneous fit of time-varying domestic equity-bond comovement and within-asset comovements. Both innovations are shown to improve the statistical fit.

The remainder of the paper is organized as follows. Section 1.2 presents the econometric model and establishes the three stylized facts. Section 1.3 solves an asset pricing model and presents estimation results for the global economic determinants. A more detailed international model is relegated to the Appendix. Section 1.4 interprets the three stylized facts in a dynamic factor model with global factors. Section 1.5 provides additional evidence with a “Jackknife” exercise. Concluding remarks are presented in Section 1.6.

1.2 Stylized Facts of Global Comovements

In this section, I first exploit a high-dimensional dynamic dependence model to establish three new stylized facts of international return comovements from three perspectives: magnitude, tail behavior, and cyclicity. Then, I obtain unconditional, non-parametric data moments to evaluate the fit of the parametric model. Sections 1.2.1 and 1.2.2 present the econometric model, while estimation methodology, data description, and estimation results follow in Sections 1.2.3–1.2.5, respectively. Section 1.2.6 evaluates the model fit of unconditional moments.

1.2.1 Setup

Consider a world economy of N countries. The log equity return of Country i during period $t + 1$ is modeled as follows, $r_{i,t+1}^E = \mu_i^E + \varepsilon_{i,t+1}^E$ where μ_i^E represents the constant mean, and $\varepsilon_{i,t+1}^E$ the return residual. The log bond return of Country i during period $t + 1$ is modeled similarly, $r_{i,t+1}^B = \mu_i^B + \varepsilon_{i,t+1}^B$. In the rest of the section, superscripts “E” and “B” denote equity and bond, respectively, and subscripts indicate country ID and time stamp.

Within each asset class, the conditional variance-covariance matrices of the residuals are

defined as,

$$\mathbf{H}_t^E \equiv E [\varepsilon_{t+1}^E \varepsilon_{t+1}^{E'} | I_t], \quad (1.1)$$

$$\mathbf{H}_t^B \equiv E [\varepsilon_{t+1}^B \varepsilon_{t+1}^{B'} | I_t], \quad (1.2)$$

where I_t denotes the information set at time t . I follow the dynamic dependence literature and express \mathbf{H}_t^E and \mathbf{H}_t^B in a quadratic form to estimate the conditional variances and the conditional correlation (off-diagonal elements) in separate steps,

$$\mathbf{H}_t^E = \Lambda_t^E \mathbf{Corr}_t^E \Lambda_t^E, \quad (1.3)$$

$$\mathbf{H}_t^B = \Lambda_t^B \mathbf{Corr}_t^B \Lambda_t^B, \quad (1.4)$$

where Λ_t^E (Λ_t^B) contains square roots of the equity (bond) return conditional variances on the diagonal, and zeros elsewhere; \mathbf{Corr}_t^E (\mathbf{Corr}_t^B) is the equity (bond) return conditional correlation matrix. Λ_t^E , Λ_t^B , \mathbf{Corr}_t^E and \mathbf{Corr}_t^B are $N \times N$ symmetric matrices. In the first step, return residuals are standardized using conditional variance estimates from univariate GARCH-class models; I relegate univariate conditional variance models and distributional assumptions to Appendices 1.1 and 1.2. The second step takes standardized residuals as given and focuses on estimating the conditional correlation matrices, \mathbf{Corr}_t^E and \mathbf{Corr}_t^B .

1.2.2 A New Econometric Model for Global Comovements

A well-known multi-dimensional dynamic dependence model is the Dynamic Equicorrelation (DECO) model introduced by Engle and Kelly (2012). They impose a strong assumption that all pairwise conditional correlations are the same for all country pairs. This assumption is suitable for my research because the goal is to obtain a series of global return comovements for each asset class.

My model highlights two new features. First, it accommodates asymmetry, which is an improvement on the original DECO model. Second, a DECO model estimates global comovement within one asset class independently; my model also ensures a simultaneous fit of the time-

varying domestic equity-bond comovement—which can be thought of as the flight-to-safety channel. In addition, my model is flexible enough to conduct three statistical tests within the model, leading to the three stylized facts.

1.2.2.1 Global Bond Comovement and the Three Tests

Denote \mathbf{z}_{t+1}^B ($N \times 1$) as the standardized residuals of country bond returns during period $t + 1$. The conditional equicorrelation matrix of \mathbf{z}_{t+1}^B is defined by,

$$E_t[\mathbf{z}_{t+1}^B \mathbf{z}_{t+1}^{B'}] = \mathbf{Corr}_t^B = (1 - \rho_t^B) \mathbf{I}_N + \rho_t^B \mathbf{J}_{N \times N}, \quad (1.5)$$

where \mathbf{I}_N is an identity matrix and $\mathbf{J}_{N \times N}$ is a matrix of 1s. The equicorrelation by definition is an equally-weighted average of correlations of unique country pairs (i.e., total of $N(N-1)/2$ pairs) at time t :

$$\rho_t^B = \frac{2}{N(N-1)} \sum_{i>j} \frac{q_{i,j,t}^B}{\sqrt{q_{i,i,t}^B q_{j,j,t}^B}}, \quad (1.6)$$

where $q_{i,j,t}^B$ is the (i, j) -th element of a symmetric matrix \mathbf{Q}_t^B ($N \times N$) which follows a generalized autoregressive heteroskedastic process. Therefore, the dynamic process of \mathbf{Q}_t^B drives the time variation in \mathbf{Corr}_t^B . In a matrix representation, $\rho_t^B = \frac{1}{N(N-1)} \left[\boldsymbol{\iota}' (\tilde{\mathbf{Q}}_t^B)^{-1/2} \mathbf{Q}_t^B (\tilde{\mathbf{Q}}_t^B)^{-1/2} \boldsymbol{\iota} - N \right]$, where $\tilde{\mathbf{Q}}_t^B$ is \mathbf{Q}_t^B with off-diagonal terms equal to zeros (i.e., Aielli (2013)'s correction) and $\boldsymbol{\iota}$ is a $N \times 1$ vector of ones.

The original DECO framework, as in Engle and Kelly (2012), models the dynamic process of \mathbf{Q}_t as follows, omitting superscript “B” for simplicity:

$$\mathbf{Q}_t = \bar{\mathbf{Q}} + \beta_1 \left(\tilde{\mathbf{Q}}_{t-1}^{\frac{1}{2}} \mathbf{z}_t \mathbf{z}_t' \tilde{\mathbf{Q}}_{t-1}^{\frac{1}{2}} - \bar{\mathbf{Q}} \right) + \beta_2 (\mathbf{Q}_{t-1} - \bar{\mathbf{Q}}), \quad (1.7)$$

where $\bar{\mathbf{Q}}$ (to be specific, $\bar{\mathbf{Q}}^B$) is the pre-determined sample bond return correlation matrix ($N \times N$); β_1 and β_2 are unknown parameters, to capture the relative importance of the cross products of shock realizations and persistence.

In this paper, I propose a more flexible dynamic process as follows:

$$\begin{aligned} \mathbf{Q}_t = & \bar{\mathbf{Q}} \circ \Phi_t + \beta_1 \left(\tilde{\mathbf{Q}}_{t-1}^{\frac{1}{2}} \mathbf{z}_t \mathbf{z}'_t \tilde{\mathbf{Q}}_{t-1}^{\frac{1}{2}} - \bar{\mathbf{Q}} \circ \Phi_{t-1} \right) + \beta_2 (\mathbf{Q}_{t-1} - \bar{\mathbf{Q}} \circ \Phi_{t-1}) \\ & + \gamma \left(\tilde{\mathbf{Q}}_{t-1}^{\frac{1}{2}} \mathbf{n}_t \mathbf{n}'_t \tilde{\mathbf{Q}}_{t-1}^{\frac{1}{2}} - \Xi \circ \bar{\mathbf{Q}} \circ \Phi_{t-1} \right), \end{aligned} \quad (1.8)$$

where “ \circ ” denotes the Hadamard product operator (i.e., element-by-element multiplication). The first term “ $\bar{\mathbf{Q}} \circ \Phi_t$ ” represents the time-varying long-run conditional mean of the conditional covariance matrix. While $\bar{\mathbf{Q}}$ captures the unconditional component of the long-run mean as before, this model also has the capacity to capture cyclical behavior of global comovement through the new term Φ_t defined below,

$$\Phi_t(N \times N) = \begin{bmatrix} 1 & 1 + \phi_t & 1 + \phi_t & \cdots \\ 1 + \phi_t & 1 & 1 + \phi_t & \cdots \\ 1 + \phi_t & 1 + \phi_t & 1 & \cdots \\ \vdots & \vdots & \vdots & \ddots \end{bmatrix}, \quad (1.9)$$

where $\phi_t = \phi \tilde{\theta}_t^{world}$ and $\tilde{\theta}_t^{world}$ is the standardized world recession indicator.¹ Therefore, by construction, the unconditional mean of Φ_t is a symmetric matrix of ones, and ϕ is an unknown constant parameter. As before, the second term captures the effect of news (scaled contemporaneous shock products) on the \mathbf{Q}_t process. The third term is an autoregressive term, capturing the persistence of the process.

To capture potential asymmetry in joint downside events, I introduce an asymmetric component to the conditional process. In the fourth term of Equation (1.8),

$$\mathbf{n}_t(N \times 1) = I_{\mathbf{z}_t < 0} \circ \mathbf{z}_t, \quad (1.10)$$

where $I_{\mathbf{z}_t < 0}$ ($N \times 1$) is assigned 1 if the standardized residual is less than 0, and assigned 0 otherwise. The constant symmetric matrix $\Xi = E [I_{\mathbf{z}_t < 0} I'_{\mathbf{z}_t < 0}]$ ($N \times N$) represents the expected

¹The recession indicator is assigned 1 during recession periods, and 0 during non-recession periods; then, I standardize the indicator so that the unconditional mean (sample mean) of ϕ_t is 0.

covariance of joint negative shocks. The γ -coefficient is not constrained to be positive. The sufficient conditions for a dynamic dependence model in the GARCH class to be positive definite for all possible realizations are that the intercept is positive semi-definite, and the initial covariance matrix is positive definite (see Ding and Engle (2001) for further details).

Three statistical tests are conducted within Equation (1.8), which leads to the three stylized facts:

(1) Equality Test. The magnitude of the long-run conditional mean of the \mathbf{Q}_t process has an unconditional component $\bar{\mathbf{Q}}$, which in the equality test is modeled as below,

$$\bar{\mathbf{Q}}^E + \nu (\mathbf{J}_{N \times N} - \mathbf{I}_N) \quad (1.11)$$

where $\bar{\mathbf{Q}}^E$ is the pre-determined equity unconditional correlation matrix, and ν is a constant. The diagonal terms of the pre-determined equity unconditional correlation matrix are equal to 1; by construction, ν increases all off-diagonal correlations by an equal amount, which is a reasonable construct because the present research focuses on international return comovements at the global level. A positive (negative) ν suggests that global bond comovement is on average greater (smaller) than global equity comovement. The null hypothesis, $\nu = 0$, is that both asset comovements have the same unconditional magnitude.

(2) Asymmetry Test. A positive γ indicates a higher left-tail (downside) comovement, whereas a negative γ indicates a higher right-tail (upside) comovement. The closest paper to introducing asymmetry to dynamic dependence models in the GARCH class is Cappiello, Engle, and Sheppard (2006); however, their model is limited to a bivariate system, whereas the present model works with a multivariate system.

(3) Cyclicity Test. A positive ϕ indicates that the long-run conditional mean of dynamic comovement behaves countercyclically, because the long-run conditional mean comoves positively with the countercyclical world recession indicator, whereas a negative ϕ indicates procyclical behavior.

In principle, business cycle news can affect returns (and thus the “new” terms in my model, $\mathbf{z}_t \mathbf{z}'_t$ and $\mathbf{n}_t \mathbf{n}'_t$) at relatively high frequency. However, my measurement of the business cycle

involves the actual observed cycles and changes only at the lower frequency. Therefore, I argue that introducing cyclicity in the long-run conditional mean is more realistic because cycles are slow-moving, and thus they are more likely to influence the levels of global comovements rather than higher-frequency dynamics. This way, my model differentiates cyclical behavior (which is economic-based) from asymmetric tail behaviors (which is return-based). Similar instrument approaches with macroeconomic variables are used in many empirical studies, a few of which include Bekaert and Harvey (1995) on estimating the world price of risk, Duffee (2005) on testing the cyclicity of the amount of consumption risk, and more recently Xu (2017) on uncovering the procyclical comovement between dividend growth and consumption growth.

1.2.2.2 Global Equity Comovement with Duo-DECO: Return Decomposition

To model global equity return comovements, I propose a “Duo-DECO” framework. The “Duo” part imposes salient feature of the time variation in *domestic* equity-bond return comovements. This time-variation is difficult to explain with economic factors (Baele et al., 2013; Ermolov, 2015) and sign-switches in the correlation are often associated with Flight-to-Safety (FTS; see Connolly, Stivers, and Sun, 2005). On a global scale, Baele et al. (2013) identify and characterize FTS episodes for 23 countries, and find that the majority of FTS events are country-specific rather than global. The correlation between country stock and bond returns is generally procyclical; that is, FTS episodes occur in a bad domestic economic environment. My model aims to accommodate the two empirical observations of domestic comovements—procyclicality and lack of synchronization—while estimating global equity return comovements in a parsimonious fashion.

To be more specific, I impose a linear equity return decomposition. Denote $z_{i,t+1}^E$ ($z_{i,t+1}^B$) as the standardized residuals of equity returns (bond returns) of Country i during period $t + 1$. Define an unknown beta process for each country i , $b_{i,t}$, to capture the time-varying sensitivity of equity

returns to bond returns.

$$z_{i,t+1}^E = b_{i,t} z_{i,t+1}^B + \sqrt{1 - (b_{i,t})^2} \tilde{z}_{i,t+1}^E, \quad (1.12)$$

$$b_{i,t} = 2 \frac{\exp(\delta_1 + \delta_2 x_{i,t})}{1 + \exp(\delta_1 + \delta_2 x_{i,t})} - 1, \quad (1.13)$$

where δ_1 and δ_2 are unknown constant parameters and $x_{i,t}$ is a country recession indicator, assigned 1 during recession months and 0 during non-recession months.

Equations (1.12)-(1.13) have four immediate implications. First, because $z_{i,t+1}^B$ and $\tilde{z}_{i,t+1}^E$ are assumed to be mutually independent,

$$\text{Var}_t(z_{i,t+1}^E) = b_{i,t}^2 \text{Var}_t(z_{i,t+1}^B) + (1 - b_{i,t}^2) \text{Var}_t(\tilde{z}_{i,t+1}^E). \quad (1.14)$$

Given that the conditional variances of standardized residuals are 1 at all times, Equation (1.12) restricts the mean and conditional variance of $\tilde{z}_{i,t+1}^E$ to 0 and 1, respectively.

Second, $b_{i,t}$ ranges from -1 to 1 (exclusively). The two unknown parameters in $b_{i,t}$ are the same across all country pairs; however, because recession periods in different countries are non-synchronized, the domestic equity-bond comovements are different across countries. Thus, $\tilde{z}_{i,t+1}^E$ can be referred to as the “bond-purified” component of equity returns.

Third, this return decomposition conveniently implies a “correlation decomposition”. In a matrix representation, I denote $\widetilde{\text{Corr}}_t^E$ ($N \times N$) as the conditional correlation matrix² of $\tilde{\mathbf{z}}_{t+1}^E$ ($N \times 1$), or $E_t[\tilde{\mathbf{z}}_{t+1}^E \tilde{\mathbf{z}}_{t+1}^{E'}] = \widetilde{\text{Corr}}_t^E$. I denote \mathbf{b}_t ($N \times 1$) as a vector of domestic equity-bond comovement. Given the decomposition in Equation (1.12), the total conditional correlation of equity returns, Corr_t^E , can be expressed as follows,

$$\text{Corr}_t^E = \text{diag}(\mathbf{b}_t) \text{Corr}_t^B \text{diag}(\mathbf{b}_t) + \text{diag}\left(\sqrt{\mathbf{1} - (\mathbf{b}_t)^{\circ 2}}\right) \widetilde{\text{Corr}}_t^E \text{diag}\left(\sqrt{\mathbf{1} - (\mathbf{b}_t)^{\circ 2}}\right), \quad (1.15)$$

where “diag(\cdot)” is a matrix operator that generates a diagonal matrix with the vector on the diagonal and 0 elsewhere, “ $(\cdot)^{\circ 2}$ ” indicates the Hadamard (element-by-element) squares, and $\mathbf{1}$

² $\widetilde{\text{Corr}}_t^E$ is a conditional correlation matrix in general; to be more accurate, I define it as a conditional equicorrelation matrix in Section 1.2.2.3.

is a $N \times 1$ vector of ones; \mathbf{Corr}_t^B is the conditional equicorrelation matrix of bond returns as formulated in Section 1.2.2.1.

1.2.2.3 Global Equity Comovement with Duo-DECO: $\widetilde{\mathbf{Corr}}_t^E$

The conditional correlation matrix of the “bond-purified” equity returns is defined as a conditional equicorrelation matrix,

$$\widetilde{\mathbf{Corr}}_t^E = (1 - \check{\rho}_t^E) \mathbf{I}_N + \check{\rho}_t^E \mathbf{J}_{N \times N}, \quad (1.16)$$

where the equicorrelation is similarly defined:

$$\check{\rho}_t^E = \frac{2}{N(N-1)} \sum_{i>j} \frac{\check{q}_{i,j,t}^E}{\sqrt{\check{q}_{i,i,t}^E \check{q}_{j,j,t}^E}}, \quad (1.17)$$

where $\check{q}_{i,j,t}^E$ is the (i, j) -th element of a symmetric matrix $\check{\mathbf{Q}}_t^E$ ($N \times N$) which follows a generalized autoregressive heteroskedastic process, omitting superscript E for simplicity:

$$\begin{aligned} \check{\mathbf{Q}}_t &= \bar{\mathbf{Q}} \circ \Phi_t + \beta_1 \left(\check{\mathbf{Q}}_{t-1}^{\frac{1}{2}} \check{\mathbf{z}}_t \check{\mathbf{z}}_t' \check{\mathbf{Q}}_{t-1}^{\frac{1}{2}} - \bar{\mathbf{Q}} \circ \Phi_{t-1} \right) + \beta_2 \left(\check{\mathbf{Q}}_{t-1} - \bar{\mathbf{Q}} \circ \Phi_{t-1} \right) \\ &+ \gamma \left(\check{\mathbf{Q}}_{t-1}^{\frac{1}{2}} \check{\mathbf{n}}_t \check{\mathbf{n}}_t' \check{\mathbf{Q}}_{t-1}^{\frac{1}{2}} - \check{\Xi} \circ \bar{\mathbf{Q}} \circ \Phi_{t-1} \right), \end{aligned} \quad (1.18)$$

where $\bar{\mathbf{Q}}$ is the pre-determined equity return correlation matrix, $\check{\mathbf{n}}_t = I_{\check{\mathbf{z}}_t < 0} \circ \check{\mathbf{z}}_t$, $\check{\Xi} = E \left[I_{\check{\mathbf{z}}_t < 0} I_{\check{\mathbf{z}}_t < 0}' \right]$, and similarly Φ_t is the cyclical component of the long-run conditional mean.

1.2.3 Estimation Procedure

I follow the dynamic conditional correlation literature (e.g., Engle, 2002; Engle and Kelly, 2012) to pre-estimate the return conditional variances of each return series independently. I use the Maximum Likelihood Estimation (MLE) methodology to obtain the conditional variance estimates for each return series, and standardize return residuals with the best conditional volatility estimates given the Akaike information criterion (AIC) and Bayesian Information Criteria (BIC).

I consider four conditional variance models (see Appendix 1.1) and four univariate distributions (see Appendix 1.2).

To estimate the global equity and bond correlations, I adopt a two-step procedure:

Step 1, Bond Comovement. Because there is no feedback from equity returns to bond returns, I first estimate global bond correlations. According to Section 1.2.2.1, the bond model has up to 4 (5) unknown parameters, $\{\beta_1, \beta_2, (\nu), \gamma, \phi\}$.³ The sufficient conditions for \mathbf{Q}_t^B to be stationary are $\beta_1 \mathbf{J}_{N \times N} + \beta_2 \mathbf{J}_{N \times N} + \gamma \mathbf{\Xi} < \mathbf{J}_{N \times N}$ and $\beta_1, \beta_2 > 0$. The proof is relegated to Appendix 1.3. No other parameter restrictions are imposed. The global bond correlation is estimated using the MLE methodology where I allow for two multivariate distributional assumptions:

1. Multivariate Gaussian MLE. The log likelihood L^B is the sum of a constant and
$$-\frac{1}{2} \sum_{t=1}^T \left(\log |\mathbf{Corr}_t^B| + \mathbf{z}_{t+1}^{B'} (\mathbf{Corr}_t^B)^{-1} \mathbf{z}_{t+1}^B \right).$$
2. Multivariate t MLE. The log likelihood L^B is the sum of a constant and
$$-\frac{1}{2} \sum_{t=1}^T \left[\log |\mathbf{Corr}_t^B| + (df + N) \log \left(1 + \frac{1}{df} \mathbf{z}_{t+1}^{B'} (\mathbf{Corr}_t^B)^{-1} \mathbf{z}_{t+1}^B \right) \right],$$
 where df is the degree of freedom of the N -variate t distribution (see Kotz and Nadarajah, 2004; Genz and Bretz, 2009).

The best estimates of \mathbf{Corr}_t^B , according to the AIC and BIC, are used in the Step 2 estimation.

Step 2, Equity Comovement. As a key feature in the Duo construct, the return decomposition implies a correlation decomposition as shown in Equation (1.15). That is, the total equity correlation \mathbf{Corr}_t^E is a “weighted” average of the estimated bond correlation (from Step 1) and the bond-purified equity correlation $\widetilde{\mathbf{Corr}}_t^E$ (this step)— $\text{diag}(\mathbf{b}_t) \mathbf{Corr}_t^B \text{diag}(\mathbf{b}_t) + \text{diag} \left(\sqrt{\mathbf{1} - (\mathbf{b}_t)^{\circ 2}} \right) \widetilde{\mathbf{Corr}}_t^E \text{diag} \left(\sqrt{\mathbf{1} - (\mathbf{b}_t)^{\circ 2}} \right)$ —where the time-varying weights (this step) are strictly positive by design. Therefore, the equity model has up to six unknown parameters, $\{\delta_1, \delta_2, \beta_1, \beta_2, \gamma, \phi\}$. It is noteworthy that DECO is a special case of Duo-DECO; when $\delta_1 = \delta_2 = 0$, b_t^i is 0 for all countries during all periods. The stationary conditions for $\check{\mathbf{Q}}_t^E$ are similar to the ones for \mathbf{Q}_t^B . As in the first step, the total global equity correlation is estimated

³The equality test parameter ν is not considered in the full model because estimation results with $\overline{\mathbf{Q}}^E + \nu (\mathbf{J}_{N \times N} - \mathbf{I}_N)$ do not exploit the full cross-country information in the true unconditional correlation matrix of bond return.

using the MLE methodology and two multivariate distributional assumptions. Model selection relies on the AIC and BIC.

1.2.4 Data

I use monthly USD-denominated log returns of eight developed countries: the United States, USA; Canada, CAN; Germany, DEU; France, FRA; United Kingdom, GBR; Switzerland, CHE; Japan, JPN; Australia, AUS. Log equity returns refer to changes in the log total return index of the domestic stock market (United States: S&P500; Canada: S&P/TSX 60; Germany: DAX 30; France: CAC 40; United Kingdom: FTSE 100; Switzerland: SMI; Japan: NIKKEI 225; Australia: S&P/ASX 200); the CRSP value-weighted return (including dividend) is used as the USA equity return; for other countries, the total return index can be obtained from DataStream. Log bond returns refer to changes in the log 10-year government bond index constructed by DataStream. The sample is from March 1987 to December 2016 (a total of 358 months). Country and world recession indicators are obtained from the OECD website.

Table 1.1 shows the summary statistics of log returns, with mean and standard deviations presented as annualized percentages. According to Panel A, the average of all pairwise unconditional correlations of raw log equity returns (before standardization) is 0.639, and that of raw log bond returns is 0.465. Using standardized returns, the average equity return correlation is 0.627, whereas the average bond return correlation is 0.461. In Panel B, U.S. equity and bond return volatilities are both the lowest among the eight countries, which is expected because returns for other countries are denominated in USD. In fact, when expressed in local currencies, the U.S. equity volatility remains the lowest. I comment on comovements in local currencies in the conclusions.

1.2.5 Estimation Results

In this section, I discuss the estimation results of the global equity and bond return comovements.

1.2.5.1 Global Bond Comovement

The parameter estimates of global bond comovement models are reported in Table 1.2. Model “B(1)” is Engle and Kelly (2012)’s DECO model. Recall, DECO is a special case of the model in the current paper (Section 1.2.2.1); therefore, the DECO model is used as an informative null hypothesis to test whether there are improvements on the statistical fit by introducing a time-varying long-run conditional mean, and correlation asymmetry. According to the standard model selection criteria (i.e. AIC and BIC), models with the asymmetry term denoted as Model “B(2)” perform the best. Between the two multivariate distributional assumptions, fitting standardized bond returns with a multivariate t distribution consistently increases the statistical fit (in terms of likelihoods, AIC, and BIC), demonstrating that the data exhibits comovement non-Gaussianity.

The conditional equicorrelation process in the best model is highly persistent ($\beta_2 = 0.9017$). The asymmetry parameter γ is borderline significant in the best model ($\gamma = 0.0263$, $t = 1.654$, one-sided p-value = 0.0645), and remains borderline significant after controlling for the time-varying long-run conditional mean ($\phi = -0.0420$) as in Model B(4). Therefore, I fail to reject the null that bond correlations are symmetric at the 5% significance level. Note that Model B(4) performs better than the best model in terms of the AIC. According to Model B(4), the cyclicity parameter ϕ is estimated to be -0.0420 ($t = -1.76$, one-sided p-value = 0.05), which indicates a weakly procyclical global bond comovement. Economically, the long-run conditional mean during recession periods is significantly lower than that during non-recession periods by an average of 0.086 (i.e., $\frac{-0.0420}{0.491}$ where 0.491 is the standard deviation of the OECD world recession indicator). As a result, I find that global bond comovement is a persistent, weakly procyclical, and symmetric process.

Model B(5) conducts the equality test.⁴ By construction, the inequality parameter ν captures the average difference between the off-diagonal terms of equity and bond return correlation matrices. Using the multivariate Gaussian distributional assumption, ν is significant and negative

⁴The equality test is discussed separately here because it does not improve statistical fit, but is applied as a way to test equality within my dynamic model.

(-0.275), suggesting that the bond correlations are on average smaller than equity correlations; a significant and negative ν is also found using the multivariate t distributional assumption.

In Figure 1.1, I graph the time variation in global bond comovement given the best model (dotted black line) together with the OECD world recessions (shaded regions). The correlation between the OECD world recession indicator and the global bond comovement is -0.0981 (two-sided p-value = 0.0635), which is consistent with the finding of weak procyclicality in the parameter estimation results above. Global bond comovement experienced a two-year drop beginning in 1992, and bounced back in 1994 for the next 17 years or so. The biggest monthly increase occurred during July 1987, which coincided with the Single European Act of 1987. The second biggest monthly increase occurred during January 1999 when the euro was formally introduced. In my sample, four out of eight countries are European. The formation of the monetary union in Europe certainly increased comovements among national assets. This increase in bond comovement around January 1999 is consistent with the pairwise evidence shown by Cappiello, Engle, and Sheppard (2006). The biggest monthly drop occurred during October 2008, the peak of financial crisis after the Lehman Brothers collapse; in two months, the global bond correlation dropped from 0.54 to 0.36. The Online Appendix shows that, during the same period, global bond return variances experienced the biggest increase since 1987—partly through an increase in currency volatilities—further contributes to the drop in correlation. However, during the full sample period, the dynamics of volatilities and correlations (given my estimations) are uncorrelated ($\rho = -0.0608$, p-value = 0.251).

1.2.5.2 Global Equity Comovement

In Table 1.3, I report the estimation results of the global equity comovement model, given the best global bond comovement estimates. The multivariate t distributional assumption improves the model fit, in terms of likelihood, the AIC, and the BIC, across all models. Model “E(1)” is the Duo system in which the purified equity return correlation is modeled with Engle and Kelly (2012)’s DECO model. The parameter estimates of γ are significant and positive whether controlling for the time-varying long-run conditional mean or not, which rejects the null

that global equity comovement is symmetric. The positive sign of γ supports excessive downside comovement. This finding is consistent with the literature (Longin and Solnik, 2001; Ang and Chen, 2002; Cappiello, Engle, and Sheppard, 2006; among many others). Next, the cyclical parameter ϕ is significant and positive—around 0.04—in all models. In particular, the ϕ estimate in the best model—Model “E(4)” with the multivariate t distribution—is 0.0457 (p-value=0.022), which can be interpreted as follows: the long-run conditional mean during recession periods is significantly higher than that during non-recession periods by an average of 0.093 (i.e., $\frac{0.0457}{0.491}$).

The Duo part—consisting of the country-specific domestic comovement process $b_{i,t}$ and the return decomposition/correlation decomposition—uses minimal assumptions to potentially capture the FTS channel. In Table 1.3, δ_2 is estimated to be significant and negative in all models, suggesting a procyclical $b_{i,t}$. The moment matching exercise in Appendix Table 1.13 enhances the estimation plausibility. In Appendix Table 1.14, I re-estimate the equity correlation models using a continuous business cycle variable: the standardized country industrial production growth, which is a procyclical business indicator. Although the standard model selection with the AIC and BIC rejects these models in Appendix Table 1.14, procyclical domestic comovement is still found with significant and negative δ_2 estimates. Moreover, I show that models that include the Duo part perform better than those that do not. In Appendix Table 1.15, Model E(13) with multivariate t distribution retains all the features of the best equity model (Table 1.3) except for the restriction that $\delta_1 = \delta_2 = 0$, and performs worse than the best equity model in terms of likelihood, the AIC, and the BIC. Note that it is hard to make an exact comparison among multivariate t models because the shapes of the multivariate t distribution (governed by df) are estimated to be different; however, the multivariate Gaussian models without the Duo part are rejected by those with the Duo part, once introducing realistic features—such as asymmetry and cyclical conditional means—according to Appendix Table 1.15.

Figure 1.1 depicts the time variation in global equity comovement (solid red line), given the best model. Two interesting observations emerge. First, at 0.218, the equity correlation has a weak (but statistically significant) positive correlation with the bond correlation. However, their movements diverge during recession periods, for instance during the early 1990’s recessions

(Gulf war), the 1994 Mexican economic crisis, and the 1998 Asian crisis. The recent 2007-08 global financial crisis and the 2012 European debt crisis witness the largest differences between global equity and bond comovements in my sample: 0.50 and 0.36, respectively. This observation confirms my findings of countercyclical global equity comovement and procyclical global bond comovement. Apart from recession periods, global equity comovements also peaked during the October 1987 global stock market crash.

Second, during the sample period, a significant and positive upward trend is found in global equity comovement. However, there is no evidence of a positive trend for global bond comovement (denominated in USD). Global equity and bond comovements both reached a low point after the euro debt crisis in January 2015, when Switzerland's central bank stunned financial markets by abandoning a cap limiting the value of the Swiss franc against the euro and caused high currency volatility. Therefore, this drop in correlations during a non-recession period is volatility-induced.

Given the estimation results of the parametric model, this paper formally establishes the following:

- Stylized Fact 1: *Bond return correlations are smaller in magnitude than equity return correlations.*
- Stylized Fact 2: *Equity return correlations are higher following joint negative shocks, while bond return correlations are symmetric.*
- Stylized Fact 3: *Equity return correlations are strongly countercyclical, while bond correlations are weakly procyclical.*

1.2.6 Model Fit

In this section, I document the stylized facts using unconditional, non-parametric data moments. Then, I compare these data moments with model moments implied from simulated datasets of the parametric models described in Sections 1.2.2.1–1.2.2.3 in order to evaluate the model fit. Given the estimation results assuming multivariate t or multivariate Gaussian distri-

butions, country equity and bond returns are simulated 1,000 times with finite samples ($T=358$) and exogenous variables (country and world OECD recession indicators). Although the multivariate Gaussian model is rejected, I simulate it for the purpose of comparison, which serves as the null hypothesis when evaluating the fit of asymmetry.

1.2.6.1 Model Fit: Equality

In Table 1.4, I test the equality between pairwise equity and bond unconditional correlations using the Jennrich (1970)'s χ^2 test (see the description in Appendix 1.4). According to Panel A of Table 1.4, the average pairwise correlation using *standardized returns* during the sample period is 0.6271 for equities and 0.4606 for bonds; the difference is significant ($\chi^2 = 227.087$ under the degree of freedom 28). The average global conditional correlations from the best models, denoted with "Conditional Model", are 0.6568 for equities and 0.4926 for bonds, which are insignificantly different from the data moments. However, the unconditional correlation does not equal the average of conditional correlations. Thus, I calculate the average of the pairwise unconditional correlations using the simulated datasets. The best model is denoted with "Simulated Model (t)", and I fail to reject that the model moments equal the data moments at the 5% significance test. In addition, I examine the fit in three 10-year subsamples and find: (1) global equity comovements are significantly higher than global bond comovements in all three subsamples; and (2) the simulation moments calculated using the best model are statistically close to the actual data moments. The subsample results also capture the widening equity-bond correlation difference after the 2007-08 financial crisis, as also found in the parametric model estimation results (see Section 1.2.5).

1.2.6.2 Model Fit: Asymmetry

In order to replicate the second stylized fact non-parametrically, I follow Longin and Solnik (2001) and Ang and Chen (2002) and use exceedance correlations to demonstrate correlation asymmetry.⁵ The core objective is to quantify the comovement of return realizations that are

⁵The exceedance correlation of standardized daily returns (\tilde{x} and \tilde{y}) at a certain threshold quantile τ is $\rho(\tilde{x}, \tilde{y} | \tilde{x} < \Phi_x^{-1}(\tau), \tilde{y} < \Phi_y^{-1}(\tau))$ if $\tau < 0.5$ or $\rho(\tilde{x}, \tilde{y} | \tilde{x} > \Phi_x^{-1}(\tau), \tilde{y} > \Phi_y^{-1}(\tau))$ if $\tau \geq 0.5$, where $\Phi_x^{-1}(\tau)$ de-

jointly in the lower or upper parts of their distributions. Figure 1.2 depicts exceedance correlations from the 20th to 80th quantiles. Apart from the data exceedance correlations, I compare exceedance correlations implied by three global comovement models from Tables 1.2 and 1.3: (1) Best models assuming the multivariate t distribution (“B (2)”, Table 1.2; “E (4)”, Table 1.3); (2) Models assuming the multivariate t distribution but with no asymmetry term (“B (1)”, Table 1.2; “E (3)”, Table 1.3); and (3) Best models assuming the multivariate Gaussian distribution (“B (2)”, Table 1.2; “E (4)”, Table 1.3). Simply put, I demonstrate the contribution of correlation asymmetry, and non-Gaussianity, by comparing the exceedance correlations implied by models in (1) and (2), and (1) and (3), respectively.

I discuss four relevant observations next. First, the data reveal significant asymmetry in equity return correlations. The equity plot in Figure 1.2 demonstrates a clear gap around the median, which is consistent with the literature. To be more specific, according to Table 1.5, the exceedance correlation jumps from 0.2619 at the 50th quantile to 0.3292 at the 49th quantile, and the gap is statistically significant. In contrast, symmetry in bond correlations is not rejected.

Second, according to the equity plot in Figure 1.2, the best model using the multivariate t distribution is able to match general patterns as seen in the data: equity exceedance correlations significantly increase around the median, whereas the bond exceedance correlation pattern is smooth. Quantitatively, bond exceedance correlations from the simulated datasets of the best model (see Row “Simulated Model (t)” of the bottom panel of Table 1.5) are within 95% confidence intervals of the data exceedance correlations across the spectrum of threshold quantiles; the Wald test that jointly test 4 quantiles-of-interest as indicated in this table fails to reject the null that the simulated best model is close to the data ($\chi^2 = 3.07$, p-value = 0.55). On the other hand, the best model for equity return comovements is able to match the general pattern and most key exceedance correlations (i.e., at the 25th, 49th, and 75th quantiles, according to the top panel of Table 1.5). However, the joint Wald test rejects the null that the model statistically matches the data. It is noteworthy that, for equities, an exact fit of asymmetry across threshold

notes the value of a given percentile τ for variable x . Global exceedance correlations can be further defined as equally-weighted bivariate exceedance correlations across 28 unique country pairs. Exceedance correlations are typically found to be smaller than time-series correlations.

quantiles is not expected because of the slightly different asymmetry identification criteria. In my model, asymmetry is introduced when both returns are *negative*, whereas in the exceedance correlation literature, asymmetry arises when both returns are *below the median*. In my sample, the 43rd quantile, rather than the median, is where all equity returns turn negative; 14 out of 28 unique country pairs show joint negative returns at the 46th quantile.

Third, I simulate models without asymmetry to demonstrate that it is the asymmetry term in the new econometric model that explains the gap (around the median). In Table 1.5 with regard to equities, the model without asymmetry is strongly rejected (see Row “Simulated Model (t), No Asymmetry”). For bonds, the model-implied point estimates are mostly within 95% confidence interval, but the joint test is rejected at the 5% level. Interestingly, among the three models, the model with a multivariate t distribution but without asymmetry is *closer* to the data than the model with a multivariate Gaussian distribution and an asymmetry term. This supports the discussion in Campbell et al. (2008) about the importance of “fat” tails in understanding correlation asymmetry.

Lastly, Gaussian models do not produce enough asymmetry or capture fat tails for either equity or bond returns, and are thus rejected. This result is consistent with the estimation results (Tables 1.2 and 1.3). The tent-shaped exceedance correlation with Gaussian fundamentals is also typically found in the literature (see e.g. Ang and Bekaert, 2002; Campbell et al., 2008). The difference between equity downside comovements calculated using data, and equity downside comovements using the simulated dataset grows wider, as the threshold quantile grows smaller. The joint test regarding fitting data for all four exceedance correlations is rejected for both equity and bond Gaussian models of the 1% level.

1.2.6.3 Model Fit: Cyclicalit

In Table 1.6, I calculate the average pairwise correlations during OECD recession and non-recession periods within both asset classes. During non-recession periods, the pairwise equity return correlation averages 0.5952, which is significantly different from the 0.6571 average found during recession periods. The bond return correlation is slightly higher during non-recession pe-

riods, which is consistent with the weak procyclicality result from the model estimation. These unconditional patterns are replicated in the parametric model. For the simulated best model (“Simulated Model (t)”), all correlations are within 95% confidence interval of the data moments and the recession / non-recession pattern is matched for both equity and bond return correlations.

1.3 Economic Determinants

Asset return innovations can be explained by either cash flow or discount rate shocks. Therefore, the economic determinants of global comovements are the second moments of these shocks that are commonly priced in individual country assets. In Section 1.3.1, I formalize this intuition and identify the economic determinants using a dynamic no-arbitrage asset pricing model that consistently prices international equities and Treasury bonds. Then, I provide the estimation strategy and results of these economic determinants in Section 1.3.2. A dynamic factor model implied from the theoretical model solution is estimated using actual return data in Section 1.4.

1.3.1 An Asset Pricing Model

The reduced-form asset pricing model is defined by a global real pricing kernel and state variables. In this paper, I focus on the perspective of a U.S. (global) investor, which is consistent with the previous empirical section (i.e., USD-denominated returns). The U.S. state variables are proxies for global state variables. The global model has closed-form solutions, which immediately motivates the economic determinants of the global conditional comovements. Given that the asset moment of interest in this paper is a second moment, the shocks structure and the dynamics of the economic determinants are modeled carefully with realistic and sophisticated dynamic processes. The focus of the present research is to evaluate the ability of a global model to interpret all three stylized facts.

Note that under the assumption of market completeness, a reduced-form international asset

pricing model assuming partial integration (i.e., the existence of different real pricing kernels for each country) can be shown to have similar model implications on the economic determinants of global comovements. A detailed solution is derived in closed form in Appendix 1.6.

1.3.1.1 The Global Real Pricing Kernel

The real pricing kernel in this paper is a variant of the Bekaert, Engstrom, and Xu (2017; BEX) kernel⁶, but accommodates more economic state variables in order to price nominal bonds. The minus real pricing kernel is,

$$-m_{t+1} = x_t + \mathcal{J}_t + \boldsymbol{\delta}'_m \begin{bmatrix} \omega_{\theta u, t+1} & \omega_{\theta d, t+1} & \omega_{\pi u, t+1} & \omega_{\pi d, t+1} & \omega_{q, t+1} \end{bmatrix}', \quad (1.19)$$

where x_t is the real short rate, \mathcal{J}_t Jensen’s inequality term (see Appendix 1.6 for a full expression) and $\boldsymbol{\delta}_m$ a 5-by-1 constant vector, $\begin{bmatrix} \delta_{m\theta u} & \delta_{m\theta d} & \delta_{m\pi u} & \delta_{m\pi d} & \delta_{mq} \end{bmatrix}'$. The five kernel shocks include real upside and downside uncertainty shocks, $\omega_{\theta u, t+1}$ and $\omega_{\theta d, t+1}$, inflation upside and downside uncertainty shocks, $\omega_{\pi u, t+1}$ and $\omega_{\pi d, t+1}$, and a preference shock $\omega_{q, t+1}$. All shocks are non-Gaussian, heteroskedastic and mutually independent. I present each of the kernel state variables and shocks in more detail in Sections 1.3.1.2–1.3.1.3.

Note that the first four shocks—filtered from two macro fundamental processes, real output growth and inflation—are referred to as “uncertainty” shocks. The non-Gaussian property of these macro shocks allows them to govern the shape of one tail of the fundamental distribution at a time, e.g. upside and downside output growth shocks. Take the real uncertainty shocks for example. Decomposed from the output growth innovation, the two real shocks also drive the dynamics of the upside and downside uncertainties, respectively, in order to capture this simple intuition: increases in upside (“good”) or downside (“bad”) uncertainty are likely to coincide with increases or decreases in the fundamentals, e.g. output growth is likely to increase when good

⁶The BEX pricing kernel is derived from the general HARA utility function $U(C) = \frac{(C/Q)^{1-\gamma}}{1-\gamma}$; when Q increases, consumption delivers less utility, and marginal utility increases. A special case can be found in Campbell and Cochrane, where $Q = \frac{C}{C-H}$ is the inverse surplus consumption ratio and H represents the habit stock. In this case, the relative risk aversion is γQ . Therefore, there are two drivers for log real pricing kernel m_{t+1} : consumption growth Δc and changes in log relative risk aversion Δq . In BEX, Δc is spanned by real economic fundamental shocks (filtered from industrial production growth) and cash flow shocks; Δq is spanned by fundamental shocks and an orthogonal preference shock.

volatility increases. Therefore, with no restrictions on δ_m , Equation (1.19) implicitly assumes that both level shocks and uncertainty shocks drive the real pricing kernel. Formal mathematical expressions are presented in Section 1.3.1.2.

Regarding the economic motivation, consumption-based models (as in Campbell and Cochrane, 1999) allow real fundamental shocks to span the real pricing kernel. BEX additionally consider in an orthogonal preference shock. The presence of inflation uncertainty shocks may induce an inflation risk premium, which is an important component of the nominal term structure.

Assets are risky to the extent that they have negative returns when the macroeconomic environment is in a “bad” state defined by realizations of macro shocks, and when risk aversion increases, as captured by a positive preference shock. The quantity of economic risk is measured by the second moments of the real and inflation shocks. Both the quantity and price of preference risk are determined by the second moment of the preference shock.

1.3.1.2 The Global Macro Environment

Macro shocks are likely to be non-Gaussian and asymmetric with time-varying volatilities (see e.g. Hamilton, 1990; Fagiolo, Napoletano, and Roventini, 2008; Gambetti, Pappa, and Canova, 2008). Therefore, I adopt the “Bad Environment-Good Environment” (BEGE) framework of Bekaert and Engstrom (2017), to construct the innovations of industrial production growth and inflation. BEGE is particularly suitable in this paper because it admits heteroskedasticity and non-Gaussianity in shocks, while the theoretical model remains in the affine asset pricing class, which demonstrates simplicity.

1.3.1.2.1 Real-Side Shocks and Uncertainties

I follow BEX in modeling the change in the log industrial production index, θ_{t+1} . The innovation is decomposed into two independent shocks each period, one governing the upside

skewness ($\omega_{\theta u,t+1}$) and the other one governing the downside skewness ($\omega_{\theta d,t+1}$):

$$\theta_{t+1} = m_{\theta,t} + \delta_{\theta\theta u}\omega_{\theta u,t+1} - \delta_{\theta\theta d}\omega_{\theta d,t+1}, \quad (1.20)$$

where the conditional mean $m_{\theta,t}$ is a persistent process to accommodate a time-varying long-run mean of output growth;⁷ the two shocks follow centered gamma distributions with time-varying shape parameters:

$$\omega_{\theta u,t+1} \sim \tilde{\Gamma}(\theta u_t, 1), \quad \omega_{\theta d,t+1} \sim \tilde{\Gamma}(\theta d_t, 1),$$

where $\tilde{\Gamma}(x, 1)$ denotes a centered gamma distribution with shape parameter x and a unit scale parameter. The shape factors, θu_t and θd_t , follow autoregressive processes,

$$\theta u_{t+1} = \bar{\theta u} + \rho_{\theta u}(\theta u_t - \bar{\theta u}) + \delta_{\theta u}\omega_{\theta u,t+1}, \quad (1.21)$$

$$\theta d_{t+1} = \bar{\theta d} + \rho_{\theta d}(\theta d_t - \bar{\theta d}) + \delta_{\theta d}\omega_{\theta d,t+1}. \quad (1.22)$$

In this paper, θu_t and θd_t govern the higher conditional moments of the real upside and downside shocks, respectively (see Appendix 1.5 for properties of a gamma-distributed shock). More specifically, because the two shocks are mutually independent, the conditional variance and the conditional unscaled skewness of output growth are as follows,

$$\begin{aligned} \text{Conditional Variance:} & \quad \delta_{\theta u}^2 \theta u_t + \delta_{\theta d}^2 \theta d_t, \\ \text{Conditional Unscaled Skewness:} & \quad 2\delta_{\theta u}^3 \theta u_t - 2\delta_{\theta d}^3 \theta d_t \end{aligned}$$

This reveals why θu_t represents “good” and θd_t represents “bad” volatility. θu_t (θd_t) increases (decreases) the skewness of industrial production growth, and thus represents the real upside (downside) uncertainty at time t . Shocks θu_{t+1} and θd_{t+1} represent real upside and downside uncertainty shocks, respectively.

⁷ $m_{\theta,t} = \bar{\theta} + \rho_{\theta}(\theta_t - \bar{\theta}) + m_{\theta u}(\theta u_t - \bar{\theta u}) + m_{\theta d}(\theta d_t - \bar{\theta d})$.

1.3.1.2.2 Nominal-Side Shocks and Uncertainties

Regarding modeling the inflation process, I allow inflation to respond to output shocks, which is approximately in line with a standard New Keynesian AS curve relating inflation to the output gap. To be specific, inflation is assumed to have constant exposures to the two real shocks, and the residual is decomposed into two nominal-side shocks governing the behavior of left- or right-tail, respectively. Denote π_t as the change in the log consumer price index for all urban consumers, πu_t the nominal upside uncertainty, and πd_t the nominal downside uncertainty. Inflation system follows these reduced-form dynamics,

$$\pi_{t+1} = m_{\pi,t} + (\delta_{\pi\theta u}\omega_{\theta u,t+1} + \delta_{\pi\theta d}\omega_{\theta d,t+1}) + (\delta_{\pi\pi u}\omega_{\pi u,t+1} - \delta_{\pi\pi d}\omega_{\pi d,t+1}), \quad (1.23)$$

where the conditional mean is a persistent process,⁸ and the two inflation shocks follow centered gamma distributions with time-varying shape parameters,

$$\omega_{\pi u,t+1} \sim \tilde{\Gamma}(\pi u_t, 1), \quad \omega_{\pi d,t+1} \sim \tilde{\Gamma}(\pi d_t, 1).$$

The time-varying shape parameters follow autoregressive processes,

$$\pi u_{t+1} = \bar{\pi u} + \rho_{\pi u}(\pi u_t - \bar{\pi u}) + \delta_{\pi u}\omega_{\pi u,t+1} \quad (1.24)$$

$$\pi d_{t+1} = \bar{\pi d} + \rho_{\pi d}(\pi d_t - \bar{\pi d}) + \delta_{\pi d}\omega_{\pi d,t+1}. \quad (1.25)$$

Similarly, πu_t and πd_t ($\omega_{\pi u,t+1}$ and $\omega_{\pi d,t+1}$) represent nominal upside and downside uncertainties (uncertainty shocks), respectively.

The four macro shocks, both real and nominal, are by design mutually independent, centered gamma shocks with heteroskedastic shape parameters. Thus, the conditional variance and

⁸ $m_{\pi,t} = \bar{\pi} + \rho_{\pi\theta}(\theta_t - \bar{\theta}) + \rho_{\pi\theta u}(\theta u_t - \bar{\theta u}) + \rho_{\pi\theta d}(\theta d_t - \bar{\theta d}) + \rho_{\pi\pi}(\pi_t - \bar{\pi}) + \rho_{\pi\pi u}(\pi u_t - \bar{\pi u}) + \rho_{\pi\pi d}(\pi d_t - \bar{\pi d})$.

the conditional unscaled skewness of inflation are,

$$\begin{aligned} \text{Conditional Variance:} & \quad (\delta_{\pi\theta u}^2 \theta u_t + \delta_{\pi\theta d}^2 \theta d_t) + (\delta_{\pi\pi u}^2 \pi u_t + \delta_{\pi\pi d}^2 \pi d_t), \\ \text{Conditional Unscaled Skewness:} & \quad (2\delta_{\pi\theta u}^3 \theta u_t - 2\delta_{\pi\theta d}^3 \theta d_t) + (2\delta_{\pi\pi u}^3 \pi u_t - 2\delta_{\pi\pi d}^3 \pi d_t). \end{aligned}$$

1.3.1.3 Global Risk Aversion

The state variable capturing risk aversion, q_t , according to BEX is motivated using a representative agent economy with a HARA utility. In the present research, the stochastic risk aversion process follows a reduced-form process:

$$q_{t+1} = m_{q,t} + \underbrace{\delta_{q\theta u} \omega_{\theta u,t+1} + \delta_{q\theta d} \omega_{\theta d,t+1} + \delta_{q\pi u} \omega_{\pi u,t+1} + \delta_{q\pi d} \omega_{\pi d,t+1}}_{\text{fundamental shock exposure}} + \delta_{qq} \omega_{q,t+1}, \quad (1.26)$$

where the conditional mean $m_{q,t}$ is a linear function of $q_t, \theta_t, \theta u_t, \theta d_t, \pi_t, \pi u_t$ and πd_t , and the preference innovation receives macro shocks and an orthogonal preference shock which follows a centered heteroskedastic gamma distribution,

$$\omega_{q,t+1} \sim \tilde{\Gamma}(q_t, 1). \quad (1.27)$$

Note that q_t does not have a feedback effect on the macro variables, which enables $\omega_{q,t+1}$ to represent a non-fundamental preference shock. The variance and unscaled skewness of $\omega_{q,t+1}$ are proportional to its level: While controlling for current business conditions, when current risk aversion is higher, there is a greater chance that the future preference shock will see a large and positive realization.

The risk aversion disturbance contains three parts: exposure to real shocks as motivated by consumption-based habit models, exposure to nominal shocks as suggested by Brandt and Wang (2003), and the preference shock as appeared in BEX. Given the distributional assumptions regarding these shocks, the model-implied conditional variance of risk aversion in the current paper is $(\delta_{q\theta u}^2 \theta u_t + \delta_{q\theta d}^2 \theta d_t) + (\delta_{q\pi u}^2 \pi u_t + \delta_{q\pi d}^2 \pi d_t) + \delta_{qq}^2 q_t$, and the conditional unscaled skewness $(2\delta_{q\theta u}^3 \theta u_t + 2\delta_{q\theta d}^3 \theta d_t) + (2\delta_{q\pi u}^3 \pi u_t + 2\delta_{q\pi d}^3 \pi d_t) + 2\delta_{qq}^3 q_t$. In other words, the higher moments of risk

aversion are perfectly spanned by macroeconomic uncertainties on one hand and pure sentiment on the other.

As mentioned before, the idea that fundamental shocks span the risk aversion process is motivated by Campbell and Cochrane (1999) where the real pricing kernel is spanned by one shock. At first glance, the CC model looks very different as non-linearities in the pricing kernel are introduced through time-varying sensitivity function of the surplus consumption ratio ($-q_t$) to consumption shocks, whereas in my model the kernel shock exposures appear time-invariant. However, the framework here, as well as in BEX, does not explicitly require a time-varying sensitivity function to induce non-linearity in the real pricing kernel. To be more specific, the conditional variance of m_{t+1} in Campbell and Cochrane (1999) is $\gamma^2(1+\lambda_t)^2\sigma_c^2$, where σ_c^2 is the constant variance of consumption growth, γ the constant curvature parameter, and λ_t the time-varying sensitivity function that causes non-linearity in the pricing kernel. In my paper, the conditional variance of m_{t+1} is $\delta_{m\theta u}^2\theta u_t + \delta_{m\theta d}^2\theta d_t + \delta_{m\pi u}^2\pi u_t + \delta_{m\pi d}^2\pi d_t + \delta_{mq}^2q_t$. The presence of q_t alone suffices to make it non-linear as it has an asymmetric non-Gaussian shock.

1.3.1.4 Real Short Rate

The reduced-form process of the real short rate is as follows,

$$x_{t+1} = m_{x,t} + \underbrace{f_x(\omega_{\theta u,t+1}, \omega_{\theta d,t+1}, \omega_{\pi u,t+1}, \omega_{\pi d,t+1}, \omega_{q,t+1})}_{\text{Fundamental \& Preference shock exposures}} + \delta_{xu}\omega_{xu,t+1} - \delta_{xd}\omega_{xd,t+1}, \quad (1.28)$$

where the conditional mean is a linear function of x_t , xu_t (later), xd_t (later), q_t , θ_t , θu_t , θd_t , π_t , πu_t and πd_t . The real short rate innovation has a systematic component which not only comprises the fundamental shocks but also the risk aversion shock. Note that this is potentially consistent with the Campbell and Cochrane model reflecting the effect of risk aversion on the real short rate (through precautionary savings and intertemporal substitution effects). The residual is then

decomposed into two centered gamma distributions with autoregressive shape parameters,

$$\omega_{xu,t+1} \sim \tilde{\Gamma}(xu_t, 1); xu_{t+1} = \overline{xu} + \rho_{xu}(xu_t - \overline{xu}) + \delta_{xu}\omega_{xu,t+1}, \quad (1.29)$$

$$\omega_{xd,t+1} \sim \tilde{\Gamma}(xd_t, 1); xd_{t+1} = \overline{xd} + \rho_{xd}(xd_t - \overline{xd}) + \delta_{xd}\omega_{xd,t+1}. \quad (1.30)$$

The two real short rate shocks can be interpreted as discretionary monetary policy shocks in my framework. There is no feedback from real short rate shocks to the risk aversion process.

1.3.1.5 Closed-Form Solution

To price U.S. equities, the cash flow growth processes are modeled to receive global real shocks ($\omega_{\theta u}$ and $\omega_{\theta d}$), and the residual is referred to as the global cash flow shock (a homoskedastic shock denoted ω_g). In order to price individual country equities, cash flow processes are projected on global shocks ($\omega_{\theta u}$, $\omega_{\theta d}$ and ω_g), and the idiosyncratic residuals are assumed to be homoskedastic and mutually independent (across countries). In order to price nominal assets, individual inflation processes are subject to global real and nominal shocks and an idiosyncratic shock.

This global model, from the perspective of a global investor, has a closed-form solution that fits in the affine class of asset pricing models because the moment generating function of a gamma shock is exponentially affine. The government bond prices can be expressed as an exact affine function of the state variables. The equity price-dividend ratios can be expressed as a quasi-affine function of the state variables. For either asset of country i , equity or long-term government bond, the log asset return can be written as the following general process,

$$\begin{aligned} \tilde{r}_{t+1}^i &= E_t(\tilde{r}_{t+1}^i) + \textit{Global Shock Exposure} + \textit{Orthogonal Idiosyncratic Residual} \\ &(+ \textit{Approximation Error}), \end{aligned}$$

where the global shocks are: the six heteroskedastic economic uncertainty shocks, the heteroskedastic preference shock (ω_q), and the homoskedastic cash flow shock (ω_g). The approximation error is primarily introduced to account for the quasi-affine solutions of equity price-dividend ratios;

for simplicity, the error is assumed homoskedastic and Gaussian. Because a linear combination of Gaussian shocks still follows a Gaussian distribution,⁹ the country return processes can be further written as a global dynamic factor model with seven heteroskedastic gamma shocks,

$$\{\omega_{\theta u}, \omega_{\theta d}, \omega_{\pi u}, \omega_{\pi d}, \omega_{xu}, \omega_{xd}, \omega_q\},$$

and a single homoskedastic Gaussian residual that is orthogonal to the seven heteroskedastic global factors and allowed to have non-zero covariances with other country residuals due to its exposure to the homoskedastic global cash flow shock.

As a result, the model solution indicates a reduced-form dynamic factor model, implying that the time variation in the global return comovement is driven by the time variation in the second moments of relevant global shocks. Therefore, the second moments of global shocks are motivated as the economic determinants of global comovements. It immediately follows that the difference in global equity and bond comovements can be explained by the different sensitivities of equity and bond returns to (some of) these global shocks.

1.3.2 The Identification of the Economic Determinants

In what follows, I describe the estimation strategy as well as estimation results of these economic determinants described in Section 1.3.1.5.

1.3.2.1 Procedure

1.3.2.1.1 Real and Inflation Uncertainties:

I pre-filter the real uncertainties θu_t and θd_t using the monthly changes in the log industrial production index (source: FRED), to ensure these variables are identified from macroeconomic information alone, and not contaminated by asset prices. I use Bates (2006)'s Approximate Maximum Likelihood estimation methodology, which allows filtering non-Gaussian shocks

⁹In data, after controlling for heteroskedastic fundamental shocks, the cash flow growth is not rejected from Gaussianity nor homoskedasticity.

and exploits exponential affine characteristic functions. Therefore, the estimation provides time series of the latent uncertainty state variables and their shocks, given the observed growth series. Next, given the filtered real uncertainty shocks, and the assumption that the real shocks are orthogonal to inflation shocks, I project inflation (changes in log Consumer Price Index; source: FRED) onto output growth, real uncertainties and real shocks. Then, I filter the nominal uncertainty shocks from the inflation residual using Bates (2006). I use the longest period of data available for the estimations of these four economic uncertainties, $\{\theta u, \theta d, \pi u, \pi d\}$; the sample period is January 1947 to December 2016.

1.3.2.1.2 Risk Aversion:

Bekaert, Engstrom, and Xu (2017) estimate a utility-based risk aversion index from a no-arbitrage framework using a wide set of macro and financial information. I argue that their risk aversion estimate is still consistent with my framework. First, as discussed earlier, my framework is a modified version of theirs to accommodate short rate shocks and uncertainties that do not feed back on risk aversion. In addition, although BEX’s risk aversion process does not control for inflation uncertainty shocks as my model here does, according to my estimation, filtered inflation shocks (after controlling for real shocks) are insignificantly correlated with the risk aversion shock in the overlapping sample ($\rho(\omega_q, \omega_{\pi u}) = 0.038, \rho(\omega_q, \omega_{\pi d}) = -0.037$). I therefore use the BEX risk aversion process in this article. The sample period spans June 1986 to February 2015.

1.3.2.1.3 Real Short Rate Uncertainties:

The estimation procedure of latent real short rate uncertainties exploits the no-arbitrage condition and the assumed pricing kernel shock structure. Given the closed-form solution (Appendix 1.6), observed nominal 30-day T-bill rate (source: CRSP), and macro and preference shocks, the real short rate as well as its shocks can be filtered using Bates (2006)’s methodology. The general estimation strategy—i.e., using the no-arbitrage condition and a pricing kernel to estimate the real term structure—is commonly used in the literature (e.g., Chen and Scott, 1993; Ang, Bekaert, and Wei, 2008). However, my model is more complicated because I also filter two

shocks from the real short rate innovation, namely upside and downside short rate uncertainties.

1.3.2.2 Results

In Figure 1.3, I show the time variation in the seven economic determinants of global co-movements. Full sample plots are shown in the Online Appendix.

First, the weak countercyclicality of the BEX risk aversion (calculated as $\gamma \exp(q_t)$ where $\gamma = 2$ represents the utility curvature) is immediately apparent, with risk aversion spiking in all three recessions, but also showing distinct peaks in other periods. The highest risk aversion of 11.58 is reached at the end of January in 2009, at the height of the Great Recession. But the risk aversion process also peaks during the October 1987 crash, the August 1998 crisis at the time of Russia default and LTCM collapse, after the TMT bull market ended in August 2002, and in August 2011 during the Euro area debt crisis.

Second, the real downside uncertainty is strongly countercyclical with a correlation coefficient of 0.71 with a NBER recession dummy (in the long sample). The correlation coefficient between the real upside uncertainty and NBER recessions is positive as well, but not statistically significant using the full sample. However, using the short sample (1987.03–2015.02), real upside uncertainty is weakly procyclical with a correlation coefficient of -0.38 with a NBER recession dummy. The two real uncertainty state variables are negatively correlated at -0.31 (statistically different from zero).

While downside uncertainty delivers the countercyclicality in real uncertainty, among inflation uncertainties, the inflation upside uncertainty exhibits more cyclical behavior than the inflation downside uncertainty. In the long sample (beginning in 1947), the time variation is less spiky, in the sense that high inflation upside uncertainty seems to appear in clusters, for example, the 1973 recession, the 1980s recession, and the recent financial crisis. The full sample plot is located in the Online Appendix. The source of the countercyclicality of inflation variation is consistent with Ball (1992). When actual and expected inflation are low, there is a consensus that the monetary authority will try to keep them low. However, when inflation is high, the public does not know whether the policy maker will disinflate or keep inflation high with the fear that dis-

inflation could result in a recession. This dispersion in beliefs potentially results in fluctuations in inflation upside uncertainty. This “high inflation-high upside uncertainty” theory is consistent with the modeling of inflation shocks appearing in both the inflation process and the inflation uncertainty processes, as in Section 1.3.1.2. Empirically, the estimated inflation *upside* uncertainty is significantly countercyclical (i.e., a 0.52 correlation with a NBER recession dummy) which may reflect the wider dispersion in general beliefs in a bad economic environment. (The two nominal uncertainty state variables are weakly positively correlated with a coefficient of 0.16.) Because macro shocks are independent by design, it is now possible to quantify the relative importance of the four shocks in explaining total inflation uncertainty. According to my estimation, inflation upside and downside uncertainties account for 47.63% and 50.25% of the total inflation variance, respectively. Surprisingly, real upside and downside uncertainties together explain less than 3% of total variance within the short sample period.

Lastly, the real short rate innovation process depends on the risk aversion shock, real-side shocks filtered from industrial production growth, and nominal-side shocks filtered from inflation; the residual is then decomposed into two shocks. Thus, these two shocks are “cleansed” from all systematic monetary policy determinants; therefore in my framework, the residuals can potentially be interpreted as discretionary monetary policy shocks. In this sample, inflation shocks explain around 64% of the total real short rate variability to reflect the close relationship between the two; for example, to disinflate, monetary authorities are likely to increase the interest rate. Risk aversion explains 17% of the variability; when risk aversion increases, investors save more, driving down the interest rate (i.e., the precautionary savings channel dominates). In the full sample, of the total variance explained by xu and xd , the downside uncertainty has a share of 73%. In the past 10 years, during which the nominal short rate is close to the zero boundary, expected inflation is positive, and real short rate is negative, the share increases to 88%. According to the last two plots of Figure 1.3, the real short rate upside uncertainty (xu) during 1986–1989 was high when the Federal Reserve responded to high inflation by raising interest rates; in the early 1990s, however, the downside uncertainty starts to become relatively more elevated. The Online Appendix provides detailed estimation results.

1.4 A Theory-Motivated Factor Model

In this section, I evaluate the ability of the asset pricing model in Section 1.3 to interpret the three stylized facts established in Section 1.2. Sections 1.4.1 and 1.4.2 present the factor model and estimation strategy. Section 1.4.3 evaluates the model fit. Section 1.4.4 conducts a global conditional comovement decomposition for both covariance and correlation, followed by a discussion of the economic significance of the factors in interpreting the three stylized facts in Section 1.4.5.

1.4.1 Dynamic Equity and Bond Return Factor Model

Suppose there are N (8) asset return series for each asset class and P (7) global factors. Denote log asset returns (raw, not standardized) of two asset classes during month $t + 1$ with \mathbf{r}_{t+1} ($2N \times 1$), which are assumed to follow:

$$\underbrace{\mathbf{r}_{t+1}}_{2N \times 1} = \underbrace{\mathbf{E}_t[\mathbf{r}_{t+1}]}_{2N \times 1} + \underbrace{\begin{bmatrix} \boldsymbol{\Omega}_{t+1} & \mathbf{0} & \cdots & \mathbf{0} \\ \mathbf{0} & \boldsymbol{\Omega}_{t+1} & \cdots & \mathbf{0} \\ & & \ddots & \\ \mathbf{0} & \mathbf{0} & \cdots & \boldsymbol{\Omega}_{t+1} \end{bmatrix}}_{2N \times 2NP} \underbrace{\begin{bmatrix} \beta_{1,t} \\ \beta_{2,t} \\ \vdots \\ \beta_{2N,t} \end{bmatrix}}_{2NP \times 1} + \underbrace{\boldsymbol{\varepsilon}_{t+1}}_{2N \times 1}, \quad (1.31)$$

where $\mathbf{E}_t[\mathbf{r}_{t+1}]$ denotes a vector of expected returns which, in my model, is a linear function of the state variables. $\boldsymbol{\Omega}_{t+1}$ denotes a row vector of the factors (shocks) introduced in Section 1.3,

$$\boldsymbol{\Omega}_{t+1} = \left[\omega_{q,t+1} \quad \omega_{\theta u,t+1} \quad \omega_{\theta d,t+1} \quad \omega_{\pi u,t+1} \quad \omega_{\pi d,t+1} \quad \omega_{xu,t+1} \quad \omega_{xd,t+1} \right],$$

where each shock follows a centered gamma distribution with time-varying shape parameters as discussed before.

Given the empirical focus of the paper, I also allow the possibility that betas of global factors are time-varying. For each country-asset class, the return sensitivity to each shock is

defined as follows:

$$\beta_t = \beta_0 + \beta_1 s_t, \tag{1.32}$$

where s_t denotes a standardized shape parameter.

Time-varying betas, or conditional betas, can be motivated both empirically and economically. *First*, empirical studies have found that the response of volatility to macroeconomic news depends on the conditional states of the business cycle (Andersen, Bollerslev, Diebold, and Vega, 2007). *Second*, time-varying betas can also arise in economic models with various be motivated by various departures of rational expectations. I discuss two plausible mechanisms below: the Bayesian Learning theory by David and Veronesi (2013), and the Confidence Risk theory by Bansal and Shaliastovich (2010). According to the Bayesian Learning theory, investors learn about (unobserved) shifts in economic states by observing signals in fundamentals and asset prices. In times of precise prior beliefs, large news is not necessary to move posterior probabilities (that is, betas are small); but when there is large uncertainty, which may be correlated with economic uncertainty measures, even small news moves posterior distributions (that is, betas are large). According to the Confidence Risk theory, a widening cross-section of variance in economic signals lowers investor's confidence placed in future growth forecasts, leading to Through this channel, large moves in the confidence measure lead to large declines (negative jumps) in asset prices, though there are no large moves in consumption.

Both empirical evidence and the economic mechanisms discussed above have been documented in the equity markets. Given that inflation upside uncertainty reflects the widening dispersion in beliefs (Ball, 1992), I consider standardized πu_t as s_t in modeling the log equity return betas; in addition, this instrument is shown to improve the empirical fit the most, among the six economic uncertainties in this paper. On the other hand, there is little research on directly examining the time-varying betas in bond returns; therefore, the beta instruments for bond returns are selected based on the best empirical fit. As a result, betas in bond returns are spanned by real uncertainties. As both real uncertainties filtered from industrial production growth exhibit strong business cycle behavior, the modeling of bond betas is potentially consistent with

the modeling of the domestic comovement channel in Section 1.2 where I use the OECD recession indicator that is also identified from industrial production growth.

The residuals in Equation (1.31) are mean zero, and assumed to be correlated:

$$E[\varepsilon_{t+1} | \Omega_{t+1}] = 0, \quad (1.33)$$

$$E[\varepsilon_{t+1} \varepsilon'_{t+1} | \Omega_{t+1}] = \Sigma. \quad (1.34)$$

The model-implied pairwise conditional covariance between country-asset i and j of the same asset class that is explained through the heteroskedastic global shocks is,

$$\beta'_{i,t} \text{Var}_t(\Omega_{t+1}) \beta_{j,t}, \quad (1.35)$$

where $\beta_{i,t}$ ($P \times 1$) and $\beta_{j,t}$ ($P \times 1$) are return sensitivities to Ω_{t+1} , and $\text{Var}_t(\Omega_{t+1})$ ($P \times P$) a conditional covariance-variance matrix of Ω_{t+1} with zeros in all off-diagonal terms because all these common shocks are by design mutually independent.

Then, the model-implied pairwise conditional correlation through the heteroskedastic global shocks is,

$$\frac{\beta'_{i,t} \text{Var}_t(\Omega_{t+1}) \beta_{j,t}}{\sqrt{\beta'_{i,t} \text{Var}_t(\Omega_{t+1}) \beta_{i,t} + \text{Var}(\varepsilon_{i,t+1})} \sqrt{\beta'_{j,t} \text{Var}_t(\Omega_{t+1}) \beta_{j,t} + \text{Var}(\varepsilon_{j,t+1})}}. \quad (1.36)$$

The global correlation is the equal-weighted average of the pairwise correlations, to be consistent with the parametric model in Section 1.2; this is referred to as the factor model-implied global correlation.

1.4.2 Estimation

The dynamic factor model is a system of regression equations with correlated residuals, which is in the class of Zellner (1962)'s Seemingly Unrelated Regression (SUR). I use feasible Generalized Least Squares (FGLS) estimators for betas and the residual covariance matrix (see

Zellner, 1962; Zellner and Huang, 1962), and estimate them jointly with MLE.¹⁰ The theoretical model (see Section 1.3.1.5) implies a multivariate Gaussian residual structure with non-zero correlations is indicated. However, the residuals could be heteroskedastic empirically; there are two potential remedies: (1) model the time series variation in Σ , and (2) change the estimation methodology to Generalized Method of Moments (GMM). The concern with (1) is misspecification error. The concern with (2) is that the estimation speed with GMM is significantly slower than MLE in this case, mainly because of the large number of moment conditions involved.¹¹

Due to the large number of parameters involved in the system, I relegate detailed equation-by-equation estimation results to Appendix Tables 1.16 (with constant betas) and 1.17 (with time-varying betas).

1.4.3 Model Fit

Figures 1.4 and 1.5 compare the factor model-implied global conditional correlations with the best global correlation estimates implied from the DECO class in Section 1.2 (henceforth, the empirical benchmarks). In both figures, the top plots assume constant betas, and the bottom plots assume time-varying betas.

The constant beta model generates a 0.55 correlation with the empirical benchmark. According to Figure 1.4, it matches the October 1987 spike, the correlation decrease during the early 1990s, and the drop during the expansion between the dot-com bubble and the 2007 financial crisis. However, the constant beta model underestimates the global comovement level during the peak of the 2007-2008 financial crisis by 0.1, and overestimates by as much as 0.2 during the 1990s. This is because constant betas do not introduce enough non-linearity, and most economic determinants considered here do not have trends, while the empirical benchmark is tested with significant and positive time trend during the sample period (see Figure 1.1).

¹⁰The reason is as follows: With correlated residuals, the Ordinary Least Squares (OLS) estimators are no longer Best Linear Unbiased Estimators (BLUE), whereas Generalized Least Squares (GLS) estimators are, by construction (Greene, 2003). Both OLS and GLS estimators are unbiased and consistent; however, the variance of the OLS estimator is biased and inefficient. Then again, GLS assumes a known residual covariance matrix, which is an unrealistic assumption. The FGLS estimator is preferred because it assumes Σ is unknown.

¹¹There are 16 asset returns, and 7 main factors; with time-varying betas, the total number of unknown parameters are 224 ($16 \times 7 \times 2$); with (at least) an exact identification, a convergence for a 3-step GMM takes 30 minutes, whereas the MLE procedure takes less than 1 minute.

According to the equity return estimation, the time-varying beta instrument is the time-varying inflation upside uncertainty; a high inflation upside uncertainty potentially captures a wide dispersion in beliefs (Ball, 1992). Linking to Bansal and Shaliastovich (2010)'s confidence risk theory for example, this wide dispersion in beliefs could result in large negative jumps in investor confidence and thus large declines in asset prices given a unit of negative fundamental shock. Given the estimation results, the time-varying beta model improves the constant beta model fit (i.e., the correlation with the empirical benchmark) from 55% to 69%. In particular, the time-varying beta model is able to match the global equity comovement during the 2007-2008 financial crisis and generate a positive albeit weak trend.

The constant beta model generates a global bond comovement that is uncorrelated with the empirical benchmark comovement from Section 1.2. However, the time-varying beta model, at a 17% correlation with the empirical benchmark, shows improvements during certain periods. Between the two real uncertainties serving as beta instruments, real upside uncertainty improves the model fit more. For example, when the Single European Act is introduced during June/July 1987, the empirical benchmark reflects this major monetary union integration event with a large spike. In Figure 1.5, while the constant beta model generates a negative jump, the time-varying beta model generates a positive jump. The economic reason behind this divergent behavior is that, in the time-varying beta model, the sensitivity of almost all foreign bond returns in this sample to the global risk aversion shock becomes positive when real upside uncertainty increases substantively (see Appendix Table 1.17), which drives up the comovement among bonds. Because beta instruments are standardized, a one standard deviation *increase* in real upside uncertainty would change the signs of bond sensitivities to the risk aversion shock from negative to positive for all four European countries (Germany, France, United Kingdom, Switzerland), which drives up global comovement. With a 2.79 standard deviation increase, all bonds are “safe”. The July 1987 integration event comprises a 1.67 standard deviation increase in real upside uncertainty. As another improvement, the time-varying beta model matches the increase in global bond comovement from 1993 to the introduction of the euro in 1999. This improvement is again due to the beta instrument reflecting good and bad states of the global economy in terms of the output

growth uncertainty; the peak corresponds to a 2.8 standard deviation increase in the instrument.

The main goal of this section is to explain the three stylized facts established in the first part of the paper. Therefore, I formally evaluate the ability of this theory-motivated dynamic factor model—featuring changes in global risk aversion and fundamental economic uncertainties as factors—in fitting the three stylized facts. To do so, I first summarize and represent the stylized facts in terms of six numerical moments, two for each fact; they are calculated from the empirical benchmarks (i.e., conditional correlations implied from the parametric model), rather than the simulated ones. Then, I obtain the factor model-implied moments to confront the benchmark moments. Both moments and their closeness tests are presented in Table 1.7. Columns with “Full” indicates that models are implied from a dynamic factor model with the full set of seven heteroskedastic global shocks. Here are several observations. The time-varying beta model is able to match all three stylized facts, whereas the constant beta model fails to match Fact 2 because the upside comovement difference 0.2245 is insignificant from the downside comovement difference 0.2368. The time-varying model is statistically closer to the empirical benchmarks according to the higher p-values in brackets, which is consistent with the dynamic fit shown in Figures 1.4 and 1.5. I conclude that, despite that fitting the true values in correlations is imperfect, the dynamic factor model with only global state variables suffices to match the three stylized fact motivated in the article.

1.4.4 Global Conditional Comovement Decomposition

I now examine the contributions of each factor to the fit by conducting global conditional covariance and correlation decompositions that are discussed in Sections 1.4.4.1 and 1.4.4.2, respectively.

1.4.4.1 Covariance

Given the total pairwise conditional covariance shown in Equation (1.35), I calculate the share of conditional covariance explained by factor ω_κ (e.g.):

$$\frac{\beta_{i,t,\kappa} \text{Var}_t(\omega_{\kappa,t+1}) \beta_{j,t,\kappa}}{\boldsymbol{\beta}'_{i,t} \text{Var}_t(\boldsymbol{\Omega}_{t+1}) \boldsymbol{\beta}_{j,t}}, \quad (1.37)$$

where $\beta_{i,t} = \beta_{i,0} + \beta_{i,1} s_t$ and $\beta_{j,t} = \beta_{j,0} + \beta_{j,1} s_t$ are scalars, indicating the beta for that particular factor; the values of $\beta_{i,0}, \beta_{i,1}, \beta_{j,0}$ and $\beta_{j,1}$ are given by the estimation results; the conditional variance of that factor, $\text{Var}_t(\omega_{\kappa,t+1})$, is a scalar.

Table 1.8 presents the average conditional covariance decomposition (across all months and across 28 unique country pairs). Three observations stand out. First, the risk aversion factor explains around 90% of the equity return covariance both in the constant beta and time-varying beta models. This quantitative result formally contributes to the ongoing debate about the relative importance of fundamental sources of risk that transmit across countries (see Miranda-Agrippino and Rey, 2015; Jotikasthira, Le, and Lundblad, 2015), and supports a potentially stronger role for the risk compensation channel in explaining international return comovement as opposed to the cash flow variables (industrial production and inflation) or the interest rate. Adding to the recent, growing literature on the strong predictive power of the variance risk premium for equity returns (see Bollerslev, Tauchen, and Zhou, 2009; Bekaert and Hoerova, 2014; Bollerslev et al., 2014; among many others), the current work establishes an important role of risk aversion for second moment dynamics.¹² Besides the dominant role of risk aversion in explaining international equity return covariances, real economic uncertainties also explain an amount (5.2% in constant beta models and 7.4% for time-varying beta models). Figure 1.6 shows the conditional covariance decomposition over time. While the share of total equity return conditional covariance explained by risk aversion dominates during my sample period, the relative weights of real and inflation uncertainties occasionally spike but their magnitudes always remain below 40%. Note that, even though the relative weight of risk aversion decreases during the fi-

¹²Bekaert, Engstrom, and Xu (2017) show that their risk aversion index is highly correlated with the variance risk premium.

nancial crisis, both the total conditional covariance and the conditional covariance accounted for by risk aversion spike. It is more of a surprising finding on the strictly dominant role of risk aversion relative to a wide range of economic uncertainties in explaining the dynamics of conditional covariance during good times, which is not suggested by extant theories.

Second, inflation upside uncertainty—the part of inflation uncertainty that comoves strongly with business cycles (see the discussion in Section 1.3.2)—explains 48.6% of the fitted bond return conditional covariance in the factor model with time-varying betas. The constant part “[β_0]”, $\frac{\beta_{i,0}Var_t(\omega_{t+1})\beta_{j,0}}{\beta'_{i,t}Var_t(\Omega_{t+1})\beta_{j,t}}$, already accounts for 43.1%. In the time-varying beta model, risk aversion is a less dominant factor (40% of the total explained covariance instead of 78% in the constant beta model), whereas inflation uncertainty (47% instead of 34%) and real short rate upside uncertainty (22% instead of a negative contribution) now play a larger role. My model reveals *non-linearities* in the effects of q_t and xu_t on global bond comovements. As mentioned in Section 1.4.3, the risk characteristics of bond returns might be different during good and bad times. The fact that all bond returns are positively correlated with risk aversion (i.e., safe) during good times drives up global bond comovement; when the world is entering a bad economic environment, several foreign bonds become risky, resulting in lower global bond return comovement. As a result, this non-linear effect of risk aversion contributes positively to the third stylized fact, a weakly procyclical global bond comovement. On the other hand, in a bad economic environment, when the real short rate upside uncertainty increases (i.e., there is a higher chance of an increase in interest rate), bond prices drop for all countries except for the USA in this sample, also indicating higher global bond comovement. Therefore, the non-linear effect of xu contributes negatively to the third stylized fact, which renders the effect of risk aversion the dominant force in fitting the stylized facts.

Third, global factor model with constant betas explains 49.4% of the total equity return covariance. Allowing for time-varying betas, the factor model explains covariances slightly better, at 54.6%.¹³ On the other hand, fitting bond return covariances with a constant-beta factor model

¹³The share of total explained covariance is calculated by dividing the time-series average of pairwise conditional covariance by the unconditional pairwise covariance matrix, and then taking the equal-weight cross-sectional average.

is not successful, with only 0.9% of the covariance explained. The fit improves with a time-varying beta model to a 15.4% explained fraction.

1.4.4.2 Correlation

While covariances can be easily decomposed, a correlation decomposition is not as straightforward. Here, I propose a new correlation decomposition test. I denote $CORR_{0,t}$ as the factor model-implied global conditional correlation using all 7 factors, $CORR_{\omega_\kappa,t}$ as the factor model-implied global conditional correlation using all factors except for factor ω_κ (where the parameters are re-estimated), and BM_t as the empirical benchmark. Then, under the null of the factor having zero contribution to the model fit, $\rho(CORR_{0,t}, BM_t) - \rho(CORR_{\omega_\kappa,t}, BM_t)$ should not be indifferent from zero. I show the statistics in Table 1.9.

The first line reports the correlations between the empirical benchmark for the case of comparison. Clearly, risk aversion has the largest marginal contribution to the correlation fit. Let's focus on the time-varying beta models which exhibit better statistical fit than the constant beta models given the previous analysis. A dynamic factor model without the risk aversion shock has -21% (-12%) correlation with the empirical benchmark for global equity comovement (global bond comovement). This indicates that risk aversion has the largest marginal contribution to the fit of global equity and bond conditional correlations, according to the second line. Moreover, I report the marginal contribution of economic uncertainties in the dynamic fit. By adding any of the 6 uncertainty shocks to the equity model, the factor model-implied global equity comovement fits the empirical benchmark better by less than 0.1—which are weakly significant, albeit small and significantly smaller than the 0.9 marginal contribution by risk aversion. In the case of the bond model, the inflation upside uncertainty shock improves the model fit the most among all 6 uncertainty shocks by around 0.14, leaving the risk aversion shock still the largest contributor in terms of statistical fit.

1.4.5 Economic Significance of Risk Aversion

The global comovement decompositions establish risk aversion as a critical economic determinant of global comovements. In this section, I formally quantify the economic significance of risk aversion (and other factors for comparison), and explain why ω_q helps interpret all three stylized facts. Because the constant beta model fits bond comovement poorly to begin with, I focus on the models with time-varying betas in this section.

In the last two columns of Table 1.7, I report the fit of a factor model omitting the risk aversion shock (ω_q). The time-varying beta model without ω_q fails to jointly fit the facts.¹⁴ The top right plot of Figure 1.7 suggests that the biggest misfit (in terms of both magnitude and dynamics) in global equity-bond correlation difference occurs during and after the 2007 financial crisis, when global equity and bond comovement decoupled. The decoupling is an interesting phenomenon, which requires more detailed examination. In my framework, the decoupling is likely an FTS effect (equity to bond) coupled with a large positive risk aversion shock. Table 1.10 evaluates the fit of factor models omitting economic uncertainty shocks is at a time. These models are still able to generate reasonable comovement differences between international equities and government bonds markets, as the three stylized facts are not rejected. That is, they are not the core factors delivering the comovement stylized facts established in the current paper.

Next, I revisit the three stylized facts and provide details on why risk aversion helps interpreting the three stylized facts:

First, equity return sensitivities to the risk aversion shock are significant and negative (i.e. risky), whereas bond return sensitivities to the risk aversion shock are not only much smaller in magnitude but have different signs in different countries. Therefore, equity comovements are higher in magnitude than bond comovements.

Second, the second moment of the risk aversion shock is positively-skewed, $skew(q_t) > 0$. With bond returns displaying relatively weaker return sensitivities to the risk aversion shock, asymmetry in bond return comovements is naturally less strong than in equity return comovements.

¹⁴The constant beta model without ω_q is also immediately rejected.

Third, the U.S. (global) investor demands higher risk compensation from risky assets when her risk aversion is high; moreover, the risk compensation channel is strengthened during periods when dispersion in beliefs is wider (captured by high inflation upside uncertainty in this model). Therefore, stock prices drop across all countries simultaneously and global equity comovement increases in a bad economic environment.

In a good economic environment when real upside uncertainty (or good volatility associated with positive skewness of future output growth) is higher than average, almost all bond prices increase with the risk aversion shock, rendering them safe assets. In a bad economic environment with low real upside uncertainty, six foreign bonds turn risky while the USA and JPN bonds remain safe assets. Therefore the commonality in bond returns is higher during good times, implying a procyclical bond comovement.

1.5 Countercyclical Divergence of Bond Risk Characteristics

In this paper, I interpret the procyclical global bond comovement with divergence in country bond risk characteristics during global economic turmoil. The sensitivities of country bond returns to the global risk aversion shock depend on different states of the world economy. In a good environment with high good real-side volatility, all country bonds are identified as safe assets, meaning their prices increase in response to increases in risk aversion. In a bad environment, some country bond prices soar when global risk aversion is higher, indicating safe heaven behaviors, whereas other country bond prices drop, constituting the higher-risk segment of the global bond market; hence, there exhibits a divergence in the risk characteristics of country government bonds. An intuition explanation is a Flight-To-Quality effect within the international bond market. In this country sample, I identify United States and Japanese government bonds as safe assets; other foreign country bonds become risky during recessions.

To further demonstrate the significant role of countercyclical divergence of bond risk characteristics in resulting in the substantive time variation in global bond correlations as observed

in Figure 1.1, in this final section, I conduct a “Jackknife” exercise. I re-estimate the global bond correlations with subsets of the full country set using the parametric model in Section 1.2, and compare them with the empirical benchmark (with a full country set).

In the first three plots of Figure 1.8, I omit one country at a time in the re-estimations. Clearly by omitting either USA or JPN bonds, global bond correlations (depicted by thin black lines) become significantly *higher* than the empirical benchmark (depicted by wide red lines). It is because the strongly comoving risky bonds now have more weights in the aggregate bond return comovement of this subsample. Note that the global bond comovement omitting Japanese government bond is higher and exhibits less time variation than the one omitting United States government bond, which suggests that the JPN bond might play a more significant role of a “safe” asset. Moreover, according to the second plot of Figure 1.8, omitting any of the European government bonds does not influence the level or cyclicity of the global bond comovement significantly.

The final plot depicts the time variation in the global bond comovement without USA and JPN government bonds. The global comovement of risky bonds is higher than the empirical benchmark value, which is expected; most importantly, it is uncorrelated with the NBER recession indicator. Major declines in global bond comovements during economic turmoil as in the empirical benchmark (e.g., 2007-08 global financial crisis, 2012 European debt crisis) do not appear in this plot. In fact, the risky bond comovement is extremely persistent ($AR(1)=0.98$) than the empirical benchmark using a full country set ($AR(1)=0.90$). Thus, this jackknife exercise further demonstrates that the divergence of bond risk characteristics is an important driver of the dynamics of global bond comovement documented in this paper. However, I do not explain why bond risk characteristics diverge in this paper; but eventually, it is closely related to the monetary policy regime and/or the exchange rate regime, which deserves more scrutiny.

1.6 Conclusion

In this paper, I formally establish three new stylized facts contrasting global equity and bond comovements, both conditionally and unconditionally. The three facts are as follows: (1) bond return correlations are smaller than equity return correlations, (2) equity returns have higher downside than upside correlations, while bond return correlations are symmetric, and (3) equity return correlations are countercyclical while bond return correlations are weakly procyclical. The stylized facts regarding bond comovements are new contributions. The new global dynamic comovement model accommodating asymmetry and domestic comovement (Duo-DECO) is potentially a methodological contribution. Next, I motivate and identify economic determinants of global comovements in a dynamic no-arbitrage asset pricing model with time-varying global economic uncertainties (of output growth, inflation, and the real short rate) and the risk aversion (of a global investor). Finally, I interpret the three stylized facts in the context of a dynamic factor model motivated by the theoretical model. I find that different sensitivities of equity returns (strongly negative) and bond returns (weakly positive or negative) to the global risk aversion shock dominantly drive all three stylized facts. While Miranda-Agrippino and Rey (2015) suggest that global risk aversion drives the global risky-asset cycle, my paper documents global risk aversion as a major source of asset return comovements across countries, for both equities and government bonds, which contributes to the ongoing debate about the relative importance of fundamental sources of risk in affecting global comovements.

The paper also leaves three puzzles for future research. First, bond comovement remains poorly explained. Second, although this paper focuses on return comovements from the perspective of a global investor, comovements denominated in local currencies are also potentially interesting given the increasing demand for currency-hedged bonds (see Viceira, Wang, and Zhou, 2017). In fact, I also examine properties of global bond comovement denominated in local currencies, and find four facts: it is smaller than global equity comovement, it is symmetric, it is acyclical, and it has a clear upward trend that disappears in the global bond comovement denominated in USD. Lastly, the three stylized facts suggest that international bond investments is

more attractive for a U.S. investor from a diversification perspective. However, world bond home bias is significantly higher than world equity home bias (Coerdacier and Rey, 2013).

Appendices

1.A Univariate Conditional Variance Models

The univariate variance model for each return series is selected using the Bayesian information criterion (BIC) from a class of models capable of capturing the common features of financial asset return variance: persistent, clustering, and (sometimes) asymmetric. Although commonly-acknowledged, these features do not appear in conditional variances of all asset returns. For example, as asymmetry in both domestic stock returns and international stock returns is widely documented (see, e.g., French, Schwert, and Stambaugh (1987), Hentschel (1995), Wu (2001), Li et al. (2005); Kenourgios, Samitas, and Paltalidis (2011) among many others), little evidence of asymmetry is found in bond returns, both domestically or internationally (see a thorough examination in Cappiello, Engle, and Sheppard (2006) for instance). As a result, in this paper, I consider four conditional variance models in the GARCH class with four residual distributional assumptions; thus, 16 models are included in the model selection.

Suppose the residual follows a conditional distribution, $\varepsilon_{t+1} \sim D(0, h_t)$ where h_t denotes the conditional variance. The first conditional variance model follows an autoregressive conditional heteroskedastic process with one lag of the innovation and one lag of volatility, or “GARCH” as in Bollerslev (1986):

$$h_t = \alpha_0 + \alpha_1 \varepsilon_t^2 + \alpha_2 h_{t-1} \quad (1.38)$$

where α_1 denotes the sensitivity of conditional variance to news and α_2 the autoregressive coefficient. Then, I use three widely-used asymmetric GARCH models that introduce non-linearity to different transformations of the conditional variance h_t . The second model is the exponential GARCH, or “EGARCH” as in Nelson (1991), which includes a signed standardized residual term to capture the (potential) higher downside risk variance. The third model is the threshold GARCH, or “TARCH” as in Zakoian (1994), which introduces asymmetry to conditional volatility, whereas the fourth model, Glosten, Jagannathan, and Runkle (1993)’s “GJR-GARCH”, introduces asymmetry to conditional variance. The model specifications are shown below:

$$\ln(h_t) = \alpha_0 + \alpha_1 \frac{|\varepsilon_t|}{\sqrt{h_{t-1}}} + \alpha_2 \ln(h_{t-1}) + \alpha_3 \frac{\varepsilon_t}{\sqrt{h_{t-1}}}, \quad (1.39)$$

$$\sqrt{h_t} = \alpha_0 + \alpha_1 |\varepsilon_t| + \alpha_2 \sqrt{h_{t-1}} + \alpha_3 I_{\varepsilon_t < 0} |\varepsilon_t|, \quad (1.40)$$

$$h_t = \alpha_0 + \alpha_1 \varepsilon_t^2 + \alpha_2 h_{t-1} + \alpha_3 I_{\varepsilon_t < 0} \varepsilon_t^2, \quad (1.41)$$

where α_3 is the asymmetry term. If the downside uncertainty is higher than the upside uncertainty, then α_3 in Equation (1.39) is expected to be negative because downside risk in these models is identified when residuals are negative, whereas α_3 in Equations (1.40) and (1.41) are expected to be positive because the asymmetry terms in last two models are sign-independent.

The standardized residuals, z_{t+1} , are defined to be $\frac{\varepsilon_{t+1}}{\sqrt{h_t}}$.

1.B Four distributional assumptions in estimating the conditional variances of return series in Section 1.1.

I consider four distributions. First, Gaussian distribution; $\varepsilon_{t+1} \sim N(0, h_t)$ with conditional probability density function equal to $\frac{1}{\sqrt{2\pi h_t}} \exp^{-\frac{\varepsilon_{t+1}^2}{2h_t}}$. Second, Student's t distribution; $\varepsilon_{t+1} \sim STD(0, h_t, \zeta_1)$ with conditional probability density function equal to

$\frac{\Gamma[\frac{1}{2}(\zeta_1+1)]}{\sqrt{\pi}\Gamma(\frac{1}{2}\zeta_1)} [(\zeta_1 - 2)h_t]^{-\frac{1}{2}} \left[1 + \frac{\varepsilon_{t+1}^2}{(\zeta_1-2)h_t}\right]^{-\frac{1}{2}(\zeta_1+1)}$ where $\zeta_1 > 2$ denotes the degree of freedom capturing the thickness of both tails and Γ denotes the gamma distribution. A higher ζ_1 indicates a thinner tail. Third, Generalized error distribution; $\varepsilon_{t+1} \sim GED(0, h_t, \zeta_1)$ with conditional probability density function equal to $\frac{\zeta_1}{2\sqrt{h_t}\Gamma(\frac{1}{\zeta_1})} \exp^{-\left(\frac{\varepsilon_{t+1}}{\sqrt{h_t}}\right)^{\zeta_1}}$. Platykurtic densities (with tails lighter than Gaussian) are defined if $\zeta_1 > 2$; on the other hand, leptokurtic densities (with tails heavier than Gaussian) are defined if $1 < \zeta_1 < 2$. Fourth, Skewed student t distribution; $\varepsilon_{t+1} \sim SKEWT(0, h_t, \zeta_1, \zeta_2)$ where conditional probability density function (according to Hansen, 1994) equals

$$f(\varepsilon_{t+1}|h_t, \zeta_1, \zeta_2) = \begin{cases} bc \left[1 + \frac{1}{\zeta_1-2} \left(\frac{b\frac{\varepsilon_{t+1}+a}{\sqrt{h_t}}}{1-\zeta_2}\right)^2\right]^{-\frac{\zeta_1+1}{2}} & \frac{\varepsilon_{t+1}}{\sqrt{h_t}} < -\frac{a}{b}, \\ bc \left[1 + \frac{1}{\zeta_1-2} \left(\frac{b\frac{\varepsilon_{t+1}+a}{\sqrt{h_t}}}{1+\zeta_2}\right)^2\right]^{-\frac{\zeta_1+1}{2}} & \frac{\varepsilon_{t+1}}{\sqrt{h_t}} \geq -\frac{a}{b}, \end{cases} \quad (1.42)$$

where $2 < \zeta_1 < \infty$, $-1 < \zeta_2 < 1$, constants $a = 4\zeta_2 c \left(\frac{\zeta_1-2}{\zeta_1-1}\right)$, $b^2 = 1 + 3\zeta_2^2 - a^2$, and $c = \frac{\Gamma[\frac{1}{2}(\zeta_1+1)]}{\sqrt{\pi}\Gamma(\frac{1}{2}\zeta_1)} [(\zeta_1 - 2)h_t]^{-\frac{1}{2}}$. The density function is continuous, and has a single mode at $-\frac{a}{b}$, which is of opposite sign with the parameter ζ_2 . Thus if $\zeta_2 > 0$, the mode of the density is to the left of zero and the distribution is right-skewed, and vice-versa when $\zeta_2 < 0$. To summarize, all distributions except for the first distribution allow for thick tails; in addition, the last distribution also captures the skewness.

1.C Prove Covariance Stationarity of the Global Dynamic Comovement Model in Equation (1.8).

In this section, I prove that \mathbf{Q}_t ($N \times N$) is a stationary process. As introduced in Section 1.2.2.1, \mathbf{Q}_t follows a generalized autoregressive heteroskedastic process,

$$\begin{aligned} \mathbf{Q}_t &= \bar{\mathbf{Q}}^* \circ \Phi_t + \beta_1 \left(\tilde{\mathbf{Q}}_{t-1}^{\frac{1}{2}} \mathbf{z}_t \mathbf{z}_t' \tilde{\mathbf{Q}}_{t-1}^{\frac{1}{2}} - \bar{\mathbf{Q}}^* \circ \Phi_{t-1} \right) + \beta_2 \left(\mathbf{Q}_{t-1} - \bar{\mathbf{Q}}^* \circ \Phi_{t-1} \right) \\ &\quad + \gamma \left(\tilde{\mathbf{Q}}_{t-1}^{\frac{1}{2}} \mathbf{n}_t \mathbf{n}_t' \tilde{\mathbf{Q}}_{t-1}^{\frac{1}{2}} - \Xi \circ \bar{\mathbf{Q}}^* \circ \Phi_{t-1} \right), \end{aligned} \quad (1.43)$$

where “ \circ ” denotes the Hadamard product operator (element-by-element); $\bar{\mathbf{Q}}^*$ is the unconditional component of the long-run conditional mean; $\tilde{\mathbf{Q}}_t$ is \mathbf{Q}_t with off-diagonal terms being zeros, which is a modification to Engle (2002) proposed by Aielli (2013); $\mathbf{n}_t (N \times 1) = I_{\mathbf{z}_t < 0} \circ \mathbf{z}_t$, where $I_{\mathbf{z}_t < 0} (N \times 1)$ is assigned 1 if the residual is less than 0, and assigned 0 otherwise; $\Xi =$

$E[I_{z_t < 0} I'_{z_t < 0}]; \Phi_t (N \times N) = \begin{bmatrix} 1 & 1 + \phi_t & 1 + \phi_t & \cdots \\ 1 + \phi_t & 1 & 1 + \phi_t & \cdots \\ 1 + \phi_t & 1 + \phi_t & 1 & \cdots \\ \vdots & \vdots & \vdots & \ddots \end{bmatrix}$ where $\phi_t = \phi \tilde{\theta}_t^{world}$, $\tilde{\theta}_t^{world}$ is the standardized θ_t^{world} and ϕ is an unknown constant parameter.

1.C.1 Time-Invariant Mean

First, given that $E_{t-1}(z_t z'_t) = Corr_{t-1} = \tilde{Q}_{t-1}^{-\frac{1}{2}} Q_{t-1} \tilde{Q}_{t-1}^{-\frac{1}{2}}$, one-period conditional mean has the following process,

$$\begin{aligned}
 E_{t-1}(Q_t) &= \bar{Q}^* \circ E_{t-1}(\Phi_t) + \beta_1 \left(\tilde{Q}_{t-1}^{\frac{1}{2}} E_{t-1}(z_t z'_t) \tilde{Q}_{t-1}^{\frac{1}{2}} - \bar{Q}^* \circ \Phi_{t-1} \right) + \beta_2 \left(Q_{t-1} - \bar{Q}^* \circ \Phi_{t-1} \right) \\
 &+ \gamma \left(\tilde{Q}_{t-1}^{\frac{1}{2}} E_{t-1}(n_t n'_t) \tilde{Q}_{t-1}^{\frac{1}{2}} - \Xi \circ \bar{Q}^* \circ \Phi_{t-1} \right), \tag{1.44}
 \end{aligned}$$

$$\begin{aligned}
 &= \bar{Q}^* \circ E_{t-1}(\Phi_t) + \beta_1 \left(\tilde{Q}_{t-1}^{\frac{1}{2}} Corr_{t-1} \tilde{Q}_{t-1}^{\frac{1}{2}} - \bar{Q}^* \circ \Phi_{t-1} \right) + \beta_2 \left(Q_{t-1} - \bar{Q}^* \circ \Phi_{t-1} \right) \\
 &+ \gamma \left(E_{t-1}(I_{z_t < 0} I'_{z_t < 0}) \circ \tilde{Q}_{t-1}^{\frac{1}{2}} Corr_{t-1} \tilde{Q}_{t-1}^{\frac{1}{2}} - \Xi \circ \bar{Q}^* \circ \Phi_{t-1} \right), \tag{1.45}
 \end{aligned}$$

$$\begin{aligned}
 &= \bar{Q}^* \circ E_{t-1}(\Phi_t) + \beta_1 \left(Q_{t-1} - \bar{Q}^* \circ \Phi_{t-1} \right) + \beta_2 \left(Q_{t-1} - \bar{Q}^* \circ \Phi_{t-1} \right) \\
 &+ \gamma \left(E_{t-1}(I_{z_t < 0} I'_{z_t < 0}) \circ Q_{t-1} - \Xi \circ \bar{Q}^* \circ \Phi_{t-1} \right). \tag{1.46}
 \end{aligned}$$

Given the law of iterated expectation and $E[E_{t-1}(I_{z_t < 0} I'_{z_t < 0})] = \Xi$, the unconditional mean of Q_t can be shown to be time-invariant as below,

$$E[E_{t-1}(Q_t)] = \bar{Q}^* \circ E[\Phi_t] + (\beta_1 \iota + \beta_2 \iota + \gamma \Xi) \circ \left(E[Q_{t-1}] - \bar{Q}^* \circ E[\Phi_{t-1}] \right), \tag{1.47}$$

$$= \bar{Q}^* \circ E[\Phi_t] + (\beta_1 \iota + \beta_2 \iota + \gamma \Xi) \circ \left(E[Q_{t-1}] - \bar{Q}^* \circ E[\Phi_{t-1}] \right), \tag{1.48}$$

where ι is a $N \times N$ matrix of 1s. Given that by construction $E[\Phi_t] = \iota$,

$$E[Q_t] (\iota - \beta_1 \iota - \beta_2 \iota - \gamma \Xi) = \bar{Q}^* \circ E[\Phi_t] (\iota - \beta_1 \iota - \beta_2 \iota - \gamma \Xi), \tag{1.49}$$

$$E[Q_t] = \bar{Q}^*. \tag{1.50}$$

1.C.2 Time-Invariant Variance

$$\begin{aligned}
 Var(Q_t) &= \bar{Q}^* \circ Var(\Phi_t) \circ \bar{Q}^* + \beta_1 \left(\underbrace{Var \left(\tilde{Q}_{t-1}^{\frac{1}{2}} z_t z'_t \tilde{Q}_{t-1}^{\frac{1}{2}} \right)}_{\equiv [A]} - \bar{Q}^* \circ Var(\Phi_{t-1}) \circ \bar{Q}^* \right) \\
 &+ \beta_2 \left(Var(Q_{t-1}) - \bar{Q}^* \circ Var(\Phi_{t-1}) \circ \bar{Q}^* \right) \\
 &+ \gamma \left(\underbrace{Var \left(\tilde{Q}_{t-1}^{\frac{1}{2}} n_t n'_t \tilde{Q}_{t-1}^{\frac{1}{2}} \right)}_{\equiv [B]} - \Xi \circ \bar{Q}^* \circ Var(\Phi_t) \circ \bar{Q}^* \circ \Xi \right), \tag{1.51}
 \end{aligned}$$

where

$$[\mathbf{A}] = \text{Var} \left(\tilde{\mathbf{Q}}_{t-1}^{\frac{1}{2}} \mathbf{z}_t \mathbf{z}'_t \tilde{\mathbf{Q}}_{t-1}^{\frac{1}{2}} \right) = E \left[\text{Var}_{t-1} \left(\tilde{\mathbf{Q}}_{t-1}^{\frac{1}{2}} \mathbf{z}_t \mathbf{z}'_t \tilde{\mathbf{Q}}_{t-1}^{\frac{1}{2}} \right) \right] + \text{Var} \left[E_{t-1} \left(\tilde{\mathbf{Q}}_{t-1}^{\frac{1}{2}} \mathbf{z}_t \mathbf{z}'_t \tilde{\mathbf{Q}}_{t-1}^{\frac{1}{2}} \right) \right], \quad (1.52)$$

$$= E \left[\tilde{\mathbf{Q}}_{t-1} \text{Var}_{t-1} (\mathbf{z}_t \mathbf{z}'_t) \tilde{\mathbf{Q}}_{t-1} \right] + \text{Var} [\mathbf{Q}_{t-1}], \quad (1.53)$$

$$= E \left[\tilde{\mathbf{Q}}_{t-1} \left[\underbrace{E_{t-1} \left[(\mathbf{z}_t \mathbf{z}'_t) (\mathbf{z}_t \mathbf{z}'_t)' \right]}_{(N \times N), \equiv [\mathbf{C1}]} - \underbrace{E_{t-1} (\mathbf{z}_t \mathbf{z}'_t) E'_{t-1} (\mathbf{z}_t \mathbf{z}'_t)}_{(N \times N), \equiv [\mathbf{C2}]} \right] \tilde{\mathbf{Q}}_{t-1} \right] + \text{Var} [\mathbf{Q}_{t-1}], \quad (1.54)$$

$$[\mathbf{B}] = \text{Var} \left(\tilde{\mathbf{Q}}_{t-1}^{\frac{1}{2}} \mathbf{n}_t \mathbf{n}'_t \tilde{\mathbf{Q}}_{t-1}^{\frac{1}{2}} \right) = E \left[\text{Var}_{t-1} \left(\tilde{\mathbf{Q}}_{t-1}^{\frac{1}{2}} \mathbf{n}_t \mathbf{n}'_t \tilde{\mathbf{Q}}_{t-1}^{\frac{1}{2}} \right) \right] + \text{Var} \left[E_{t-1} \left(\tilde{\mathbf{Q}}_{t-1}^{\frac{1}{2}} \mathbf{n}_t \mathbf{n}'_t \tilde{\mathbf{Q}}_{t-1}^{\frac{1}{2}} \right) \right], \quad (1.55)$$

$$= E \left[\tilde{\mathbf{Q}}_{t-1} \text{Var}_{t-1} (\mathbf{n}_t \mathbf{n}'_t) \tilde{\mathbf{Q}}_{t-1} \right] + \text{Var} \left[E_{t-1} (I_{\mathbf{z}_t < 0} I'_{\mathbf{z}_t < 0}) \right] \circ \text{Var} [\mathbf{Q}_{t-1}], \quad (1.56)$$

$$= E \left[\tilde{\mathbf{Q}}_{t-1} \left[\underbrace{E_{t-1} \left[(I_{\mathbf{z}_t < 0} I'_{\mathbf{z}_t < 0}) (I_{\mathbf{z}_t < 0} I'_{\mathbf{z}_t < 0})' \right]}_{(N \times N), \equiv [\mathbf{D1}]} \circ [\mathbf{C1}] - \underbrace{E_{t-1} (I_{\mathbf{z}_t < 0} I'_{\mathbf{z}_t < 0}) E'_{t-1} (I_{\mathbf{z}_t < 0} I'_{\mathbf{z}_t < 0})}_{(N \times N), \equiv [\mathbf{D2}]} \circ [\mathbf{C2}] \right] \tilde{\mathbf{Q}}_{t-1} \right] + \text{Var} \left[E_{t-1} (I_{\mathbf{z}_t < 0} I'_{\mathbf{z}_t < 0}) \right] \circ \text{Var} [\mathbf{Q}_{t-1}]. \quad (1.57)$$

Given that \mathbf{z}_t is assumed to be a stationary vector, higher moments of \mathbf{z}_t is time-invariant; it immediately suggests that the unconditional means of Components $[\mathbf{C1}]$ and $[\mathbf{C2}]$ in the equation above are time-invariant. Given the stationary $\tilde{\mathbf{Q}}_{t-1}$ process as shown earlier, the unconditional mean of products of stationary processes in $[\mathbf{A}]$ are time-invariant. Similar arguments can be applied to $[\mathbf{B}]$.

1.D The Jennrich (1970) Correlation Test

Suppose two N -variate sample correlation matrices, \mathbf{R}_1 ($N \times N$) and \mathbf{R}_2 ($N \times N$) with sample sizes t_1 and t_2 (per variate), the test statistics is, $\chi^2 = \frac{1}{2} \text{tr}(\mathbf{Z}\mathbf{Z}) - \text{diag}(\mathbf{Z})' \mathbf{S}^{-1} \text{diag}(\mathbf{Z})$ where “tr” calculates the matrix trace and “diag” the diagonal terms; \mathbf{Z} ($N \times N$) = $c^{1/2} \bar{\mathbf{R}}^{-1} (\mathbf{R}_1 - \mathbf{R}_2)$ where $c = \frac{t_1 t_2}{t_1 + t_2}$ and $\bar{\mathbf{R}} = (t_1 \mathbf{R}_1 + t_2 \mathbf{R}_2) / (t_1 + t_2)$; \mathbf{S} ($N \times N$) = $\mathbf{I}_N + \bar{\mathbf{R}} \circ \bar{\mathbf{R}}^{-1}$ where \mathbf{I}_N is the identity matrix and “o” denotes the Hadamard product operator (element-by-element). The test statistics (see further details in Jennrich, 1970) has an asymptotic χ^2 distribution with degrees of freedom $N(N-1)/2$.

1.E Review on the Statistical Properties of a Gamma Distribution

For a Gamma random variable, $y \sim \Gamma(s, \theta)$ where s denotes the shape parameter and θ the scale parameter, it has the following PDF,

$$f_Y^{\text{Gamma}}(y; s, \theta) = \frac{1}{\Gamma(s) \theta^s} y^{s-1} \exp\left(-\frac{y}{\theta}\right), \quad (1.58)$$

where $\Gamma(v)$ is a complete Gamma function.

The moment generating function is,

$$M_Y^{Gamma}(t; s, \theta) = (1 - \theta t)^{-s}, \forall t < \frac{1}{\theta}. \quad (1.59)$$

The mean is θs ; the variance is $\theta^2 s$; the unscaled skewness is $2\theta^3 s$.

1.F Solving an International Asset Pricing Model

In the main text (Section 1.3), for simplicity, I assume that there exists a global investor who prices both U.S. and foreign country assets (equities and Treasury bonds), and thus the asset prices are solved from the perspective of this global investor. The advantage of that parsimonious framework is to motivate a global dynamic factor model examined in Section 1.4.

In this appendix section, I acknowledge the exchange rates dynamics and different real pricing kernel of each country. For each country, its domestic investor prices domestic assets where (1) the domestic macro environment and investor risk aversion receive global state variable exposures, and (2) the domestic investor's pricing kernel reflects partial integration. Section 1.6.1 introduces the U.S. state variables and real pricing kernel and solves the U.S. asset prices; Section 1.6.2 discusses the individual country real pricing kernels and state variables as well as model solutions.

The main take-away is that a global dynamic factor model still holds.

1.F.1 The U.S. Asset Market

1.F.1.1 U.S. State Variable Dynamics

1.F.1.1.a Matrix representation

In a matrix representation, the U.S. state vector at time t is denoted as \mathbf{X}_{t+1} (11×1),

$$\begin{bmatrix} \theta_{t+1} & \text{Industrial production growth} \\ \theta u_{t+1} & \text{Real upside uncertainty} \\ \theta d_{t+1} & \text{Real downside uncertainty} \\ \pi_{t+1} & \text{Inflation} \\ \pi u_{t+1} & \text{Nominal upside uncertainty} \\ \pi d_{t+1} & \text{Nominal downside uncertainty} \\ x_{t+1} & \text{Real short rate} \\ x u_{t+1} & \text{Real short rate upside uncertainty} \\ x d_{t+1} & \text{Real short rate downside uncertainty} \\ g_{t+1} & \text{Dividend growth} \\ q_{t+1} & \text{Global risk aversion} \end{bmatrix},$$

which follows this general dynamics:

$$\mathbf{X}_{t+1} = \boldsymbol{\xi}_{\mathbf{X},t} + \text{Jensen's}(\boldsymbol{\delta}_{\mathbf{X}}, \mathbf{S}_t) + \boldsymbol{\delta}_{\mathbf{X}} \boldsymbol{\omega}_{t+1}, \quad (1.60)$$

$$\boldsymbol{\omega}_{t+1} \sim \Gamma(\mathbf{S}_t, \mathbf{1}) - \mathbf{S}_t, \quad (1.61)$$

where $\boldsymbol{\xi}_{\mathbf{X},t}$ (11×1) denotes the conditional mean vector; $\boldsymbol{\omega}_{t+1}$ (8×1) denotes the global state variable shock matrix $[\omega_{\theta u, t+1} \ \omega_{\theta d, t+1} \ \omega_{\pi u, t+1} \ \omega_{\pi d, t+1} \ \omega_{x u, t+1} \ \omega_{x d, t+1} \ \omega_{g, t+1} \ \omega_{q, t+1}]'$ where the shocks are mutually independent; $\boldsymbol{\delta}_{\mathbf{X}}$ (11×8) denotes the constant coefficient matrix to the state variable shocks $\boldsymbol{\omega}_{t+1}$; \mathbf{S}_t (8×1) is the vector of the shock shape parameters $[\theta u_t \ \theta d_t \ \pi u_t \ \pi d_t \ x u_t \ x d_t \ v \ q_t]'$; $\text{Jensen's}(\boldsymbol{\delta}_{\mathbf{X}}, \mathbf{S}_t)$ denotes the Jensen's inequality term

from Gamma distributions; $\Gamma(s, 1)$ denotes the Gamma random variable with a shape parameter s and a scale parameter 1.

The six uncertainty state variables and their shocks are denoted as,

$$\mathbf{U}_t = [\theta u_t \quad \theta d_t \quad \pi u_t \quad \pi d_t \quad x u_t \quad x d_t]' ,$$

$$\boldsymbol{\omega}_{\mathbf{U}, t+1} = [\omega_{\theta u, t+1} \quad \omega_{\theta d, t+1} \quad \omega_{\pi u, t+1} \quad \omega_{\pi d, t+1} \quad \omega_{x u, t+1} \quad \omega_{x d, t+1}]' .$$

1.F.1.1.b Output growth and uncertainties

I follow Bekaert, Engstrom, and Xu (2017) to model industrial production growth innovation with two centered independent gamma shocks where each shock has a time-varying shape parameter that governs the higher moments of the shock. I name the shape parameter that governs the right-tail (left-tail) skewness the real upside (downside) uncertainty, θu (θd).¹⁵ Formally, θ_{t+1} has the following process,

$$\theta_{t+1} = \bar{\theta} + \rho_{\theta\theta}(\theta_t - \bar{\theta}) + \rho_{\theta\theta u}(\theta u_t - \bar{\theta}u) + \rho_{\theta\theta d}(\theta d_t - \bar{\theta}d) + u_{t+1}^\theta, \quad (1.62)$$

where the growth shock is decomposed into two independent shocks,

$$u_{t+1}^\theta = \delta_{\theta\theta u}\omega_{\theta u, t+1} - \delta_{\theta\theta d}\omega_{\theta d, t+1}. \quad (1.63)$$

The shocks follow centered Gamma distributions with time-varying shape parameters,

$$\omega_{\theta u, t+1} \sim \tilde{\Gamma}(\theta u_t, 1) \quad (1.64)$$

$$\omega_{\theta d, t+1} \sim \tilde{\Gamma}(\theta d_t, 1), \quad (1.65)$$

where $\tilde{\Gamma}(y, 1)$ denotes a centered Gamma-distributed random variable with shape parameter y and a unit scale parameter. The shape factors, θu_t and θd_t , follow autoregressive processes,

$$\theta u_{t+1} = \bar{\theta}u + \rho_{\theta u}(\theta u_t - \bar{\theta}u) + \delta_{\theta u}\omega_{\theta u, t+1} \quad (1.66)$$

$$\theta d_{t+1} = \bar{\theta}d + \rho_{\theta d}(\theta d_t - \bar{\theta}d) + \delta_{\theta d}\omega_{\theta d, t+1}, \quad (1.67)$$

where ρ_y denotes the autoregressive term of process y_{t+1} , δ_y the sensitivity to $\omega_{y, t+1}$, and \bar{y} the constant long-run mean. Given that Gamma distributions are right-skewed by design, the growth shock with a negative loading on $\omega_{\theta d, t+1}$ models the left-tail events; hence, $\omega_{\theta d, t+1}$ is interpreted as the downside uncertainty shocks, and θd_t the real downside uncertainty.

State variables: $\{\theta, \theta u, \theta d\}$.

State variable shocks: $\{\omega_{\theta u}, \omega_{\theta d}\}$.

1.F.1.1.c Inflation and uncertainties

Inflation process receives contemporaneous shocks from the real side. Denote π_{t+1} as the change in the log consumer price index for all urban consumers, πu_t the nominal upside uncertainty and πd_t the nominal downside uncertainty. The inflation system follows this reduced-form dynamics,

$$\pi_{t+1} = \bar{\pi} + \rho_{\pi\theta}(\theta_t - \bar{\theta}) + \rho_{\pi\theta u}(\theta u_t - \bar{\theta}u) + \rho_{\pi\theta d}(\theta d_t - \bar{\theta}d) + \rho_{\pi\pi}(\pi_t - \bar{\pi}) + \rho_{\pi\pi u}(\pi u_t - \bar{\pi}u) + \rho_{\pi\pi d}(\pi d_t - \bar{\pi}d) + u_{t+1}^\pi, \quad (1.68)$$

where the inflation disturbance is sensitive to the two real uncertainty shocks, and the residual is decomposed into two nominal uncertainty shocks that are mutually independent of one another,

$$u_{t+1}^\pi = (\delta_{\pi\theta u}\omega_{\theta u, t+1} + \delta_{\pi\theta d}\omega_{\theta d, t+1}) + (\delta_{\pi\pi u}\omega_{\pi u, t+1} - \delta_{\pi\pi d}\omega_{\pi d, t+1}). \quad (1.69)$$

¹⁵Note that Bekaert, Engstrom, and Xu (2017) name them ‘‘good’’ and ‘‘bad’’ uncertainties to assign economic meanings of real uncertainties, whereas my notation here is more general and consistent as, for example, inflation upside uncertainty (later) is not typically considered as ‘‘good’’ uncertainty.

The shocks follow centered Gamma distributions with time-varying shape parameters,

$$\omega_{\pi u, t+1} \sim \tilde{\Gamma}(\pi u_t, 1) \quad (1.70)$$

$$\omega_{\pi d, t+1} \sim \tilde{\Gamma}(\pi d_t, 1), \quad (1.71)$$

$$\pi u_{t+1} = \bar{\pi u} + \rho_{\pi u}(\pi u_t - \bar{\pi u}) + \delta_{\pi u} \omega_{\pi u, t+1} \quad (1.72)$$

$$\pi d_{t+1} = \bar{\pi d} + \rho_{\pi d}(\pi d_t - \bar{\pi d}) + \delta_{\pi d} \omega_{\pi d, t+1}. \quad (1.73)$$

Importantly, the theoretical structural representation of the inflation dynamics above is,

$$\pi_{t+1} = \xi_{\pi, t} + [\boldsymbol{\delta}_{\pi} - \ln(\mathbf{1} + \boldsymbol{\delta}_{\pi})] \mathbf{S}_t + \boldsymbol{\delta}_{\pi} \boldsymbol{\omega}_{t+1}, \quad (1.74)$$

where $\boldsymbol{\delta}_{\pi} = [\delta_{\pi\theta u} \ \delta_{\pi\theta d} \ \delta_{\pi\pi u} \ -\delta_{\pi\pi d} \ 0 \ 0 \ 0 \ 0]$ so that the relevant shocks are $\omega_{\theta u, t+1}$, $\omega_{\theta d, t+1}$, $\omega_{\pi u, t+1}$, and $\omega_{\pi d, t+1}$. The signs of the the innovation loadings on the two real uncertainty shocks, $\omega_{\theta u, t+1}$ and $\omega_{\theta d, t+1}$, are not restricted in the model, whereas $\delta_{\pi\pi u}$ and $\delta_{\pi\pi d}$ are assumed to be positive.

State variables: $\{\pi, \pi u, \pi d\}$.

State variable shocks: $\{\omega_{\pi u}, \omega_{\pi d}\}$.

1.F.1.1.d Risk aversion

Denote q_t as the time-varying risk aversion variable,¹⁶

$$\begin{aligned} q_{t+1} = & \bar{q} + \rho_{q\theta}(\theta_t - \bar{\theta}) + \rho_{q\theta u}(\theta u_t - \bar{\theta u}) + \rho_{q\theta d}(\theta d_t - \bar{\theta d}) \\ & + \rho_{q\pi}(\pi_t - \bar{\pi}) + \rho_{q\pi u}(\pi u_t - \bar{\pi u}) + \rho_{q\pi d}(\pi d_t - \bar{\pi d}) + \rho_{qq}(q_t - \bar{q}) + u_{t+1}^q, \end{aligned} \quad (1.75)$$

where the risk aversion shock is sensitive to the real and nominal uncertainty shocks, the short rate shock and a risk aversion-specific heteroskedastic shock,

$$u_{t+1}^q = (\delta_{q\theta u} \omega_{\theta u, t+1} + \delta_{q\theta d} \omega_{\theta d, t+1}) + (\delta_{q\pi u} \omega_{\pi u, t+1} + \delta_{q\pi d} \omega_{\pi d, t+1}) + \delta_{qq} \omega_{q, t+1}, \quad (1.76)$$

where the risk aversion-specific shock follows a centered heteroskedastic Gamma distribution,

$$\omega_{q, t+1} \sim \tilde{\Gamma}(q_t, 1). \quad (1.77)$$

State variables: $\{q\}$.

State variable shocks: $\{\omega_q\}$.

1.F.1.1.e Real short rate and uncertainties

Denote x_t as the latent real short rate,

$$\begin{aligned} x_{t+1} = & \bar{x} + \rho_{x\theta}(\theta_t - \bar{\theta}) + \rho_{x\theta u}(\theta u_t - \bar{\theta u}) + \rho_{x\theta d}(\theta d_t - \bar{\theta d}) \\ & + \rho_{x\pi}(\pi_t - \bar{\pi}) + \rho_{x\pi u}(\pi u_t - \bar{\pi u}) + \rho_{x\pi d}(\pi d_t - \bar{\pi d}) \\ & + \rho_{xx}(x_t - \bar{x}) + \rho_{xxu}(x u_t - \bar{x u}) + \rho_{xxd}(x d_t - \bar{x d}) + \rho_{xq}(q_t - \bar{q}) + u_{t+1}^x, \end{aligned} \quad (1.78)$$

where the short rate shock is sensitive to the real and nominal uncertainty shocks as well as a short rate-specific homoskedastic shock,

$$u_{t+1}^x = (\delta_{x\theta u} \omega_{\theta u, t+1} + \delta_{x\theta d} \omega_{\theta d, t+1}) + (\delta_{x\pi u} \omega_{\pi u, t+1} + \delta_{x\pi d} \omega_{\pi d, t+1}) + \delta_{xq} \omega_{q, t+1} + \delta_{xxu} \omega_{xu, t+1} - \delta_{xxd} \omega_{xd, t+1}, \quad (1.79)$$

where the (exogenous) short rate shocks follow centered Gamma distributions with time-varying shape parameters,

$$\omega_{xu, t+1} \sim \tilde{\Gamma}(x u_t, 1), \quad x u_{t+1} = \bar{x u} + \rho_{xu}(x u_t - \bar{x u}) + \delta_{xu} \omega_{xu, t+1}, \quad (1.80)$$

$$\omega_{xd, t+1} \sim \tilde{\Gamma}(x d_t, 1), \quad x d_{t+1} = \bar{x d} + \rho_{xd}(x d_t - \bar{x d}) + \delta_{xd} \omega_{xd, t+1}. \quad (1.81)$$

State variables: $\{x, x u, x d\}$.

¹⁶It is a risk aversion variable, because the exact definition is risk aversion (motivated from a HARA utility is $\gamma \exp(q_t)$).

State variable shocks: $\{\omega_{xu}, \omega_{xd}\}$.

1.F.1.1.f Real dividend growth

Denote g_t as the change in log real dividend per share,

$$g_{t+1} = \bar{g} + \rho_{g\theta}(\theta_t - \bar{\theta}) + \rho_{g\theta u}(\theta u_t - \bar{\theta}u) + \rho_{g\theta d}(\theta d_t - \bar{\theta}d) + \rho_{gg}(g_t - \bar{g}) + u_{t+1}^g, \quad (1.82)$$

where the dividend growth shock is sensitive to the real and nominal uncertainty shocks as well as a dividend-specific homoskedastic shock,

$$u_{t+1}^g = (\delta_{g\theta u}\omega_{\theta u,t+1} + \delta_{g\theta d}\omega_{\theta d,t+1}) + \delta_{gg}\omega_{g,t+1}, \quad (1.83)$$

where the sign of δ_{gg} is not restricted, and the dividend-specific shock is assumed to follow a homoskedastic Gamma distribution,

$$\omega_{g,t+1} \sim \tilde{\Gamma}(v, 1). \quad (1.84)$$

Importantly, the theoretical structural representation of the real growth dynamics above is,

$$g_{t+1} = \xi_{g,t} + [\boldsymbol{\delta}_g + \ln(\mathbf{1} - \boldsymbol{\delta}_g)]\mathbf{S}_t + \boldsymbol{\delta}_g\boldsymbol{\omega}_{t+1}, \quad (1.85)$$

where $\boldsymbol{\delta}_g = [\delta_{g\theta u} \ \delta_{g\theta d} \ 0 \ 0 \ 0 \ 0 \ \delta_{gg} \ 0]$ so that the relevant shocks are $\omega_{\theta u,t+1}$, $\omega_{\theta d,t+1}$, and $\omega_{g,t+1}$.

State variables: $\{g\}$.

State variable shocks: $\{\omega_g\}$.

1.F.1.2 U.S. Real Pricing Kernel

I specify the (minus) logarithm of the real global pricing kernel to be affine to the global state variable levels and shocks,

$$-m_{t+1} = x_t + [\boldsymbol{\delta}_m - \ln(\mathbf{1} + \boldsymbol{\delta}_m)]\mathbf{S}_t + \boldsymbol{\delta}_m\boldsymbol{\omega}_{t+1}, \quad (1.86)$$

where the drift x_t is the real short rate, $\boldsymbol{\delta}_m$ (1×8) prices of risks, $\boldsymbol{\omega}_{t+1}$ (8×1) the state variable shock matrix defined earlier, and $[\boldsymbol{\delta}_m - \ln(\mathbf{1} + \boldsymbol{\delta}_m)]\mathbf{S}_t$ the Jensen's inequality term given the Gamma distributional assumptions.

The real global pricing kernel is spanned by five global shocks: the real upside and downside uncertainty shocks ($\omega_{\theta u}$ and $\omega_{\theta d}$), the inflation upside and downside uncertainty shocks ($\omega_{\pi u}$ and $\omega_{\pi d}$), and the risk aversion shock (ω_q). First, the two real-side uncertainty shock and the risk aversion shock span the pricing kernel, which can be motivated in Campbell and Cochrane (1999) and Bekaert, Engstrom, and Xu (2017). Second, the two inflation uncertainty shocks span the real pricing kernel, which is to induce the inflation risk premium.

1.F.1.3 U.S. Asset Prices and Risk Premiums

1.F.1.3.a Nominal Treasury Bonds

The real global short rate ($y_{t,1} = -\ln\{[E_t[\exp(m_{t+1})]]\}$) and the nominal global short rate ($\tilde{y}_{t,1} = -\ln\{[E_t[\exp(m_{t+1} - \pi_{t+1})]]\}$) are solved in closed forms,

$$y_{t,1} = x_t, \quad (1.87)$$

$$\tilde{y}_{t,1} = x_t + \underbrace{\xi_{\pi,t} + \ln[(\mathbf{1} + \boldsymbol{\delta}_m + \boldsymbol{\delta}_\pi) \circ (\mathbf{1} + \boldsymbol{\delta}_m)^{\circ-1} \circ (\mathbf{1} + \boldsymbol{\delta}_\pi)^{\circ-1}]}_{\text{inflation compensation}}\mathbf{S}_t, \quad (1.88)$$

¹⁷ where “ $\ln(\cdot)$ ” is the element-wise logarithm operator, “ \circ ” the Hadamard product of two identically sized matrices (or element-by-element matrix multiplication), and “ $(\cdot)^{\circ-1}$ ” the Hadamard inverse. The three components in nominal short rate are the real short rate (x_t), the expected inflation rate ($\xi_{\pi,t}$), and the inflation risk premium to compensate investors for bearing the inflation risk associated with the nominal bonds. It is noteworthy that the linear approximation of the inflation risk premium, $\ln[(\mathbf{1} + \boldsymbol{\delta}_m + \boldsymbol{\delta}_\pi) \circ (\mathbf{1} + \boldsymbol{\delta}_m)^{\circ-1} \circ (\mathbf{1} + \boldsymbol{\delta}_\pi)^{\circ-1}]$, is $-(\boldsymbol{\delta}_m \circ \boldsymbol{\delta}_\pi) \mathbf{S}_t$, or $Cov_t(m_{t+1}, \pi_{t+1})$ as derived in the Gaussian-augmented nominal term structure literature (see, e.g., Campbell, Sunderam, and Viceira, 2017).

The price of the n -period zero-coupon nominal bond ($\tilde{P}_{t,n}^b$) can be then solved recursively in exact closed forms, and is an exponential affine function of a set of time-varying state variables.

$$\tilde{P}_{t,n}^b = E_t \left[\exp \left(\tilde{p}_{t+1,n-1}^b + m_{t+1} - \pi_{t+1} \right) \right] \quad (1.89)$$

$$= E_t \left[\exp \left(x_{t+1} + \xi_{\pi,t+1} + \ln \left[(\mathbf{1} + \boldsymbol{\delta}_m + \boldsymbol{\delta}_\pi) \circ (\mathbf{1} + \boldsymbol{\delta}_m)^{\circ-1} \circ (\mathbf{1} + \boldsymbol{\delta}_\pi)^{\circ-1} \right] \mathbf{S}_{t+1} + m_{t+1} - \pi_{t+1} \right) \right] \quad (1.90)$$

$$= \exp \left(\mathbf{A}_{0,n} + \mathbf{A}_{1,n} \mathbf{X}_t \right), \quad (1.91)$$

where $\mathbf{A}_{0,n}$, $\mathbf{A}_{1,n}$ are constant scalars or matrices.

The log return of the global nominal n -period zero-coupon bonds from t to $t + 1$ can be expressed as follows,

$$\begin{aligned} \tilde{r}_{t+1,n}^b &\equiv \ln \left(\frac{\tilde{P}_{t+1,n-1}^b}{\tilde{P}_{t,n}^b} \right), \\ &= \Omega_{0,n}^b + \Omega_{1,n}^b \mathbf{X}_t + \Omega_{2,n}^b \boldsymbol{\omega}_{t+1} + \left[\Omega_{2,n}^b + \ln \left(1 - \Omega_{2,n}^b \right) \mathbf{S}_t \right] + \epsilon_{t+1,n}^b, \end{aligned} \quad (1.92)$$

where $\epsilon_{t+1,n}^b \sim N(0, \sigma_b^2)$ is a homoskedastic Gaussian shock to potentially capture approximation error.

1.F.1.3.b Bond Risk Premium

Given the no-arbitrage condition, $E_t[\exp(\tilde{m}_{t+1} + \tilde{r}_{t+1,n}^b)] = 1$, the global bond risk premium (ignoring the Jensen’s inequality terms) has a closed-form solution,

$$E_t[\tilde{r}_{t+1,n}^b] - \tilde{y}_{t,1} + \frac{1}{2} \sigma_b^2 = \ln \left[(\mathbf{1} + \boldsymbol{\delta}_m + \boldsymbol{\delta}_\pi - \Omega_{2,n}^b) \circ (\mathbf{1} + \boldsymbol{\delta}_m + \boldsymbol{\delta}_\pi)^{\circ-1} \circ (\mathbf{1} - \Omega_{2,n}^b)^{\circ-1} \right] \mathbf{S}_t, \quad (1.93)$$

¹⁸ which in a quadratic Gaussian approximation has the following expression,

$$\approx \left[(\boldsymbol{\delta}_m + \boldsymbol{\delta}_\pi) \circ \Omega_{2,n}^b \right] \mathbf{S}_t = -Cov_t(\tilde{m}_{t+1}, \tilde{r}_{t+1,n}^b). \quad (1.94)$$

¹⁹ where $\boldsymbol{\delta}_m$ is the SDF loading on the four global uncertainty shocks subject to the time-varying global risk aversion as discussed in Section 1.6.1.2, and $\boldsymbol{\delta}_\pi$ is the inflation rate loading on the four global uncertainty shocks as discussed in Section 1.6.1.1.

¹⁷In this paper, $\tilde{(\cdot)}$ denotes nominal variables.

¹⁸Note that, the non-linearity is due to the non-linearities in the moment generating function of gamma shocks.

¹⁹The quadratic Taylor approximation for “ $y - \ln(1 + y)$ ” is $\frac{1}{2}y^2$.

1.F.1.3.c Equities

Bekaert, Engstrom, and Xu (2017) show that log equity returns is quasi-affine to the state variable levels and shocks as below,

$$\tilde{r}_{t+1}^e \equiv \ln \left(\frac{PD_{t+1} + 1}{PD_t} \frac{\tilde{D}_{t+1}}{\tilde{D}_t} \right), \quad (1.95)$$

$$= \Omega_0^e + \mathbf{\Omega}_1^e \mathbf{X}_t + \mathbf{\Omega}_2^e \boldsymbol{\omega}_{t+1} + [\mathbf{\Omega}_2^e + \ln(1 - \mathbf{\Omega}_2^e) \mathbf{S}_t] + \epsilon_{t+1}^e, \quad (1.96)$$

where $\epsilon_{t+1}^e \sim N(0, \sigma_e^2)$ is a homoskedastic Gaussian shock to potentially capture approximation error.

1.F.1.3.d Equity Risk Premium

Given the no-arbitrage condition, $E_t[\exp(\tilde{m}_{t+1} + \tilde{r}_{t+1}^e)] = 1$, the global equity risk premium has a closed-form solution using the return process,

$$E_t[\tilde{r}_{t+1}^e] - \tilde{y}_{t,1} + \frac{1}{2}\sigma_e^2 = \ln[(1 + \boldsymbol{\delta}_m + \boldsymbol{\delta}_\pi - \mathbf{\Omega}_2^e) \circ (1 + \boldsymbol{\delta}_m + \boldsymbol{\delta}_\pi)^{\circ-1} \circ (1 - \mathbf{\Omega}_2^e)^{\circ-1}] \mathbf{S}_t, \quad (1.97)$$

$$\approx [(\boldsymbol{\delta}_m + \boldsymbol{\delta}_\pi) \circ \mathbf{\Omega}_2^e] \mathbf{S}_t = -Cov_t(\tilde{m}_{t+1}, \tilde{r}_{t+1}^e). \quad (1.98)$$

1.F.1.3.e Variances

The physical variance for Asset $a \in \{b, e\}$,

$$V_t^{a,P} \equiv E_t \left[(\tilde{r}_{t+1}^a - E_t(\tilde{r}_{t+1}^a))^2 \right], \quad (1.99)$$

$$= \mathbf{\Omega}_2^a \mathbf{S}_t \mathbf{\Omega}_2^{a'} + \sigma_a^2, \quad (1.100)$$

where the parameter matrices are discussed in Equations (1.92) and (1.95).

The risk-neutral variance for Asset $a \in \{b, e\}$,

$$V_t^{a,Q} \equiv E_t^Q \left[(\tilde{r}_{t+1}^a - E_t(\tilde{r}_{t+1}^a))^2 \right] \quad (1.101)$$

$$= \frac{\partial^2 mgf_t^Q(\tilde{r}_{t+1}^a; \nu)}{\partial \nu^2} \Big|_{\nu=0} - \left(\frac{\partial mgf_t^Q(\tilde{r}_{t+1}^a; \nu)}{\partial \nu} \Big|_{\nu=0} \right)^2 \quad (1.102)$$

$$= \left[\mathbf{\Omega}_2^a \circ (\mathbf{1} + \boldsymbol{\delta}_m + \boldsymbol{\delta}_\pi)^{\circ-1} \right] \mathbf{S}_t \left[\mathbf{\Omega}_2^a \circ (\mathbf{1} + \boldsymbol{\delta}_m + \boldsymbol{\delta}_\pi)^{\circ-1} \right]' + \sigma_a^2, \quad (1.103)$$

where the moment generating function is $mgf_t^Q(\tilde{r}_{t+1}^a; \nu) = \frac{E_t[\exp(\tilde{m}_{t+1} + \nu \tilde{r}_{t+1}^a)]}{E_t[\exp(\tilde{m}_{t+1})]}$. “ \circ ” is the Hadamard product of two identically sized matrices (or element-by-element matrix multiplication), and “ $(\cdot)^{\circ-1}$ ” is the Hadamard inverse. $\mathbf{\Omega}_2^a$ is the asset return loading vector on the common shocks, or an “amount-of-risk” loading vector; $(\boldsymbol{\delta}_m + \boldsymbol{\delta}_\pi)$ represents the nominal pricing kernel loading vector on the common shocks, or a “price-of-risk” loading vector. Intuitively, a positive downside uncertainty shock is perceived as bad news, driving up the intertemporal marginal rates of substitution; the sensitivity of the pricing kernel on the downside uncertainty shock is expected to be higher (positive) than that on the upside uncertainty shock, or $\delta_{m\theta d,t}$ in the minus m_{t+1} expression is smaller than 0 and less than $\delta_{m\theta u,t}$.

1.F.1.3.f Variances as Assets: Variance Risk Premium

Hence, the solutions of variances in closed form imply a premium of $V_t^{a,Q}$ over $V_t^{a,P}$. For asset $a \in \{b, e\}$,

$$\begin{aligned} VRP_t^a &= V_t^{a,Q} - V_t^{a,P} \\ &= \left[\Omega_2^a \circ (\mathbf{1} + \delta_m + \delta_\pi)^{\circ-1} \right] \mathbf{S}_t \left[\Omega_2^a \circ (\mathbf{1} + \delta_m + \delta_\pi)^{\circ-1} \right]' - \Omega_2^a \mathbf{S}_t \Omega_2^{a'}. \end{aligned} \quad (1.104)$$

1.F.2 Other Asset Markets

This world economy is partially integrated. Each market is complete. Each country-level state variable has a global component with constant exposures to the global levels and shocks and an idiosyncratic component. Idiosyncratic shocks are uncorrelated across countries. Under the no-arbitrage assumption, there exists closed-form solutions for country equity and bond prices.

1.F.2.1 Local State Variables: Matrix representation

In a matrix representation, the regional state vector denoted as \mathbf{X}_{t+1}^i (11×1),

$$\left[\theta_{t+1}^i \quad \theta u_{t+1}^i \quad \theta d_{t+1}^i \quad \pi_{t+1}^i \quad \pi u_{t+1}^i \quad \pi d_{t+1}^i \quad x_{t+1}^i \quad x u_{t+1}^i \quad x d_{t+1}^i \quad g_{t+1}^i \quad q_{t+1}^i \right]',$$

follows this general dynamics:

$$\begin{aligned} \mathbf{X}_{t+1}^i &= \alpha_{\mathbf{X}}^i \circ \boldsymbol{\xi}_{\mathbf{X},t} + (\mathbf{1} - \alpha_{\mathbf{X}}^i) \circ \boldsymbol{\xi}_{\mathbf{X},t} + \underbrace{\text{Jensen's } \left(\alpha_{\mathbf{X}}^i \circ \boldsymbol{\delta}_{\mathbf{X}}^i, \mathbf{S}_t \right) + \text{Jensen's } \left((\mathbf{1} - \alpha_{\mathbf{X}}^i) \circ \mathbf{X}_{\omega}^i, \mathbf{S}_t^i \right)}_{\text{Jensen's inequality terms}} \\ &\quad + \left(\alpha_{\mathbf{X}}^i \circ \boldsymbol{\delta}_{\mathbf{X}}^i \right) \boldsymbol{\omega}_{t+1} + \left((\mathbf{1} - \alpha_{\mathbf{X}}^i) \circ \mathbf{X}_{\omega}^i \right) \boldsymbol{\omega}_{t+1}^i, \end{aligned} \quad (1.105)$$

$$\boldsymbol{\omega}_{t+1}^i \sim \Gamma(\mathbf{S}_t^i, \mathbf{1}) - \mathbf{S}_t^i, \quad (1.106)$$

where $\boldsymbol{\xi}_{\mathbf{X},t}$ (11×1) denotes the conditional mean vector of the global state variables \mathbf{X}_{t+1} in Section 1.6.1.1, $\boldsymbol{\omega}_{t+1}$ (9×1) the global state variable shock matrix, $\boldsymbol{\delta}_{\mathbf{X}}^i$ (11×9) the constant local coefficient vector to the global state variable shocks $\boldsymbol{\omega}_{t+1}$ (which are not constraint to be the same with global state variable loadings on global shocks $\boldsymbol{\delta}_{\mathbf{X}}$), \mathbf{S}_t (9×1) the time-varying shape parameters of global shocks, and $\Upsilon(\alpha_{\mathbf{X}}^i \circ \boldsymbol{\delta}_{\mathbf{X}}^i, \mathbf{S}_t)$ is the Jensen's inequality term from Gamma distributions. The local counterparts are defined as follows. $\boldsymbol{\xi}_{\mathbf{X},t}^i$ (11×1) denotes the local component of the conditional mean vector of the regional state variables, $\boldsymbol{\omega}_{t+1}^i$ (11×1) the local state variable shock matrix,

$$\left[\omega_{\theta u, t+1}^i \quad \omega_{\theta d, t+1}^i \quad \omega_{\pi u, t+1}^i \quad \omega_{\pi d, t+1}^i \quad \omega_{x, t+1}^i \quad \omega_{x u, t+1}^i \quad \omega_{x d, t+1}^i \quad \omega_{g, t+1}^i \quad \omega_{q, t+1}^i \right]',$$

\mathbf{X}_{ω}^i (11×9) the constant coefficient vector to the local state variable shocks $\boldsymbol{\omega}_{t+1}^i$, \mathbf{S}_t^i (9×1) the time-varying shape parameters of local shocks,

$$\left[\theta u_t^i \quad \theta d_t^i \quad \pi u_t^i \quad \pi d_t^i \quad x u_t^i \quad x d_t^i \quad v^i \quad q_t^i \right]'$$

Most important, $\alpha_{\mathbf{X}}^i$ (11×1) captures the constant global exposures.

The shock structures of each local state variables follow the global counterparts to ensure local shocks are also mutually independent from each other.

1.F.2.2 Local Real Pricing Kernel

I specify the logarithm of the local real local pricing kernel to be affine to the global and local state variable levels and shocks,

$$-m_{t+1}^i = \alpha_m^i \left(x_t + \delta_m^i \omega_{t+1} \right) + (1 - \alpha_m^i) \left(x_t^i + m_\omega^i \omega_{t+1}^i \right) + \underbrace{\left[\alpha_m^i \delta_m^i - \ln \left(1 + \alpha_m^i \delta_m^i \right) \right] \mathbf{S}_t + \left[(1 - \alpha_m^i) m_\omega^i - \ln \left(1 + (1 - \alpha_m^i) m_\omega^i \right) \right] \mathbf{S}_t^i}_{\text{Jensen's Inequality Terms}} \quad (1.107)$$

where ω_{t+1} (9×1) and ω_{t+1}^i (9×1) are the global and local state variable shock matrix defined earlier. δ_m^i (1×9) denotes a vector of constant sensitivities to global shocks. Similarly, m_ω^i (1×7) denotes a vector of constant sensitivities to local shocks.

The drift term, $\alpha_m^i x_t + (1 - \alpha_m^i) x_t^i$, is the real regional short rate.

1.F.2.3 Local Asset Prices and Risk Premiums

1.F.2.3.a Nominal Treasury Bonds

The real local short rate ($y_{t,1}^i = -\ln\{[E_t[\exp(m_{t+1}^i)]]\}$) and the nominal regional short rate ($\tilde{y}_{t,1}^i = -\ln\{[E_t[\exp(m_{t+1}^i - \pi_{t+1}^i)]]\}$) are solved in closed forms,

$$\begin{aligned} y_{t,1}^i &= \alpha_m^i x_t + (1 - \alpha_m^i) x_t^i, \\ \tilde{y}_{t,1}^i &= \alpha_m^i x_t + \alpha_\pi^i \xi_{\pi,t} + (1 - \alpha_m^i) x_t^i + (1 - \alpha_\pi^i) \xi_{\pi,t}^i \\ &+ \ln \left[\left(1 + \alpha_m^i \delta_m^i + \alpha_\pi^i \delta_\pi^i \right) \circ \left(1 + \alpha_m^i \delta_m^i \right)^{\circ-1} \circ \left(1 + \alpha_\pi^i \delta_\pi^i \right)^{\circ-1} \right] \mathbf{S}_t \\ &+ \ln \left[\left(1 + (1 - \alpha_m^i) m_\omega^i + (1 - \alpha_\pi^i) \pi_\omega^i \right) \circ \left(1 + (1 - \alpha_m^i) m_\omega^i \right)^{\circ-1} \circ \left(1 + (1 - \alpha_\pi^i) \pi_\omega^i \right)^{\circ-1} \right] \mathbf{S}_t^i. \end{aligned} \quad (1.108)$$

where “ $\ln(\cdot)$ ” is the element-wise logarithm operator, “ \circ ” is the Hadamard product of two identically sized matrices (or element-by-element matrix multiplication), and “ $(\cdot)^{\circ-1}$ ” is the Hadamard inverse. The three components in nominal short rate represent the real short rate ($\alpha_m^i x_t + (1 - \alpha_m^i) x_t^i$), the expected inflation rate ($\alpha_\pi^i \xi_{\pi,t} + (1 - \alpha_\pi^i) \xi_{\pi,t}^i$), and the inflation risk premium (+ Jensen’s inequality term).

The price of n -period zero-coupon nominal bond ($\tilde{P}_{t,n}^{b,i}$) can be then solved recursively in exact closed forms, given the shock specifications. The nominal local bond return from t to $t+1$ can be approximately expressed as follows,

$$\tilde{r}_{t+1,n}^{b,i} \equiv \ln \left(\frac{\tilde{P}_{t+1,n-1}^{b,i}}{\tilde{P}_{t,n}^{b,i}} \right), \quad (1.110)$$

$$\begin{aligned} &= \Omega_{0,n}^{b,i} + \Omega_{1,n}^{b,i} \mathbf{X}_t + \Omega_{2,n}^{b,i} \omega_{t+1} + \left[\Omega_{2,n}^{b,i} + \ln \left(1 - \Omega_{2,n}^{b,i} \right) \right] \mathbf{S}_t \\ &+ \Omega_{3,n}^{b,i} \mathbf{X}_t^i + \Omega_{4,n}^{b,i} \omega_{t+1}^i + \left[\Omega_{4,n}^{b,i} + \ln \left(1 - \Omega_{4,n}^{b,i} \right) \right] \mathbf{S}_t^i + \epsilon_{t+1}^{b,i}, \end{aligned} \quad (1.111)$$

where $\epsilon_{t+1}^{b,i}$ is a homoskedastic Gaussian shock with volatility σ_b^i to capture approximation error.

1.F.2.3.b Bond Risk Premium

Given the no-arbitrage condition, $E_t[\exp(\tilde{m}_{t+1}^i + \tilde{r}_{t+1,n}^{b,i})] = 1$ where $\tilde{r}_{t+1,n}^{b,i}$ is the nominal bond return, the regional bond risk premium has a closed-form solution,

$$\begin{aligned}
E_t[\tilde{r}_{t+1,n}^{b,i}] - \tilde{y}_{t,1}^i + \frac{1}{2}\sigma_b^{i2} &= \ln \left[\underbrace{\left(1 + \alpha_m^i \delta_m + \alpha_\pi^i \delta_\pi - \Omega_{2,n}^{b,i}\right) \circ \left(1 + \alpha_m^i \delta_m + \alpha_\pi^i \delta_\pi\right)^{\circ-1} \circ \left(1 - \Omega_{2,n}^{b,i}\right)^{\circ-1}}_{(1) \text{ compensation for global risk exposure}} \right] \mathbf{S}_t \\
&+ \ln \left[\underbrace{\left(1 + (1 - \alpha_m^i) \mathbf{m}_\omega^i + (1 - \alpha_\pi^i) \boldsymbol{\pi}_\omega^i - \Omega_{4,n}^{b,i}\right) \circ \left(1 + (1 - \alpha_m^i) \mathbf{m}_\omega^i + (1 - \alpha_\pi^i) \boldsymbol{\pi}_\omega^i\right)^{\circ-1} \circ \left(1 - \Omega_{4,n}^{b,i}\right)^{\circ-1}}_{(2) \text{ compensation for regional risk exposure}} \right] \mathbf{S}_t^i,
\end{aligned} \tag{1.112}$$

²⁰ which in a quadratic Gaussian approximation has the following expression,

$$\begin{aligned}
&\approx \underbrace{\left(\alpha_m^i \delta_m + \alpha_\pi^i \delta_\pi\right) \circ \Omega_{2,n}^{b,i} \mathbf{S}_t}_{\approx(1)} + \underbrace{\left[(1 - \alpha_m^i) \mathbf{m}_\omega^i + (1 - \alpha_\pi^i) \boldsymbol{\pi}_\omega^i\right] \circ \Omega_{4,n}^{b,i} \mathbf{S}_t^i}_{\approx(2)} = -Cov_t(\tilde{m}_{t+1}^i, \tilde{r}_{t+1,n}^{b,i}).
\end{aligned} \tag{1.113}$$

21

1.F.2.3.c Equities

The nominal local equity return from t to $t + 1$ can be approximately expressed as follows,

$$\tilde{r}_{t+1}^{e,i} \equiv \ln \left(\frac{\tilde{P}_{t+1,n-1}^{e,i}}{\tilde{P}_t^{e,i}} \right), \tag{1.114}$$

$$\begin{aligned}
&= \Omega_0^{e,i} + \Omega_1^{e,i} \mathbf{X}_t + \Omega_2^{e,i} \boldsymbol{\omega}_{t+1} + \left[\Omega_2^{b,i} + \ln \left(1 - \Omega_2^{b,i}\right) \mathbf{S}_t \right] \\
&+ \Omega_3^{e,i} \mathbf{X}_t^i + \Omega_4^{e,i} \boldsymbol{\omega}_{t+1}^i + \left[\Omega_4^{b,i} + \ln \left(1 - \Omega_4^{b,i}\right) \mathbf{S}_t^i \right] + \epsilon_{t+1}^{e,i}.
\end{aligned} \tag{1.115}$$

where $\epsilon_{t+1}^{e,i}$ is a homoskedastic Gaussian shock with volatility σ_e^i to capture approximation error.

1.F.2.3.d Equity Risk Premium

Given the no-arbitrage condition, $E_t[\exp(\tilde{m}_{t+1}^i + \tilde{r}_{t+1}^{e,i})] = 1$ where $\tilde{r}_{t+1}^{e,i}$ is the nominal equity return, the regional equity risk premium has a closed-form solution,

$$\begin{aligned}
E_t[\tilde{r}_{t+1}^{e,i}] - \tilde{y}_{t,1}^i + \frac{1}{2}\sigma_b^{i2} &= \ln \left[\underbrace{\left(1 + \alpha_m^i \delta_m + \alpha_\pi^i \delta_\pi - \Omega_2^{e,i}\right) \circ \left(1 + \alpha_m^i \delta_m + \alpha_\pi^i \delta_\pi\right)^{\circ-1} \circ \left(1 - \Omega_2^{e,i}\right)^{\circ-1}}_{(1) \text{ compensation for global risk exposure}} \right] \mathbf{S}_t \\
&+ \ln \left[\underbrace{\left(1 + (1 - \alpha_m^i) \mathbf{m}_\omega^i + (1 - \alpha_\pi^i) \boldsymbol{\pi}_\omega^i - \Omega_4^{e,i}\right) \circ \left(1 + (1 - \alpha_m^i) \mathbf{m}_\omega^i + (1 - \alpha_\pi^i) \boldsymbol{\pi}_\omega^i\right)^{\circ-1} \circ \left(1 - \Omega_4^{e,i}\right)^{\circ-1}}_{(2) \text{ compensation for regional risk exposure}} \right] \mathbf{S}_t^i,
\end{aligned} \tag{1.116}$$

²⁰Note that, the non-linearity is due to the non-linearities in the moment generating function of Gamma shocks.

²¹The quadratic Taylor approximation for “ $y - \ln(1 + y)$ ” is $\frac{1}{2}y^2$.

²² which in a quadratic Gaussian approximation has the following expression,

$$\approx \underbrace{\left(\alpha_m^i \delta_m + \alpha_\pi^i \delta_\pi \right) \circ \Omega_2^{e,i} \mathbf{S}_t}_{\approx (1)} + \underbrace{\left[(1 - \alpha_m^i) \mathbf{m}_\omega^i + (1 - \alpha_\pi^i) \boldsymbol{\pi}_\omega^i \right] \circ \Omega_4^{e,i} \mathbf{S}_t^i}_{\approx (2)} = -Cov_t(\tilde{m}_{t+1}^i, \tilde{r}_{t+1}^{e,i}). \quad (1.117)$$

1.F.2.3.e Variances

The physical variance for Asset $a \in \{b, e\}$,

$$V_t^{a,i,P} \equiv E_t \left[\left(\tilde{r}_{t+1}^{a,i} - E_t(\tilde{r}_{t+1}^{a,i}) \right)^2 \right], \quad (1.118)$$

$$= \Omega_2^{a,i} \mathbf{S}_t \Omega_2^{a,i'} + \Omega_4^{a,i} \mathbf{S}_t^i \Omega_4^{a,i'} + \sigma_a^{i^2}, \quad (1.119)$$

where the parameter matrices are discussed in Equations (1.110) and (1.114).

The risk-neutral variance for Asset $a \in \{b, e\}$,

$$V_t^{a,i,Q} \equiv E_t^Q \left[\left(\tilde{r}_{t+1}^{a,i} - E_t^Q(\tilde{r}_{t+1}^{a,i}) \right)^2 \right], \quad (1.120)$$

$$\begin{aligned} &= \left[\Omega_2^{a,i} \circ (\mathbf{1} + \boldsymbol{\delta}_m + \boldsymbol{\delta}_\pi)^{\circ -1} \right] \mathbf{S}_t \left[\Omega_2^{a,i} \circ (\mathbf{1} + \boldsymbol{\delta}_m + \boldsymbol{\delta}_\pi)^{\circ -1} \right]' \\ &+ \left[\Omega_4^{a,i} \circ (\mathbf{1} + \mathbf{m}_\omega^i + \boldsymbol{\pi}_\omega^i)^{\circ -1} \right] \mathbf{S}_t^i \left[\Omega_4^{a,i} \circ (\mathbf{1} + \mathbf{m}_\omega^i + \boldsymbol{\pi}_\omega^i)^{\circ -1} \right]' + \sigma_a^{i^2}. \end{aligned} \quad (1.121)$$

1.F.2.3.f Variances as Assets: Variance Risk Premium

The present tripartite model derives closed-form solutions for VRP which show potentials to capture its empirical time variation characteristics. For asset $a \in \{b, e\}$,

$$\begin{aligned} VRP_t^a &= V_t^{a,Q} - V_t^{a,P} \\ &= \left[\Omega_2^a \circ (\mathbf{1} + \boldsymbol{\delta}_m + \boldsymbol{\delta}_\pi)^{\circ -1} \right] \mathbf{S}_t \left[\Omega_2^a \circ (\mathbf{1} + \boldsymbol{\delta}_m + \boldsymbol{\delta}_\pi)^{\circ -1} \right]' - \Omega_2^a \mathbf{S}_t \Omega_2^{a'} \\ &+ \left[\Omega_4^{a,i} \circ (\mathbf{1} + \mathbf{m}_\omega^i + \boldsymbol{\pi}_\omega^i)^{\circ -1} \right] \mathbf{S}_t^i \left[\Omega_4^{a,i} \circ (\mathbf{1} + \mathbf{m}_\omega^i + \boldsymbol{\pi}_\omega^i)^{\circ -1} \right]' - \Omega_4^{a,i} \mathbf{S}_t^i \Omega_4^{a,i'}, \end{aligned} \quad (1.122)$$

where Ω_2^a and $\Omega_4^{a,i}$ are the “amount-of-risk” coefficients, and $\boldsymbol{\delta}_m$ and \mathbf{m}_ω^i are the “price-of-risk” coefficients that are linear to the global and regional risk aversions respectively. In the tripartite framework, the variance risk premium can be decomposed into a global component and a regional component.

1.F.2.3.g Foreign Exchange Returns

Denote $s^{\$/i}$ as the log of the spot exchange rate in units of dollars per foreign currency i at region i . As stated in the Proposition 1 of Backus, Foresi, and Telmer (2011), the change in the nominal exchange rate, $\Delta s_{t+1}^{\$/i} = s_{t+1}^{\$/i} - s_t^{\$/i}$, in a frictionless world is equivalent to the nominal pricing kernel difference,

$$\Delta s_{t+1}^{\$/i} = m_{t+1}^i - m_{t+1} + \pi_{t+1} - \pi_{t+1}^i. \quad (1.123)$$

²²Note that, the non-linearity is due to the non-linearities in the moment generating function of Gamma shocks.

An increase in $s^{\$/i}$ means a depreciation in dollars (and an appreciation in region i currency). In this model, a hypothetical world with perfect integration (i.e. $\alpha_m^i = 1\forall^i$) still obtains a time-varying spot rate to address the inflation risk amid the real macroeconomic risks. The regional currency excess return is the log return to U.S. investors of borrowing in dollars to hold foreign investment currency i can be expressed as an exact dynamic factor model,

$$\tilde{r}_{t+1}^{fx,i} \equiv \Delta s_{t+1}^{\$/i} + \tilde{y}_{t,1}^i, \quad (1.124)$$

$$= \Omega_0^{fx,i} + \Omega_1^{fx,i} \mathbf{X}_t + \Omega_2^{fx,i} \boldsymbol{\omega}_{t+1} + \Omega_3^{fx,i} \mathbf{X}_t^i + \Omega_4^{fx,i} \boldsymbol{\omega}_{t+1}^i + \varepsilon_{t+1}^{fx,i} + Jensen's + \epsilon_{t+1}^{fx,i}, \quad (1.125)$$

where $\Omega_0^{fx,i}$, $\Omega_1^{fx,i}$, $\Omega_2^{fx,i}$, $\Omega_3^{fx,i}$ and $\Omega_4^{fx,i}$ are constant matrices; $\epsilon_{t+1}^{fx,i}$ is the approximation error term that follows a homoskedastic Gaussian distribution with volatility σ_{fx}^i .

1.F.2.3.h Foreign Exchange Risk Premium

Given the no-arbitrage condition, $E_t[\exp(\tilde{m}_{t+1} + \tilde{r}_{t+1}^{fx,i})] = 1$ where $\tilde{r}_{t+1}^{fx,i}$ is the nominal foreign exchange return (from the U.S. investor's view point), the foreign exchange risk premium has a closed-form solution,

$$E_t[\tilde{r}_{t+1}^{fx,i}] - \tilde{y}_{t,1}^i + \frac{1}{2} \sigma_{fx}^i{}^2 = \ln \left[\left(1 + \boldsymbol{\delta}_m + \boldsymbol{\delta}_\pi - \boldsymbol{\Omega}_2^{fx,i} \right) \circ (1 + \boldsymbol{\delta}_m + \boldsymbol{\delta}_\pi)^{\circ-1} \circ (1 - \boldsymbol{\Omega}_2^{fx,i})^{\circ-1} \right] \mathbf{S}_t, \quad (1.126)$$

²³ which in a quadratic Gaussian approximation has the following expression,

$$\approx (\boldsymbol{\delta}_m + \boldsymbol{\delta}_\pi) \circ \boldsymbol{\Omega}_2^{fx,i} \mathbf{S}_t = -Cov_t(\tilde{m}_{t+1}, \tilde{r}_{t+1}^{fx,i}). \quad (1.127)$$

²³Note that, the non-linearity is due to the non-linearities in the moment generating function of Gamma shocks.

Table 1.1: Summary Statistics.

This table presents the unconditional correlation matrices of USD-denominated log returns of 8 developed countries (United States, USA; Canada, CAN; Germany, DEU; France, FRA; United Kingdom, GBR; Switzerland, CHE; Japan, JPN; Australia, AUS) in Panel A and unconditional univariate moments (with bootstrapped standard errors in parentheses) in Panel B. Mean and standard deviations are presented in annualized percentages. “Equity” return refers to the change in log total return index of domestic country stock market (United States: S&P500; Canada: S&P/TSX 60; Germany: DAX 30; France: CAC 40; United Kingdom: FTSE 100; Switzerland: SMI; Japan: NIKKEI 225; Australia: S&P/ASX 200); CRSP value-weighted return is used to obtain the USA equity return; other return series are obtained from DataStream. “Bond” (“Gov-Bond”) return refers to the change in log 10-year government bond index constructed by DataStream. Data is at monthly frequency. The sample is from March 1987 to December 2016 (T=358). Bold (italics) values indicate <5% (10%) significance level.

Panel A. Unconditional Correlation Matrices, 8 countries, 1987/03 - 2016/12								
	<i>North America</i>		<i>Europe</i>				<i>Australasia</i>	
	USA	CAN	DEU	FRA	GBR	CHE	JPN	AUS
(A.1) Equity								
USA	1	0.782	0.725	0.720	0.759	0.671	0.434	0.672
CAN		1	0.649	0.649	0.696	0.578	0.442	0.723
DEU			1	0.872	0.743	0.726	0.436	0.606
FRA				1	0.763	0.740	0.477	0.625
GBR					1	0.741	0.509	0.720
CHE						1	0.472	0.594
JPN							1	0.473
AUS								1
(A.2) Bond								
USA	1	0.457	0.436	0.436	0.343	0.344	0.324	0.282
CAN		1	0.415	0.439	0.396	0.267	0.201	0.599
DEU			1	0.958	0.685	0.812	0.503	0.440
FRA				1	0.666	0.768	0.464	0.460
GBR					1	0.573	0.402	0.385
CHE						1	0.540	0.360
JPN							1	0.239
AUS								1
Panel B. Unconditionanl Univariate Moments (annualized percentages)								
	<i>North America</i>		<i>Europe</i>				<i>Australasia</i>	
	USA	CAN	DEU	FRA	GBR	CHE	JPN	AUS
(B.1) Equity								
Mean	9.321 (2.741)	8.331 (3.552)	<i>7.476</i> (4.220)	<i>7.138</i> (3.907)	7.347 (3.120)	8.820 (3.195)	<i>2.299</i> (3.853)	9.284 (4.198)
S.D.	15.017 (0.950)	19.551 (1.317)	23.143 (1.224)	21.340 (1.018)	17.177 (0.948)	17.497 (0.890)	21.169 (0.907)	23.174 (2.264)
Skewness	-1.149 (0.364)	-1.374 (0.386)	-0.961 (0.252)	-0.566 (0.255)	-1.244 (0.596)	-1.265 (0.441)	-0.504 (0.244)	<i>-3.175</i> (1.661)
(B.2) Bond								
Mean	5.863 (0.984)	7.348 (1.652)	6.287 (1.879)	7.333 (1.861)	7.178 (1.823)	6.224 (2.001)	5.112 (2.180)	9.781 (2.173)
S.D.	7.240 (0.330)	9.972 (0.500)	11.537 (0.520)	11.360 (0.509)	11.135 (0.526)	12.307 (0.539)	13.238 (0.672)	13.170 (0.616)
Skewness	0.016 (0.230)	-0.416 (0.261)	-0.006 (0.186)	-0.014 (0.188)	0.049 (0.197)	0.230 (0.181)	0.278 (0.244)	-0.550 (0.195)

Table 1.2: Estimation Results of Global Bond Comovement.

This table presents the estimation results of the global bond return comovement models as described in Section 1.2. The full model builds on Engle and Kelly (2012)'s Dynamic Equicorrelation (DECO) model and features three new tests: (1) whether global equity and bond comovements are equal, (2) whether global bond comovement is symmetric and (3) whether it is cyclical. **Model details:** Denote \mathbf{z}_{t+1}^B ($N \times 1$) as the standardized residuals of country bond returns during period $t + 1$. The conditional equicorrelation matrix of \mathbf{z}_{t+1}^B is defined by $E_t[\mathbf{z}_{t+1}^B \mathbf{z}_{t+1}^{B'}] = \mathbf{Corr}_t^B$ ($N \times N$),

$$\mathbf{Corr}_t^B = (1 - \rho_t^B) \mathbf{I}_N + \rho_t^B \mathbf{J}_{N \times N}, \quad (1.T1)$$

where \mathbf{I}_N is an identity matrix; $\mathbf{J}_{N \times N}$ is a matrix of ones. The equicorrelation (by definition) is an equal-weighted average of correlations of unique country pairs (i.e., total of $N(N-1)/2$ pairs) conditional given information set at t :

$$\rho_t^B = \frac{2}{N(N-1)} \sum_{i>j} \frac{q_{i,j,t}^B}{\sqrt{q_{i,i,t}^B q_{j,j,t}^B}}, \quad (1.T2)$$

where $q_{i,j,t}^B$ is the (i, j) -th element of a symmetric matrix \mathbf{Q}_t^B ($N \times N$) which follows a generalized autoregressive heteroskedastic process, (omitting superscript "B" below for simplicity)

$$\begin{aligned} \mathbf{Q}_t = & \bar{\mathbf{Q}}^* \circ \Phi_t + \beta_1 \left(\tilde{\mathbf{Q}}_{t-1}^{\frac{1}{2}} \mathbf{z}_t \mathbf{z}_t' \tilde{\mathbf{Q}}_{t-1}^{\frac{1}{2}} - \bar{\mathbf{Q}}^* \circ \Phi_{t-1} \right) + \beta_2 \left(\mathbf{Q}_{t-1} - \bar{\mathbf{Q}}^* \circ \Phi_{t-1} \right) \\ & + \gamma \left(\tilde{\mathbf{Q}}_{t-1}^{\frac{1}{2}} \mathbf{n}_t \mathbf{n}_t' \tilde{\mathbf{Q}}_{t-1}^{\frac{1}{2}} - \Xi \circ \bar{\mathbf{Q}}^* \circ \Phi_{t-1} \right), \end{aligned} \quad (1.T3)$$

where "o" denotes the Hadamard product operator (element-by-element); $\tilde{\mathbf{Q}}_t$ is \mathbf{Q}_t with off-diagonal terms being zeros, which is a modification to Engle (2002) proposed by Aielli (2013). **Tests:** [1. Equality] The constant part of the long-run conditional mean ($\bar{\mathbf{Q}}^* \circ \Phi_t$), $\bar{\mathbf{Q}}^*$, can be defined as $\bar{\mathbf{Q}}^E + \nu (\mathbf{J}_{N \times N} - \mathbf{I}_N)$ (to test) or $\bar{\mathbf{Q}}^B$, where $\bar{\mathbf{Q}}^E$ ($\bar{\mathbf{Q}}^B$) is the pre-determined unconditional correlation matrix of equity (bond) returns respectively. [2. Asymmetry] \mathbf{n}_t ($N \times 1$) = $\mathbf{I}_{z_t < 0} \circ \mathbf{z}_t$, where $\mathbf{I}_{z_t < 0}$ ($N \times 1$) is assigned 1 if the residual is less than 0, and assigned 0 otherwise; $\Xi = E[\mathbf{I}_{z_t} \mathbf{I}_{z_t}']$. [3. Cyclical] Φ_t ($N \times N$) = $\mathbf{J}_{N \times N} + \phi_t (\mathbf{J}_{N \times N} - \mathbf{I}_N)$, where $\phi_t = \phi \tilde{\theta}_t^{world}$ and $\tilde{\theta}_t^{world}$ is the standardized world recession indicator (source: OECD). **Estimation:** The unknown parameters are $\{\beta_1, \beta_2, \nu, \gamma, \phi\}$, where ν is estimated separately. Sufficient stationarity conditions for \mathbf{Q}_t^B are $\beta_1 \mathbf{J}_{N \times N} + \beta_2 \mathbf{J}_{N \times N} + \gamma \Xi < \mathbf{J}_{N \times N}$ and $\beta_1, \beta_2 > 0$. Two distributions are considered to obtain log likelihood function: (1) multivariate Gaussian: $L^B[n] \propto -\frac{1}{2} \sum_t \left[\log |\mathbf{Corr}_t^B| + \mathbf{z}_{t+1}^{B'} (\mathbf{Corr}_t^B)^{-1} \mathbf{z}_{t+1}^B \right]$; (2) multivariate t : $L^B[t] \propto -\frac{1}{2} \sum_t \left[\log |\mathbf{Corr}_t^B| + (df + N) \log \left(1 + \frac{1}{df} \mathbf{z}_{t+1}^{B'} (\mathbf{Corr}_t^B)^{-1} \mathbf{z}_{t+1}^B \right) \right]$, where df is the degree of freedom of the N -variate t distribution. Best estimates of \mathbf{Corr}_t^B according to AIC and BIC are used in the second step estimation. Model estimation uses MLE at monthly frequency covering period from March 1987 to December 2016 (T=358), and model selection follows BIC. Bold (italics) values indicate <5% (10%) significance level.

	<i>Multivariate Gaussian</i>					<i>Multivariate t</i>				
	B (1)	B (2)	B (3)	B (4)	B (5)	B (1)	B (2)	B (3)	B (4)	B (5)
β_1	0.0808 (0.0332)	0.0705 (0.0330)	0.0701 (0.0287)	0.0581 (0.0279)	0.0858 (0.0334)	0.0845 (0.0060)	<i>0.0407</i> (0.0218)	0.0894 (0.0144)	<i>0.0311</i> (0.0159)	0.0745 (0.0222)
β_2	0.9121 (0.0406)	0.9073 (0.0423)	0.9255 (0.0304)	0.9245 (0.0325)	0.9141 (0.0335)	0.9155 (0.0060)	0.9017 (0.0284)	0.9106 (0.0144)	0.9216 (0.0246)	0.8776 (0.0285)
ν					-0.2746 (0.0551)					-0.1665 (0.0621)
γ		0.0195 (0.0138)		0.0170 (0.0166)			<i>0.0263</i> (0.0158)		<i>0.0214</i> (0.0129)	
ϕ			-0.0375 (0.0253)	-0.0572 (0.0466)				-0.0434 (0.0284)	<i>-0.0420</i> (0.0238)	
df						11.0408 (2.5590)	9.5987 (2.0717)	11.1170 (2.6198)	9.8033 (2.3917)	10.0123 (2.1231)
LL	-3509.93	-3506.17	-3507.87	-3504.27	-3508.88	-3374.47	-3339.31	-3373.51	-3337.75	-3345.14
AIC	7023.87	7018.34	7021.74	7016.53	7023.75	6754.93	6686.62	6755.01	6685.50	6698.29
BIC	7031.63	7029.99	7033.38	7032.06	7035.40	6766.57	6702.14	6770.53	6704.90	6713.81
							BEST			

Table 1.3: Estimation Results of Global Equity Comovement.

This table presents the estimation results of the global equity return comovement models that ensures the simultaneous fit of domestic equity-bond comovement, as described in Section 1.2. The model is also referred to as “Duo-DECO” in this paper. **Model details:** Denote $z_{i,t+1}^E$ as the standardized residual of Country i ’s equity return during period $t + 1$. Define an unknown beta process of each country i , $b_{i,t}$, that captures the time-varying beta of equity standardized residual to bond standardized residual of the same country:

$$z_{i,t+1}^E = b_{i,t} z_{i,t+1}^B + \sqrt{1 - (b_{i,t})^2} z_{i,t+1}^E, \quad (1.T4)$$

$$b_{i,t} = 2 \frac{\exp(\delta_1 + \delta_2 x_{i,t})}{1 + \exp(\delta_1 + \delta_2 x_{i,t})} - 1, \quad (1.T5)$$

where δ_1 and δ_2 are unknown constant parameters and $x_{i,t}$ is a country recession indicator assigned 1 during recession months and 0 during non-recession months (source: OECD). By design, the bond-purified equity return residual \check{z}_{t+1}^E ($N \times 1$) has variance equal to 1. The conditional equicorrelation matrix of \check{z}_{t+1}^E is defined by $E_t[\check{z}_{t+1}^E \check{z}_{t+1}^{E'}] = \widetilde{\text{Corr}}_t^E(N \times N) = (1 - \check{\rho}_t^E) \mathbf{I}_N + \check{\rho}_t^E \mathbf{J}_{N \times N}$. The equicorrelation is $\check{\rho}_t^E = \frac{2}{N(N-1)} \sum_{i>j} \frac{\check{q}_{i,j,t}^E}{\sqrt{\check{q}_{i,i,t}^E \check{q}_{j,j,t}^E}}$,

where $\check{q}_{i,j,t}^E$ is the (i, j) -th element of a symmetric matrix \check{Q}_t^E ($N \times N$) which follows an isomorphic generalized autoregressive heteroskedastic process (see Equation (1.18)). **Tests:** The asymmetry and cyclical tests are similarly conducted within the model. **Estimation:** Given the return decomposition above, total equity conditional correlation is:

$$\text{Corr}_t^E = \text{diag}(\mathbf{b}_t) \text{Corr}_t^B \text{diag}(\mathbf{b}_t) + \text{diag}\left(\sqrt{\mathbf{J}_{N \times N} - (\mathbf{b}_t)^{\circ 2}}\right) \widetilde{\text{Corr}}_t^E \text{diag}\left(\sqrt{\mathbf{J}_{N \times N} - (\mathbf{b}_t)^{\circ 2}}\right), \quad (1.T6)$$

where “diag(\cdot)” is a matrix operator that generates a diagonal matrix with the vector on the diagonal and 0 elsewhere and “(\cdot) $^{\circ 2}$ ” indicates the element-by-element (Hadamard) squares; Corr_t^B is the best bond model according to Table 1.2. The unknown parameters are $\{\delta_1, \delta_2, \beta_1, \beta_2, \gamma, \phi\}$. Sufficient stationarity conditions for \check{Q}_t^E (and thus \check{Q}_t^E given stationary \mathbf{Q}_t^B) are $\beta_1 \mathbf{J}_{N \times N} + \beta_2 \mathbf{J}_{N \times N} + \gamma \mathbf{\Xi} < \mathbf{J}_{N \times N}$ and $\beta_1, \beta_2 > 0$. Similarly, I consider multivariate Gaussian and multivariate t distributions. Model estimation uses MLE at monthly frequency, and model selection follows AIC and BIC. The sample period is from March 1987 to December 2016 ($T=358$). Bold (italics) values indicate $<5\%$ (10%) significance level.

	<i>Multivariate Gaussian</i>					<i>Multivariate t</i>				
	E (1)	E (2)	E (3)	E (4)	E (5)	E (1)	E (2)	E (3)	E (4)	E (5)
β_1	0.0883 (0.0296)	0.0775 (0.0560)	0.0722 (0.0346)	0.0630 (0.2528)	0.0515 (0.1016)	0.0745 (0.0364)	0.0182 (0.0087)	0.0476 (0.0488)	0.0173 (0.0176)	0.0225 (0.0104)
β_2	0.8708 (0.0397)	0.8803 (0.0460)	0.8961 (0.0496)	<i>0.9015</i> (0.4759)	0.9058 (0.1418)	0.8879 (0.0568)	0.9069 (0.0115)	0.9341 (0.0808)	0.9089 (0.0169)	0.9617 (0.0142)
ν										
γ		0.0554 (0.0172)		0.0583 (0.0112)	0.0588 (0.0136)		0.0521 (0.0158)		0.0507 (0.0128)	0.0533 (0.0065)
ϕ			<i>0.0381</i> (0.0198)	<i>0.0366</i> (0.0187)	0.0394 (0.0201)			<i>0.0426</i> (0.0246)	0.0457 (0.0199)	<i>0.0386</i> (0.0207)
δ_1	0.6126 (0.0333)	0.5997 (0.0376)	0.6114 (0.0334)	0.6000 (0.0354)		0.6470 (0.0306)	0.6303 (0.0316)	0.6461 (0.0308)	0.6296 (0.0354)	
δ_2	-0.1383 (0.0429)	-0.1315 (0.0483)	-0.1387 (0.0426)	-0.1319 (0.0457)		-0.1539 (0.0404)	-0.1372 (0.0425)	-0.1549 (0.0404)	-0.1389 (0.0353)	
df						6.7254 (0.9285)	6.6772 (0.8372)	6.6921 (0.9195)	6.7167 (0.8433)	6.1025 (1.9130)
LL	-3117.02	-3107.47	-3110.08	-3103.18	-3114.15	-3041.22	-3025.99	-3037.92	-3021.07	-3027.17
AIC	6242.04	6224.94	6230.15	6218.37	6236.31	6092.44	6063.99	6087.85	6056.15	6064.33
BIC	6257.56	6244.34	6249.55	6241.65	6251.83	6111.84	6087.27	6111.13	6083.31	6083.74
										BEST

Table 1.4: Model Fit: (In)Equality between Global Equity Comovement and Global Bond Comovement.

This table replicates the test results on the inequality between global equity comovement and global bond comovement with data. **Data Moments & Test Statistics:** Rows “Data” report the equally-weighted unconditional pairwise correlations (excluding diagonal terms) of returns denominated in USD. Bootstrapped standard errors are reported in parentheses. “Jennrich’s χ^2 (E-B)” is a statistical test adapted from Jennrich (1970) to test the equality of two sample correlation matrices (in this paper, equity and bond). Test details are relegated to Appendix 1.4. “***” denotes <1% significance level, or the equality hypothesis is rejected. **Model Moments:** Three model moments are considered. (1) Rows “Conditional Model” reports time-series averages of the model-implied global equity and bond comovements obtained from the best model according to Tables 1.2 and 1.3. (2 and 3) Given the estimation results assuming multivariate t or multivariate Gaussian distributions, Rows “Simulated Model (t)” (“Simulated Model (n)”) report averages of 1000 unconditional global correlations obtained from finite-sample simulations assuming multivariate t distribution (multivariate Gaussian distribution). Bold (italics) values indicate the model point estimates are within 95% (99%) confidence intervals of the corresponding data moments. **Panels:** Full sample and three subsample periods are considered.

	Equity	Bond	Equity	Bond
	Panel A. Full Sample		Panel B. 1987/03 - 1997/02	
Data	0.6271	0.4606	0.5923	0.3907
S.E.	(0.0254)	(0.0233)	(0.0299)	(0.0213)
Jennrich’s χ^2	227.087(***)		91.701(***)	
Conditional Model	0.6568	0.4926	0.5784	0.3997
Simulated Model (t)	0.6712	0.4179	0.6151	0.3563
Simulated Model (n)	0.5831	0.4184	0.5502	0.3568
	Panel C. 1997/03 - 2007/02		Panel D. 2007/03 - 2017/01	
Data	0.6401	0.5469	0.7538	0.5021
S.E.	(0.0270)	(0.0223)	(0.0268)	(0.0225)
Jennrich’s χ^2	116.729(***)		124.005(***)	
Conditional Model	0.6614	0.5391	0.7319	0.5384
Simulated Model (t)	0.6409	0.4637	0.7578	0.4336
Simulated Model (n)	0.5997	0.5088	0.5993	0.3896

Table 1.5: Model Fit: (A)symmetry in Global Comovements.

This table evaluates the fit of global dynamic comovement model(s) to the non-parametric estimates of global upside and downside comovements. **Data Moments:** Following Longin and Solnik (2001) and Ang and Chen (2002), the exceedance correlation of standardized daily returns (\tilde{x} and \tilde{y}) at a certain threshold quantile τ is $\rho(\tilde{x}, \tilde{y} | \tilde{x} < \Phi_x^{-1}(\tau), \tilde{y} < \Phi_y^{-1}(\tau))$ if $\tau < 0.5$ or $\rho(\tilde{x}, \tilde{y} | \tilde{x} > \Phi_x^{-1}(\tau), \tilde{y} > \Phi_y^{-1}(\tau))$ if $\tau \geq 0.5$. Global exceedance correlations are equally-weighted bivariate exceedance correlations across 28 unique country pairs. Daily returns (from 1987/03 to 2016/12) are standardized using the best GARCH-class conditional volatility estimates. Standard errors for “bivariate” exceedance correlations are obtained using Cohen and Cohen (2003); then, standard errors for global exceedance correlations are obtained using Delta’s Method. **Model Moments:** Three global comovement models are considered: (1) Best models assuming multivariate t (“B (2)”, Table 1.2; “E (4)”, Table 1.3). (2) Models assuming multivariate t but with no asymmetry term (“B (1)”, Table 1.2; “E (3)”, Table 1.3). (3) Best models assuming multivariate Gaussian (“B (2)”, Table 1.2; “E (4)”, Table 1.3). Column “Distance” reports the sum of squared standardized distance between model and data moments (of the four quantiles); p-value of the distance is reported in the last column. Bold (italics) values indicate the model point estimates are within 95% (99%) confidence intervals of the corresponding data moments. More quantile choices can be found in Figure 1.2.

	Equity				Distance, $\chi^2(4)$	p-value
	25%	49%	51%	75%		
Data	0.3682	0.3292	0.2619	0.2469	0.00	-
S.E.	(0.0199)	(0.0147)	(0.0153)	(0.0216)	-	-
Simulated Model (t)	<i>0.3229</i>	0.3326	0.3024	0.2872	15.68	0.35%
Simulated Model (n)	0.2316	0.2763	0.2631	0.2161	62.12	0.00%
Simulated Model (t), No Asymmetry	0.3094	0.3133	0.3115	0.3197	31.67	0.00%
	Bond				Distance, $\chi^2(4)$	p-value
	25%	49%	51%	75%		
Data	0.3029	0.3024	0.3079	0.3245	0.00	-
S.E.	(0.0209)	(0.0149)	(0.0149)	(0.0206)	-	-
Simulated Model (t)	0.3365	0.3098	0.3114	0.3337	3.07	54.69%
Simulated Model (n)	0.2165	0.2767	<i>0.2774</i>	0.2394	41.26	0.00%
Simulated Model (t), No Asymmetry	0.2718	0.2865	0.2888	<i>0.2723</i>	11.41	2.23%

Table 1.6: Model Fit: Cyclicalities of Global Equity Comovement and Global Bond Comovement.

This table evaluates the fit of best global models for cyclicity moments in data. **Data Moments:** “Non-recession” (“Recession”) periods are identified when the OECD world recession indicator is 0 (1). Then the average pairwise unconditional correlations are calculated within each subsample. **Model Moments:** Three model moments are considered. (1) Rows “Conditional Model” reports time-series averages of the model-implied global equity and bond comovements as shown in Tables 1.2 and 1.3. (2 and 3) Given the estimation results assuming multivariate t or multivariate Gaussian distribution, Rows “Simulated Model (t)” (“Simulated Model (n)”) report averages of 1000 unconditional global correlations obtained from finite-sample simulations assuming multivariate t distribution (multivariate Gaussian distribution). Bold (italics): point estimates within 95% (99%) confidence intervals of the data moments.

	Equity		Bond	
	Non-Recession	Recession	Non-Recession	Recession
Data	0.5952	0.6571	0.4705	0.4520
S.E.	(0.0334)	(0.0161)	(0.0302)	(0.0480)
t Statistics	1.67 (*)		-0.33	
Conditional Model	0.6479	0.6740	0.5285	0.4437
Simulated Model (t)	0.6364	0.6761	0.4188	0.4169
Simulated Model (n)	0.5777	0.5885	0.4112	0.4256

Table 1.7: Dynamic Factor Model Fit & Economic Significance of Risk Aversion

This table evaluates the fit of the full models and demonstrates the economic significance of risk aversion in explaining global return correlations. **Models:** “Empirical BM” denotes the empirical benchmarks obtained from the first part of the paper. Four dynamic factor models are considered: (a full set of factors, a subset of factors excluding the risk aversion shock ω_q) \times (constant betas, time-varying betas). Details estimation results of the return loadings are relegated to Tables 1.16 (constant beta) and 1.17 (time-varying beta). **Fact Checks:** Each stylized fact is summarized by 2 moments in this table to be matched. On Fact 1, average conditional global correlations are calculated over the sample. On Fact 2, periods are considered “downside” (“upside”) when the world return (equal average of all 8 countries) is less than or equal to 0. On Fact 3, the model-implied conditional correlations are regressed on the OECD world recession indicator. The p-values in brackets correspond to the t test results of the closeness between the empirical benchmark moments and the factor model-implied moments; standard errors of the empirical benchmark moments are calculated using Delta’s method. Bold (italics) values indicate the point estimates are within 95% (99%) confidence intervals of the corresponding data moments. “Yes” (“No”) indicates that the model fits (fails to fit) the stylized facts.

		<i>Empirical BM:</i>		<i>Dynamic Factor Models:</i>	
		constant Full	time-varying Full	constant Exclud. ω_q	time-varying Exclud. ω_q
<i>Test Fact 1: Equity Correlation > Bond Correlation</i>					
{Moment 1: Average Conditional Global Correlations}					
Global Equity Correlation	0.6568	0.6919	0.6762	0.5000	0.5008
Closeness to BM [p-value]		[41.5%]	[64.9%]	[0.3%]	[0.4%]
Global Bond Correlation	0.4926	0.4628	0.4523	0.6219	0.4482
		[42.1%]	[28.4%]	[0.5%]	[24.1%]
Fit Fact 1?		Yes	Yes	No	No
<i>Test Fact 2: Excessive Left-Tail Global Correlation in Equities</i>					
{Moment 2: Global Equity Correlation – Global Bond Correlation}					
$r^{World} > 0$	0.1579	0.2245	0.2191	-0.1219	<i>0.0523</i>
		[13.6%]	[16.7%]	[0.0%]	[2.8%]
$r^{World} \leq 0$	0.1725	0.2368	0.2322	-0.1220	0.0530
		[10.5%]	[12.9%]	[0.0%]	[0.8%]
Fit Fact 2?		No	Yes	No	No
<i>Test Fact 3: Countercyclical Equity Correlation, Weakly Procyclical Bond Correlation</i>					
{Moment 3: Sensitivity to OECD World Output Growth}					
Global Equity Correlation	-1.2511	-0.6688	-0.7710	<i>0.0646</i>	0.2851
		[19.7%]	[28.1%]	[1.1%]	[0.4%]
Global Bond Correlation	0.5880	0.5114	0.5288	<i>0.0382</i>	<i>-0.0258</i>
		[72.5%]	[78.6%]	[2.7%]	[1.6%]
Fit Fact 3?		Yes	Yes	No	No

Table 1.8: Global Return Covariance Decomposition.

This table calculates the extent to which each state variable contributes to the global equity conditional covariance and global bond conditional covariance. For Country i and Country j ($i \neq j$), the covariance share explained by factor ω_κ is,

$$\frac{\beta_{i,t,\kappa} Var_t(\omega_{\kappa,t+1}) \beta_{j,t,\kappa}}{\beta'_{i,t} Var_t(\Omega_{t+1}) \beta_{j,t}},$$

where $\beta_{i,t,\kappa} Var_t(\omega_{\kappa,t+1}) \beta_{j,t,\kappa}$ can be further decomposed into a constant-beta part, $\beta_{i,0,\kappa} Var_t(\omega_{\kappa,t+1}) \beta_{j,0,\kappa}$, and a time-varying beta part, $\beta_{i,1,\kappa} Var_t(\omega_{\kappa,t+1}) \beta_{j,1,\kappa} s_t^2$ (s_t is the standardized instrument). Lines in bold indicate the four types of factors; “[β_0]” (“[β_1]”) indicates the constant (time-varying) part of the explained covariance. The share of total explained comovement is obtained by dividing the time-series average of the pairwise conditional covariance by the unconditional pairwise covariance matrix.

		o Constant Beta		o Time-Varying Beta			
		Equity	Bond	Equity	Bond		
Risk Aversion:	ω_q	90.3%	78.2%	90.5%			
				[β_0]	88.6%	[β_0]	27.2%
				[β_1]	1.9%	[β_1]	12.9%
Real Uncertainties:	Total	5.2%	-1.9%	7.4%		-3.8%	
	$\omega_{\theta u}$	5.5%	-0.4%	5.1%		3.2%	
				[β_0]	4.9%	[β_0]	-3.8%
				[β_1]	0.2%	[β_1]	7.0%
	$\omega_{\theta d}$	-0.3%	-1.5%	2.3%		-6.9%	
				[β_0]	0.9%	[β_0]	-5.3%
				[β_1]	1.4%	[β_1]	-1.7%
Inflation Uncertainties:	Total	2.8%	33.6%	1.1%		46.8%	
	$\omega_{\pi u}$	1.8%	10.8%	1.3%		48.6%	
				[β_0]	0.1%	[β_0]	43.1%
				[β_1]	1.2%	[β_1]	5.5%
	$\omega_{\pi d}$	1.0%	22.8%	-0.2%		-1.8%	
				[β_0]	0.3%	[β_0]	0.7%
				[β_1]	-0.5%	[β_1]	-2.5%
Real Short Rate Uncertainties:	Total	1.7%	-9.9%	1.0%		17.0%	
	ω_{xu}	-0.2%	-10.1%	-0.1%		21.9%	
				[β_0]	-0.3%	[β_0]	14.7%
				[β_1]	0.2%	[β_1]	7.2%
	ω_{xd}	1.9%	0.1%	1.1%		-4.9%	
				[β_0]	1.1%	[β_0]	-5.5%
				[β_1]	-0.1%	[β_1]	0.5%
Share of Explained Comovement		49.4%	0.9%	54.6%		15.4%	
Excluding Risk Aversion		4.8%	0.2%	5.2%		9.2%	

Table 1.9: Global Return Correlation Decomposition.

This table presents the extent to which each factor contributes to fitting the global correlations (empirical benchmarks). Row “All Shocks” shows the correlation between factor model-implied correlation and the empirical benchmarks where the factor model includes all shocks, denoted as $\rho(CORR_{0,t}, BM_t)$; asymptotic standard errors are shown in the parentheses. Then, denote the correlation between factor model-implied correlation and the empirical benchmarks where the factor model excludes shock ω_κ as $\rho(CORR_{\setminus\kappa,t}, BM_t)$. In rest of the rows, $\rho(CORR_{0,t}, BM_t) - \rho(CORR_{\setminus\kappa,t}, BM_t)$ are reported with the corresponding shock name in the first column.

	Constant Beta				Time-Varying Beta			
	Equity		Bond		Equity		Bond	
All Shocks	0.549	(0.046)	0.004	(0.055)	0.685	(0.040)	0.172	(0.054)
Risk Aversion	0.332		0.029		0.898		0.292	
Real Upside Uncertainty	0.028		0.063		0.086		0.121	
Real Downside Uncertainty	0.024		0.063		0.095		0.111	
Inflation Upside Uncertainty	0.032		0.069		0.076		0.136	
Inflation Downside Uncertainty	0.027		0.062		0.095		0.115	
Real Short Rate Upside Uncertainty	0.037		0.062		0.090		0.078	
Real Short Rate Downside Uncertainty	0.030		0.060		0.092		0.122	

Table 1.10: Dynamic Factor Model Fit & Economic Significance of Other State Variables

This table evaluates the fit of the models excluding a specific factor shock and illustrate the economic significance of that shock in explaining global asset comovements. Panel A considers constant beta models, and Panel B considers time-varying beta models. Details on the model fit are described in Table 1.7. Bold (italics) values indicate the point estimates are within 95% (99%) confidence intervals of the corresponding data moments.

<i>A. Dynamic Factor Model with Constant Betas:</i>						
Excluding:	$\omega_{\theta u}$	$\omega_{\theta d}$	$\omega_{\pi u}$	$\omega_{\pi d}$	ω_{xu}	ω_{xd}
<i>Test Fact 1: Equity Correlation > Bond Correlation</i>						
	{Moment 1: Average Conditional Global Correlations}					
Global Equity Correlation	<i>0.7732</i>	<i>0.7733</i>	<i>0.7751</i>	<i>0.7737</i>	<i>0.7729</i>	<i>0.7747</i>
Closeness to BM [p-value]	[1.8%]	[1.8%]	[1.7%]	[1.8%]	[1.8%]	[1.7%]
Global Bond Correlation	0.4713	0.4624	0.4622	0.4656	0.4602	0.4641
	[56.2%]	[41.5%]	[41.2%]	[46.5%]	[38.4%]	[44.1%]
Fit Fact 1?	Yes	Yes	Yes	Yes	Yes	Yes
<i>Test Fact 2: Excessive Left-Tail Global Correlation in Equities</i>						
	{Moment 2: Global Equity Correlation – Global Bond Correlation}					
$r^{World} > 0$	<i>0.2852</i>	0.2937	0.2957	0.2912	0.2955	0.2935
	[1.1%]	[0.8%]	[0.7%]	[0.9%]	[0.7%]	[0.8%]
$r^{World} \leq 0$	0.3213	0.3309	0.3330	0.3278	0.3326	0.3304
	[0.2%]	[0.1%]	[0.1%]	[0.2%]	[0.1%]	[0.1%]
Fit Fact 2?	Yes	Yes	Yes	Yes	Yes	Yes
<i>Test Fact 3: Countercyclical Equity Correlation, Weakly Procyclical Bond Correlation</i>						
	{Moment 3: Sensitivity to OECD World Output Growth}					
Global Equity Correlation	<i>-0.2929</i>	-0.3227	<i>-0.2849</i>	<i>-0.2868</i>	<i>-0.2898</i>	<i>-0.2854</i>
	[4.6%]	[5.2%]	[4.5%]	[4.5%]	[4.6%]	[4.5%]
Global Bond Correlation	0.5518	0.5408	0.5819	0.5464	0.5463	0.5547
	[86.8%]	[82.8%]	[97.8%]	[84.8%]	[84.8%]	[87.8%]
Fit Fact 3?	Yes	Yes	Yes	Yes	Yes	Yes
<i>B. Dynamic Factor Model with Time-Varying Betas:</i>						
Excluding:	$\omega_{\theta u}$	$\omega_{\theta d}$	$\omega_{\pi u}$	$\omega_{\pi d}$	ω_{xu}	ω_{xd}
<i>Test Fact 1: Equity Correlation > Bond Correlation</i>						
	{Moment 1: Average Conditional Global Correlations}					
Global Equity Correlation	<i>0.7601</i>	<i>0.7600</i>	<i>0.7645</i>	<i>0.7622</i>	<i>0.7592</i>	<i>0.7618</i>
Closeness to BM [p-value]	[3.1%]	[3.1%]	[2.6%]	[2.9%]	[3.2%]	[2.9%]
Global Bond Correlation	0.3527	0.3458	0.3528	0.3501	0.3596	0.3599
	[0.3%]	[0.2%]	[0.3%]	[0.2%]	[0.4%]	[0.4%]
Fit Fact 1?	Yes	Yes	Yes	Yes	Yes	Yes
<i>Test Fact 2: Excessive Left-Tail Global Correlation in Equities</i>						
	{Moment 2: Global Equity Correlation – Global Bond Correlation}					
$r^{World} > 0$	0.3844	0.3905	0.3888	0.3887	0.3756	0.3789
	[0.0%]	[0.0%]	[0.0%]	[0.0%]	[0.0%]	[0.0%]
$r^{World} \leq 0$	0.4347	0.4423	0.4383	0.4398	0.4289	0.4292
	[0.0%]	[0.0%]	[0.0%]	[0.0%]	[0.0%]	[0.0%]
Fit Fact 2?	Yes	Yes	Yes	Yes	Yes	Yes
<i>Test Fact 3: Countercyclical Equity Correlation, Weakly Procyclical Bond Correlation</i>						
	{Moment 3: Sensitivity to OECD World Output Growth}					
Global Equity Correlation	-0.4693	-0.5162	-0.4105	-0.4639	-0.4943	-0.4624
	[9.3%]	[11.2%]	[7.4%]	[9.1%]	[10.3%]	[9.1%]
Global Bond Correlation	0.7083	0.7324	0.7009	0.7736	0.9312	0.7756
	[58.3%]	[51.1%]	[60.6%]	[40.2%]	[13.7%]	[39.7%]
Fit Fact 3?	Yes	Yes	Yes	Yes	Yes	Yes

Table 1.11: Conditional Variance Decomposition.

Panel A. Constant Beta															
	ω_q		$\omega_{\theta u}$		$\omega_{\theta d}$		$\omega_{\pi u}$		$\omega_{\pi d}$		ω_{xu}		ω_{xd}		Explained
USA Equity	93.6%		4.0%		0.0%		1.2%		0.2%		0.3%		0.6%		56.7%
CAN Equity	71.3%		7.2%		0.2%		2.4%		17.1%		0.0%		1.7%		47.4%
DEU Equity	95.4%		0.5%		0.1%		1.6%		0.9%		1.0%		0.6%		39.6%
FRA Equity	88.1%		3.9%		0.2%		2.9%		0.2%		3.2%		1.5%		37.3%
GBR Equity	84.6%		8.8%		2.0%		1.0%		0.6%		2.6%		0.4%		33.9%
CHE Equity	89.8%		7.0%		0.8%		0.4%		0.4%		0.1%		1.5%		33.7%
JPN Equity	76.2%		1.8%		7.8%		3.4%		3.7%		0.1%		7.1%		8.2%
AUS Equity	72.9%		15.0%		2.2%		1.7%		3.1%		1.3%		3.9%		33.8%
USA Gov-Bond	43.4%		0.2%		5.6%		9.0%		40.5%		0.1%		1.3%		13.9%
CAN Gov-Bond	57.0%		0.6%		7.7%		18.1%		10.6%		1.9%		4.0%		9.4%
DEU Gov-Bond	3.2%		1.2%		2.4%		12.2%		80.7%		0.2%		0.1%		8.7%
FRA Gov-Bond	0.9%		0.3%		1.3%		17.5%		79.8%		0.1%		0.1%		7.4%
GBR Gov-Bond	38.7%		6.4%		0.5%		8.6%		30.7%		15.1%		0.0%		5.1%
CHE Gov-Bond	20.7%		7.6%		2.0%		15.5%		43.8%		10.0%		0.4%		2.1%
JPN Gov-Bond	78.8%		1.7%		0.5%		5.2%		13.0%		0.3%		0.6%		3.3%
AUS Gov-Bond	36.3%		16.2%		7.3%		9.4%		21.1%		4.4%		5.3%		14.3%
Panel B. Time-Varying Beta															
	ω_q		$\omega_{\theta u}$		$\omega_{\theta d}$		$\omega_{\pi u}$		$\omega_{\pi d}$		ω_{xu}		ω_{xd}		Explained
	β_0	β_1													
USA Equity	87.6%	0.1%	3.6%	0.2%	0.9%	0.8%	2.4%	0.2%	0.6%	2.0%	0.0%	0.7%	0.9%	0.0%	60.2%
CAN Equity	68.1%	0.2%	8.2%	0.3%	0.6%	1.8%	1.3%	0.1%	14.2%	0.1%	0.4%	1.8%	2.4%	0.6%	52.7%
DEU Equity	87.2%	2.2%	0.4%	0.0%	1.7%	0.7%	0.0%	1.9%	1.3%	2.9%	1.5%	0.1%	0.2%	0.1%	50.3%
FRA Equity	86.0%	1.1%	3.0%	0.4%	0.2%	0.7%	0.4%	1.2%	0.1%	2.8%	3.2%	0.2%	0.7%	0.0%	41.3%
GBR Equity	82.1%	0.2%	7.6%	0.1%	0.5%	2.6%	0.1%	1.0%	0.3%	2.7%	2.7%	0.1%	0.0%	0.1%	38.3%
CHE Equity	87.4%	2.6%	5.1%	1.9%	0.0%	0.3%	0.0%	0.8%	0.5%	0.3%	0.2%	0.1%	0.7%	0.1%	35.8%
JPN Equity	55.0%	6.7%	0.7%	2.0%	19.0%	1.1%	0.1%	1.0%	0.3%	9.1%	0.4%	0.0%	4.1%	0.4%	19.5%
AUS Equity	72.3%	2.8%	15.2%	0.0%	0.3%	0.8%	0.0%	1.1%	0.9%	0.2%	2.2%	1.3%	2.7%	0.0%	38.6%
USA Gov-Bond	33.2%	0.3%	0.2%	0.5%	8.8%	1.9%	0.1%	5.4%	31.2%	7.0%	0.3%	4.1%	4.4%	2.7%	24.1%
CAN Gov-Bond	46.9%	3.7%	0.2%	0.3%	17.1%	10.1%	2.8%	12.0%	2.4%	1.0%	2.4%	0.8%	0.3%	0.0%	20.1%
DEU Gov-Bond	0.2%	18.6%	1.6%	4.7%	5.8%	2.3%	0.1%	3.5%	52.8%	3.3%	1.9%	0.7%	3.8%	0.8%	15.8%
FRA Gov-Bond	2.2%	17.8%	0.8%	6.6%	5.7%	3.5%	0.1%	4.0%	44.6%	6.9%	2.2%	1.9%	3.3%	0.4%	16.9%
GBR Gov-Bond	10.6%	16.9%	7.8%	10.9%	0.5%	0.4%	1.5%	1.7%	11.6%	0.2%	18.2%	5.1%	10.1%	4.4%	10.6%
CHE Gov-Bond	0.1%	38.6%	6.6%	7.8%	0.3%	0.5%	1.7%	1.7%	20.7%	3.2%	10.7%	1.0%	7.1%	0.2%	8.5%
JPN Gov-Bond	33.8%	0.0%	1.0%	2.6%	1.0%	2.4%	1.6%	3.5%	5.4%	43.9%	1.4%	0.6%	2.8%	0.0%	15.8%
AUS Gov-Bond	40.3%	7.6%	9.8%	0.0%	4.0%	1.5%	4.8%	7.0%	5.6%	8.8%	6.2%	3.5%	0.9%	0.0%	29.0%

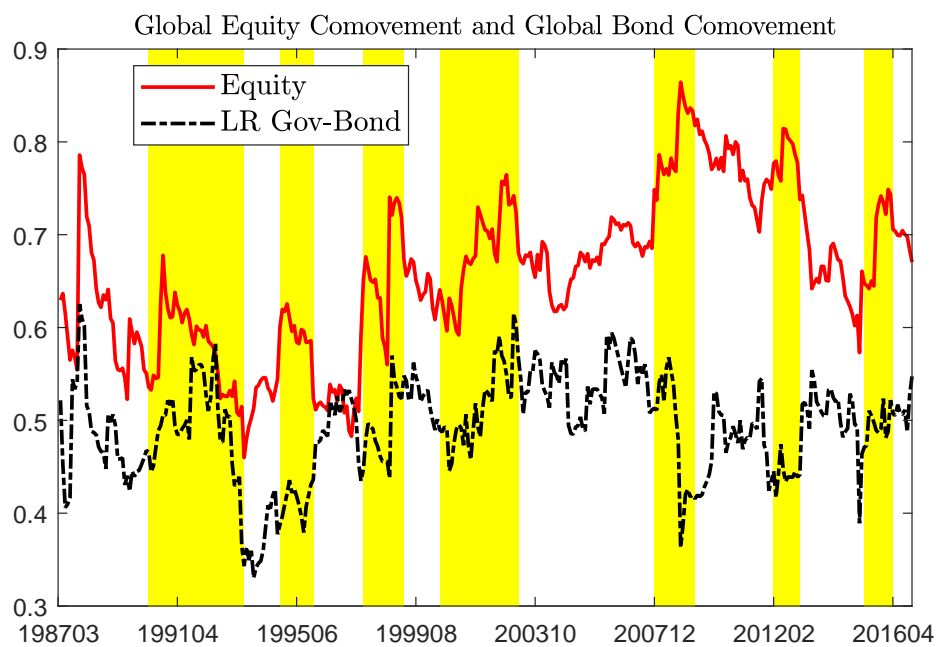


Figure 1.1: Global Dynamic Comovement Estimates.

The red line depicts the global equity correlations and the black dashed line the global bond correlations. The shaded regions are OECD world recession months from the OECD website. Model details are presented in Tables 1.2 and 1.3.

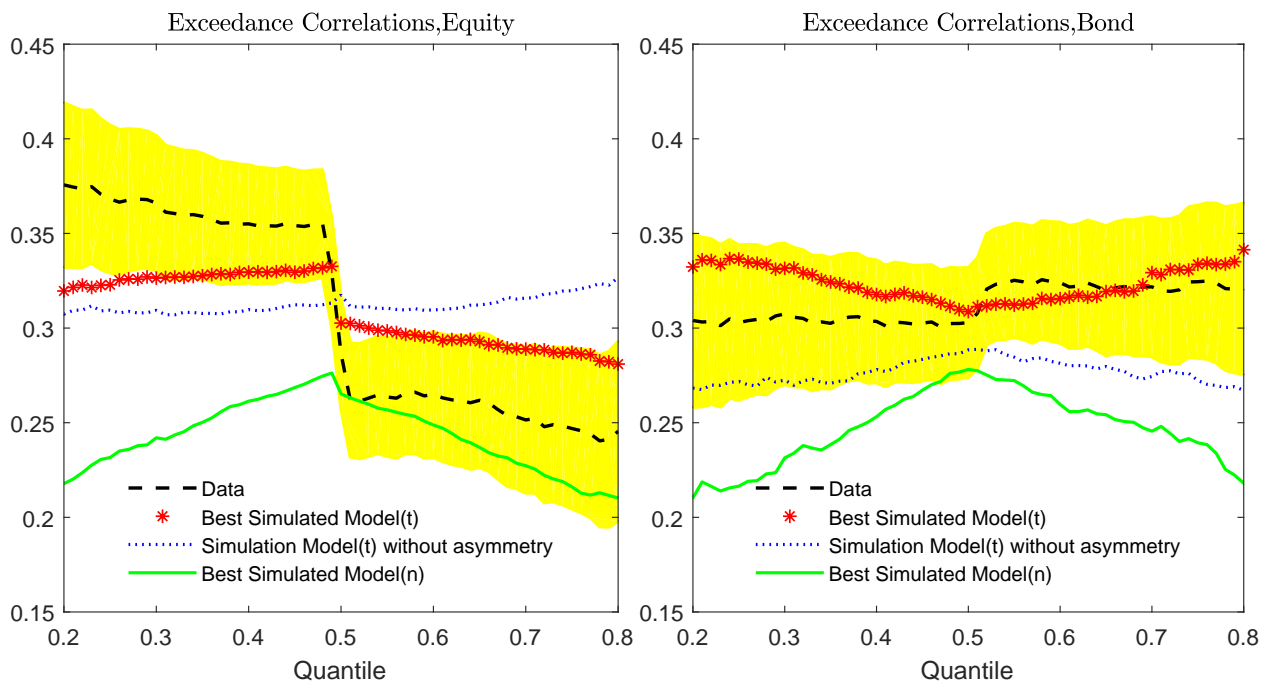


Figure 1.2: Global Exceedance Correlations of Asset Returns Denominated in USD.

This plot compares empirical global exceedance correlations calculated using standardized returns with model exceedance correlations calculated using simulated datasets, at full spectrum of the distribution. Table 1.5 provides more details on data moment and model moments (from simulated data). **Lines:** In this plot, black dashed lines and the yellow bandwidth depict the empirical global exceedance correlations and their 95% confidence intervals. Three global models from Tables 1.2 and 1.3 are considered. (1) Best models assuming multivariate t (“B (2)”, Table 1.2; “E (4)”, Table 1.3). (2) Models assuming multivariate t but with no asymmetry term (“B (1)”, Table 1.2; “E (3)”, Table 1.3). (3) Best models assuming multivariate Gaussian (“B (2)”, Table 1.2; “E (4)”, Table 1.3).

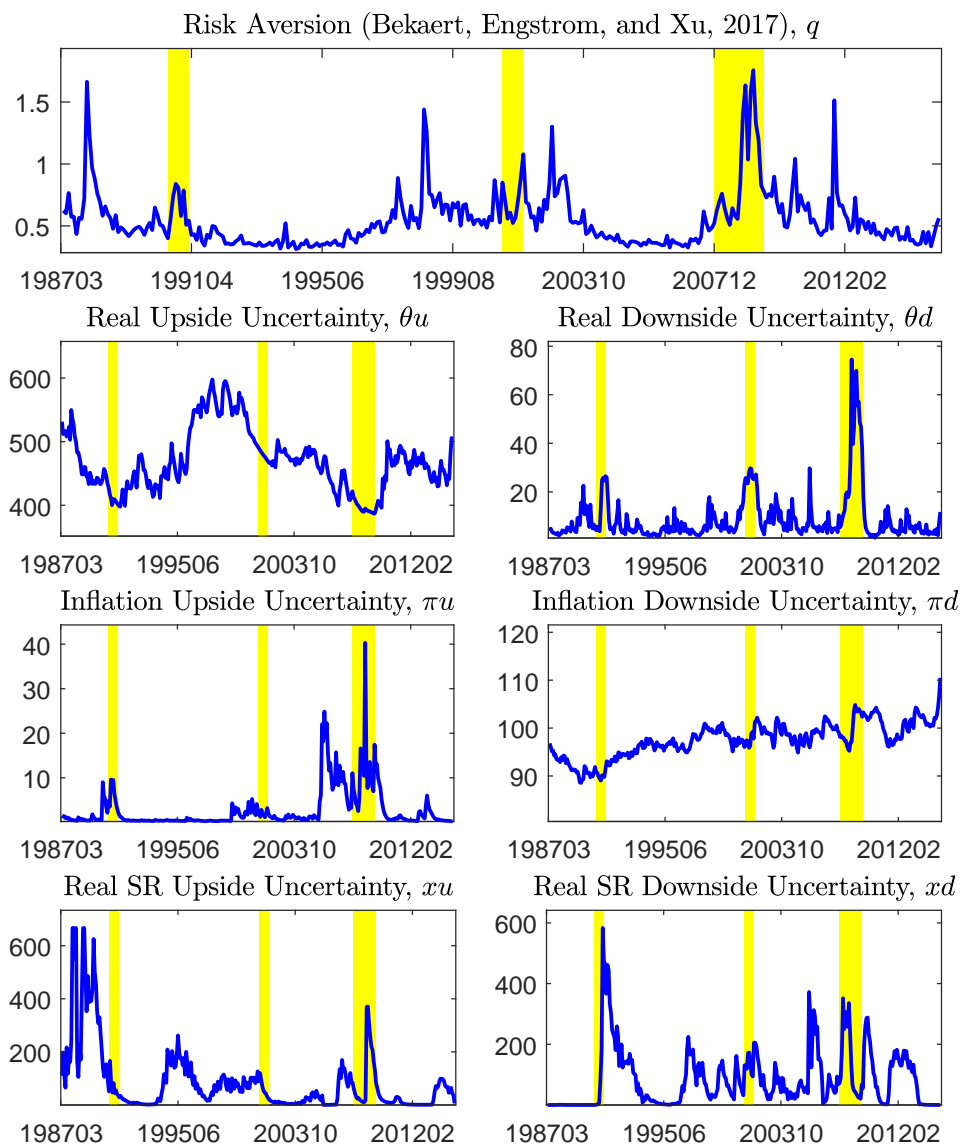


Figure 1.3: Dynamics of the Seven Economic Determinants.

The U.S. state variables used as global proxies. They are estimated at monthly frequency. For economic uncertainties, each state variable is estimated using the longest sample available: real and inflation upside and downside uncertainties, 1947/01–2016/12; real short rate, 1987/03–2015/02. The shaded regions are NBER world recession month from the NBER website.

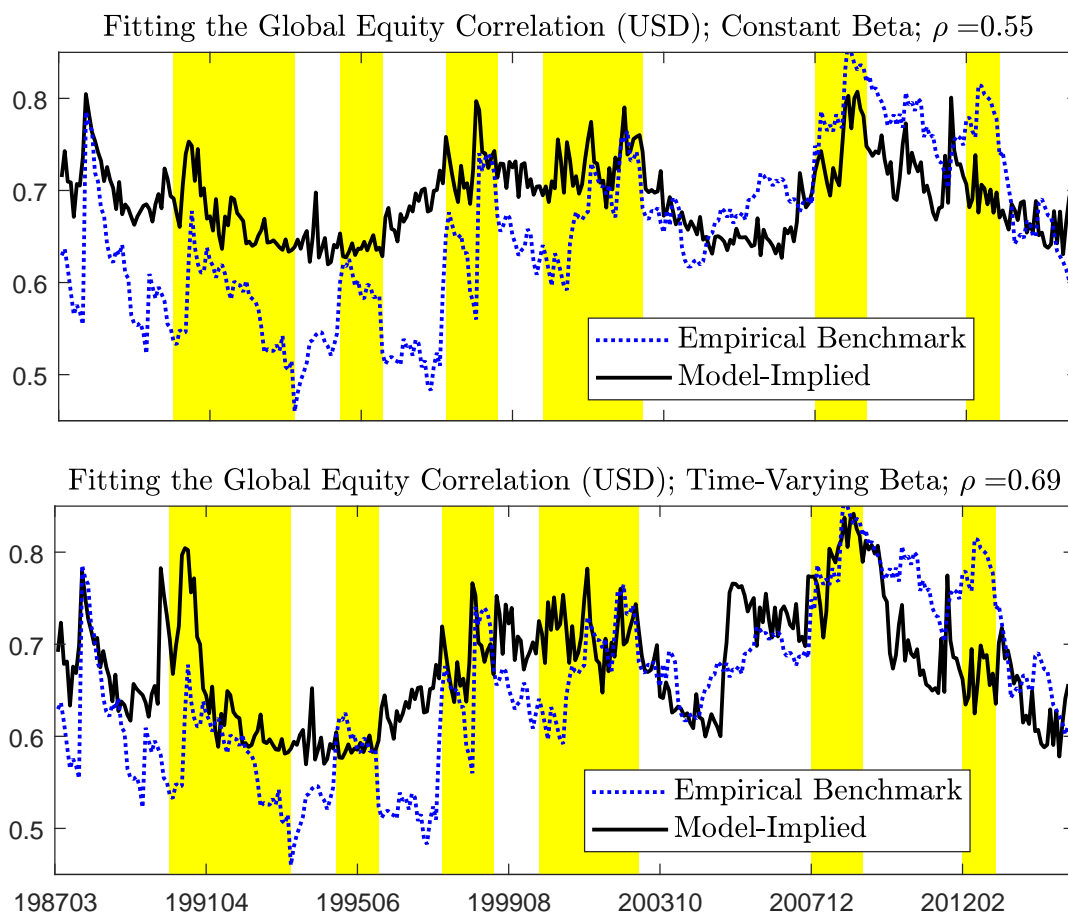


Figure 1.4: Data-Implied (Empirical Benchmark) and Model-Implied (Dynamic Factor Model) Global Equity Return Comovements.

The shaded regions are OECD world recession months from the OECD website.

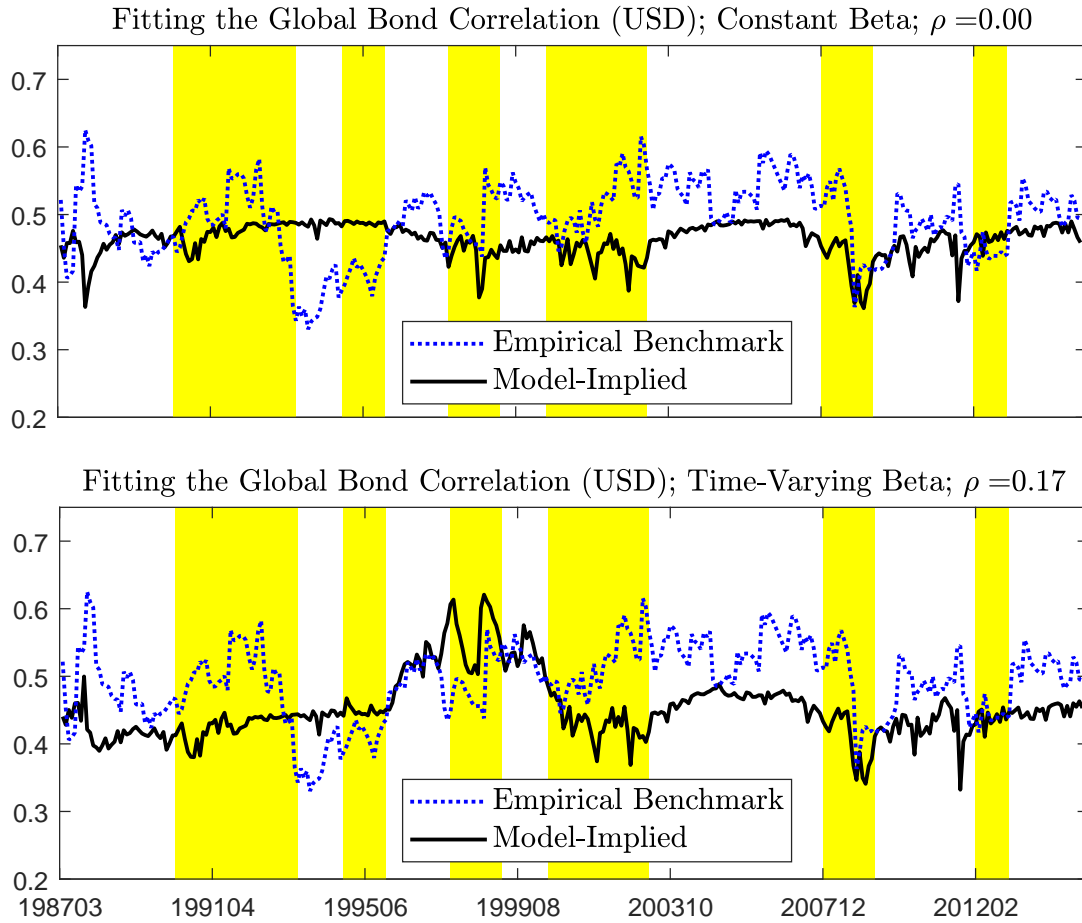


Figure 1.5: Data-Implied (Empirical Benchmark) and Model-Implied (Dynamic Factor Model) Global Bond Return Comovements.

The shaded regions are OECD world recession months from the OECD website.

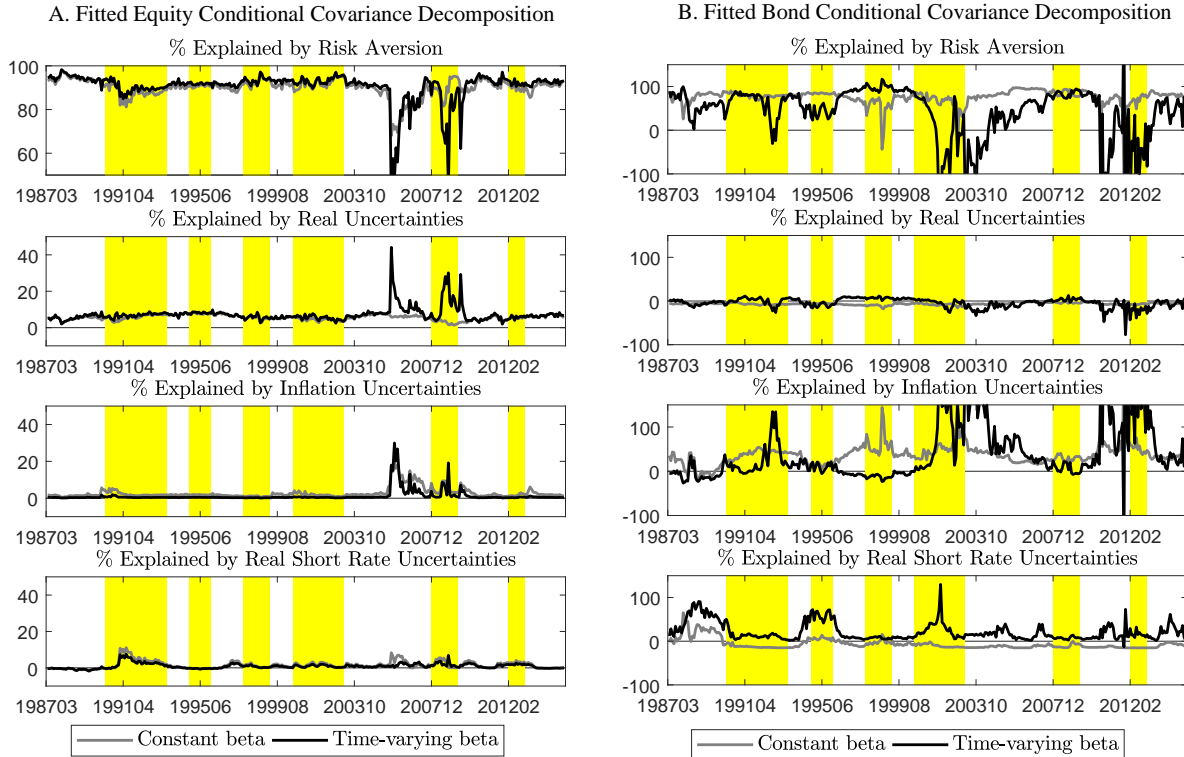


Figure 1.6: Time Variation in Shares of Economic Determinants in Explaining the Fitted Conditional Covariance Decomposition.

The share is first calculated within each country pair (excluding self pairs), and then obtain the cross-section average across all country pairs. The shaded regions are OECD world recession months from the OECD website.

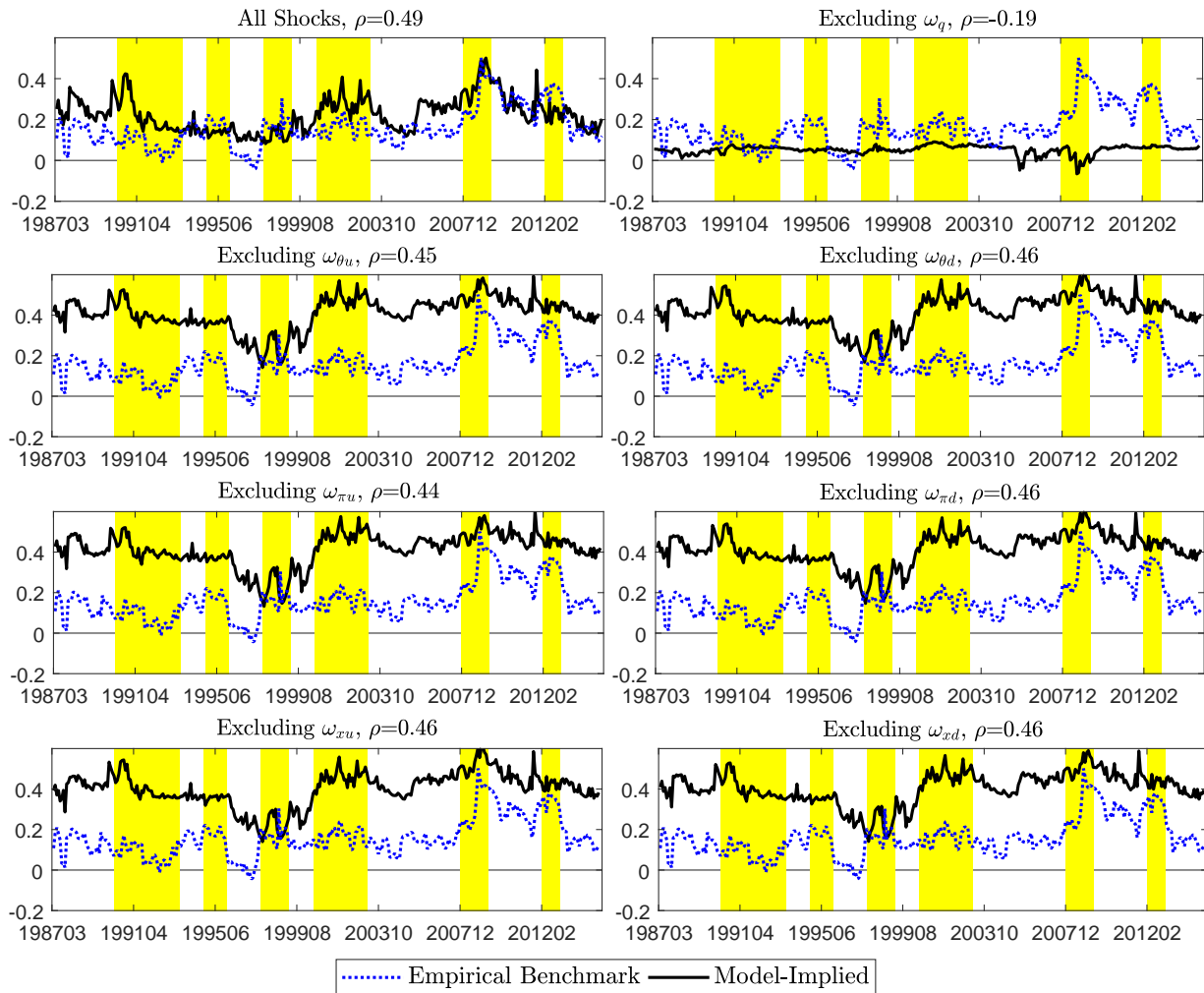


Figure 1.7: Fit of Equity and Bond Comovement Differences. Global Return Comovements When Omitting One Factor.

The data-implied differences are depicted in dashed blue lines, and the model-implied differences in solid black lines. The shaded regions are OECD world recession months from the OECD website.

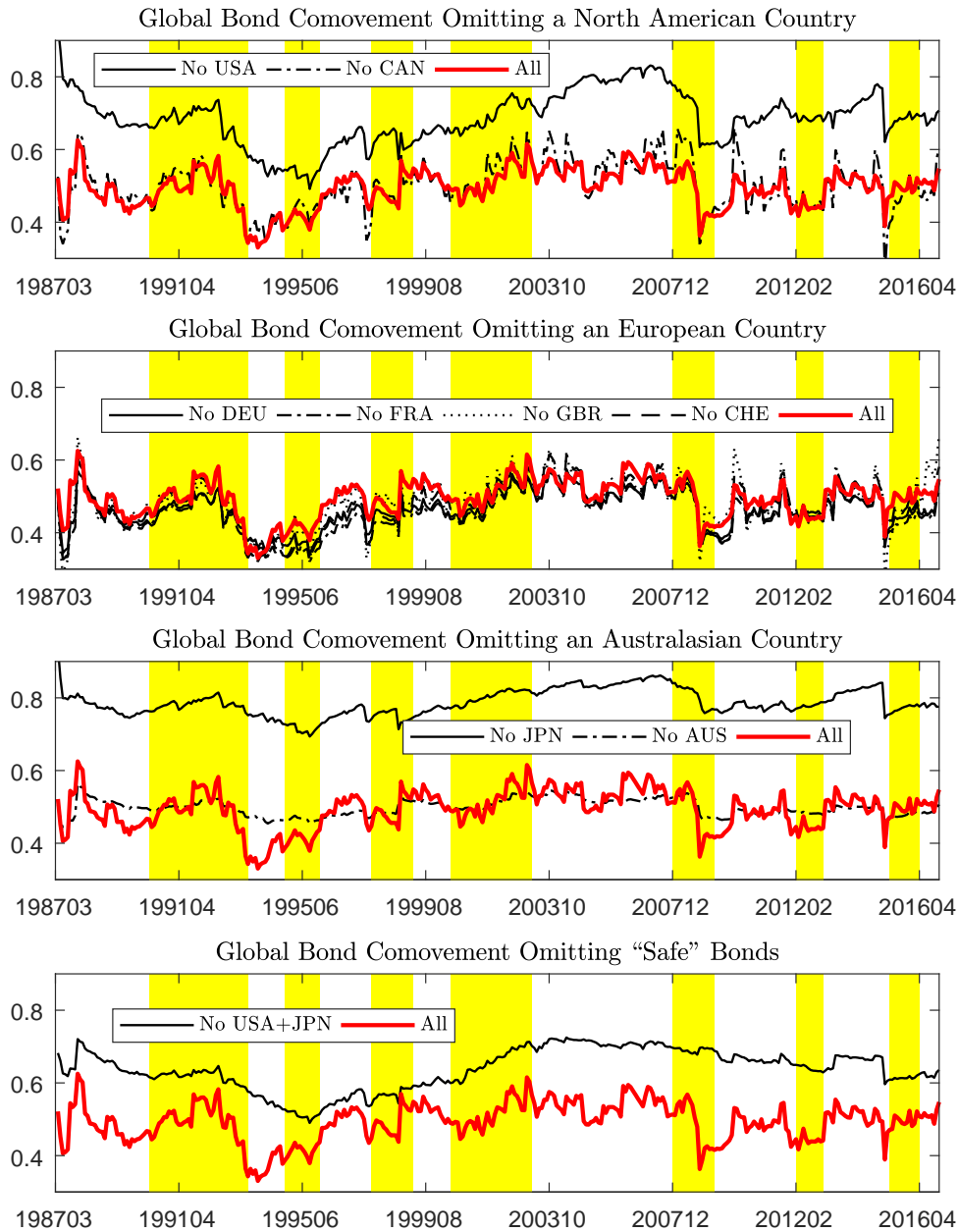


Figure 1.8: Global Dynamic Comovement Estimates, Omitting Certain Countries

The thick red lines in all four plots depict the empirical benchmark of global bond return correlations (from Figure 1.1). In the top three plots, the rest of the lines depict the (re-estimated) time-varying global bond return correlations omitting one country at a time. The three plots correspond to the three regions in my sample. In the fourth plot, the black line shows the (re-estimated) time-varying global bond return correlations omitting both USA and JPN bonds; both are identified as safe assets in this sample. The shaded regions are OECD world recession months from the OECD website.

Table 1.12: Conditional Volatility Models for Asset Returns.

This table presents best GARCH-class models and distributional assumptions for asset return conditional volatility. The four GARCH-class models are GARCH (“GARCH”), exponential GARCH (“EGARCH”), Threshold GARCH (“TARCH”), and Glosten-Jagannathan-Runkle GARCH (“GJRGARCH”). The four distributions-of-interest are Gaussian (“ ”), Student t (“t” characterized by a tail parameter ζ_1), GED (“GED” characterized by a tail parameter ζ_1), and Skewed t (“Skewt” characterized by a tail parameter ζ_1 and an asymmetry parameter ζ_2) distributions. Suppose $r_{t+1} = \mu + \varepsilon_{t+1}$, where $\varepsilon_{t+1} \sim D(0, h_t)$.

- (1) GARCH, Bollerslev (1986) : $h_t = \alpha_0 + \alpha_1 \varepsilon_t^2 + \alpha_2 h_{t-1}$
- (2) EGARCH, Nelson (1991) : $\ln(h_t) = \alpha_0 + \alpha_1 \frac{|\varepsilon_t|}{\sqrt{h_{t-1}}} + \alpha_2 \ln(h_{t-1}) + \alpha_3 \frac{\varepsilon_t}{\sqrt{h_{t-1}}}$
- (3) TARCH, Zakoian (1994) : $\sqrt{h_t} = \alpha_0 + \alpha_1 |\varepsilon_t| + \alpha_2 \sqrt{h_{t-1}} + \alpha_3 I_{\varepsilon_t < 0} |\varepsilon_t|$
- (4) GJRGARCH, Glosten, Jagannathan, and Runkle (1993) : $h_t = \alpha_0 + \alpha_1 \varepsilon_t^2 + \alpha_2 h_{t-1} + \alpha_3 I_{\varepsilon_t < 0} \varepsilon_t^2$.

Model estimation uses MLE at monthly frequency covering period from March 1987 to December 2016 (T=358), and model selection follows BIC. Bold values indicate <5% significance level.

Asset	Best Model	Variance Equation Parameters			Distribution Parameters	
		α_1	α_2	α_3	Thick Tail (ζ_1)	Skew (ζ_2)
USA Equity	EGARCH-Skewt	0.2652	0.8694	-0.1635	7.9925	-0.3664
CAN Equity	GARCH-Skewt	0.1111	0.8079		7.5999	-0.2775
DEU Equity	EGARCH-Skewt	0.2178	0.8603	-0.1164	7.3323	-0.2923
FRA Equity	EGARCH-Skewt	0.1749	0.8325	-0.2215	21.9996	-0.2914
GBR Equity	EGARCH-Skewt	0.1515	0.8269	-0.1881	11.3674	-0.1898
CHE Equity	GJRGARCH-Skewt	0.0345	0.2317	0.2989	6.5014	-0.1673
JPN Equity	EGARCH	0.2339	0.9369	-0.1193		
AUS Equity	EGARCH-Skewt	0.1257	0.9192	-0.0685	6.4191	-0.2395
USA Gov-Bond	TARCH	0.3669	0.6959	-0.1259		
CAN Gov-Bond	GARCH-t	0.0702	0.6549		9.4227	
DEU Gov-Bond	TARCH	0.2506	0.7814	-0.0644		
FRA Gov-Bond	GARCH	0.0774	0.8484			
GBR Gov-Bond	GARCH-GED	0.0463	0.9278		1.3353	
CHE Gov-Bond	GARCH	0.1284	0.4380			
JPN Gov-Bond	GARCH-GED	0.1093	0.7756		1.3036	
AUS Gov-Bond	GARCH-Skewt	0.1330	0.5543		13.7548	-0.2537

Table 1.13: Model Fit: Flight-to-Safety Channel, Given Best Model in Table 1.3

The model implicitly include a FTS channel. To provide the right empirical moments to be compared with, “Empirical” reports the average of time-varying correlation (estimated using a parsimonious dynamic conditional correlation model as in Engle, 2002) between standardized monthly equity returns and bond returns—both denominated in USD as consistently used in this paper. Three model moments are reported. (1) “Conditional Model” reports the time-series averages of the model-implied equity beta Table 1.3. (2 and 3) Because simulations do not effect the beta realizations, “Simulated Model (t)” and “Simulated Model (n)” report averages of model-implied beta averages given parameter estimates in Table 1.3. Because best conditional model is also the best model assuming multivariate t distribution, (1) and (2) report the same numbers. **States:** Good (Bad) states, when country recession indicator = 0 (1). Bold (italics) values indicate the model point estimates are within 95% (99%) confidence intervals of the corresponding data moments.

	Full States	Good	Bad
Empirical	0.3360	0.3799	0.2946
S.E.	(0.0481)	(0.0468)	(0.0494)
Conditional Model	0.2829	0.3051	0.2417
Simulated Model (t)	0.2829	0.3051	0.2417
Simulated Model (n)	0.2698	0.2913	0.2299

Table 1.14: Estimation Results of Global Equity Comovement: $x_{i,t}$ = Standardized Country Output Growth.

This table provides one of the robustness checks of the global equity correlation estimates involving the FTS channel (as in Table 1.3). Here, I use standardized country output growth (industrial production growth) as $x_{i,t}$ in the FTS process. Model estimation uses MLE at monthly frequency covering period from March 1987 to December 2016 (T=358), and model selection follows BIC. Bold (italics) values indicate <5% (10%) significance level.

	<i>Multivariate Gaussian</i>				<i>Multivariate t</i>			
	E (6)	E (7)	E (8)	E (9)	E (6)	E (7)	E (8)	E (9)
β_1	0.0884 (0.0291)	0.0777 (0.0355)	0.0724 (0.0341)	0.0634 (0.0539)	0.0753 (0.0353)	0.0176 (0.0082)	0.0490 (0.0566)	0.0172 (0.0200)
β_2	0.8708 (0.0390)	0.8801 (0.0450)	0.8958 (0.0487)	0.9008 (0.0828)	0.8864 (0.0547)	0.9676 (0.0111)	0.9315 (0.0935)	0.9692 (0.1289)
ν								
γ		0.0555 (0.0124)		<i>0.0305</i> (0.0183)		0.0518 (0.0155)		0.0505 (0.0081)
ϕ			-0.0382 (0.0190)	<i>-0.0364</i> (0.0195)			-0.0421 (0.0257)	-0.0457 (0.0223)
δ_1	0.5958 (0.0265)	0.5856 (0.0270)	0.5943 (0.0263)	0.5855 (0.0263)	0.4238 (0.0243)	0.4130 (0.0185)	0.4221 (0.0242)	0.4123 (0.0656)
δ_2	0.0686 (0.0214)	0.0623 (0.0219)	0.0678 (0.0212)	0.0605 (0.0214)	0.0387 (0.0175)	<i>0.0328</i> (0.0185)	0.0377 (0.0176)	0.0331 (0.0166)
df					7.0510 (2.5636)	6.6308 (1.6799)	7.1301 (2.6175)	6.8784 (1.9001)
LL	-3116.94	-3108.74	-3110.54	-3104.85	-3041.29	-3028.77	-3037.87	-3025.04
AIC	6241.87	6227.48	6231.07	6221.70	6092.58	6069.53	6087.75	6064.08
BIC	6257.39	6246.88	6250.47	6244.99	6111.99	6092.82	6111.03	6091.24

Table 1.15: Estimation Results of Global Equity Comovement: DECO Estimates, No Domestic Comovement Part.

This table provides one of the robustness checks of the global equity correlation estimates involving the FTS channel (as in Table 1.3). Here, I directly estimate the DECO model with tests. Model estimation uses MLE at monthly frequency covering period from March 1987 to December 2016 (T=358), and model selection follows BIC. Bold (italics) values indicate <5% (10%) significance level.

	<i>Multivariate Gaussian</i>					<i>Multivariate t</i>				
	E (10)	E (11)	E (12)	E (13)	E (14)	E (10)	E (11)	E (12)	E (13)	E (14)
β_1	0.0883 (0.0313)	<i>0.0725</i> (0.0384)	0.0497 (0.0219)	0.0515 (0.1016)	0.0985 (0.0329)	0.0612 (0.0138)	0.0281 (0.0249)	0.0599 (0.0117)	0.0225 (0.0104)	0.1041 (0.0287)
β_2	0.8905 (0.0431)	0.8942 (0.0449)	0.9485 (0.0281)	0.9058 (0.1418)	0.8693 (0.0444)	0.9388 (0.0143)	0.9520 (0.0348)	0.9401 (0.0123)	0.9617 (0.0142)	0.8482 (0.0349)
ν					0.2072 (0.0539)					0.2800 (0.0358)
γ		0.0559 (0.0106)		0.0588 (0.0136)			0.0579 (0.0135)		0.0533 (0.0065)	
ϕ			<i>0.0432</i> (0.0252)	0.0394 (0.0201)				<i>0.0259</i> (0.0141)	<i>0.0386</i> (0.0207)	
δ_1										
δ_2										
df						7.3522 (2.5334)	5.8748 (1.8115)	7.6657 (2.6764)	6.1025 (1.9130)	6.6052 (2.1257)
LL	-3120.24	-3118.03	-3117.13	-3114.15	-3120.47	-3042.07	-3030.19	-3038.64	-3027.17	-3042.15
AIC	6244.48	6242.06	6240.25	6236.31	6246.94	6090.13	6068.37	6085.28	6064.33	6092.29
BIC	6252.24	6253.70	6251.89	6251.83	6258.58	6101.77	6083.90	6100.80	6083.74	6107.81
				BEST					BEST	

Table 1.16: Factor Exposures of Global Asset Returns in a Seemingly Unrelated Regression (SUR) Frameworks; Constant Beta.

In this table, I jointly estimate the constant exposures of global equity and bond returns to global factor shocks in a SUR framework. The error terms may have cross-equation contemporaneous correlations. SUR models are estimated with MLE. The sample period covers from March 1987 to February 2015; February 2015 is the last month given the availability of the risk aversion estimate from Bekaert, Engstrom, and Xu, 2017. Standard errors are shown in the parentheses. Bold (italics) values indicate <5% (10%) significance level.

Seemingly Unrelated Regressions with Returns in USD; Constant Beta														
	ω_g		ω_{θ_u}		ω_{θ_d}		ω_{π_u}		ω_{π_d}		ω_{x_u}		ω_{x_d}	
USA Equity	-0.1734	(0.0128)	-0.0003	(0.0001)	-0.0001	(0.0008)	-0.0022	(0.0010)	0.0001	(0.0004)	0.0002	(0.0002)	0.0003	(0.0002)
CAN Equity	-0.1811	(0.0178)	-0.0005	(0.0001)	-0.0006	(0.0011)	-0.0038	(0.0015)	-0.0016	(0.0005)	-0.0001	(0.0003)	<i>0.0006</i>	(0.0003)
DEU Equity	-0.2245	(0.0218)	-0.0001	(0.0001)	0.0004	(0.0014)	<i>-0.0032</i>	(0.0018)	-0.0004	(0.0006)	0.0004	(0.0003)	0.0003	(0.0004)
FRA Equity	-0.1942	(0.0202)	-0.0003	(0.0001)	-0.0005	(0.0013)	-0.0040	(0.0016)	-0.0001	(0.0006)	0.0007	(0.0003)	0.0005	(0.0003)
GBR Equity	-0.1452	(0.0163)	-0.0004	(0.0001)	-0.0014	(0.0010)	-0.0017	(0.0013)	-0.0002	(0.0005)	<i>-0.0005</i>	(0.0003)	0.0002	(0.0003)
CHE Equity	-0.1524	(0.0170)	-0.0003	(0.0001)	-0.0009	(0.0011)	-0.0010	(0.0014)	0.0002	(0.0005)	0.0001	(0.0003)	0.0004	(0.0003)
JPN Equity	-0.0833	(0.0225)	-0.0001	(0.0002)	0.0018	(0.0014)	-0.0021	(0.0018)	-0.0003	(0.0006)	-0.0001	(0.0004)	0.0005	(0.0004)
AUS Equity	-0.1829	(0.0220)	-0.0007	(0.0001)	-0.0020	(0.0014)	<i>-0.0031</i>	(0.0018)	-0.0007	(0.0006)	-0.0005	(0.0004)	0.0008	(0.0004)
USA Gov-Bond	0.0280	(0.0076)	0.0000	(0.0001)	0.0007	(0.0005)	-0.0016	(0.0006)	0.0005	(0.0002)	0.0000	(0.0001)	-0.0001	(0.0001)
CAN Gov-Bond	-0.0345	(0.0103)	0.0000	(0.0001)	0.0009	(0.0007)	-0.0027	(0.0008)	-0.0003	(0.0003)	-0.0001	(0.0002)	0.0002	(0.0002)
DEU Gov-Bond	0.0095	(0.0123)	0.0000	(0.0001)	0.0005	(0.0008)	-0.0024	(0.0010)	-0.0009	(0.0004)	0.0000	(0.0002)	0.0000	(0.0002)
FRA Gov-Bond	0.0043	(0.0121)	0.0000	(0.0001)	0.0004	(0.0008)	-0.0027	(0.0010)	-0.0008	(0.0003)	0.0000	(0.0002)	0.0000	(0.0002)
GBR Gov-Bond	0.0241	(0.0119)	0.0001	(0.0001)	0.0002	(0.0008)	-0.0014	(0.0010)	-0.0004	(0.0003)	<i>-0.0003</i>	(0.0002)	0.0000	(0.0002)
CHE Gov-Bond	0.0125	(0.0134)	0.0001	(0.0001)	0.0003	(0.0009)	-0.0014	(0.0011)	-0.0003	(0.0004)	-0.0002	(0.0002)	0.0000	(0.0002)
JPN Gov-Bond	0.0334	(0.0142)	0.0000	(0.0001)	0.0002	(0.0009)	0.0010	(0.0012)	-0.0002	(0.0004)	0.0000	(0.0002)	0.0001	(0.0002)
AUS Gov-Bond	-0.0467	(0.0132)	-0.0003	(0.0001)	<i>-0.0014</i>	(0.0008)	-0.0030	(0.0011)	<i>-0.0006</i>	(0.0004)	-0.0003	(0.0002)	<i>0.0004</i>	(0.0002)

Table 1.17: Factor Exposures of Global Asset Returns in Seemingly Unrelated Regression (SUR) Framework; USD; Time-Varying Beta.

In this table, I jointly estimate the time-varying exposures of global equity and bond returns (in USD) to global factor shocks in a SUR framework. The error terms may have cross-equation contemporaneous correlations. SUR models are estimated with MLE. The sample period covers from March 1987 to February 2015. Standard errors are shown in the parentheses. Bold (italics) values indicate <5% (10%) significance level.

β_0	ω_q	$\omega_{\theta u}$	$\omega_{\theta d}$	$\omega_{\pi u}$	$\omega_{\pi d}$	$\omega_{\pi u}$	$\omega_{\pi d}$	$\omega_{\pi u}$	$\omega_{\pi d}$	ω_{xu}	ω_{xd}	ω_{xu}	ω_{xd}	
USA Equity	-0.1687	(0.0129)	-0.0003	(0.0001)	0.0011	(0.0010)	<i>-0.0034</i>	(0.0018)	0.0002	(0.0004)	0.0001	(0.0002)	0.0003	(0.0002)
CAN Equity	-0.1790	(0.0179)	-0.0005	(0.0001)	0.0011	(0.0015)	-0.0031	(0.0024)	-0.0015	(0.0005)	-0.0003	(0.0003)	<i>0.0007</i>	(0.0003)
DEU Equity	-0.2254	(0.0220)	-0.0001	(0.0002)	0.0020	(0.0018)	0.0001	(0.0030)	-0.0005	(0.0007)	0.0006	(0.0004)	0.0002	(0.0004)
FRA Equity	-0.1932	(0.0205)	-0.0003	(0.0001)	0.0007	(0.0017)	-0.0016	(0.0028)	-0.0001	(0.0006)	0.0008	(0.0004)	0.0003	(0.0004)
GBR Equity	-0.1432	(0.0163)	-0.0004	(0.0001)	0.0007	(0.0013)	-0.0006	(0.0022)	-0.0002	(0.0005)	<i>-0.0005</i>	(0.0003)	-0.0001	(0.0003)
CHE Equity	-0.1493	(0.0172)	-0.0003	(0.0001)	0.0001	(0.0014)	-0.0003	(0.0023)	0.0002	(0.0005)	0.0001	(0.0003)	0.0003	(0.0003)
JPN Equity	-0.0858	(0.0225)	-0.0001	(0.0002)	<i>0.0035</i>	(0.0018)	0.0005	(0.0031)	-0.0001	(0.0007)	-0.0001	(0.0004)	0.0005	(0.0004)
AUS Equity	-0.1846	(0.0222)	-0.0007	(0.0002)	-0.0008	(0.0018)	0.0004	(0.0030)	-0.0004	(0.0007)	<i>-0.0006</i>	(0.0004)	<i>0.0007</i>	(0.0004)
USA Gov-Bond	0.0303	(0.0078)	0.0000	(0.0001)	<i>0.0010</i>	(0.0006)	0.0001	(0.0013)	0.0005	(0.0002)	0.0001	(0.0001)	-0.0002	(0.0002)
CAN Gov-Bond	-0.0386	(0.0105)	0.0000	(0.0001)	<i>0.0016</i>	(0.0008)	0.0013	(0.0017)	-0.0002	(0.0003)	-0.0002	(0.0002)	0.0001	(0.0002)
DEU Gov-Bond	-0.0024	(0.0125)	0.0001	(0.0001)	0.0010	(0.0010)	0.0003	(0.0020)	-0.0008	(0.0004)	-0.0002	(0.0002)	-0.0002	(0.0002)
FRA Gov-Bond	-0.0083	(0.0122)	0.0000	(0.0001)	0.0009	(0.0010)	0.0002	(0.0020)	-0.0007	(0.0003)	-0.0002	(0.0002)	-0.0002	(0.0002)
GBR Gov-Bond	0.0134	(0.0122)	0.0001	(0.0001)	0.0002	(0.0010)	0.0006	(0.0020)	-0.0003	(0.0003)	-0.0004	(0.0002)	-0.0003	(0.0002)
CHE Gov-Bond	-0.0012	(0.0137)	0.0001	(0.0001)	-0.0001	(0.0011)	0.0005	(0.0022)	-0.0003	(0.0004)	-0.0003	(0.0002)	-0.0002	(0.0003)
JPN Gov-Bond	0.0314	(0.0146)	0.0000	(0.0001)	-0.0003	(0.0012)	-0.0008	(0.0024)	-0.0002	(0.0004)	-0.0001	(0.0002)	0.0002	(0.0003)
AUS Gov-Bond	-0.0614	(0.0132)	-0.0002	(0.0001)	-0.0013	(0.0010)	0.0027	(0.0022)	-0.0004	(0.0004)	-0.0005	(0.0002)	0.0002	(0.0003)
β_1 for Equities	$\omega_q * s_e$	$\omega_{\theta u} * s_e$	$\omega_{\theta d} * s_e$	$\omega_{\pi u} * s_e$	$\omega_{\pi d} * s_e$	$\omega_{\pi u} * s_e$	$\omega_{\pi d} * s_e$	$\omega_{\pi u} * s_e$	$\omega_{\pi d} * s_e$	$\omega_{xu} * s_e$	$\omega_{xd} * s_e$	$\omega_{xu} * s_e$	$\omega_{xd} * s_e$	
USA Equity	-0.0068	(0.0142)	0.0001	(0.0001)	<i>-0.0011</i>	(0.0006)	0.0006	(0.0008)	0.0006	(0.0006)	-0.0004	(0.0003)	0.0000	(0.0002)
CAN Equity	-0.0144	(0.0198)	-0.0001	(0.0002)	-0.0020	(0.0008)	-0.0004	(0.0011)	0.0002	(0.0008)	<i>-0.0009</i>	(0.0005)	-0.0003	(0.0003)
DEU Equity	-0.0527	(0.0243)	0.0000	(0.0002)	-0.0016	(0.0010)	-0.0029	(0.0014)	-0.0011	(0.0010)	0.0003	(0.0006)	-0.0001	(0.0004)
FRA Equity	-0.0299	(0.0226)	0.0002	(0.0002)	-0.0013	(0.0010)	-0.0018	(0.0013)	-0.0009	(0.0009)	-0.0003	(0.0005)	-0.0001	(0.0003)
GBR Equity	-0.0109	(0.0181)	0.0001	(0.0002)	-0.0020	(0.0008)	-0.0013	(0.0010)	-0.0007	(0.0007)	-0.0001	(0.0004)	0.0001	(0.0003)
CHE Equity	<i>-0.0349</i>	(0.0190)	0.0003	(0.0002)	-0.0007	(0.0008)	-0.0010	(0.0011)	-0.0002	(0.0008)	0.0001	(0.0005)	0.0001	(0.0003)
JPN Equity	-0.0537	(0.0249)	0.0002	(0.0002)	-0.0013	(0.0011)	-0.0015	(0.0014)	0.0011	(0.0010)	-0.0001	(0.0006)	0.0003	(0.0004)
AUS Equity	-0.0500	(0.0245)	0.0000	(0.0002)	-0.0014	(0.0010)	-0.0017	(0.0014)	0.0002	(0.0010)	-0.0008	(0.0006)	0.0000	(0.0004)
β_1 for Bonds	$\omega_q * s_b$	$\omega_{\theta u} * s_b$	$\omega_{\theta d} * s_b$	$\omega_{\pi u} * s_b$	$\omega_{\pi d} * s_b$	$\omega_{\pi u} * s_b$	$\omega_{\pi d} * s_b$	$\omega_{\pi u} * s_b$	$\omega_{\pi d} * s_b$	$\omega_{xu} * s_b$	$\omega_{xd} * s_b$	$\omega_{xu} * s_b$	$\omega_{xd} * s_b$	
USA Gov-Bond	0.0035	(0.0068)	0.0000	(0.0001)	0.0006	(0.0005)	<i>0.0018</i>	(0.0010)	-0.0003	(0.0003)	-0.0003	(0.0001)	-0.0002	(0.0001)
CAN Gov-Bond	0.0138	(0.0092)	0.0000	(0.0001)	0.0017	(0.0007)	0.0036	(0.0013)	-0.0001	(0.0003)	0.0001	(0.0002)	0.0000	(0.0002)
DEU Gov-Bond	0.0372	(0.0109)	<i>0.0002</i>	(0.0001)	0.0008	(0.0008)	0.0018	(0.0015)	-0.0003	(0.0004)	0.0001	(0.0002)	-0.0002	(0.0002)
FRA Gov-Bond	0.0370	(0.0106)	0.0002	(0.0001)	0.0011	(0.0008)	0.0020	(0.0015)	-0.0004	(0.0004)	0.0002	(0.0002)	-0.0001	(0.0002)
GBR Gov-Bond	0.0276	(0.0106)	0.0002	(0.0001)	0.0003	(0.0008)	0.0010	(0.0015)	0.0001	(0.0004)	0.0003	(0.0002)	-0.0003	(0.0002)
CHE Gov-Bond	0.0411	(0.0120)	0.0002	(0.0001)	-0.0003	(0.0009)	0.0010	(0.0017)	0.0002	(0.0004)	0.0001	(0.0002)	0.0000	(0.0002)
JPN Gov-Bond	-0.0011	(0.0128)	0.0001	(0.0001)	-0.0010	(0.0009)	-0.0021	(0.0018)	-0.0012	(0.0005)	0.0001	(0.0002)	0.0000	(0.0003)
AUS Gov-Bond	0.0350	(0.0116)	0.0000	(0.0001)	0.0010	(0.0008)	0.0042	(0.0016)	<i>-0.0007</i>	(0.0004)	0.0005	(0.0002)	0.0000	(0.0002)

2

PROCYCLICALITY OF THE COMOVEMENT BETWEEN DIVIDEND GROWTH AND CONSUMPTION GROWTH

I document that dividend growth and consumption growth comove procyclically. This new stylized fact empirically resolves the “Duffee Puzzle”—stock returns and consumption growth covary procyclically (Duffee, 2005)—but contradicts extant theoretical assumptions in asset pricing models. I then design a new data generating process (DGP) for the joint consumption-dividend dynamics which fits the procyclical comovement and a wide set of other related second moments. Lastly, I solve a variant of Campbell and Cochrane’s habit formation model with this new DGP and the procyclical consumption-dividend growth comovement as a new state variable. The new procyclical component in the amount of risk induces a more volatile price-dividend ratio at the cost of a lower equity premium due to the now counterbalancing dynamics of the price (countercyclical) and amount (procyclical) of risk. In addition, the new state variable accounts for 13% of the variability of the price dividend ratio in the data and carries a positive price of risk in the cross-section of stock returns.

2.1 Introduction

Duffee (2005) documents that the amount of consumption risk, that is the conditional covariance between equity returns and consumption growth, is procyclical. Provided that many well-accepted theories imply a constant (e.g., Bansal and Yaron, 2004) or countercyclical (e.g.,

Campbell and Cochrane, 1999) amount of risk, I identify and coin Duffee (2005)’s finding the “Duffee Puzzle.”

In this article, I first empirically demonstrate that this procyclicality is generated by a procyclical comovement between the cash flow part of the market return and consumption growth, and establish a set of new empirical facts regarding consumption growth, dividend growth, and the amount of risk. Then, I propose a new data generating process (DGP) for the joint dynamics of consumption and dividend growth that makes the empirical findings amenable to consumption-based asset pricing models. Lastly, I explore how incorporating more realistic dynamics into the amount of risk affects the performance of extant dynamic asset pricing models.

Using a flexible empirical framework and a longer sample period (January 1959–June 2014) than the one used in Duffee (2005), the empirical part of this article continues to find robust evidence for the procyclical conditional correlation *and* conditional covariance between market returns and consumption growth. Then, I decompose the amount of risk into two components,

$$Cov_t(r_{t+1}^m, \Delta c_{t+1}) = \underbrace{Cov_t(\Delta d_{t+1}, \Delta c_{t+1})}_{\text{Exogenous}} + \underbrace{Cov_t(r_{t+1}^m - \Delta d_{t+1}, \Delta c_{t+1})}_{\text{Endogenous}}, \quad (2.T1)$$

where r_{t+1}^m is the log market return, Δc_{t+1} the log consumption growth, and Δd_{t+1} the log dividend growth. The decomposition of the amount of consumption risk yields a conditional covariance, $Cov_t(\Delta d_{t+1}, \Delta c_{t+1})$, which is modeled *exogenously* in the extant consumption-based asset pricing literature, and an *endogenous* conditional covariance, $Cov_t(r_{t+1}^m - \Delta d_{t+1}, \Delta c_{t+1})$. Although there is limited research on the cyclicity of the endogenous component above, both extant theories and empirical evidence suggest that the comovement between changes in the log price dividend ratio—a linear proxy for the non-dividend part of the market return—and consumption growth is not procyclical. Therefore, the covariance between dividend and consumption growth must be strongly procyclical in order to explain the Duffee Puzzle. Such procyclical comovement between dividend and consumption growth could arise from managers’ preference for dividend smoothing. According to Lintner (1956) and a follow-up study by Brav, Graham, Harvey, and Michaely (2005), a “prudent foresighted” manager is reluctant to cut dividends when

the economy is in a downturn unless he/she expects the decrease in earnings to be persistent.¹ As a result, changes in financial payouts are expected to be less associated with macroeconomic shocks during bad times than during normal times.

Indeed, I find that the exogenous component of the amount of risk behaves *procyclically* and the endogenous component behaves *countercyclically*. My results are robust to using various measures of the consumption growth innovations, different estimates of the conditional variances, and different proxies for cash flow growth rates (e.g., earnings growth instead of dividend growth). To quantify the significance of the procyclical exogenous component in explaining the procyclical amount of risk, my empirical results reveal that the share, $\frac{Cov_t(\Delta d_{t+1}, \Delta c_{t+1})}{Cov_t(r_{t+1}^m, \Delta c_{t+1})}$, is surprisingly volatile over the business cycle, reaching a peak of 106% during the 1960s expansion and a trough of -89% following the 1969-70 recession. The empirical part of the paper concludes with a comprehensive list of ten stylized facts pertinent to the Duffee Puzzle and its components. In particular, all three comovement statistics (the conditional correlation, covariance and beta of dividend growth to consumption growth) are shown to be procyclical, while the conditional variance of consumption growth is heteroskedastic and countercyclical.

Next, I formulate a parsimonious DGP for the joint dynamics of consumption and dividend growth with a minimum number of state variables that matches the stylized facts. In contrast, as I discuss in detail in Section 3.3, state-of-the-art consumption-based asset pricing models mostly assume unrealistic joint dynamics between consumption growth (which enters the utility function) and dividend growth (which constitutes the cash flow process of the equity claim to be priced).

The new DGP exhibits two empirically salient features. First, I introduce a new state variable b capturing a time-varying sensitivity of dividend growth to consumption growth (or dividend-consumption beta). In particular, this state variable is procyclical as it comoves positively with consumption growth (the only macroeconomic variable in consumption-based asset pricing framework). The procyclical dividend beta is new to the literature, both empirically and

¹Since Lintner (1956), theories of why firms smooth their dividends are primarily based on either asymmetric information (Kumar, 1988; Brennan and Thakor, 1990; Fudenberg and Tirole, 1995; DeMarzo and Sannikov, 2008; Guttman, Kadan, and Kandel, 2010) or agency considerations (Allen, Bernardo, and Welch, 2000; DeAngelo and DeAngelo, 2007; Lambrecht and Myers, 2012).

theoretically.

Second, to ensure the simultaneous fit of (1) procyclical correlation and covariance between consumption and dividend growth and (2) countercyclical consumption growth variance, I allow consumption growth to receive two independent shocks each period, a homoskedastic Gaussian shock named the “fundamental shock” and an asymmetric heteroskedastic gamma shock named the “event shock”. To justify the decomposition, I apply the filtration-based maximum likelihood methodology (Bates, 2006) to obtain the fundamental and event shock realizations, and provide economic interpretations of the two consumption shocks:

The (filtered) fundamental shock, behaving procyclically, explains most of the total consumption growth variability during the sample period and has a significant and negative correlation with the detrended consumption-wealth ratio introduced by Lettau and Ludvigson (2001)—which is consistent with my DGP. In my DGP, dividend growth is sensitive to the contemporaneous consumption fundamental shock with a persistent procyclical beta that also comoves positively with the fundamental shock. Suppose a positive fundamental shock arrives this period. The persistent procyclical dividend beta is expected to remain *high* in the future. Because dividend growth variance increases with dividend beta, it is the persistently *high* dividend growth variance in expectations that gets capitalized in financial wealth, driving up the wealth-consumption ratio in the current period. The event shocks, behaving countercyclically, drive the countercyclicality of the consumption growth variance. The conditional variance of the event shock constitutes the second state variable of the new DGP: macroeconomic uncertainty, denoted as n .

In the last part of the paper, I formally demonstrate the ability of the new DGP to generate realistic dynamics of the amount of risk in a variant of the Campbell and Cochrane model (henceforth, CC)—thus accommodating the Duffee Puzzle—and explore new asset pricing implications of the new state variable b . While the time variation in the price of risk, as in the standard CC model, is driven by the procyclical surplus consumption ratio (s), the time variation in the amount of risk is now determined by two countervailing sources, which is consistent with the empirical evidence of the Duffee Puzzle decomposition. More precisely, the amount of risk now

contains both procyclical and countercyclical sources generated from the dividend-consumption comovement (b) and the macroeconomic uncertainty (n), respectively. Hence, in my model, the procyclical comovement risk counteracts the countercyclical volatility risk and the endogenous countercyclical price of risk, rendering the equity claim less risky. In addition, this economy generates a more volatile price-dividend ratio than a standard CC model due to the additional variability introduced by the additional amount-of-risk state variables (b and n). The relationship between the price-dividend ratio and the new state variable b , controlling for the pricing effects of the other two state variables in this economy, is positive through a dominant cash flow channel: the persistent procyclical consumption-dividend comovement results in persistent procyclical cash flow volatility, which gets capitalized in equity prices.

As an important byproduct, this theoretical framework allows me to study the relative importance of time-varying price and quantity of risk in price variability. According to both empirical and simulated datasets, I find that the two amount-of-risk state variables (b and n) jointly explain about 30% of the fitted price-dividend ratio variance, leaving the only price-of-risk state variable (s) the dominant source.

To further support the procyclical comovement channel, I provide direct evidence for the pricing of the consumption-dividend comovement risk in the cross section, controlling for market excess returns and innovations to the other two state variables. Using Fama and MacBeth (1973) regressions for the 25 size- and book-to-market-sorted portfolios of Fama and French (1993), I find a significant and positive price of consumption-dividend comovement risk, consistent with the theory. That is, stocks covarying more with aggregate dividend risk are riskier, because the dividend risk is procyclical. Growth stocks exhibit significantly lower (or even negative for the Large-Growth bin) b loadings than value stocks; this model thus explains 75% of the value premium.

The outline of the paper is as follows. Section 3.2 replicates the main empirical finding in Duffee (2005) and examines the cyclicity of the exogenous and endogenous amount-of-risk components. Section 3.3 formulates and estimates the new DGP. Section 3.4 analyzes a variant of Campbell and Cochrane's habit formation model that accommodates the Duffee Puzzle. Sec-

tion 3.6 provides the cross-sectional evidence. Concluding comments are offered in Section 3.7.

2.2 The Duffee Puzzle Revisited, Econometrically

The decomposition of the amount of consumption risk, as shown in Equation (2.T1), yields an *exogenous* conditional covariance, $Cov_t(\Delta d_{t+1}, \Delta c_{t+1})$, and an *endogenous* conditional covariance, $Cov_t(r_{t+1}^m - \Delta d_{t+1}, \Delta c_{t+1})$. In this section, I exploit a bivariate dynamic dependence model in the GARCH class in a flexible way to replicate the Duffee Puzzle and identify the cyclicity of the two conditional comovements that constitute the puzzle.

2.2.1 The Model

The empirical analysis uses four variables as follows: consumption growth, the change in the log monthly consumption level, $\Delta c_{t+1} = \log(C_{t+1}) - \log(C_t)$; dividend growth, $\Delta d_{t+1} = \log(D_{t+1}) - \log(D_t)$; the log market return, $r_{t+1}^m = \log\left(\frac{P_{t+1} + D_{t+1}}{P_t}\right)$; and the difference between the log market return and dividend growth (namely, the non-dividend part of the market return), $r_{t+1}^m - \Delta d_{t+1}$. First, I project each series or its filtered counterpart (see Section 3.3) onto an exogenous business cycle indicator (1=recession, 0=non-recession) to obtain the series residuals. Consider a bivariate system,

$$\tilde{\boldsymbol{\epsilon}}_{t+1} \equiv \begin{bmatrix} \tilde{\epsilon}_{1,t+1} & \tilde{\epsilon}_{2,t+1} \end{bmatrix}', \quad (2.T2)$$

where, in this paper, $\tilde{\epsilon}_{1,t+1}$ is the consumption growth residual (denoted by $\tilde{\epsilon}_{c,t+1}$) from t to $t + 1$, and $\tilde{\epsilon}_{2,t+1}$ is either the market return residual ($\tilde{\epsilon}_{rm,t+1}$), the dividend growth residual ($\tilde{\epsilon}_{d,t+1}$), or the non-dividend part residual ($\tilde{\epsilon}_{rmd,t+1}$). The conditional variance-covariance matrix of the residuals is defined as,

$$\mathbf{H}_t \equiv E_t [\tilde{\boldsymbol{\epsilon}}_{t+1} \tilde{\boldsymbol{\epsilon}}_{t+1}']. \quad (2.T3)$$

I follow Engle (2002) and express \mathbf{H}_t in a quadratic form in order to estimate the conditional variances (diagonal elements) and the conditional correlation (off-diagonal elements) in two sepa-

rate steps,

$$\mathbf{H}_t = \mathbf{\Lambda}_t \mathbf{Corr}_t \mathbf{\Lambda}_t, \quad (2.T4)$$

where the diagonal terms of $\mathbf{\Lambda}_t$ (2×2) are the square roots of the conditional variances of $\tilde{\epsilon}_{1,t+1}$ and $\tilde{\epsilon}_{2,t+1}$ and the off-diagonal terms of $\mathbf{\Lambda}_t$ equal 0, or $\mathbf{\Lambda}_t \mathbf{\Lambda}_t' = \begin{bmatrix} h_{1,t} & 0 \\ 0 & h_{2,t} \end{bmatrix}$ (discussed in Section 2.2.1.1); \mathbf{Corr}_t (2×2) is the conditional correlation matrix (discussed in Section 2.2.1.2).

2.2.1.1 Conditional Volatility

The empirical literature lacks consensus about how to model the dynamics of consumption and dividend growth volatility, although researchers have provided empirical evidence for heteroskedasticity (e.g., Kandel and Stambaugh, 1990; Lettau, Ludvigson, and Wachter, 2008) and non-Gaussianity (e.g., Bekaert and Engstrom, 2017). In contrast, the evidence for heteroskedasticity and non-Gaussianity in market returns is usually found to be strong and robust. Here, I consider four conditional variance models (in the GARCH class) that identify the cyclicity of the conditional variance within the model and test for heteroskedasticity and non-Gaussianity.

The first conditional variance model assumes constant variances that are allowed to be different during recession and non-recession periods. Suppose the residual follows a conditional Gaussian distribution, $\tilde{\epsilon}_{t+1} \sim N(0, h_t)$,² and the conditional variance follows a process,

$$h_t = \bar{h} (1 + q_t). \quad (2.T5)$$

where \bar{h} denotes the predetermined unconditional variance and the process of q_t is a multiple of the standardized NBER recession indicator (denoted as $SNBER_t$)³ so that the average condi-

²The subscript i to denote a specific series in all conditional variance models of Section 2.2.1.1 is omitted for simplicity.

$$SNBER_t \equiv \frac{I_{NBER,t} - E(I_{NBER,t})}{SD(I_{NBER,t})} = \begin{cases} SNBER^{recc.} > 0 & \text{during recession periods} \\ SNBER^{non-recc.} < 0 & \text{during non-recession periods} \end{cases},$$

where $I_{NBER,t}$ is the NBER recession indicator obtained from the NBER website.

tional variance, $E(h_t)$, is \bar{h} ,

$$q_t = \nu SNBER_t, \quad (2.T6)$$

where ν is a scalar. The zero-mean business cycle indicator, q_t , is the key variable to identify the cyclicity within the model. A positive (negative) coefficient estimate of ν suggests a counter-cyclical (procyclical) conditional variance; a zero estimate fails to reject the null of a constant variance.⁴

In the second and third models, the conditional variances follow autoregressive conditional heteroskedastic processes where the long-run conditional means are allowed to be different during recession and non-recession periods,

$$h_t = \bar{h}(1 + q_t) + \alpha [\tilde{\epsilon}_t^2 - \bar{h}(1 + q_{t-1})] + \beta [h_{t-1} - \bar{h}(1 + q_{t-1})], \quad (2.T7)$$

where $\alpha + \beta < 1$, $\alpha > 0$, $\beta > 0$; “ $\bar{h}(1 + q_t)$ ” denotes the long-run conditional mean of the conditional variance and q_t was introduced in Equation (2.T6). The second and third models impose different distributional assumptions: the second model assumes a conditional Gaussian distribution, $\tilde{\epsilon}_{t+1} \sim N(0, h_t)$, and the third model assumes a symmetric leptokurtic conditional Generalized Error Distribution, $\tilde{\epsilon}_{t+1} \sim GED(0, h_t, \tau)$ where the shape parameter τ determines the thickness of both tails. In particular, a zero ν estimate reduces Equation (2.T7) to a GARCH model (Bollerslev, 1987) in the second model or a GED-GARCH model (Nelson, 1991) in the third model. The first model is a special case of the second model.

The fourth model is introduced to account for conditional asymmetry. I adapt the “Bad Environment-Good Environment” (BEGE) framework in Bekaert, Engstrom, and Ermolov (2015) to include a long-run conditional mean that depends on the cycle variable q_t . The residual is a composite shock with two centered gamma shocks: $\tilde{\epsilon}_{t+1} = \sigma_{cp}\tilde{\omega}_{cp,t+1} - \sigma_{cn}\tilde{\omega}_{cn,t+1}$ where $\tilde{\omega}_{cp,t+1} \sim \tilde{\Gamma}(\bar{cp}, 1)$ denotes a centered homoskedastic gamma shock governing the right-tail skewness and $\tilde{\omega}_{cn,t+1} \sim \tilde{\Gamma}(cn_t, 1)$ denotes a centered heteroskedastic gamma shock governing

⁴This instrument approach is popular in empirical studies (see, e.g., Campbell, 1987; Shanken, 1990; Bekaert and Harvey, 1995; Duffee, 2005, among many others).

the left-tail skewness (given the minus sign); \overline{cp} (> 0) and cn_t (> 0) denote the shape parameters of the two independent gamma shocks, respectively; σ_{cp} and σ_{cn} denote the scale parameters (> 0), and the conditional variance and unscaled skewness are $h_t = \sigma_{cp}^2 \overline{cp} + \sigma_{cn}^2 cn_t$ and $skew_t = 2\sigma_{cp}^3 \overline{cp} - 2\sigma_{cn}^3 cn_t$, respectively. Thus, cn_t drives the time variation in the total conditional variance, and has the following process:

$$cn_t = \overline{cn}(1 + q_t) + \alpha_{cn} \left[\frac{\tilde{\epsilon}_t^2}{2\sigma_{cn}^2} - \overline{cn}(1 + q_{t-1}) \right] + \beta_{cn} [cn_{t-1} - \overline{cn}(1 + q_{t-1})], \quad (2.T8)$$

where $\alpha_{cn} + \beta_{cn} < 1$, $\alpha_{cn} > 0$, $\beta_{cn} > 0$; “ $\overline{cn}(1 + q_t)$ ” denotes the long-run conditional mean of the downside uncertainty where \overline{cn} (> 0) is the long-run unconditional mean. Note that, as in Bekaert, Engstrom, and Ermolov (2015), the squared residual is scaled by the squared scale parameter of the respective gamma distribution. Because the dynamics of the shape parameter cn_t depend on the observed residual $\tilde{\epsilon}_t$ and not the latent gamma shock $\tilde{\omega}_{cn,t}$, the model remains in the GARCH class without requiring filtering these gamma shocks.

2.2.1.2 Conditional Correlation

I follow Engle (2002) to model the conditional correlation matrix \mathbf{Corr}_t in Equation (2.T4) with a quadratic form, $(\mathbf{Q}_t^*)^{-1} \mathbf{Q}_t (\mathbf{Q}_t^*)^{-1}$, where \mathbf{Q}_t^* is the diagonal matrix with the square roots of the diagonal elements of \mathbf{Q}_t on the diagonal (so the diagonal entries of \mathbf{Corr}_t are strictly equal to 1). The off-diagonal element of \mathbf{Corr}_t is the conditional correlation (or equivalently, the conditional covariance) of the standardized residuals, $\mathbf{z}_{t+1} \equiv \begin{bmatrix} z_{1,t+1} & z_{2,t+1} \end{bmatrix}' = \mathbf{\Lambda}_t^{-1} \tilde{\epsilon}_{t+1}$.

The present model differs from Engle (2002)’s dynamic conditional correlation model (DCC), who assumes a constant long-run mean of the dynamic correlation, and from Colacito, Engle, and Ghysels (2011), who use a weighted average of past correlations to model the long-run conditional mean. Instead, the DCC- q_t model proposed here models the long-run conditional mean as a linear function of an exogenous business cycle indicator. Thus, the DCC- q_t model

directly tests the cyclicity of the conditional correlation between the two variables-of-interest:

$$\mathbf{Q}_t = \bar{Q}_{12} \begin{bmatrix} 1 & 1 + q_t \\ 1 + q_t & 1 \end{bmatrix} + \alpha_{12} \left[\mathbf{z}_t \mathbf{z}_t' - \bar{Q}_{12} \begin{bmatrix} 1 & 1 + q_{t-1} \\ 1 + q_{t-1} & 1 \end{bmatrix} \right] + \beta_{12} \left[\mathbf{Q}_{t-1} - \bar{Q}_{12} \begin{bmatrix} 1 & 1 + q_{t-1} \\ 1 + q_{t-1} & 1 \end{bmatrix} \right], \quad (2.T9)$$

where the parameter \bar{Q}_{12} denotes the the predetermined constant conditional correlation between the standardized residuals. Note that Engel (2002)'s DCC model is a special case with $\nu = 0$. To summarize, the bivariate GARCH DCC- q_t model captures correlation clustering as observed in data, while the long-run conditional mean links the conditional correlation to the business cycle.⁵

2.2.2 Data

The empirical part of the paper involves four key variables: consumption growth, dividend growth, the equity market return, and the non-dividend part of the market return. I follow Duffee (2005) to use monthly data indexed with t . The sample spans the period from January 1959 to June 2014. Monthly real consumption per capita is defined as the sum of seasonally adjusted real aggregate expenditures on nondurable goods and services divided by monthly estimates of population (source: U.S. Bureau of Economic Analysis, BEA). Note that the realized deflators for aggregate nondurable and services consumption are different (source: BEA). Monthly seasonally adjusted dividend and earnings per market share are collected by Shiller (1989) and available on his website. The number of market shares is obtained by dividing the monthly total market value by the S&P 500 index (source: Center for Research in Security Prices, CRSP). Hence, monthly nominal dividends (earnings) per capita are calculated by multiplying the monthly dividends (earnings) per market share with the number of market shares and then dividing the aggregate dividends (earnings) by the monthly estimates of population. I use changes in the log Personal Consumption Expenditures (PCE) to calculate monthly real dividend (earnings) per

⁵In earlier versions of the paper, I use a wide set of instruments to approximate business conditions such as output growth, the employment rate and changes in the yield spread. In this version, I keep the NBER recession indicator as the only instrument for simplicity without loss of economic significance.

capita. Monthly real consumption (dividend or earnings) growth is defined as log-differenced real consumption (dividend or earnings) per capita. The market return is defined as the change in the log market index including dividends (source: CRSP) minus the change in the log PCE. The non-dividend part of the market return is the difference between the market return and dividend growth.

It is well-known that measured aggregate consumption data are flow data which are reported as total consumption over an extended period; this temporal aggregation results in a non-zero autoregressive coefficient of aggregate consumption growth (Working, 1960) even if the *true* consumption growth is i.i.d.. The temporal aggregation effect could also potentially induce biases in the estimated conditional covariances.⁶ Therefore, I follow Duffee (2005) and construct a measure of monthly consumption growth removes the autoregressive terms up to the third order, $\Delta c_{t+1} - \sum_1^3 \phi_i(\Delta c_{t+1-i} - \bar{c})$ where ϕ_i is the i^{th} -order autoregressive coefficient and \bar{c} is the unconditional mean.⁷

2.2.3 Estimation Methodology and Cyclicity Inferences

2.2.3.1 A Two-Stage Procedure

Many dynamic covariance models in the GARCH class (such as the bivariate model in Engle (2002) and the multivariate model in Engle and Kelly (2012)) are estimated using a two-stage quasi-maximum likelihood (QML) estimator. Bollerslev and Wooldridge (1992) and White (1994) show that, under standard regularity conditions, the quasi-maximum likelihood estimator is still consistent and asymptotically Gaussian when a Gaussian log likelihood is maximized even though the distributional assumption of Gaussianity is violated. Thus, the log quasi-likelihood of the dynamic covariance model can be written as the sum of a volatility part and a correlation part (as is true for the log likelihood of a Gaussian model). Therefore, it is customary to maximize

⁶Duffee (2005), 1691-1694, provides a thorough discussion on why the purely contemporaneous covariance between returns and consumption growth underestimates the true covariance.

⁷In all the Tables and Figures of the current section, “consumption growth” refers to this new measure that controls for the temporal aggregation issue. In Tables OA1, OA4~OA6 of the Online Appendix, I replicate the main results using one-period consumption growth (Δc_{t+1}) and AR(1)-de-meaned consumption growth ($\Delta c_{t+1} - \phi_1(\Delta c_t - \bar{c})$) and two de-meaned dividend growth measures to provide a comprehensive set of robustness checks.

the sum of log quasi-likelihoods of individual conditional variance models in the first stage, and maximize the log quasi-likelihood of the bivariate conditional correlation model in the second stage, given the first-stage estimation results of conditional variances.

Here, I modify the two-stage QML estimation methodology and estimate the four conditional variance models of each residual series using the maximum likelihood estimation (MLE) methodology with the actual density functions. For each residual series, the best conditional variance estimate according to the Bayesian Information Criteria (BIC) is selected to standardize the residuals for use in the second-stage estimation. Note that the four conditional variance models impose different time-series and distributional assumptions, and identifying the correct conditional distribution and volatility model is important for the theoretical modeling of the new DGP in Section 3.3.

Then, the second stage appeals to the QML asymptotic theory to estimate the conditional covariance/correlation of the standardized residuals in two dynamic dependence models: the DCC model and the DCC- q_t model as introduced in Section 2.2.1.2. The standard errors of the quasi-maximum likelihood estimators are calculated following Engle and Sheppard (2001).

2.2.3.2 Cyclical Inference

Recall that the primary goal of my empirical framework is to parameterize the dynamic comovement processes in a flexible way so as to simultaneously identify the cyclicalities of the comovements between consumption growth and (1) market returns (i.e., the Duffee Puzzle), (2) dividend growth (i.e., the exogenous component), and (3) the non-dividend part of market returns (i.e., the endogenous component).

To test the cyclicalities of the relevant correlations, I use the estimation results of parameter ν within the model, and conduct Wald and Likelihood Ratio tests using post estimation inference. By design, the DCC model is the null hypothesis of the DCC- q_t model with the cyclicalities coefficient ν equal to 0. The probability distribution of both test statistics is a χ^2 distribution with a unit degree of freedom. Lastly, given the estimates of the conditional correlations and variances from the empirical model, conditional covariances and betas are obtained *ex post*. The regression

coefficients of the implied covariances and betas on the NBER indicator provide direct tests on their cyclicity. This inference may differ from the t-test because the variance process itself may induce cyclicity.

2.2.4 Empirical Analysis

In this section, I begin with a discussion of the first-stage conditional variance estimation results. Then, I report the second-stage conditional comovement estimation results on the decomposition of the Duffee Puzzle.

2.2.4.1 Conditional Variance Estimation Results

Table 2.1 presents the first-stage estimation results of the univariate conditional variance models for each of the four variables in the empirical framework—consumption growth (Panel A), market return (Panel B), dividend growth (Panel C) and the non-dividend part of the market return (Panel D). First, the empirical evidence supports that the conditional variances of all the four variables are heteroskedastic with the conditional models in all panels outperforming the unconditional models (according to both the BIC and AIC criteria). Moreover, in all panels, the best models feature a long-run mean depending on the cyclical indicator (q_t), supporting cyclicity.

According to Panel A of Table 2.1, the conditional variance of consumption growth behaves countercyclically, given the significant and positive coefficient estimates of the standardized NBER recession indicator in all four models. The best q_t -conditional model (“GED-GARCH, q_t ” with BIC = -5808.60) identifies a smaller cyclicity coefficient estimate ($\hat{\nu}=0.0428$, SE=0.0099) than the unconditional model ($\hat{\nu}=0.1014$, SE=0.0066) because the GARCH process already captures some cyclical variations in the conditional variance through the squared residuals. This significant cyclicity coefficient estimate indicates that the long-run conditional mean of monthly consumption growth volatility reaches as high as 0.0034 (annualized=0.0117) during recession periods and as low as 0.0032 (annualized=0.0110) during normal periods. The finding of countercyclical consumption growth volatility is in line with the literature (see, Kandel and Stambaugh,

1990; Bansal and Yaron, 2004; Bekaert and Engstrom, 2017). Moreover, given that the GED-GARCH model assumes a symmetric distribution with fat tails and that this model outperforms other conditional variance models, excess kurtosis is a salient feature of the consumption growth innovations.

The conditional variance of market returns also exhibits countercyclical behavior, which is consistent with the literature (see, e.g., Bollerslev, Engle, and Wooldridge, 1988; Schwert, 1989; Hamilton and Lin, 1996). According to Panel B of Table 2.1, the cyclical coefficient estimate in the best model (“GED-GARCH, q_t ”) is significant and positive ($\hat{\nu}=0.6935$, $SE=0.1084$). In economic terms, the long-run conditional mean of market volatility varies between 0.0616 (annualized=0.2138) during NBER recession periods and 0.0310 (annualized=0.1100) during non-recession periods; the monthly unconditional market volatility in the sample is 0.0374 (annualized=0.1298).

The market return contains a dividend part (Δd) and a non-dividend part ($r^m - \Delta d$). The conditional variance of dividend growth is found to be (weakly) procyclical, according to the best model (“BEGE- n_t -GARCH, q_t ”) in Panel C of Table 2.1. The cyclical coefficient is estimated to be -0.1114 ($SE=0.0592$) in the best model, indicating that the long-run conditional mean of dividend growth volatility varies between 0.0058 (annualized=0.0201) during recession periods and 0.0069 (annualized=0.0241) during normal periods.

On the non-dividend part of the market return, the estimation results in Panel D of Table 2.1 indicate strong evidence for countercyclical conditional volatility, given that all the cyclical coefficient estimates in all the four models are significant and positive. In particular, the significant and positive coefficient estimate in the best model (“GED-GARCH, q_t ”), 0.6689 ($SE=0.0991$), indicates that the long-run conditional volatility is around 0.0611 (annualized=0.2117) during NBER recession periods, and around 0.0311 (annualized= 0.1077) during non-recession periods; the sample monthly volatility is 0.0375 (annualized=0.1299).

Table 2.2 displays the detailed estimation results of the *best* conditional variance models for each of the four variable residuals. Apart from the main result on cyclical volatility, the consumption growth variance is found to be highly persistent ($\alpha + \beta = 0.9985$). Consumption growth (Panel

A), the market return (Panel B) and the non-dividend part of the market return (Panel D) are best fitted with leptokurtic distributions of which the shape parameters (τ) are between 1 and 2. Note that the generalized error distributions allow for tails that are either heavier than normal (when $\tau < 2$) or lighter than normal (when $\tau > 2$). The best model for dividend growth (“BEGE- n_t -GARCH, q_t ”) features conditional non-Gaussianity including time-varying skewness. This is not surprising as the unconditional scaled skewness of monthly dividend growth is -1.2271 (SE=0.5145).

2.2.4.2 The Duffee Puzzle Revisited

As illustrated in Equation (2.T1), variation in the amount of risk (the conditional covariance between market returns and consumption growth) are driven by variation in either the amount of dividend risk (the conditional covariance between dividend growth and consumption growth) or the amount of non-dividend risk (the conditional covariance between the non-dividend part of market returns and consumption growth). In this section, I identify the source of procyclicality in the Duffee Puzzle by formally examining the cyclicity of the three comovements. I report the core results in Table 2.3.

I first replicate the Duffee Puzzle using a longer sample. The cyclicity coefficient estimate in the consumption-return correlation is significant and negative ($\hat{\nu}=-0.1539$, SE=0.0359), according to the third column of Table 2.3, Panel A. In other words, the long-run conditional mean of the consumption-return conditional correlation is higher during non-recession periods (at 0.2147) and decreases during recession periods (to 0.1251), and the difference is statistically significant. The Likelihood Ratio test indicates that the less restrictive DCC- q_t model fits the data significantly better than the more restrictive DCC model; namely, a constant long-run conditional correlation is rejected with a p-value of 0.329%. Given the conditional correlation estimates and the conditional volatility estimates, the conditional covariance and the conditional beta are calculated. To test the cyclicity of the other two comovement measures, Panels B and C of Table 2.3 report the regression results of the model-implied conditional covariance and beta on the NBER indicator. Both are procyclical and the beta significantly so. This is particularly surpris-

ing for the conditional covariance (between consumption growth and market returns) because, as established before, both the conditional volatilities of market returns and consumption growth are countercyclical. Thus, these results support the main findings in Duffee (2005)—procyclical conditional correlation and covariance between consumption growth and market returns—using 13 additional years of data.

Next, I examine the consumption-dividend comovements. According to the fourth and the fifth columns of Table 2.3, both the Wald test and the LR test reject a constant long-run mean of the consumption-dividend conditional correlation at a significance level smaller than 1%. The cyclical coefficient estimate is significant and negative ($\hat{\nu}=-0.7999$, $SE=0.0987$), which implies procyclical behavior of the conditional correlation—the main result of this article. The magnitude of $\hat{\nu}$ implies that the long-run conditional correlation can drop to close to zero during bad times and increase to around 0.3039 during good times, with the sample correlation of the residuals being 0.2298. Given the estimated conditional correlation from Panel A and the estimated conditional variances from Table 2.2, Panels B and C of Table 2.3 show strong evidence that the conditional covariance and the conditional beta are both procyclical, with the procyclicality of the conditional beta stronger due to the countercyclicality of the consumption growth volatility in the denominator.

To support the claim that the exogenous component is the source of procyclicality of the puzzle, I complement the analysis on the exogenous component with an analysis on the endogenous component. The empirical evidence shows that the endogenous component behaves countercyclically. According to the seventh column of Panel A of Table 2.3, the long-run conditional correlation between the non-dividend part of the market return and consumption growth covaries positively with the countercyclical NBER recession indicator ($\hat{\nu}=0.0445$, $SE=0.0221$). In economic terms, the long-run conditional mean of the conditional correlation increases to around 0.2363 during recession periods and decreases to 0.2090 during non-recession periods, with the long-run unconditional mean being 0.2128 during the sample period; this difference is statistically significant. The Wald test and the LR test confirm this result at significance levels of 5% and 10% respectively. Panels B and C show that the conditional covariance and the conditional

beta are both strongly countercyclical with this countercyclical endogenous component in the amount of risk counteracting the procyclical exogenous component. The procyclicality of the return-consumption correlation ($\hat{\nu}=-0.1539$, $SE=0.0359$) is naturally weaker than the procyclicality of the consumption-dividend correlation ($\hat{\nu}=-0.7999$, $SE=0.0987$), comparing the third and the fifth columns of Table 2.3. Analogously, Panel C shows the market return-consumption beta w.r.t. the NBER indicator to be less negative than the dividend-consumption beta.

One interesting implication of these findings is that the share of the exogenous component in the Duffee Puzzle varies greatly through time. Figure 2.1 depicts the implied exogenous (solid black line) and endogenous (dashed red line) components in the top plot, and the time-varying share of the exogenous component in the amount of risk in the bottom plot. The weights of the two counteracting forces vary drastically over the business cycle. In particular, the share of dividend risk in the total amount of risk is procyclical. Given my estimates, the exogenous part explains on average 13.79% ($SE=1.12\%$) of the total risk during the sample period. Its share drops to 0.54% during recession periods, which is statistically significantly lower than the share (16.58%) during non-recession periods ($t\ stat=-6.35$); it becomes as high as 106% during the 1960s expansion and as low as -89% following the 1969-70 recession.

2.2.4.3 Robustness

I conduct three robustness checks of the main empirical finding in this paper—the procyclical comovement between consumption and dividend growth. All estimation results can be found in the Online Appendix.

First, I use the best conditional variance estimates *without* the NBER indicator to standardize the residual series innovations that are used in the second-stage estimation. According to Table OA3 of the Online Appendix, the cyclicity coefficient estimate remains significant and negative ($\hat{\nu}=-0.5544$, $SE=0.1298$), indicating a procyclical conditional correlation; analogously, the conditional covariance and beta coefficients are also significant and negative, indicating procyclicality.

Second, I use different consumption growth data. In particular, I conduct the same two-

stage estimation procedure using (1) the original consumption growth and (2) the AR(1)-de-meaned consumption growth. Again, the procyclicality result is shown to be robust (see Tables OA4~OA6 of the Online Appendix).

Third, while many consumption-based asset pricing papers use dividend data to measure the actual cash flows received by the representative agent investing in equities, Longstaff and Piazzesi (2004) propose to use earnings data to proxy for aggregate economic dividends. Using earnings instead of dividend growth, I continue to find a procyclical comovement with consumption growth ($\hat{\nu}=-1.0875$, SE=0.2314; LR=15.41, p-value=0.009%), according to Table OA7 of the Online Appendix. Earnings growth—which is not smoothed over time—and consumption growth comove procyclically because of the dividend part of earnings growth. Log earnings growth has two components, dividend growth and the change in the log payout ratio. The comovement between the non-dividend part of earnings growth and consumption growth is acyclical ($\hat{\nu}=0.1734$, SE=1.0125). Therefore, my results consistently explain the procyclical comovement between cash flow growth and consumption growth through dividend smoothing.

2.2.5 Summary of the Empirical Part of the Paper

This section has confirmed Duffee (2005)'s main finding that the amount of risk behaves procyclically using a longer sample, despite several major recessions during this period. I then provide strong and robust evidence that it is the procyclical exogenous component (covariance between consumption and dividend growth) that accounts for the procyclicality in the amount of risk, given the endogenous component being strictly countercyclical. Figure 2.1 illustrates the core of the empirical section. To build a DGP for the joint dynamics of consumption and dividend growth, it is useful to summarize the results of this section in 10 stylized facts:

(a).	The conditional variance of Δc is countercyclical.	<i>Kandel & Stambaugh (1990)</i>
(b).	The conditional variance of Δd is procyclical.	<i>New</i>
(c).	The conditional correlation between Δc and Δd is procyclical.	<i>New</i>
(d).	The conditional covariance between Δc and Δd (i.e., dividend risk) is procyclical.	<i>New</i>
(e).	The conditional sensitivity of Δd to Δc is procyclical.	<i>New</i>
(f).	The conditional variance of $r^m - \Delta d$ is countercyclical.	<i>New</i>
(g).	The conditional variance of r^m is countercyclical.	<i>Schwert (1989)</i>
(h).	The conditional covariance between Δc and $r^m - \Delta d$ is countercyclical.	<i>New</i>
(i).	The conditional covariance between Δc and r^m (i.e., amount of risk) is procyclical.	<i>Duffee (2005)</i>
(j).	The share of dividend risk in the total amount of risk varies procyclically.	<i>New</i>

Note that some stylized facts are implied by other two facts; for example, (a) and (d) immediately implies (e), and (d) and (h) immediately implies (j).

2.3 A New DGP for the Joint Consumption-Dividend Dynamics

State-of-the-art consumption-based asset pricing models tend to assume unrealistic joint dynamics between consumption and dividend growth. In a Lucas tree economy (Lucas, 1978), dividends equal consumption. Most of the literature since then has separated the modeling of consumption from dividends. Often, these two processes are modeled as unit root processes with constant correlations. For example, Campbell and Cochrane (1999) assume constant comovement (and variances). Bansal and Yaron (2004) assume a zero consumption-dividend conditional comovement because their model imposes independence among all level and uncertainty shocks. Bansal, Kiku, and Yaron (2012) allow the dividend growth innovations to have a constant exposure to the consumption shock. However, it can be easily shown that all three consumption-dividend comovement measures (correlation, covariance and beta) are not procyclical in their models.

In Table 2.4, I report a thorough evaluation of the (in)abilities of seven extant representative consumption-based asset pricing models to match the key empirical facts established in

the present research (see Section 2.2.5): three models fall within the habit-formation workhorse framework, i.e. Campbell and Cochrane (1999), and four long-run risk workhorse framework, i.e. Bansal and Yaron (2004). Note that there is a large literature on improving the performance of these two workhorse models; however, these seven models especially focus on accommodating more realistic dynamics of fundamental shocks, which is in line with the theme of this article. I find that all models fail to match the procyclical consumption-dividend comovement and the Duffee Puzzle, i.e. Facts (c, b, i).⁸

In this section, I formulate a parsimonious DGP for the consumption-dividend joint dynamics with only two state variables that has the potential to fit all stylized facts analytically, which is then verified empirically. In addition, I am able to assign economic interpretations to these state variables and their shocks using actual data and direct evidence, which enhances the plausibility of the new DGP. While the ultimate goal is to accommodate stylized facts into an asset pricing model, the GARCH-class dynamic dependence model in Section 3.2 is not appealing because it involves at least four state variables to generate realistic consumption-dividend joint dynamics.⁹

⁸All three habit-formation models show the potential to fit the countercyclical endogenous component (Fact (h)), whereas all four long-run risk models fail to fit this empirical fact. This advantage becomes one of the key reasons why this paper focuses on a variant of the Campbell-Cochrane model to accommodate the Duffee Puzzle in Section 3.4.

⁹They are (1) consumption and (2) dividend variances, $h_{c,t}$ and $h_{d,t}$, (3) the consumption-dividend correlation, $Corr_t$, and (3) the time-varying long-run conditional mean of the conditional correlation, q_t .

2.3.1 The New DGP

Consumption and dividend growth have the following joint dynamics:

$$\Delta c_{t+1} = \bar{c} + \sigma_c \tilde{\omega}_{c,t+1} + \sigma_n \tilde{\omega}_{n,t+1}, \quad (2.T10)$$

$$n_{t+1} = (1 - \phi_n) \bar{n} + \phi_n n_t + \sigma_{nn} \tilde{\omega}_{n,t+1}, \quad (2.T11)$$

$$\Delta d_{t+1} = \bar{d} + \phi_d (V_{c,t} - \bar{V}_c) + b_t \sigma_c \tilde{\omega}_{c,t+1} + \sigma_d \tilde{\omega}_{d,t+1}, \quad (2.T12)$$

$$b_{t+1} = (1 - \phi_b) \bar{b} + \phi_b b_t + \lambda_b \sigma_c \tilde{\omega}_{c,t+1}, \quad (2.T13)$$

$$V_{c,t} = \sigma_c^2 + \sigma_n^2 n_t, \quad (2.T14)$$

$$\bar{V}_c = \sigma_c^2 + \sigma_n^2 \bar{n}, \quad (2.T15)$$

where consumption and dividend growth are observables; the two latent state variables in the system are the macroeconomic uncertainty n_t and the sensitivity of dividend growth to consumption growth b_t (which is new to the literature). Both state variables are assumed to follow autoregressive processes. $V_{c,t}$ denotes the conditional variance of consumption growth, which is a linear function of n_t , and \bar{V}_c represents the average conditional variance. A constant parameter \bar{x} denotes the unconditional mean of process x_t , and ϕ_x denotes the conditional mean feedback of process x_t to itself or another variable.

This model allows time variation in expected dividend growth that may help generate a negative effect of macroeconomic uncertainty on valuation ratios through a cash flow effect ($\phi_d < 0$), but assumes a constant mean in the consumption growth equation. According to Table OA1 of the Online Appendix, regressing AR(3)-de-meaned consumption growth on a NBER recession indicator delivers an insignificant coefficient of -0.0008 (SE=0.0005), whereas the corresponding coefficient for dividend growth is significant and negative, -0.0042 (SE=0.0008). Therefore, the conditional mean specifications are consistent with the data. The autoregressive coefficients for the state variables (ϕ_n and ϕ_b) are expected to be positive.

The new DGP features three mutually independent shocks. The consumption “fundamental shock”, $\tilde{\omega}_{c,t+1}$, is a Gaussian shock with unit standard deviation; the consumption “event

shock”, $\tilde{\omega}_{n,t+1}$, follows a centered heteroskedastic gamma distribution with a strictly positive shape parameter n_t (using a subscript to denote that n_t varies over time) and a unit scale parameter; the dividend-specific shock, $\tilde{\omega}_{d,t+1}$, follows a centered homoskedastic gamma distribution with a strictly positive shape parameter V_d and a unit scale parameter. That is,

$$\tilde{\omega}_{c,t+1} \sim i.i.d.N(0, 1); \tilde{\omega}_{n,t+1} \sim \Gamma(n_t, 1) - n_t; \tilde{\omega}_{d,t+1} \sim \Gamma(V_d, 1) - V_d.$$

In particular, the probability density function for $\tilde{\omega}_{n,t+1}$, denoted $f(\tilde{\omega}_{n,t+1})$, is given by,

$$f(\tilde{\omega}_{n,t+1}) = \frac{1}{\Gamma(n_t)} (\tilde{\omega}_{n,t+1} + n_t)^{n_t-1} \exp(-\tilde{\omega}_{n,t+1} - n_t), \quad (2.T16)$$

for $\tilde{\omega}_{n,t+1} > -n_t$ and with $\Gamma(\cdot)$ representing a complete gamma function. The moment generating function of $\tilde{\omega}_{n,t+1}$, denoted $M(\kappa) \equiv E[\exp(\kappa\tilde{\omega}_{n,t+1})]$, is $\exp[-\kappa n_t - \ln(1 - \kappa)n_t]$. It can be easily shown that the conditional mean of $\tilde{\omega}_{n,t+1}$ is zero, the conditional variance n_t (> 0), the conditional unscaled skewness $2n_t$ (> 0)¹⁰ and the conditional unscaled excess kurtosis $6n_t$ (> 0). Similar results hold for the distribution of $\tilde{\omega}_{d,t+1}$ with V_d governing the shape of the distribution.

Gamma shocks are not as commonly used as Gaussian shocks in the literature, but they are appealing for my purposes for two reasons. First, they help fit the evidence of thick and skewed tails found in consumption and dividend growth residuals (see Section 3.2). Second, higher-order moments of gamma-distributed variables can be expressed as linear functions of their shape parameters (see above), which helps produce neat and tractable analytical solutions given that this paper focuses on second (cross) moments. It turns out that, conditional on the constant shock sensitivity parameters having the appropriate signs ($\sigma_c, \sigma_{nn}, \lambda_b > 0$; $\sigma_n, \sigma_d < 0$), the new DGP has the ability to match all five stylized facts about the consumption-dividend joint dynamics (Facts (a)~(e) as documented in Section 3.2) and match their distributional properties.

To see this, let me first discuss the consumption system. Each period, consumption growth responds positively to the “Gaussian” fundamental shock ($\sigma_c > 0$) and negatively to the “gamma”

¹⁰It is noteworthy that a gamma shock is always right-skewed, and thus the minus gamma shock is left-skewed.

event shock ($\sigma_n < 0$). Given the moment generating functions of Gaussian- and gamma-distributed shocks and that the two shocks are assumed to be independent, the total consumption growth variance has an analytical solution, $\sigma_c^2 + \sigma_n^2 n_t$ in which σ_c^2 captures the “fundamental-shock” variability and $\sigma_n^2 n_t$ captures the “event-shock” variability. With $\tilde{\omega}_{n,t+1}$ right-skewed, a negative σ_n implies that the event-shock component of the consumption innovation provides a source of heteroskedasticity that is coming from the left tail of consumption growth (with large negative events). It is a realistic and parsimonious assumption because Bekaert and Engstrom (2017) who model consumption innovations with both positively- and negatively-skewed gamma shocks find that the shape parameter of the positively-skewed gamma shock is large (or, the shock is Gaussian-like) and time-invariant (or, the shock is homoskedastic). In addition, the negative σ_n enables the new DGP to generate countercyclical consumption growth volatility:

- Fact Check (a): n_{t+1} is countercyclical, given that $Cov_t[\Delta c_{t+1}, n_{t+1}] = \sigma_n \sigma_{nn} n_t < 0$. Thus, the conditional variance of consumption growth, $\sigma_c^2 + \sigma_n^2 n_t$, is countercyclical.

Dividend growth loads on the fundamental consumption shock with a time-varying beta (b_t), and is further influenced by a homoskedastic left-skewed gamma disturbance (given that σ_d is negative and $\tilde{\omega}_{d,t+1}$ is right-skewed). The time-varying b_t is procyclical as σ_c and λ_b are strictly positive constants:

- Fact Check (e): b_{t+1} is procyclical, given that $Cov_t[\Delta c_{t+1}, b_{t+1}] = \lambda_b \sigma_c^2 > 0$.

The conditional variance of dividend growth, $b_t^2 \sigma_c^2 + \sigma_d^2 V_d$, increases with b_t (if $b_t > 0$), which immediately implies a procyclical dividend growth variance. Given the countercyclicity of the consumption volatility state variable n_t above, the new dividend growth process is thus modeled conveniently to generate a strictly procyclical comovement between dividend growth and consumption growth (i.e., correlation, covariance, and beta).

- Fact Check (b): the conditional variance of dividend growth, $b_t^2 \sigma_c^2 + \sigma_d^2$, is procyclical.
- Fact Check (c): the conditional correlation between dividend and consumption growth, $\frac{b_t \sigma_c^2}{\sqrt{\sigma_c^2 + \sigma_d^2 n_t} \sqrt{b_t^2 \sigma_c^2 + \sigma_d^2 V_d}}$, is procyclical given a countercyclical n_t and a procyclical b_t .
- Fact Check (d): the conditional covariance between dividend and consumption growth, $b_t \sigma_c^2$, is procyclical.

2.3.2 DGP Estimation Results

In this section, I first present the estimation results for the new DGP. To enhance the plausibility of the new DGP, I then discuss the economic interpretation of the latent shocks in Section 2.3.2.2, the evidence on fitting the cyclical with over-identification in Section 2.3.2.3, and the possibility of other DGPs that might satisfy the 5 exogenous facts in Section 2.3.2.4. The parameter estimates are used when exploring the theoretical economy later in Section 3.4.

2.3.2.1 Parameter Estimation Results of the New DGP

Given that there is no feedback from dividend growth dynamics to consumption growth dynamics, I estimate the consumption growth system $(\{\Delta c, n\})$ and the dividend growth system $(\{\Delta d, b\})$ in a two-step estimation procedure. During the first step, the consumption growth system is estimated using a filtration-based approximate maximum likelihood methodology developed by Bates (2006) to obtain parameter estimates, realizations of the latent macroeconomic uncertainty state variable $(\{\hat{n}_t\}_{t=1}^T)^{11}$ and realizations of the two consumption shocks $(\{\hat{\omega}_{c,t}\}_{t=2}^T, \{\hat{\omega}_{n,t}\}_{t=2}^T)$. Given the first-step estimation results, the dividend growth system is estimated using the maximum likelihood methodology to obtain the remaining parameter estimates, estimates of the comovement state variable $(\{\hat{b}_t\}_{t=1}^T)$ and the dividend-specific shock $(\{\hat{\omega}_{d,t}\}_{t=2}^T)$. I provide a detailed description of the estimation procedure in Appendix 2.1.

According to Panel A of Table 2.5, consumption growth depends positively on the symmetric homoskedastic fundamental shock ($\hat{\sigma}_c=0.0029$, SE=0.0001) and negatively on the right-skewed heteroskedastic event shock ($\hat{\sigma}_n=-0.0023$, SE=0.0005). Moreover, the sensitivity of the macroeconomic uncertainty state variable n_t to the event shock is positive, $\hat{\sigma}_{nn}=0.2772$ (SE=0.1027), which analytically implies a countercyclical n_t as it covaries negatively with consumption growth. Therefore, the first-step estimation results deliver countercyclical consumption growth volatility, i.e. Fact (a); I defer its graphical evidence (Figure 2.2) to Section 2.3.2.2.

The estimation results of the dividend growth system show that the sensitivity of b_t to the fundamental shock is significant and positive ($\hat{\lambda}_b=14.0978$, SE=1.3764), which immediately

¹¹In this paper, “ \hat{x} ” indicates an estimate of the unknown parameter/variable/shock x .

implies that the conditional beta b_t is procyclical given that $\widehat{Cov}_t(\Delta c_{t+1}, \hat{b}_{t+1}) = \hat{\lambda}_b \hat{\sigma}_c^2 > 0$. Thus, the conditional covariance and correlation between dividend and consumption growth are also procyclical, given the analytical solutions derived before. Next, because the b_t estimates are positive (see Figure 2.3), admitting an one-to-one correspondence between \hat{b}_t and \hat{b}_t^2 , the conditional variance of dividend growth—that increases with b_t^2 —is also procyclical. Therefore, the parameter estimation results demonstrate the ability of the new DGP to fit Facts (b)~(e) analytically.

In addition, I find the unconditional distribution of $\hat{\omega}_{d,t+1}$ to be right-skewed (skewness=0.3070, SE=0.0751; Panel C of Table 2.5), and the estimate of σ_d is significant and negative ($\hat{\sigma}_d = -0.0008$, SE=1.88E-05). Because the consumption fundamental shock is a Gaussian shock, the dividend-specific disturbance ($\sigma_d \tilde{\omega}_d$) is designed to capture the strong negative skewness of dividend growth innovations as observed in data (skewness=-1.2271, SE=0.5145) and the conditional evidence in Table 2.1 featuring time-varying negative conditional skewness. Therefore, the new DGP has the potential to match the distributional properties of the dividend growth innovations.

2.3.2.2 Economic Interpretation

Here, I analyze the time variation in the estimated state variables (\hat{n} and \hat{b}) in Figures 2.2 and 2.3. Moreover, given that the DGP shock structure plays a crucial role in simultaneously matching all five stylized facts, I compare the time variation in the filtered shocks ($\hat{\omega}_n$ and $\hat{\omega}_c$) against various business cycle indicators in Figure 2.4 to motivate their economic interpretation and thus to enhance the plausibility of the new DGP.

Figure 2.2 depicts the two estimated components of the total consumption growth variability, $\hat{\sigma}_c^2$ contributed by the fundamental shock and $\hat{\sigma}_n^2 \hat{n}_t$ contributed by the event shock. While the fundamental shock clearly plays a dominant role in explaining the total consumption growth variability during normal periods, the event shock accounts for as high as 57.95% of the total variance during NBER recessions. For example, the largest spikes occurred during the 1973 oil crisis and during the oil crisis followed by Volcker's monetary policy tightening in the early 1980s. The third largest spike occurred in the early 1960s, again coinciding with an NBER recession.

During the recent 2007-08 financial crisis, the fraction of the total consumption variance explained by the event shock soared to around 34%, but did not exceed the three largest spikes mentioned above. These spikes also clearly show up in the quarterly shocks graphed in the bottom panel of Figure 2.4.¹²

The filtered homoskedastic consumption shock explains (on average) 82.29% of the total consumption growth variability during the sample period. The correlation between the fundamental shock and the NBER recession indicator is -0.182*** at the monthly frequency and -0.2703*** at the quarterly frequency. It immediately follows that this shock is procyclical. The top panel of Figure 2.4 depicts filtered fundamental shocks aggregated to a quarterly frequency. The shock is consistently negative during NBER recessions, with the largest negative shocks occurring during the 2007-08 recessions.

The fundamental shock is the only shock that determines both the consumption and dividend growth innovations. According to Panel D of Table 2.5, I find that the detrended quarterly consumption-wealth ratio from Lettau and Ludvigson (2001) (source: Martin Lettau's website) has a significant and negative correlation (-0.215***) with the filtered fundamental shock, but is uncorrelated with the filtered event shock (0.0561) and the dividend-specific shock (0.0350). The top panel of Figure 2.4 illustrates the negative correlation between the fundamental shock and the detrended \widehat{cay} . Therefore, the fundamental shock is not only a procyclical shock but is also positively correlated with the wealth-consumption ratio. Because the dividend-consumption beta, b_t , is persistent (with a half life of 5.5 months), a unit fundamental shock at time t increases b_t and will have persistent effects on expected future dividend-consumption comovement and cash flow variance. It is the persistent effects that get capitalized in financial wealth, inducing a higher wealth-consumption ratio.

Several extant models in the consumption-based literature have modeled consumption growth disturbances with two independent shocks. The continuous-time model in Longstaff and Piazzesi (2004) models the consumption growth innovation with a Brownian motion (analogous

¹²The quarterly shocks are calculated as the sum of monthly shocks in the same quarter; quarterly aggregation is necessary for computing correlations with Lettau and Ludvigson (2001)'s *cay* variable which is only available at the quarterly (or lower) frequency (see Panel D of Table 2.5).

to the Gaussian fundamental shock here) and a jump process (analogous to the gamma event shock here). My model is also related to the “BEGE” model in Bekaert and Engstrom (2017) featuring two independent shocks, one associated with the “good” volatility and the other one “bad” volatility. Segal, Shaliastovich, and Yaron (2015) adapt this model in a long-run risk framework. However, my model also ensures the fit of realistic dynamics of dividend volatility and dividend-consumption comovements, which potentially improves all three models above.

Lastly, Figure 2.3 depicts the heteroskedastic part ($\hat{b}_t^2 \hat{\sigma}_c^2$) and the homoskedastic part ($\hat{\sigma}_d^2 \hat{V}_d$) of the total dividend growth variance. Consumption shocks explain on average 3.18% of the total dividend variance.

2.3.2.3 Fitting the Cyclicity: Evidence and Over-identification

Even though the empirical evidence regarding cyclicity in Section 3.2 pertains to dynamic conditional moments, I replicate it here in terms of moments calculated during recession and non-recession periods. Specifically, I simulate the DGP for 100,000 months given the shock distributional assumptions and the parameter estimates, and then test the closeness between sample moments and simulation moments during recession and non-recession periods.

Because the empirical recession dummy variable uses the NBER recession indicator which (according to the NBER White Paper) is created based on patterns in GDP growth, I therefore develop an algorithm to identify recession patterns in the consumption growth—the only macroeconomic variable in consumption-based asset pricing models (see Appendix 2.2 for a detailed description). When applying this algorithm to consumption growth during January 1959 – June 2014, it identifies seven out of the eight NBER recessions. More formally, the consumption-based recession indicator is highly correlated with the actual NBER recession indicator at 0.80, and projecting the consumption-based recession indicator onto the actual NBER recession indicator produces a coefficient of 0.9038 (SE=0.0507), which is insignificantly different from 1.

In Table 2.6, I calculate cyclical data moments regarding the five stylized facts established in Section 3.2 on consumption and dividend growth (i.e., Facts (a)~(e)). The evidence for the procyclicality of the comovement (correlation, covariance, and beta) between dividend and con-

sumption growth remains strong in the data moments, which is consistent with the strong and robust empirical evidence found in the conditional framework in Section 3.2. Column “M(3)”¹³ in Panel A shows that all the model moment point estimates calculated from both recession and non-recession periods are within 95% confidence intervals of the data moments. The DGP-implied moments also look economically very close to the data moments, with a few exceptions. For example, the correlation between dividend and consumption growth is 0.0639 in comparison to 0.0148 in the data. Given an imperfect recession identification scheme, such gap is understandable.

In Table 2.7, I investigate the fit of the DGP with respect to a number of other data moments as an over-identification test. These moments include the means, standard deviations, skewness, and excess kurtosis of consumption and dividend growth (8), the heteroskedastic nature of their innovations (2), and their unconditional comovement moments (3). According to Column “M(3)” of Table 2.7, these moments are matched statistically well except for the skewness and excess kurtosis of dividend growth, which are underestimated.

2.3.2.4 On the Uniqueness of DGPs Accommodating the Duffee Puzzle

Duffee (2005) uses a simplified two-asset model with constant discount rate and growth rates to show that consumption growth is more positively correlated with stock returns when stock market wealth is relatively more important in determining consumption than other asset wealth—this is what he calls the “composition effect”. Therefore, his framework essentially suggests a procyclical component in the consumption variance.

Inspired by the Duffee model, one intuitive alternative (to the new DGP) is to assume a “constant” exposure of dividend growth to the consumption fundamental shock but assign this consumption shock a “procyclical” conditional variance, whereas the current model assumes a procyclical exposure and a homoskedastic fundamental shock. Then, each period, the consumption growth innovation in this alternative DGP receives a heteroskedastic Gaussian shock with procyclical volatility and a heteroskedastic gamma shock with countercyclical volatility. This

¹³In short, “M(3)” denotes the model in this paper; I defer further explanation to Section 2.4.3.

alternative model can in theory generate a procyclical consumption-dividend covariance, correlation and beta.

However, this alternative DGP generates two problems. First, the identification of consumption growth variance becomes harder. Analytically, the consumption growth conditional variance is now the sum of a procyclical component (through the fundamental shock) and a countercyclical component (through the event shock), which makes the ultimate cyclicity unclear. However, both the empirical evidence in Section 3.2 and the recession/non-recession sample moments in this section suggest strongly countercyclical consumption growth variance. From the viewpoint of an econometrician, given that a Gaussian distribution is symmetric and *not* bounded, the heteroskedastic fundamental shock might act as the event shock to try to fit the left-tail events in the estimation. Hence, the estimation results might generate countercyclical fundamental shock volatility and thus countercyclical consumption-dividend comovement, which contradicts the empirical findings. Restricting the fundamental shock volatility to be procyclical (e.g., restricting the signs of certain parameters) could resolve the technical problem; then, the estimation results obtained from a constrained estimation usually become harder to interpret, which makes this alternative DGP less appealing.

Second, and more importantly, this alternative DGP likely generates a *positive* correlation between consumption and dividend growth variances because the heteroskedastic fundamental shock now positively explains the dynamics of both variances. However, the best GARCH-class conditional variance estimation results suggest that the consumption growth variance is weakly negatively correlated with dividend growth variance ($\rho=-20.41\%$, $SE=3.82\%$). This negative correlation is consistent with Fact (a), countercyclical consumption growth variance, and Fact (b), procyclical dividend growth variance. The new DGP nails this moment: according to the estimation results, my model implies a correlation of -13.11% , which is within the 95% confidence interval of the data moment.

2.4 An External Habit Model

In this section, I explore how incorporating more realistic dynamics into the amount of risk affects the performance of the extant dynamic asset pricing models. In Section 2.4.1, I describe the assumptions regarding the preferences of the representative agent. In Section 2.4.2, I provide approximate analytical solutions of asset prices that demonstrate various features of the model. In Section 2.4.3, I confront the numerical solution of the model with a wide range of empirical moments.

The key moments to be matched by the model are the cyclicity of the two components of the Duffee Puzzle. The procyclical conditional covariance between dividend and consumption growth (or the exogenous component) is immediately satisfied given the new DGP (see Section 3.3). However, different consumption-based asset pricing models have different implications regarding the cyclicity of the conditional covariance between the non-dividend part of the market return and consumption growth (or the endogenous component). The (external) habit-formation framework naturally entails a countercyclical endogenous component through countercyclical risk aversion; the effects of consumption shocks on the valuation ratio are amplified during bad times when risk aversion is higher. On the other hand, the long-run risk framework assumes that shocks (i.e., consumption shock, dividend shock, volatility shock, long-run expected growth shock) are independent of one another, resulting in a zero covariance between the price dividend ratio and consumption growth and thus a zero endogenous component. In addition, I show later that an endowment economy with procyclical dividend risk requires a countercyclical price of risk to generate realistic cyclical behavior for the price dividend ratio and the equity premium. As a result, in this paper, I consider the more natural external habit paradigm as developed in Campbell and Cochrane (1999).

2.4.1 Habit-Based Preferences

In this economy, the representative agent maximizes:

$$E_0 \left[\sum_{t=0}^{\infty} \beta^t \frac{(C_t - X_t)^{1-\gamma} - 1}{1-\gamma} \right], \quad (2.T17)$$

where C_t is the real consumption level and X_t the external habit level at time t ($C_t > X_t$). The parameter β is the time discount factor, and γ is the curvature parameter. The relative risk aversion (the local curvature of the utility function) is $\gamma \frac{C_t}{C_t - X_t} \equiv \frac{\gamma}{S_t}$, where the surplus consumption ratio S_t is defined as the percentage gap between consumption and habit level. When the consumption level is closer to the habit level (i.e., lower surplus consumption ratio), the agent becomes more risk averse (instantaneously). The log surplus consumption ratio s_t , $\log(S_t)$, follows an AR(1) process with its shock structure perfectly spanned by the two aforementioned consumption shocks:

$$s_{t+1} = (1 - \phi_s) \bar{s}_t + \phi_s s_t + \lambda_t (\sigma_c \tilde{\omega}_{c,t+1} + \sigma_n \tilde{\omega}_{n,t+1}), \quad (2.T18)$$

where ϕ_s is the persistence coefficient of s_t , \bar{s}_t the time-varying long-run mean, and λ_t the sensitivity function. Note that \bar{s}_t is assumed constant in the CC model, but countercyclical in my model (see Section 2.4.2.1). The stochastic discount factor (SDF) is the ratio of marginal utilities, $M_{t+1} = \beta \frac{U_C(C_{t+1}, X_{t+1})}{U_C(C_t, X_t)} = \beta \left(\frac{C_{t+1} S_{t+1}}{C_t S_t} \right)^{-\gamma}$; the log real pricing kernel is,

$$\begin{aligned} m_{t+1} &= \ln \beta - \gamma \Delta c_{t+1} - \gamma \Delta s_{t+1} \\ &= \ln \beta - \gamma \bar{c} - \gamma(1 - \phi_s)(\bar{s}_t - s_t) - \gamma(1 + \lambda_t) (\sigma_c \tilde{\omega}_{c,t+1} + \sigma_n \tilde{\omega}_{n,t+1}). \end{aligned} \quad (2.T19)$$

2.4.2 Asset Prices

In this section, I present salient features of asset prices implied by the model with (quasi) analytical solutions.

2.4.2.1 The Risk Free Rate and the Sensitivity Function

The risk free rate, rf_t , is solved from the usual first-order condition for the consumption-saving ratio, $rf_t = \ln\{E_t[\exp(m_{t+1})]^{-1}\}$. Given the moment generating functions of the two independent shocks in the kernel process (Equation (2.T19)), the risk free rate has an exact closed-form solution,

$$rf_t = -\ln \beta + \underbrace{\gamma \bar{c} + \gamma(1 - \phi_s)(\bar{s}_t - s_t)}_{\text{intertemporal substitution}} - \underbrace{\frac{1}{2}\gamma^2(1 + \lambda_t)^2\sigma_c^2 - [\gamma(1 + \lambda_t)\sigma_n - \ln(1 + \gamma(1 + \lambda_t)\sigma_n)]}_{\text{precautionary savings}} n_t. \quad (2.T20)$$

Similar to the Campbell and Cochrane model, one source for time variation in the risk free rate is the “intertemporal substitution effect”. When risk appetite is low ($s_t < \bar{s}_t$) and thus expected to be high in the future, the agent borrows to smooth marginal utility, driving up the interest rate. Another source is the “precautionary savings effect”, when the agent wants to save more during volatile periods, driving down the interest rate.

The literature proposes various ways of specifying the sensitivity function, which plays an important role in the Campbell and Cochrane (1999) model as it represents the price of consumption risk. First, in Campbell and Cochrane (1999), the two effects perfectly cancel out, rendering the risk free rate constant; however, a constant short rate is counterfactual. Second, in Wachter (2005, 2006), the intertemporal substitution effect dominates in order to generate an upward sloping real yield curve and a positive bond risk premium. This framework results in a countercyclical risk free rate—which is counterfactual given that Ang, Bekaert, and Wei (2008) find the U.S. real risk free rate to be procyclical. Third, Bekaert and Engstrom (2017) propose a time-varying risk free rate such that the relative importance of the two effects varies over time. Their risk free rate also depends on n_t .

I propose a fourth way delivering a risk free rate that is strictly procyclical (i.e., the precautionary savings effect dominates). The sensitivity function is solved such that the second-order Taylor approximation of Equation (2.T20) is a constant, which is referred to as the rf_{CC} compo-

ment of the exact risk free rate (see Equation (2.T24) below or Appendix 2.3):

$$\lambda_t = \begin{cases} \frac{1}{\bar{S}_t} \sqrt{1 - 2(s_t - \bar{s}_t)} - 1, & s_t \leq s_{max,t} \\ 0, & s_t > s_{max,t} \end{cases} \quad (2.T21)$$

where $\bar{s}_t = \log(\bar{S}_t)$ and $s_{max,t}$ are derived as functions of the free parameters and n_t ,

$$\bar{S}_t = \sqrt{(\sigma_c^2 + \sigma_n^2 n_t) \frac{\gamma}{1 - \phi_s}}, \quad (2.T22)$$

$$s_{max,t} = \bar{s}_t + \frac{1}{2}(1 - \bar{S}_t^2). \quad (2.T23)$$

Note that \bar{S}_t is defined endogenously to CC's \bar{S} with the only difference that the consumption growth variance varies through time. The $s_{max,t}$ variable is likewise the time-varying equivalent to the expression in CC. The dynamics of the sensitivity function are thus determined by s_t and n_t . The surplus consumption ratio state variable s_t has an intuitive negative effect on λ_t (as in the Campbell and Cochrane model); when the consumption level is closer to the habit level, the price of risk increases. The uncertainty state variable n_t has a negative effect on λ_t through \bar{S}_t (as also assumed in Bekaert and Engstrom, 2017) and a positive effect through \bar{s}_t . Given the parameter choices in this paper (see Section 2.4.3 for more details), the countercyclical n_t exhibits an overall negative effect on λ_t . The negative effect of the procyclical s_t on λ_t dominates the negative effect of the countercyclical n_t , implying an overall countercyclical sensitivity function in my model.

With this sensitivity function, a third order Taylor approximation of the risk free rate is given by:

$$rf_t \approx \underbrace{-\ln \beta + \gamma \bar{c} - \frac{(1 - \phi_s)\gamma}{2}}_{\equiv rf_{CC}} + \frac{1}{3}\gamma^3(1 + \lambda_t)^3 \underbrace{\sigma_n^3}_{<0} n_t. \quad (2.T24)$$

In this expression, the constant term “ rf_{CC} ” is identical to the risk free rate in Campbell and Cochrane (1999). The appended “precautionary savings” term, $\frac{1}{3}\gamma^3(1 + \lambda_t)^3 \sigma_n^3 n_t$, is determined by the countercyclical sensitivity function (ultimately driving the price of risk) in Equation (2.T21)

and the countercyclical macroeconomic uncertainty. Because σ_n is negative according to Table 2.5, the appended term and the risk free rate are strictly procyclical. The actual risk free rate has a negative and procyclical nonlinear term appended to rf_{CC} instead of the approximate cubic term above (see Appendix 2.3).

2.4.2.2 Approximate Analytical Solution for Equity Prices

The endowment economy features three state variables: the procyclical risk appetite (s_t), the countercyclical macroeconomic uncertainty (n_t), and the procyclical consumption-dividend comovement (b_t).¹⁴ Campbell and Cochrane (1999)'s state variable, s_t , ensures variation in the price of risk; the two *new* state variables, n_t and b_t , introduce dynamics into the amount of risk. Note that the model does not have exact closed-form solutions and thus is formally solved with numerical methods (see Section 2.4.3). Nevertheless, approximation analytical solutions help provide economic intuitions.

First, I conjecture an approximate process for the log valuation ratio $pd_t \equiv \ln\left(\frac{P_t}{D_t}\right)$,

$$pd_t = A_0 + A_1s_t + A_2b_t + A_3b_t^2 + A_4n_t. \quad (2.T25)$$

The analytical solutions rely on two additional approximations. First, I apply the Campbell and Shiller linearization to the log market return, $r_{t+1}^m = \ln\left(\frac{P_{t+1}+D_{t+1}}{P_t}\right) \approx \Delta d_{t+1} + a_1pd_{t+1} - pd_t + a_0$ where a_0 and a_1 are linearization constants that only depend on the average level of pd . The approximate market return is used in the Euler equation. Second, given the shock assumptions and the pd conjecture, there are three types of shocks in the log market return: a Gaussian shock, a $\chi^2(1)$ shock, and a gamma shock. I then use a quasi quadratic Taylor approximation to the Euler equation: $1 = E_t[\exp(m_{t+1} + r_{t+1}^m)] \approx \exp\left[E_t(m_{t+1} + r_{t+1}^m) + \frac{1}{2}V_t(E(m_{t+1} + r_{t+1}^m))\right]$ (see Appendix 2.4). Conditional on these three approximations, the coefficients in the conjectured price dividend ratio are solved in closed form in Appendix 2.5. The state variables affect the

¹⁴The cyclicity of the state variables can be easily proved. Risk appetite (introduced in Section 2.4.1) is procyclical because $Cov_t(s_{t+1}, \Delta c_{t+1}) = \lambda(s_t)(\sigma_c^2 + \sigma_n^2 n_t) > 0$. As discussed in Section 3.3, macroeconomic uncertainty is countercyclical because $Cov_t(n_{t+1}, \Delta c_{t+1}) = \sigma_n \sigma_{nn} n_t < 0$, and consumption-dividend comovement is procyclical because $Cov_t(b_{t+1}, \Delta c_{t+1}) = \sigma_c^2 b_t > 0$.

price dividend ratio via a discount rate (DR) channel and/or via a cash flow (CF) channel:

2.4.2.2.1 [1]. The risk aversion effects:

$$A_1 > 0.$$

When risk appetite (risk aversion) is low (high), the required compensation per unit of consumption risk to investing in risky assets increases; hence, the price dividend ratio decreases as the risk compensation demanded increases.

Risk aversion has another DR channel, operating through the interest rate. As shown in Equation (2.T24), the precautionary savings effect on the interest rate is amplified when risk aversion is high. Thus, interest rate decreases with risk aversion, driving down the total return demanded; hence, price the dividend ratio increases. This effect is, however, dominated by the risk premium effect above, given the parameter choices and numerical solutions in Section 2.4.3.

2.4.2.2.2 [2]. The comovement effects (New):

$$A_2, A_3 > 0.$$

Through a pure CF channel, the price dividend ratio can be interpreted as reflecting the outlook on future dividend growth. The persistent procyclical b_t induces a persistent procyclical dividend growth variance, which gets capitalized in equity prices. Analytically, the expected value of the exponential of dividend growth increases with both the expected growth and conditional variance.¹⁵ The conditional variance component has a closed-form solution that strictly increases with b_t^2 . Therefore, this pure CF channel suggests a positive relationship between b_t and pd_t .

However, there is a potentially countervailing risk premium effect. The total risk premium to compensate changes in dividend growth can be intuitively approximated with $-Cov_t(m_{t+1}, \Delta d_{t+1}) = \gamma(1 + \lambda_t)b_t\sigma_c^2$. The compensation for cash flow risk increases with both b_t and λ_t . When a positive fundamental shock arrives, b_t and s_t increase and λ_t decreases simultaneously. If λ_t was not countercyclical, the model would generate a higher risk premium, potentially resulting in a coun-

¹⁵The Gaussian analogue is, $E_t[\exp(\Delta d_{t+1})] = \exp[E_t(\Delta d_{t+1}) + \frac{1}{2}V_t(\Delta d_{t+1})]$.

terintuitive negative relationship between the procyclical b_t and the procyclical pd_t . Given the parameter choices and numerical solutions, this habit formation model has the ability to generate a positive $pd_t \sim b_t$ relationship. This is *another* reason why the habit formation paradigm is preferred in comparison with the long-run risk framework (which assumes a constant price of risk).

2.4.2.2.3 [3]. The macroeconomic uncertainty effects:

$$A_4 > 0.$$

The CF channel of uncertainty is well-recognized. When macroeconomic uncertainty (n_t) is higher, future dividend growth is expected to be lower, driving down the current price—which is in the spirit of the long-run risk story. On the other hand, a higher n_t induces more precautionary savings, driving down the interest rate and lowering the total return demanded; this DR channel of n_t also appears in Bekaert and Engstrom (2017). Given my parameter choices, the DR channel dominates the CF channel in the current model during almost all periods.

Given these results, I verify Facts (f) and (g) regarding the cyclicity of price-dividend ratio and market return variances.

■ Fact Check (f) and (g): *The log market return in the approximate analytical solution is $\Delta d_{t+1} + a_1 pd_{t+1} - pd_t + a_0$. Given the dividend growth dynamics in the new DGP and the price dividend ratio conjecture, the conditional variances of the log price dividend ratio and the log market return have the following approximate expressions,*

$$Var_t(pd_{t+1}) \approx \varsigma_{pd} + \varsigma_1 \lambda_t + \varsigma_2 b_t + \varsigma_3 n_t + \varsigma_4 \lambda_t^2 + \varsigma_5 b_t^2 + \varsigma_6 \lambda_t b_t + \varsigma_7 \lambda_t n_t + \varsigma_8 \lambda_t^2 n_t, \quad (2.T26)$$

$$\begin{aligned} Var_t(r_{t+1}^m) \approx & \varsigma_{rm} + a_1^2 \varsigma_1 \lambda_t + [a_1^2 \varsigma_2 + 2a_1 \lambda_b \sigma_c^2 (A_2 + 2A_3(1 - \phi_b) \bar{b})] b_t + a_1^2 \varsigma_3 n_t + a_1^2 \varsigma_4 \lambda_t^2 \\ & + (a_1^2 \varsigma_5 + 2a_1 \varsigma_2 + \sigma_c^2) b_t^2 + (a_1^2 \varsigma_6 + 2a_1 \varsigma_1) \lambda_t b_t + a_1^2 \varsigma_7 \lambda_t n_t + a_1^2 \varsigma_8 \lambda_t^2 n_t, \end{aligned} \quad (2.T27)$$

where ς_{pd} , ς_{rm} , ς_1 , ς_2 , ς_3 , ς_4 , ς_5 , ς_6 , ς_8 , a_1 , λ_b , σ_c , ϕ_b and \bar{b} are strictly positive constants, and $\varsigma_7 = 2A_1 A_4 \sigma_n \sigma_{nn}$ is negative when the discount rate effect of n_t dominates its cash flow effect, and positive vice versa. Thus, the model has the potential to generate a countercyclical price dividend ratio (a linear proxy for the variance of the non-dividend part of the market return) and market return variances.

2.4.2.3 The Duffee Puzzle Revisited, Theoretically

The empirical evidence in Section 3.2 finds that the exogenous component $Cov_t(\Delta d_{t+1}, \Delta c_{t+1})$ is procyclical, the endogenous component $Cov_t(r_{t+1}^m - \Delta d_{t+1}, \Delta c_{t+1})$ countercyclical, and the amount of risk $Cov_t(r_{t+1}^m, \Delta c_{t+1})$ procyclical. In particular, the latter two empirical facts are important testable hypotheses in evaluating the theoretical model.

According to the approximate analytical solution (see Appendix 2.5), the model-implied amount of risk contains a procyclical exogenous component as assumed in the new DGP; the model-implied endogenous component contains three parts from the three state variables respec-

tively:

$$\begin{aligned}
& \underbrace{b_t \sigma_c^2}_{\textcircled{1}. \text{ Exogenous Component}} \\
+ & \underbrace{a_1 A_1 \lambda_t \sigma_c^2}_{\textcircled{2}. \text{ Endogenous Component: benchmark amount of risk in Campbell and Cochrane (1999)}} \\
+ & \underbrace{[a_1 A_2 \lambda_b + 2a_1 A_3 (1 - \phi_b) \bar{b} \lambda_b + 2a_1 A_3 \phi_b \lambda_b b_t] \sigma_c^2}_{\textcircled{3}. \text{ Endogenous Component: additional amount of risk induced by comovement}} \\
+ & \underbrace{a_1 [A_1 \lambda_t \sigma_n^2 + A_4 \sigma_{nm} \sigma_n] n_t}_{\textcircled{4}. \text{ Endogenous Component: additional amount of risk induced by uncertainty}}, \\
& \tag{2.T28}
\end{aligned}$$

where the parameters $\sigma_c, \sigma_{nn}, \bar{b}, \phi_b, \lambda_b$ and a_1 are positive and σ_n is negative according to the DGP estimation results in Table 2.5. The procyclical exogenous component, Term $\textcircled{1}$, is directly obtained from the new DGP. The next three terms constitute the endogenous component. The strictly countercyclical Term $\textcircled{2}$ captures the amount of risk implied from linearizing the original Campbell and Cochrane model. As discussed in Section 2.4.2.2, it reflects the positive effect of risk appetite on the valuation ratio. Term $\textcircled{3}$ captures the procyclical amount of “comovement risk” that emerges from the positive sensitivity of the valuation ratio to the time-varying consumption-dividend comovement. The last term captures the amount of risk that is associated with the countercyclical macroeconomic uncertainty; the cyclicity of Term $\textcircled{4}$ is parameter-dependent, but has the potential to generate a countercyclical process.

With these expressions, I examine the model’s ability to deliver Facts (h)~(j).

- Fact Check (h): *The model has the potential to generate a countercyclical endogenous component if the procyclical part(s) is counteracted by the countercyclical part(s).*
- Fact Check (i): *The procyclical terms (Terms ① and ③) in the amount of risk expression (Equation (2.T28)) must counteract the countercyclical sources in order to obtain procyclical amount of risk, thus resolving the Duffee Puzzle.*
- Fact Check (j): *The share of the procyclical exogenous component in the total amount of risk has the potential to be procyclical if the implied endogenous component is not strongly procyclical.*

2.4.2.4 The Equity Premium

The equity premium in this revised habit formation model is approximately the product of a countercyclical price of risk, $\gamma(1 + \lambda_t)$, and a time-varying amount of risk that comprises both procyclical and countercyclical sources according to Equation (2.T28). The detailed derivation is included in Appendix 2.5.

The interactions between the two additional risk sources from the two new state variables (the countercyclical volatility risk and the procyclical dividend risk) and the countercyclical price of risk have direct implications for the magnitude of the equity risk premium. On the one hand, the introduction of the countercyclical volatility risk makes the asset riskier as the volatility risk is higher when risk aversion is higher during economic turmoil; from this perspective, a higher unconditional equity premium is expected. On the other hand, the introduction of the procyclical dividend risk—the core contribution of the present research—potentially lowers the level of the unconditional equity premium. This is because the amount of risk now contains a procyclical component which counteracts the countercyclical price of risk; in other words, the asset becomes less risky. Moreover, the conditional equity premium no longer monotonically increases with the price of risk.

2.4.3 Numerical Solutions and Results

The final model features three state variables: the habit state variable, s , and two new state variables, n and b . Therefore, in the numerical analysis, I introduce two intermediate models to analyze the effects of the two new state variables in the final model.

The first intermediate model “M(1)” is an adapted Campbell and Cochrane model which features homoskedastic fundamentals. To be more precise, consumption growth innovations depend on a homoskedastic Gaussian fundamental shock and a homoskedastic gamma event shock (i.e., shape parameter = \bar{n}), and dividend growth has a constant exposure to the consumption fundamental shock (i.e., the dividend beta = \bar{b}). M(1) features only one state variable, as present in Campbell and Cochrane (1999), the surplus consumption ratio. The second intermediate model “M(2)” is an adapted Bekaert and Engstrom (2017) model that builds on M(1) but incorporates countercyclical macroeconomic uncertainty as the second state variable. Thus, the final model “M(3)” can be viewed as a generalization of M(2) where the consumption-dividend comovement is now procyclical. The comparison between the numerical solutions of M(3) and M(2) (M(2) and M(1)) reveals the pricing implications of b_t (n_t). All three models price dividend claims. Appendix 2.3 presents M(1) and M(2) in detail.

In the remainder of the section, Section 2.4.3.1 describes the calibration of the preference (non-DGP) parameters. Then, I confront the three models with a wide range of asset price statistics. Specifically, in Section 2.4.3.2, I evaluate the model fit in terms of conventional asset price statistics and over-identify the models with additional unconditional fundamental and cross moments. In Section 2.4.3.3, I focus on the implications of the uncertainty and comovement state variables on fitting the 10 stylized facts revolving the Duffee Puzzle. I conclude by revisiting how the three state variables affect price dividend ratios and then their relative importance in driving equity prices in Section 2.4.3.4.

2.4.3.1 Calibration and Simulation

There are four non-DGP parameters to be determined: γ , ϕ_s , rf_{CC} , and β . I fix the utility curvature parameter γ at 2. As commonly assumed in the literature, the AR(1) coefficient of the

s_t process, ϕ_s , equals the AR(1) coefficient of monthly log price dividend ratio. The benchmark constant risk free rate, rf_{CC} , as appeared in Equation (2.T20), is chosen to match the average monthly real short rate proxied by the difference between the change in log nominal 90-day Treasury index constructed by CRSP and the continuously compounded inflation rate. β is the time discount parameter inferred from the rf_{CC} equation. Table 2.8 summarizes the non-DGP parameters.

The log valuation ratios are solved numerically using the “series method” from Wachter (2005). M(1) is solved using a one-dimensional grid (20×1) for the one state variable: the log surplus consumption ratio; M(2) is solved over a two-dimensional grid (20×20) for the two state variables: the log surplus consumption ratio and macroeconomic uncertainty. The final model M(3) uses a three-dimensional grid ($20 \times 20 \times 20$) for all three state variables.

For each model, I draw 100,000 months of fundamental shocks and then construct the state variable processes according to their data generating processes. Given the grid solutions, I apply the piecewise polynomial cubic interpolation for M(1), and the piecewise polynomial spline interpolation for M(2) and M(3) to obtain the log price dividend ratio for each simulated month given the state variable values. All the reported theoretical moments in this paper are calculated using the second half of the simulated dataset, i.e., 50,001-100,000. As mentioned in Section 2.3.2.3, the recession periods in the simulated dataset are identified using patterns in simulated consumption growth (see Appendix 2.2 for details).

2.4.3.2 Unconditional Moments

Table 2.9 reports the fit of the models with respect to the unconditional moments of fundamentals and asset prices. The equity risk premium increases a lot from 4.4520% in M(1) to 5.9374% in M(2) because the time-varying macroeconomic uncertainty introduces additional countercyclical dynamics into the amount of risk, which also results in a lower price dividend ratio. The average price dividend ratio implied from M(2) is below the sample 95% confidence interval. However, the log valuation ratio variability implied from M(2), 0.2882, is not statistically significantly different from the data moment, which is an improvement to M(1) and is consis-

tent with Bekaert and Engstrom (2017). The standard CC model and its adapted version fail to generate sufficient price dividend ratio variability.

Adding procyclical dividend risk, in M(3), the unconditional equity premium is slightly lower compared to that in M(2) with a constant dividend risk, which is consistent with economic intuition. In M(3), the amount of risk now contains a procyclical component which counteracts the countercyclical macroeconomic uncertainty in the amount of risk and the countercyclical risk aversion in the price of risk. Thus, equities are less risky in M(3). Quantitatively, the annualized equity premium drops from 5.9374% in M(2) to 5.3537% in M(3)—both not rejected by the sample counterpart (4.8780%). With procyclical dividend risk affecting the price dividend ratio positively, $\sigma(pd)$ implied from M(3) increases to 0.3037, which is the closest to the data moment (0.3946) in this row.

The variability of the market excess return in M(1) is below the sample 95% confidence interval of the data moment (14.8816%). The fit significantly improves when introducing heteroskedasticity into consumption growth in M(2), because of the more volatile price dividend ratio as discussed earlier. Although M(3) incorporates one more state variable, the market return implied from M(3) is less variable, $\sigma(r^m - rf) = 14.5441\%$, than that implied from M(2). Here is the interpretation. The unconditional variance of market return can be approximately decomposed into three components: the variance of pd , the variance of Δd , and the covariance between pd and Δd . M(1) and M(2) by construction impose a strictly positive covariance between pd and Δd through their positive exposures to the consumption fundamental shock. The unconditional covariance between the two in M(3) contains an additional negative term, because $Cov(\lambda_t, b_t) < 0$, reflecting the procyclical dividend risk serving as an internal “buffer” against the countercyclical risk aversion in the economy.¹⁶

¹⁶As a simplified version of Equation (2.T27), the conditional covariance between the dividend growth and price changes (ignoring the quadratic term) in M(3) is

$$\begin{aligned} Cov_t(pd_{t+1}, \Delta d_{t+1}) &\approx A_1 Cov_t(s_{t+1}, \Delta d_{t+1}) + A_2 Cov_t(b_{t+1}, \Delta d_{t+1}) + A_4 Cov_t(n_{t+1}, \Delta d_{t+1}) \\ &= A_1 \lambda_t b_t \sigma_c^2 + A_2 \lambda_b b_t \sigma_c^2 + 0. \end{aligned} \quad (2.T29)$$

Then the unconditional covariance becomes,

$$E[Cov_t(pd_{t+1}, \Delta d_{t+1})] \approx A_1 \sigma_c^2 E(\lambda_t) E(b_t) + A_1 \sigma_c^2 \underbrace{Cov(\lambda_t, b_t)}_{<0} + A_2 \lambda_b \sigma_c^2 E(b_t). \quad (2.T30)$$

Despite failing to fit return variability, the M(1)-implied Sharpe Ratio is within the sample 95% confidence interval of the data point estimate (0.3278). The implied Sharpe Ratio from the M(3) economy, 0.3681, has the best fit among the three models. The kurtosis moment is also matched statistically well by all three models. However, the equity return skewness implied by all three models is indifferent from zero, although M(2) and M(3) do generate negative skewness.

M(2) and M(3) generate the same risk free rate dynamics because they only differ in the dividend growth processes. Their risk free rate is slightly higher than the one in M(1), but both risk free rates have means that are within the 95% confidence interval of the data point estimate, 1.4209%.

In addition, I over-identify the models with a set of 18 unconditional first, second, and cross moments of economic fundamentals and market returns. Table 2.7, as discussed before in Section 3.3 when I evaluated the fit of the new DGP, also shows that M(1) and M(2) can fit reasonably well with respect to these unconditional higher moments, with the exception of return-based volatilities.

2.4.3.3 Duffee Puzzle

In Table 2.10, I evaluate the fit of the theoretical models with respect to the cyclical moments related to the endogenous part of the Duffee Puzzle, i.e. Facts (f)~(j). To begin with, the risk aversion channel does not suffice to explain the strongly countercyclical volatility dynamics of asset prices as I observe in data; thus, M(1) fails to match Facts (f) and (g). Nevertheless, M(1) matches the endogenous part of the puzzle, the countercyclical $C(r^m - \Delta d, \Delta c)$ or Fact (h), which further demonstrates the advantage of a habit formation framework.

The countercyclical uncertainty n_t introduces additional countercyclicality into the variances of r^m and $r^m - \Delta d$, which are now significantly higher during recession periods and statistically close to the data moments. Moreover, M(2) improves M(1) towards generating a more realistic endogenous component. The difference between the two $C(r^m - \Delta d, \Delta c)$ values calculated during recession and non-recession periods is $2.54 \times 10^{-5} - 2.23 \times 10^{-5} = 0.31 \times 10^{-5}$ in M(2) and $2.45 \times 10^{-5} - 2.25 \times 10^{-5} = 0.20 \times 10^{-5}$ in M(1), whereas the difference calculated using data is

$2.36 \times 10^{-5} - 2.06 \times 10^{-5} = 0.30 \times 10^{-5}$ (one-sided p-value=0.039). The difference in M(2) is within the 95% confidence interval of the data moment.

Next, I discuss the implications of the comovement state variable b_t . The simulation results further demonstrate the ability of this procyclical exogenous component (driven by b_t) to counterbalance the countercyclical endogenous component in the total amount of risk and thus resolve the Duffee Puzzle. To be more specific, Table 2.10, Fact (i), shows that M(3) generates a higher covariance between market returns and consumption growth during non-recession periods ($C(r^m, \Delta c)(I_{recc.=0}) = 2.7672 \times 10^{-5}$) than during recession periods ($C(r^m, \Delta c)(I_{recc.=1}) = 2.6743 \times 10^{-5}$); both point estimates are not rejected by their sample counterparts. In the same row, M(1) and M(2) without the procyclical comovement state variable b_t generate a countercyclical amount of risk.

Lastly, and more importantly, the *share* of the amount of risk explained by the exogenous component is already weakly procyclical in M(1) and M(2). This is true because the endogenous components, which enter the denominator, are countercyclical through the risk aversion channel. However, without a procyclical exogenous component, M(1) and M(2) do not fit Fact (j). More specifically, the implied shares during non-recession periods in all three models are statistically close to the sample counterparts: 15.980% in data, 14.136% in M(1), 14.248 in M(2), and 13.443% in M(3). However, the implied shares during recession periods are statistically significantly higher in M(1), 13.120%, and M(2), 12.717%, than in the data, 1.322%. Only model M(3) generates the share, 4.196%, that is within the 95% confidence interval of the data. This in turn demonstrates the economic significance of the procyclical comovement documented in this article.

2.4.3.4 Price Dividend Ratio Dynamics

In this section, I analyze the dependence of the price dividend ratio on the three state variables both economically and quantitatively. In Figure 2.5, lines with squares illustrate the dependence of the price dividend ratio on s (n) given the numerical solution of M(3), conditional on *different* combinations of the other two state variables n and b (s and b); regarding *different* combinations, I consider mean and critical values for each of the other two variables. Since M(2)

has only two dimensions, s and n , I fix one when evaluating the relationship between pd and the other variable as shown in solid lines with triangles. M(1) with only one dimension, s , is depicted in solids lines with circles.

All lines in the top plot of Figure 2.5 demonstrate the positive relationship between the price dividend ratio and the surplus consumption ratio, consistent with the literature and the analytical prediction earlier. Next, the dotted line with squares shows that the price dividend ratio is higher in states of high n (1.4246, the 95% quantile value in the n_t simulation), controlling for the same b . This “high n ”–“high PD ” line indicates that the DR effect of n_t on the valuation ratio via the risk free rate dominates the CF effect via the expected dividend growth in this model. However, both analytical (see Appendix 2.5) and numerical (here) solutions confirm that the price dividend ratio does not have a monotonic relationship with n . The bottom plot of Figure 2.5 shows that, after certain cutoff point around $n = 4.5$, the price dividend ratio decreases with n ; namely, the CF effect of macroeconomic uncertainty becomes dominant during periods with “extremely” bad events (i.e., 0.1% according to the simulation). This non-monotonic relationship precisely reflects the countervailing DR and CF effects of the macroeconomic uncertainty state variable, as discussed in the analytical part (see Section 2.4.2.2). In the top plot of Figure 2.5, the DR effect dominates because the 95% quantile value (1.4246) is less than the cutoff value (4.5).

Figure 2.6 analyzes the relationship between the price dividend ratio and b , conditional on s and n . The three lines with squares show the positive relationship between the valuation ratio and the comovement state variable in M(3) by fixing s and n at mean or critical values, confirming the dominant CF channel mentioned in Section 2.4.2.2. In addition, the price dividend ratio implied from M(3) at the “low s ”–“ \bar{n} ” plane ($s = -3.5281, n = 0.3742$; dotted line) is lower than at the “ $E(s)$ ”–“ \bar{n} ” plane¹⁷ ($s = -2.6595, n = 0.3742$; solid line), indicating a positive relationship between PD and s . Analogously, the price dividend ratio is higher at the “ $E(s)$ ”–“high n ” plane ($s = -2.6595, n = 1.4246$; dashed line) than at the $E(s)$ – \bar{n} plane (solid line), indicating a positive

¹⁷Note that the long-run mean of s_t is by design time-varying in M(2) and M(3), as discussed in Section 2.4.1. The long-run mean of s in M(1) is constant, $\bar{s} = -2.6677$, as shown in Table 2.8. In Figure 2.6, I use the unconditional mean of s simulated from M(3) as the s intercept value for all five lines for consistency.

relationship between PD and n .¹⁸ Both observations are consistent with Figure 2.5. Lastly, the $M(1)$ and $M(2)$ horizontal lines intersect the $E(s)-\bar{n}$ plane of $M(3)$ at around $b = 0.45$, which is expected because $\hat{b} = 0.4447$.

Next, I examine the log price dividend ratio dynamics quantitatively. In Table 2.11, I conduct univariate and multivariate contemporaneous regressions of the log price dividend ratio on the state variables, and confront the parameter estimates and variance decomposition results in each model with their sample counterparts. In the last row, I note the R^2 of the univariate or multivariate regression within each model.

I obtain the empirical proxies for the three state variables as follows. I follow Wachter (2006) to construct a monthly empirical proxy for s_t , $\sum_{i=1}^{108} \phi_s^i \Delta c_{t-i}$ where ϕ_s at the monthly frequency is 0.9957 (Table 2.8) and Δc_t is the AR(3)-de-meaned consumption growth. Because of the cumulative sum, the empirical proxy for s_t (thus the sample regressions) starts in March 1968. I then scale the empirical proxy to match the mean and volatility of s_t implied from the theoretical model. The monthly empirical proxies for n_t and b_t are obtained from the DGP estimation results in Table 2.5.

The univariate coefficient estimate of pd_t on b_t in the empirical regression is 1.2807 (SE=0.1292); economically, that means that a unit standard deviation increase in b_t (0.10) is associated with $\frac{1}{3}$ unit standard deviation increase in pd_t (0.14). The univariate model explains 12.900% of the total variability of pd_t . The multivariate model has a higher R^2 of 49.587%. The log surplus consumption ratio accounts for 72.779% of the fitted log price dividend ratio variability (or variance decomposition, $\text{VARC}(s_t) \equiv \hat{b}(s_t) \text{cov}(s_t, \widehat{pd}_t) / \text{var}(\widehat{pd}_t) = 72.779\%$ where \widehat{pd}_t denotes the fitted value), the macroeconomic uncertainty for 14.102%, and the consumption-dividend comovement for 13.386%. The log surplus consumption ratio s_t and the procyclical comovement b_t positively predict pd_t in the multivariate regression, while n_t has a negative coefficient. Hence, empirically, the relationship between the log valuation ratio and b_t remains significant and positive after controlling for other state variables, providing empirical evidence of the CF channel as discussed in Section 2.4.2.2.

¹⁸ “ \bar{n} ” (0.3742) and “high n ” (1.4246) are within the lower region in the bottom plot of Figure 2.5 where the DR effect still dominates the CF effect; thus, a positive relationship is expected.

With the simulated dataset of M(1), the s_t coefficient of 0.6693 is higher than the sample 95% confidence interval. The regression R^2 is 96.933% given that the M(1) economy is spanned by only one state variable; it is not 100% because the CC channel builds in a non-linearity through the sensitivity function. The bivariate regression using the simulated dataset of M(2) shows a significant and positive coefficient estimate of s_t (0.5564) with a large variance decomposition percentage (69.091%). The bivariate regression of M(2) appears parsimonious to capture the additional non-linearity introduced by the uncertainty state variable, thus obtaining a lower R^2 of only 62.012%. However, the linear models are potentially useful to evaluate first order effects.¹⁹

The M(3) model is the only model with the new state variable b_t . With the simulated dataset of M(3), the univariate coefficient estimate of pd_t on b_t is 1.1146, which is statistically close to the empirical coefficient estimate. Given that M(3) is a non-linear model with no exact closed-form solutions, I use the approximate linear conjecture (Equation (2.T25)) underlying the approximate analytical solution in Section 2.4.2.2, for the multivariate analysis. Thus, the multivariate regression model has four explanatory variables, $\{s_t, n_t, b_t, b_t^2\}$. The multivariate regression delivers a significant and positive coefficient estimate for s_t (0.5368) with a 64.317% variance decomposition percentage; the estimate is within two standard errors of the empirical coefficient. The b_t coefficient estimate is 0.8951, which is higher than the empirical coefficient (0.5480) but would not be rejected at the 1% significance level. In contrast to the empirical finding on the dominating CF effect of n_t on pd_t (i.e., a negative n_t coefficient), the multivariate regression results using the simulated datasets of both M(2) and M(3) show a dominating DR effect (i.e., positive n_t coefficients) as also seen in Figures 2.5 and 2.6. The M(3) model also underestimates the significance of b_t in explaining price variability: the VARC is 6.657% using the simulated dataset of M(3), but 13.386% using actual data. The R^2 of the M(3) approximate model is 65.255%, suggesting that higher order terms are important in explaining price dividend ratio.

Lastly, Table 2.11 reveals two more economic insights. First, controlling for macroeconomic uncertainty and dynamic cash flow comovement, changes in risk aversion play a significant and

¹⁹Note that in the long-run risk literature, it is common to use linear approximations.

dominant role (data VARC = 72.799%) in explaining the price variability even with a rough proxy. Thus, risk aversion appears to be a more economically important factor in explaining risky asset prices than are second moment state variables, which is a testable hypothesis for future research. Second, the data VARCs of the procyclical consumption-dividend comovement (13.386%) and the countercyclical uncertainty (14.102%) are relatively close. Thus, while the countercyclical uncertainty is well-acknowledged in the literature, the procyclical dividend risk introduced in this article appears to also have nontrivial economic significance.

2.5 The Cross Section of Expected Returns

Macroeconomic variables are widely-acknowledged candidates for systematic risk factors that are correlated with consumption and investment opportunities and thus maybe priced in the cross-section of expected returns (see Maio and Santa-Clara, 2015). There is a small but burgeoning literature using macro factors to explain the cross-section of expected returns (see e.g. Lettau and Ludvigson, 2001; Bansal, Dittmar, and Lundblad, 2005; Bali, Brown, and Tang, 2017).

To enhance the plausibility of the procyclical comovement state variable introduced in this article, I now examine the cross-sectional pricing abilities of the three state variables. A four-factor pricing model with market returns and the innovations to the three state variables is estimated using the Fama and MacBeth (1973) methodology and the 25 size- and book-to-market-sorted portfolios constructed by Fama and French (1993). The sample period is March 1968–June 2014. Market returns are included to acknowledge systematic financial asset risk factors that are orthogonal to macroeconomic shocks in a parsimonious way. The first four panels in Table 2.12 report the portfolio loadings on the four factors, the 5th bin–1st bin (“5-1”) differences along each dimension and their significance. The last panel reports the second-stage cross-sectional regression results for the prices of risk and their significance.

I find that the price of volatility risk is negative ($\hat{\lambda}_{innov} = -0.0697$, $SE = 0.0413$; Panel E of Table 2.12). Investors pay for insurance against increases in macroeconomic uncertainty. In

the cross section, value stocks and small stocks comove more negatively with changes in volatility than growth and large stocks and thus require higher risk premiums, whereas large growth stocks exhibit positive betas and thus provide volatility risk insurance. Note that the macroeconomic uncertainty in this paper is simply proxied by consumption growth volatility; its role in cross-sectional pricing supports the recent findings in Bali, Brown, and Tang (2017) who use the well-known economic uncertainty index of Jurado, Ludvigson, and Ng (2015). In addition, the price of comovement risk is positive ($\hat{\lambda}_{binnow}=0.0474$, $SE=0.0216$; Panel E of Table 2.12)—which is consistent with the theory in the current paper. Investors consider stocks that covary more positively with aggregate dividend risk riskier, because dividend risk is procyclical. This is new to the cross-section of expected-return literature.

Given the cross-sectional findings in Table 2.12, value stocks exhibit higher b_t loadings than growth stocks, and small stocks exhibit higher loadings than large stocks. As the extreme example in the 5×5 panel, the loading of the VALUE-SMALL portfolio on the b_t innovations in the four-factor pricing model is significant and positive ($\hat{\beta}_{i,binnow}=17.1760$, $SE=6.3492$). Furthermore, I test the significance of the loading differences between the 5th bin (“VALUE”) and the 1-st bin (“GROWTH”), conditional on different sizes. For portfolios with above-medium sizes, the “5-1” differences are significant and positive (8.5369* for the “Size 4” stocks, and 19.6829*** for the “LARGE” stocks). The empirical value premium is calculated as the average spread in returns between the 5th bin (“VALUE”) and the 1-st bin (“GROWTH”) stocks across time and across all sizes. The explained value premium through the comovement channel is calculated as the average loading difference (“5-1”) multiplied by the price of comovement risk across all sizes. As an immediate implication, the comovement channel explains 75% of the value premium, that is 0.39% out of 0.51%, through the lens of this model.

This paper provides a framework to evaluate the explanatory power of the economic state variables for both time-varying price variation and cross-sectional variation in expected returns. Among the three economic factors motivated from the theoretical model, while in Section 2.4.3.4 I find that changes in risk aversion is a dominant factor explaining aggregate price-dividend ratio variability (VARC=72.79% according to Table 2.11), but changes in macroeconomic uncertainty

and cash flow comovement (higher-order-moment factors) account for 94.65% of the explained *cross-sectional* variation in expected returns.

2.6 Conclusion

This paper contributes to the literature in the following ways. First, it recognizes and replicates the puzzling finding in Duffee (2005) in which he provides empirical evidence for the procyclicality of the amount of risk, $Cov_t(r_{t+1}^m, \Delta c_{t+1})$. To resolve the Duffee Puzzle, I decompose the covariance into two components, providing strong and robust empirical evidence for a procyclical component, $Cov_t(\Delta d_{t+1}, \Delta c_{t+1})$ and a countercyclical component, $Cov_t(r_{t+1}^m - \Delta d_{t+1}, \Delta c_{t+1})$. Because the procyclical component dominates, the puzzle is resolved. In contrast, most of the literature assumes that the amount of risk is acyclical or strictly countercyclical. I establish 10 stylized facts (of which 7 are new) related to the Duffee Puzzle that serve as testable hypotheses for a proposed theoretical model.

Second, I formulate a new DGP for the consumption-dividend joint dynamics with a minimum number of state variables to be used in consumption-based asset pricing models. The new DGP features two new state variables: countercyclical macroeconomic uncertainty and procyclical consumption-dividend comovement. Both the analytical solutions and estimation results of this parsimonious DGP demonstrate the ability to accommodate all stylized facts related to consumption and dividend growth, which is an improvement to the existing DGPs in the literature.

Then, I solve a variant of the Campbell and Cochrane model that uses the new DGP and accommodates the Duffee Puzzle. The three state variables are the procyclical risk appetite and two new ones from the new DGP. Numerical solutions demonstrate that the revised model fits all cyclical moments related to the Duffee Puzzle, which is a contribution to the literature. I also confront the model with a broad array of unconditional fundamental moments, asset price statistics and price dividend ratio variance decompositions to over-identify the model. In particular, the comovement state variable positively predicts the log price dividend ratio through the cash flow channel, which is quantitatively confirmed using actual data. Furthermore, a multivariate

contemporaneous regression of the log price dividend ratio on the three state variables reveals that the procyclical comovement state variable explains 13% of the fitted log price dividend ratio variability. Other notable asset pricing implications are (1) a lower equity premium and (2) a more volatile price dividend ratio. The procyclical amount of dividend risk “hedges” the countercyclical price of risk and the countercyclical volatility in the total amount of risk, rendering equity less risky.

To substantiate the plausibility of the procyclical comovement as the new state variable, I also examine its ability to help price the cross section of expected returns. I find a significant and positive price of comovement risk: investors demand higher compensation from stocks that comove more positively with the consumption-dividend comovement. Value stocks have significantly higher comovement loadings than growth stocks, which explains 75% of the value premium in this sample. Second-moment state variables (countercyclical macroeconomic uncertainty and procyclical consumption-dividend comovement) account for 95% of the total explanatory power of the three state variables in explaining the *cross section* of asset returns, whereas risk aversion accounts for 72% of price dividend ratio variability and thus is a dominant factor in explaining the *time variation* in market returns.

Appendices

2.A Estimation procedure for the new DGP in Section 2.3.1

The consumption-dividend dynamics in Section 2.3.1 accommodates the Duffee Puzzle and the time-varying macroeconomic uncertainty, and thus introduces several new parameters. I provide parameter choices based on a two-step estimation procedure. Consumption growth and dividend growth have the following joint dynamics:

$$\Delta c_{t+1} = \bar{c} + \sigma_c \tilde{\omega}_{c,t+1} + \sigma_n \tilde{\omega}_{n,t+1}, \quad (2.T1)$$

$$n_{t+1} = (1 - \phi_n) \bar{n} + \phi_n n_t + \sigma_{nn} \tilde{\omega}_{n,t+1}, \quad (2.T2)$$

$$\Delta d_{t+1} = \bar{d} + \phi_d (V_{c,t} - \bar{V}_c) + b_t \sigma_c \tilde{\omega}_{c,t+1} + \sigma_d \tilde{\omega}_{d,t+1}, \quad (2.T3)$$

$$b_{t+1} = (1 - \phi_b) \bar{b} + \phi_b b_t + \lambda_b \sigma_c \tilde{\omega}_{c,t+1}, \quad (2.T4)$$

$$V_{c,t} = \sigma_c^2 + \sigma_n^2 n_t, \quad (2.T5)$$

$$\bar{V}_c = \sigma_c^2 + \sigma_n^2 \bar{n}, \quad (2.T6)$$

where the consumption fundamental shock, $\tilde{\omega}_{c,t+1}$, is a centered Gaussian shock with standard deviation equal to 1, the consumption event shock, $\tilde{\omega}_{n,t+1}$, follows a centered heteroskedastic gamma distribution with a strictly positive shape parameter equal to n_t and a scale parameter equal to 1, and the dividend-specific shock, $\tilde{\omega}_{d,t+1}$, follows a centered homoskedastic gamma distribution with a strictly positive shape parameter equal to V_d and a scale parameter equal to 1. Or,

$$\tilde{\omega}_{c,t+1} \sim i.i.d.N(0, 1); \tilde{\omega}_{n,t+1} \sim \Gamma(n_t, 1) - n_t; \tilde{\omega}_{d,t+1} \sim \Gamma(V_d, 1) - V_d.$$

The three fundamental shocks are mutually independent. Consumption growth and dividend growths are observables; the two latent processes in the system are the macroeconomic uncertainty state variable n_t and the conditional sensitivity of dividend growth to consumption growth b_t . $V_{c,t}$ denotes the total consumption conditional variance, which is a linear function of n_t . \bar{x} denotes the unconditional mean of process x , and ϕ_x denotes the conditional mean feedback of process x to itself or another variable. Here is the full set of parameters in the joint dynamics: consumption, $\{\bar{c}, \sigma_c, \sigma_n, \bar{n}, \phi_n, \sigma_{nn}\}$; cash flow, $\{\bar{d}, \phi_d, \sigma_d, \bar{b}, \phi_b, \lambda_b\}$.

By design, there is no feedback from the cash flow growth process to the consumption growth process. The estimation procedure is described with two steps. The first step estimates the consumption growth system. I use a filtration-based maximum likelihood methodology of Bates (2006) to estimate the latent time series n_t and extract the two consumption shock realizations, the fundamental shock $\tilde{\omega}_{c,t+1}$ and the event shock $\tilde{\omega}_{n,t+1}$. The conditional consumption growth variance and its long-run average is then implied, $\hat{V}_{c,t}$ and $\hat{V}_{c,t}$.

The second step takes the dividend growth data, Δd_{t+1} , and the predetermined state variable levels and shocks from the previous step, $\{\hat{V}_{c,t}, \hat{V}_{c,t}, \hat{\sigma}_c, \hat{\omega}_{c,t+1}\}$, and finds the cash flow parameters such that the sum of the log likelihoods of the implied cash flow-specific shock $\tilde{\omega}_{d,t+1}$ is maximized. To provide estimation convenience without loss of statistical power, I first project dividend growth onto a vector of ones and $\hat{V}_{c,t} - \hat{V}_{c,t}$, and obtain the estimates for $\{\bar{d}, \phi_d\}$. Then, I use the residuals to estimate the rest of the cash flow parameters. The MLE estimation does not impose constraints on the non-negativity of b_t estimates, but imposes one constraint to ensure a valid gamma density function for $\tilde{\omega}_{d,t+1}$ at any time stamp t :

$$-\sigma_d V_d \geq \max_{\forall t \in 1, \dots, T} \left(\Delta d_{t+1} - \bar{d} - \hat{\phi}_d (\hat{V}_{c,t} - \hat{V}_{c,t}) - b_t \hat{\omega}_{c,t+1} \right). \quad (2.T7)$$

A gamma distribution is right-tailed and is bounded below; σ_d is expected to be negative given the strongly negative dividend growth skewness; therefore, the zero-mean dividend-specific shock $\sigma_d \tilde{\omega}_{d,t+1}$ is expected to be left-tailed with an upper bound at $-\sigma_d V_d > 0$. The constraint above states that the maximum dividend-specific shock is within the upper bound, and thus a gamma density function at any time stamp t is defined.

2.B Recession identification criteria in simulated monthly series

In the moment matching exercises, data moments and simulation moments during recession and non-recession months are calculated in Table 2.6. The empirical recession dummy variable uses the NBER recession indicator (from the NBER website) which is based on patterns in quarterly GDP growth. However, theoretical models in this paper do not generate output. Instead, I use patterns in consumption growth (the only macroeconomic variable in the model) to identify

recessions in the simulated months. Here is the algorithm:

1. **Quarterly Growth:** aggregate the monthly consumption growth data into a quarterly frequency;
2. **Standardization:** de-mean the quarterly consumption growth by a 49-quarter moving average (24+1+24), and divide it with its long-term/unconditional standard deviation;
3. **Fundamental Cyclical Events:** identify the quarters as recessions if there are at least two consecutive standardized consumption growth drops that are < -0.9 ;
4. **Extreme Events:** for an extreme event (when standardized consumption growth values are ≤ -2), if its *adjacent* quarter(s) before and/or after exhibit(s) negative standardized growths, then the extreme event and its adjacent quarter(s) are considered as recession periods. If the *second adjacent* quarters before and/or after also have standardized growth < -0.9 , then these quarters + adjacent one(s) + extreme event are identified as recession periods. Evaluate backward and forward until the “ripple” effect is considered diminished, or ≥ -0.9 .
5. **Trough Points with Positive Growths:** given the recessions identified in (3) and (4), if there is a recession period lasting for at least three quarters and the following quarter has a positive growth rate (usually large), then this quarter is also considered as a recession period.

I test the algorithm using the actual monthly consumption data, and compare the identified recessions with the NBER recession periods. This methodology is able to identify 7 out of the 8 NBER recessions between January 1959 and June 2014, with a significant correlation 80%. The quarterly regression coefficient is 0.9038 (SE=0.0507), which fails to reject the null hypothesis of 1 at the 5% significance level.

2.C Intermediate models in Section 2.4

In this section, I introduce the two intermediate models and the final model as analyzed in Section 2.4. The first intermediate model “M(1)” is an adapted Campbell and Cochrane model that features one state variable (the surplus consumption ratio), homoskedastic shocks, constant expected dividend growth, and a constant consumption-dividend comovement. The second intermediate model “M(2)” is an adapted Bekaert and Engstrom model that builds on M(1) to incorporate a countercyclical macroeconomic uncertainty as a salient state variable. Lastly, the final model in this paper “M(3)” can be viewed as a generalization of M(2) where the consumption-dividend comovement is now procyclical. All three models price dividend claims.

- Fundamentals:

$$M(1): \Delta c_{t+1} = \bar{c} + \sigma_c \tilde{\omega}_{c,t+1} + \sigma_n \tilde{\omega}_{n,t+1}, \quad (2.T1)$$

$$\tilde{\omega}_{c,t+1} \sim i.i.d.N(0, 1), \tilde{\omega}_{n,t+1} \sim \Gamma(\bar{n}, 1) - \bar{n}, \quad (2.T2)$$

$$\Delta d_{t+1} = \bar{d} + \bar{b} \sigma_c \tilde{\omega}_{c,t+1} + \sigma_d \tilde{\omega}_{d,t+1}, \quad (2.T3)$$

$$\tilde{\omega}_{d,t+1} \sim \Gamma(V_d, 1) - V_d, \quad (2.T4)$$

$$\bar{c} = 0.0025, \sigma_c = 0.0029, \sigma_n = -0.0023, \bar{n} = 0.3742,$$

$$\bar{d} = 0.0025, \sigma_d = -0.0008, V_d = 89.9322, \bar{b} = 0.4447;$$

$$M(2): \Delta c_{t+1} = \bar{c} + \sigma_c \tilde{\omega}_{c,t+1} + \sigma_n \tilde{\omega}_{n,t+1}, \quad (2.T5)$$

$$n_{t+1} = (1 - \phi_n) \bar{n} + \phi_n n_t + \sigma_{nn} \tilde{\omega}_{n,t+1}, \quad (2.T6)$$

$$\tilde{\omega}_{c,t+1} \sim i.i.d.N(0, 1), \tilde{\omega}_{n,t+1} \sim \Gamma(n_t, 1) - n_t, \quad (2.T7)$$

$$\Delta d_{t+1} = \bar{d} + \phi_d (V_{c,t} - \bar{V}_c) + \bar{b} \sigma_c \tilde{\omega}_{c,t+1} + \sigma_d \tilde{\omega}_{d,t+1}, \quad (2.T8)$$

$$V_{c,t} = Var_t(\Delta c_{t+1}) = \sigma_c^2 + \sigma_n^2 n_t, \bar{V}_c = E(V_{c,t}), \quad (2.T9)$$

$$\tilde{\omega}_{d,t+1} \sim \Gamma(V_d, 1) - V_d, \quad (2.T10)$$

$$\bar{c} = 0.0025, \sigma_c = 0.0029, \sigma_n = -0.0023, \bar{n} = 0.3742, \phi_n = 0.9500, \sigma_{nn} = 0.2772,$$

$$\bar{d} = 0.0025, \phi_d = -568.0871, \sigma_d = -0.0008, V_d = 89.9322, \bar{b} = 0.4447;$$

M(3): The new DGP in this paper (as shown in Table 2.5).

- The surplus consumption ratio, M(1)~M(3):

$$s_{t+1} = (1 - \phi_s) \bar{s} + \phi_s s_t + \lambda_t (\Delta c_{t+1} - \bar{c}). \quad (2.T11)$$

- The sensitivity functions:

$$\lambda_t = \begin{cases} \frac{1}{\bar{S}_t} \sqrt{1 - 2(s_t - \bar{s}_t)} - 1, & s_t \leq s_{max,t} \\ 0, & s_t > s_{max,t} \end{cases}, \quad (2.T12)$$

$$\bar{s}_t = \log(\bar{S}_t), \quad (2.T13)$$

$$s_{max,t} = \bar{s}_t + \frac{1}{2}(1 - \bar{S}_t^2), \quad (2.T14)$$

$$M(1): \bar{S}_t = \sqrt{(\sigma_c^2 + \sigma_n^2 \bar{n}) \frac{\gamma}{1 - \phi_s}}, \quad (2.T15)$$

$$M(2/3): \bar{S}_t = \sqrt{(\sigma_c^2 + \sigma_n^2 n_t) \frac{\gamma}{1 - \phi_s}}. \quad (2.T16)$$

- The real risk free rates (approximated at the third order for demonstration purpose):

$$\begin{aligned}
\text{M(1): } rf_t &= -\ln \beta + \gamma \bar{c} + \gamma(1 - \phi_s)(\bar{s}_t - s_t) - \frac{1}{2}\gamma^2(1 + \lambda_t)^2\sigma_c^2 - [\gamma(1 + \lambda_t)\sigma_n - \ln(1 + \gamma(1 + \lambda_t)\sigma_n)]\bar{n} \\
&\approx -\ln \beta + \gamma \bar{c} + \gamma(1 - \phi_s)(\bar{s}_t - s_t) - \underbrace{\frac{1}{2}\gamma^2(1 + \lambda_t)^2\sigma_c^2 - \frac{1}{2}\gamma^2(1 + \lambda_t)^2\sigma_n^2\bar{n} + \frac{1}{3}\gamma^3(1 + \lambda_t)^3\sigma_n^3\bar{n}}_{\text{fix} = -\frac{(1-\phi_s)\gamma}{2}} \\
&\approx rf_{CC} + \frac{1}{3}\gamma^3(1 + \lambda_t)^3 \underbrace{\sigma_n^3}_{<0} \bar{n}, \tag{2.T17}
\end{aligned}$$

$$\begin{aligned}
\text{M(2/3): } rf_t &= -\ln \beta + \gamma \bar{c} + \gamma(1 - \phi_s)(\bar{s}_t - s_t) - \frac{1}{2}\gamma^2(1 + \lambda_t)^2\sigma_c^2 - [\gamma(1 + \lambda_t)\sigma_n - \ln(1 + \gamma(1 + \lambda_t)\sigma_n)]n_t \\
&\approx -\ln \beta + \gamma \bar{c} + \gamma(1 - \phi_s)(\bar{s}_t - s_t) - \underbrace{\frac{1}{2}\gamma^2(1 + \lambda_t)^2\sigma_c^2 - \frac{1}{2}\gamma^2(1 + \lambda_t)^2\sigma_n^2n_t + \frac{1}{3}\gamma^3(1 + \lambda_t)^3\sigma_n^3n_t}_{\text{fix} = -\frac{(1-\phi_s)\gamma}{2}} \\
&\approx rf_{CC} + \frac{1}{3}\gamma^3(1 + \lambda_t)^3 \underbrace{\sigma_n^3}_{<0} n_t, \tag{2.T18}
\end{aligned}$$

$$rf_{CC} = -\ln \beta + \gamma \bar{c} - \frac{(1 - \phi_s)\gamma}{2}. \tag{2.T19}$$

2.D Quadratic approximation to the moment generating function of a random variable that is a linear combination of Gaussian, χ^2 , and gamma shocks

Suppose a random variable x receives three shocks,

$$\begin{aligned}
x &= \mu + x_1\omega + x_2(\omega^2 - 1) + x_3(\varepsilon - \alpha), \\
\omega &\sim i.i.d.N(0, 1), \\
\omega^2 &\sim i.i.d.\chi^2(1), \\
\varepsilon &\sim \Gamma(\alpha, 1),
\end{aligned} \tag{2.T1}$$

where μ is the unconditional mean of variable x , and $\{x_1, x_2, x_3\}$ are constant coefficients. Recall the moment generating function (mgf) for a standard Gaussian shock is $mgf_\omega(\nu) = \exp(\nu^2/2)$, the mgf for a χ^2 shock is $mgf_{\omega^2}(\nu) = (1 - 2\nu)^{-1/2}$, and the mgf for a gamma shock with a unit scale parameter is $mgf_\varepsilon(\nu) = (1 - \nu)^{-\alpha}$ where α is the shape parameter. The three shocks are uncorrelated. Therefore,

$$\begin{aligned}
mgf_x(\nu) &= E[\exp(\nu x)] \\
&= \exp(\nu\mu)E_t[\exp(\nu x_1\omega + \nu x_2(\omega^2 - 1) + \nu x_3(\varepsilon - \alpha))] \\
&= \exp(\nu\mu - \nu x_2 - \nu x_3\alpha)mgf_\omega(\nu x_1)mgf_{\omega^2}(\nu x_2) + mgf_\varepsilon(\nu x_3) \\
&= \exp(\nu\mu - \nu x_2 - \nu x_3\alpha) \exp\left\{\frac{1}{2}(\nu x_1)^2\right\} (1 - 2\nu x_2)^{-1/2} (1 - \nu x_3)^{-\alpha} \\
&= \exp(\nu\mu - \nu x_2 - \nu x_3\alpha) \exp\left\{\frac{1}{2}(\nu x_1)^2 - \frac{1}{2}\ln(1 - 2\nu x_2) - \alpha \ln(1 - \nu x_3)\right\}. \tag{2.T2}
\end{aligned}$$

It can be easily shown that the quadratic approximation to $\ln(1-x)$ is $-x - \frac{1}{2}x^2$. Applying the quadratic approximation to $\ln(1-2\nu x_2)$ and $\ln(1-\nu x_3)$, the mgf becomes,

$$\begin{aligned} mgf_x(\nu) &\approx \exp(\nu\mu - \nu x_2 - \nu x_3\alpha) \exp\left\{\frac{1}{2}(\nu x_1)^2 + \nu x_2 + (\nu x_2)^2 + \nu x_3\alpha + \frac{1}{2}(\nu x_3)^2\alpha\right\} \\ &= \exp(\nu\mu) \exp\left\{\frac{1}{2}(\nu x_1)^2 + (\nu x_2)^2 + \frac{1}{2}(\nu x_3)^2\alpha\right\} \\ &= \exp(\nu E(x)) \exp\left\{\frac{1}{2}\nu^2 V(x)\right\}. \end{aligned} \quad (2.T3)$$

Define $X = \exp(x)$ and set $\nu = 1$,

$$E(X) \approx \exp\left\{E(x) + \frac{1}{2}V(x)\right\}. \quad (2.T4)$$

2.E Solving the theoretical model from Section 2.4 (approximate analytical solution)

In this section, I solve the theoretical model in Section 2.4, or M(3), with an approximate analytical solution using a similar procedure in the spirit of Bansal and Yaron (2004). The log linearization of the Euler equation becomes complex with gamma shocks and $\chi^2(1)$ shocks. Thus, to derive an ‘‘approximate’’ analytical solution, I use a quadratic approximation to the moment generating functions of the random variable $m_{t+1} + r_{t+1}^m$ (Appendix 2.4), and impose a linear approximation to obtain the log market return. In this economy, the log valuation ratio pd_t has the conjecture as follows:

$$pd_t = A_0 + A_1 s_t + A_2 b_t + A_3 b_t^2 + A_4 n_t. \quad (2.T1)$$

The Campbell and Shiller linearization to market return shows,

$$r_{t+1}^m = \Delta d_{t+1} + a_1 pd_{t+1} - pd_t + a_0. \quad (2.T2)$$

Given equations above, the log market return can be approximately expressed as a linear function of the state variables and four independent shocks to the economy:

$$\begin{aligned} r_{t+1}^m &= \bar{d} - \phi_d \sigma_d^2 \bar{n} + a_1 (A_0 + A_1(1 - \phi_s)\bar{s} + A_2(1 - \phi_b)\bar{b} + A_3((1 - \phi_b)\bar{b})^2 + A_4(1 - \phi_n)\bar{n}) - A_0 + a_0 \\ &\quad + A_1(a_1\phi_s - 1)s_t + (a_1A_2\phi_b + 2a_1A_3(1 - \phi_b)\bar{b}\phi_b - A_2)b_t \\ &\quad + A_3(a_1\phi_b^2 - 1)b_t^2 + (a_1A_4\phi_n - A_4 + \phi_d\sigma_d^2)n_t \\ &\quad + (a_1A_1\lambda_t + a_1A_2\lambda_b + 2a_1A_3(1 - \phi_b)\bar{b}\lambda_b + (1 + 2a_1A_3\phi_b\lambda_b)b_t)\sigma_c\tilde{\omega}_{c,t+1} \\ &\quad + a_1A_3\sigma_c^2\lambda_b^2(\tilde{\omega}_{c,t+1})^2 + a_1(A_1\lambda_t\sigma_n + A_4\sigma_{nn})\tilde{\omega}_{n,t+1} + \sigma_d\tilde{\omega}_{d,t+1}. \end{aligned} \quad (2.T3)$$

With the approximate logarithm of the Euler equation and by equating the terms for the state variables, the coefficients in the price-dividend ratio equation are solved:

$$A_1 = \frac{\gamma(1 - \phi_s)}{1 - a_1\phi_s}, \quad (2.T4)$$

$$0 < A_1 < \gamma.$$

$$A_2 = \frac{(1 + 2a_1A_3\phi_b\lambda_b) [\gamma(1 + \lambda_t) - (a_1A_1\lambda_t + 2a_1A_3(1 - \phi_b)\bar{b}\lambda_b)] \sigma_c^2 - 2a_1A_3(1 - \phi_b)\phi_b\bar{b}}{a_1\phi_b - 1 + a_1\lambda_b(1 + 2a_1A_3\phi_b\lambda_b)\sigma_c^2} > 0. \quad (2.T5)$$

$$A_3 = \frac{-2a_1\phi_b\lambda_b\sigma_c^2 + 1 - a_1\phi_b^2 \pm \sqrt{(2a_1\phi_b\lambda_b\sigma_c^2 - 1 + a_1\phi_b^2)^2 - 4a_1^2\phi_b^2\lambda_b^2\sigma_c^4}}{4a_1^2\phi_b^2\lambda_b^2\sigma_c^2} > 0. \quad (2.T6)$$

$$A_4 = \frac{\xi_t \pm \sqrt{\xi_t^2 - 2\sigma_{nn}^2 a_1^2 \left(\phi_d \sigma_d^2 + \frac{1}{2} (A_1 \lambda_t a_1 - \gamma(1 + \lambda_t))^2 \sigma_n^2 \right)}}{2\sigma_{nn}^2 a_1^2}, \quad (2.T7)$$

$$\xi_t = 1 - \phi_n a_1 - a_1^2 A_1 \lambda_t \sigma_n \sigma_{nn} + \gamma(1 + \lambda_t) a_1 \sigma_n \sigma_{nn}, \quad (2.T8)$$

$$A_4 < 0 \iff \phi_d \sigma_d^2 < -\frac{1}{2} (A_1 \lambda_t a_1 - \gamma(1 + \lambda_t))^2 \sigma_n^2.$$

The equity premium equation is well-approximated with $-Cov_t(r_{t+1}^m, m_{t+1})$ given the quadratic approximation,

$$\begin{aligned} E_t(r_{t+1}^m) - rft &+ \frac{1}{2} Var_t(r_{t+1}^m) \approx -Cov_t(r_{t+1}^m, m_{t+1}) \\ &= \underbrace{\gamma(1 + \lambda_t)}_{\text{price of consumption risk}} \\ &\times \underbrace{\{a_1 A_1 \lambda_t \sigma_c^2\}}_{\text{price of consumption risk}} \\ &+ \underbrace{[a_1 A_2 \lambda_b + 2a_1 A_3(1 - \phi_b)\bar{b}\lambda_b + (1 + 2a_1 A_3 \phi_b \lambda_b) b_t]}_{\text{price of consumption risk}} \sigma_c^2 \\ &+ \underbrace{a_1 [A_1 \lambda_t \sigma_n^2 + A_4 \sigma_{nn} \sigma_n]}_{\text{price of consumption risk}} n_t \\ &+ \underbrace{\dots}_{\text{price of consumption risk}} \end{aligned} \quad (2.T9)$$

2.0

Table 2.1: Models of the Univariate Conditional Variances.

This table presents the estimation results of eight univariate conditional variance models with a constant long-run mean or with a time-varying long-run mean that is a linear function of the standardized NBER recession indicator for four variables: consumption growth, log market return, dividend growth, and the non-dividend part of the market return. **Data** “Consumption Growth” is the AR(3)-de-meanned change in log real consumption (non-durable goods and services) per capita (source: BEA). “Market Return” is the change in log real market index (including dividends) (source: CRSP). “Dividend Growth” is the change in log real dividend level per capita (source: Shiller’s website). “Market Return–Dividend Growth” is the linear difference between log market return and log dividend growth. The NBER recession indicator ($I_{NBER,t}$) is obtained from the NBER website (1=recession; 0=otherwise), the standardized NBER indicator ($SNBER_t$) is predetermined as $(I_{NBER,t} - E(I_{NBER,t}))/SD(I_{NBER,t})$. To obtain the residuals, the four variables are regressed on the NBER recession indicator to account for the the cyclical conditional mean (if any). **Models without q_t** “Unconditional” denotes a model with a time-invariant variance. “GARCH” is adapted from Bollerslev (1987) assuming symmetric heteroskedastic Gaussian shocks. “GED-GARCH” is adapted from Nelson (1991) assuming symmetric heteroskedastic GED shocks with thick tails. “BEGE- n_t -GARCH” is adapted from Bekaert, Engstrom, and Ermolov (2015) assuming asymmetric heteroskedastic gamma shocks with thick tails. **Models with q_t** see Section 3.2 for modeling details. Model estimation uses the maximum likelihood estimation (MLE) methodology given the specified shock distributions. The estimations for “GARCH” and “GED-GARCH” use variance targeting. The robust standard errors are shown in parentheses. Values in bold (italics) are statistically significance at a significant level of 5% (10%). Underlined models are the best models among the eight models, given the Bayesian Information Criteria (BIC). N=665 months (1959/02~2014/06).

Panel A. Consumption Growth						
	Loglikelihood	Nparams	AIC	BIC	$SNBER_t$ coefficient	(SE)
Unconditional	2884.42	1	-5766.84	-5762.34		
GARCH	2911.44	2	-5816.87	-5803.37		
GED-GARCH	2913.30	3	-5820.59	-5807.10		
BEGE- n_t -GARCH	2919.62	6	-5827.23	-5800.24		
Unconditional, q_t	2885.92	1	-5767.84	-5758.84	0.1014	(0.0066)
GARCH, q_t	2913.14	3	-5820.28	-5806.78	0.0270	(0.0060)
GED-GARCH, q_t	2917.30	4	-5826.59	<u>-5808.60</u>	0.0428	(0.0099)
BEGE- n_t -GARCH, q_t	2924.92	7	<u>-5835.85</u>	-5804.35	0.1941	(0.0173)
Panel B. Market Return						
	Loglikelihood	Nparams	AIC	BIC	$SNBER_t$ coefficient	(SE)
Unconditional	1241.50	1	-2481.01	-2476.51		
GARCH	1275.84	2	-2547.68	-2538.68		
GED-GARCH	1293.13	3	-2580.25	-2566.75		
BEGE- n_t -GARCH	1307.83	6	-2603.65	-2576.65		
Unconditional, q_t	1284.04	1	-2566.09	-2561.59	0.6541	(0.0888)
GARCH, q_t	1298.05	3	-2590.10	-2576.60	0.6944	(0.0938)
GED-GARCH, q_t	1307.41	4	<u>-2606.82</u>	<u>-2588.82</u>	0.6935	(0.1084)
BEGE- n_t -GARCH, q_t	1309.54	7	-2605.09	-2573.59	0.6077	(0.4930)
Panel C. Dividend Growth						
	Loglikelihood	Nparams	AIC	BIC	$SNBER_t$ coefficient	(SE)
Unconditional	2374.99	1	-4747.98	-4743.48		
GARCH	2441.71	2	-4879.43	-4870.43		
GED-GARCH	2485.82	3	-4965.63	-4952.13		
BEGE- n_t -GARCH	2495.86	6	-4979.73	-4952.73		
Unconditional, q_t	2376.52	1	-4751.05	-4746.55	-0.0897	(0.0441)
GARCH, q_t	2444.05	3	-4882.11	-4868.61	-0.1316	(0.0413)
GED-GARCH, q_t	2486.82	4	-4965.63	-4947.63	-0.0714	(0.0620)
BEGE- n_t -GARCH, q_t	2499.63	7	<u>-4985.26</u>	<u>-4953.76</u>	<i>-0.1114</i>	(0.0592)

continue previous page

Panel D. Market Return–Dividend Growth (Non-Dividend Part of the Market Return)						
	Loglikelihood	Nparams	AIC	BIC	$SNBER_t$ coefficient	(SE)
Unconditional	1241.08	1	-2480.17	-2475.67		
GARCH	1276.97	2	-2549.95	-2540.95		
GED-GARCH	1294.55	3	-2583.10	-2569.60		
BEGE- n_t -GARCH	1303.12	6	-2594.24	-2567.24		
Unconditional, q_t	1284.03	1	-2566.05	-2561.55	0.6577	(0.0888)
GARCH, q_t	1300.38	3	-2594.76	-2581.26	0.6822	(0.0873)
GED-GARCH, q_t	1308.63	4	-2609.27	<u>-2591.27</u>	0.6689	(0.0991)
BEGE- n_t -GARCH, q_t	1313.71	7	<u>-2613.43</u>	-2581.93	0.7571	(0.1036)

Table 2.2: Parameter Estimates for the Best Univariate Conditional Variance Models.

This table presents the best univariate conditional variance models (denoted with underlines in Table 2.1) of consumption growth, log market return, dividend growth, and the non-dividend part of the market return. Denote $\tilde{\epsilon}_{t+1}$ as the zero-mean innovation at time $t + 1$, and h_t as the conditional variance of $\tilde{\epsilon}_{t+1}$. The best conditional variance model for consumption growth (Panel A of Table 2.1), log market return (Panel B of Table 2.1) and the non-dividend part of the market return (Panel D of Table 2.1) is “GED-GARCH- q_t ”:

$$\begin{aligned} \tilde{\epsilon}_{t+1} &\sim GED(0, h_t, \tau); \\ V_t(\tilde{\epsilon}_{t+1}) &\equiv h_t = \bar{h}(1 + q_t) + \alpha [\tilde{\epsilon}_t^2 - \bar{h}(1 + q_{t-1})] + \beta [h_{t-1} - \bar{h}(1 + q_{t-1})], \end{aligned}$$

where $\alpha + \beta < 1$, $\alpha > 0$, $\beta > 0$; $\tau > 0$ is the shape parameter of the Generalized Error Distribution. The best conditional variance model for dividend growth (Panel C of Table 2.1) is “BEGE- n_t -GARCH- q_t ”:

$$\begin{aligned} \tilde{\epsilon}_{t+1} &= \sigma_p \tilde{\omega}_{p,t+1} - \sigma_n \tilde{\omega}_{n,t+1}; \quad \tilde{\omega}_{p,t+1} \sim \Gamma(\bar{p}, 1) - \bar{p}, \quad \tilde{\omega}_{n,t+1} \sim \Gamma(n_t, 1) - n_t; \\ V_t(\tilde{\epsilon}_{t+1}) &\equiv h_t = \sigma_p^2 \bar{p} + \sigma_n^2 n_t; \quad n_t = \bar{n}(1 + q_t) + \alpha_n \left[\frac{\tilde{\epsilon}_t^2}{2\sigma_n^2} - \bar{n}(1 + q_{t-1}) \right] + \beta_n [n_{t-1} - \bar{n}(1 + q_{t-1})], \end{aligned}$$

where $\alpha_n + \beta_n < 1$, $\alpha_n > 0$, $\beta_n > 0$; \bar{p} (σ_p) is the shape (scale) parameter of the zero-mean homoskedastic good-environment gamma shock $\{\tilde{\omega}_{p,t+1}\}$, and $\{n_t\}$ (σ_n) the shape parameter of the zero-mean heteroskedastic bad-environment gamma shock $\{\tilde{\omega}_{n,t+1}\}$; $\sigma_p, \sigma_n, \bar{p}$ and $\{n_t\}$ are strictly positive to satisfy statistical properties of gamma distributions. The time-varying long-run conditional mean of the conditional variances is a multiple of the standardized NBER recession indicator:

$$q_t = \nu SNBER_t.$$

More model descriptions and estimation methodologies are discussed in Section 3.2. Robust standard errors are shown in parentheses. Values in bold (italics) are statistically significant at a significant level of 5% (10%). N=665 months (1959/02~2014/06).

Panel A. Consumption Growth, GED-GARCH-q_t							
	$\sqrt{\bar{h}}$	α	β	τ	ν		
Est.	0.0032	0.0129	0.9856	1.4708	0.0428		
SE	(fix)	(0.0704)	(0.0710)	(0.3442)	(0.0099)		
Panel B. Market Return, GED-GARCH-q_t							
	$\sqrt{\bar{h}}$	α	β	τ	ν		
Est.	0.0374	0.1407	0.7668	1.4659	0.6935		
SE	(fix)	(0.0390)	(0.0662)	(0.1042)	(0.1084)		
Panel C. Dividend Growth, BEGE-n_t-GARCH-q_t							
	\bar{p}	σ_p	\bar{n}	σ_n	α_n	β_n	ν
Est.	19.6778	0.0009	0.8751	0.0032	0.5179	0.4124	<i>-0.1114</i>
SE	(0.4408)	(0.0002)	(0.1592)	(0.0003)	(0.1141)	(0.1044)	(0.0592)
Panel D. Market Return–Dividend Growth, GED-GARCH-q_t							
	$\sqrt{\bar{h}}$	α	β	τ	ν		
Est.	0.0375	0.1570	0.7621	1.4854	0.6689		
SE	(fix)	(0.0360)	(0.0633)	(0.1078)	(0.0991)		

Table 2.3: Cyclicity of the Conditional Comovements between Consumption Growth and Market Return Components: Decomposing the Duffee Puzzle.

Given the best univariate conditional variance estimates from Table 2.2, this table formally identifies the cyclicity of the conditional comovements (correlation in Panel A, covariance in Panel B, and beta in Panel C) between the innovations of consumption growth and the innovations of different components of the market return using the DCC- q_t framework. In particular, the amount of risk ($Cov_t(\Delta c_{t+1}, r_{t+1}^m)$) is decomposed into two components: the “exogenous” component ($Cov_t(\Delta c_{t+1}, \Delta d_{t+1})$) and the “endogenous” component ($Cov_t(\Delta c_{t+1}, r_{t+1}^m - \Delta d_{t+1})$). **The DCC- q_t Model** The bivariate dependence framework is designed to jointly estimate and test the cyclicity of the conditional correlation. The conditional correlation matrix $Corr_t$ is modeled with a quadratic form, $(Q_t^*)^{-1} Q_t (Q_t^*)^{-1}$, where Q_t^* is the diagonal matrix with the square root of the diagonal element of Q_t on the diagonal (so the diagonal entries of $Corr_t$ are strictly equal to 1). The off-diagonal element of $Corr_t$ is the conditional correlation (or equivalently, the conditional covariance) of the standardized disturbance obtained from Table 2.2, $z_{t+1} \equiv [z_{1,t+1}, z_{2,t+1}]'$. The DCC- q_t model is expressed as follows,

$$Q_t = \bar{Q}_{12} \begin{bmatrix} 1 & 1 + q_t \\ 1 + q_t & 1 \end{bmatrix} + \alpha_{12} \left[z_t z_t' - \bar{Q}_{12} \begin{bmatrix} 1 & 1 + q_{t-1} \\ 1 + q_{t-1} & 1 \end{bmatrix} \right] + \beta_{12} \left[Q_{t-1} - \bar{Q}_{12} \begin{bmatrix} 1 & 1 + q_{t-1} \\ 1 + q_{t-1} & 1 \end{bmatrix} \right],$$

where parameter \bar{Q}_{12} is the off-diagonal term of the predetermined constant conditional correlation matrix $\bar{Q} = \frac{1}{T} \sum_{t=1}^T z_t z_t'$, and q_t is a multiple of the standardized NBER recession indicator,

$$q_t = \nu SNBER_t.$$

The DCC Model With $\nu = 0$ (or a constant long-run mean), the DCC model (Engle, 2002) is a natural null hypothesis of the DCC- q_t model. **Implied Conditional Covariance and Conditional Beta** Given the conditional correlation estimates from Panel A of this table and the conditional variance estimates from Table 2.2, the conditional covariance and the conditional beta of dividend growth to consumption growth innovations are derived and regressed on the NBER recession indicator ($I_{NBER}=1$ during recessions; 0 otherwise) in Panel B and Panel C. **Other Notations** “LL”, loglikelihood; “LR”, likelihood ratio; $b(I_{NBER})$, OLS coefficient on the NBER recession indicator. Robust standard errors are shown in parentheses. Values in bold (italics) are statistically significant at a significant level of 5% (10%). N=665 months (1959/02~2014/06).

<i>Series 1:</i>	<i>Consumption Growth (Δc)</i>			<i>Market Return (r^m)</i>		
<i>Series 2:</i>	<i>Market Return (r^m)</i>	<i>Dividend Growth (Δd)</i>	<i>$r^m - \Delta d$</i>			
Panel A. Conditional Correlation						
Conditional Correlation Parameters:	DCC	DCC- q_t	DCC	DCC- q_t	DCC	DCC- q_t
\bar{Q}_{12}	0.2022 (fix)	0.2022 (fix)	0.2298 (fix)	0.2298 (fix)	0.2128 (fix)	0.2128 (fix)
α_{12}	0.0223 (0.1463)	0.0227 (0.1636)	0.1431 (0.0637)	0.1405 (0.0644)	0.0211 (0.1804)	0.0210 (0.1823)
β_{12}	0.9657 (0.0740)	0.9340 (0.0830)	0.8300 (0.0255)	0.8324 (0.0262)	0.9735 (0.1147)	0.9740 (0.0502)
ν		-0.1539 (0.0645)		-0.7999 (0.0987)		0.0445 (0.0221)
LL	112.30	116.62	57.62	62.42	17.23	19.08
N(param)	2	3	2	3	2	3
Wald test stats. (H0=DCC)	-	5.69	-	65.73	-	4.05
P-value	-	1.702%	-	0.000%	-	4.405%
LR test stats. (H0=DCC)	-	8.64	-	9.60	-	3.69
P-value	-	0.329%	-	0.195%	-	5.463%

Panel B. Conditional Covariance						
	DCC	DCC- q_t	DCC	DCC- q_t	DCC	DCC- q_t
$b(I_{NBER}) (\times 10^{-5})$	-0.2849	-0.5030	-0.5358	-0.8919	0.2389	0.3776
$SE(b(I_{NBER})) (\times 10^{-5})$	(0.1505)	(0.2697)	(0.2562)	(0.2564)	(0.0987)	(0.0993)

Panel C. Conditional Beta						
	DCC	DCC- q_t	DCC	DCC- q_t	DCC	DCC- q_t
$b(I_{NBER})$	-0.1418	-0.3501	-0.3268	-0.7131	0.1850	0.3630
$SE(b(I_{NBER}))$	(0.0719)	(0.0713)	(0.0482)	(0.0493)	(0.0719)	(0.0719)

Table 2.4: Seven extant consumption-based asset pricing models, and their implications on the cyclicalities of the exogenous component, $Cov_t(\Delta d_{t+1}, \Delta c_{t+1})$, and the endogenous component, $Cov_t(r_{t+1}^m - \Delta d_{t+1}, \Delta c_{t+1})$, of the amount of risk.

In addition to Campbell and Cochrane (1999)'s habit-formation model and Bansal and Yaron (2004)'s long-run risk model, five variants of the two models that focus on modeling more realistic *higher moments* of shocks are evaluated at their abilities to meet the stylized facts established in Section 3.2. To provide intuitions about the non-dividend part of the market return ($r_{t+1}^m - \Delta d_{t+1}$), I follow the convention in the long-run risk literature to approximate $r_{t+1}^m - \Delta d_{t+1}$ with changes in log price dividend ratio according to the Campbell and Shiller linearization. **Habit-formation Models** “CC1999”: Campbell and Cochrane (1999, JPE). “BEX2009”: Bekaert, Engstrom, and King (2009, JFE) allow time variation in both uncertainty and risk aversion in square root-type processes to identify the relative importance of changes in uncertainty and changes in risk aversion in equity prices and risk premiums. “BE2017”: Bekaert and Engstrom (2017, JPE) decompose aggregate consumption innovation into “good” and “bad” shocks and allow the two shocks to affect other state variables in the economy. **Long-run Risk Models** “BY2004”: Bansal and Yaron (2004, JF). “BTZ2009”: Bollerslev, Tauchen, and Zhou (2009, JFQA) assume a time-varying volatility of volatility in a square root-type process that is shown to be a crucial state variable for the equity variance premium (VRP). “BKY2012”: Bansal, Kiku, and Yaron (2012, CFR) are the first to model a positive covariance between consumption growth and dividend growth under the LRR setting. “SSY2015”: Segal, Shaliastovich, and Yaron (2015, JFE) introduce the good volatility-bad volatility idea as in BE2017 in a long-run risk framework. **Notations** “Const.”, constant; “counter-”, countercyclical; “pro-”, procyclical.

	(1)	(2)	(3)	(4)	(5)	(6)	(7)
(a). $Var_t(\Delta c_{t+1})$	CC1999 Habit Const.	BEX2009 Habit ✓	BE2017 Habit ✓	BY2004 LRR Counter- (⊗)	BTZ2009 LRR Counter- (⊗)	BKY2012 LRR Counter- (⊗)	SSY2015 LRR Counter- (⊗)
(b). $Var_t(\Delta d_{t+1})$	Pro- Const.	Counter- Const.	Counter- Const.	Counter- (⊗) Counter- (⊗)	Counter- (⊗) Counter- (⊗)	Counter- (⊗) Counter- (⊗)	Const. Const.
(c). $Corr_t(\Delta d_{t+1}, \Delta c_{t+1})$	Pro- Const. (0.2)	Const. (>0)	Unclear (>0)	0	1	Const. (>0)	0
(d). $Cov_t(\Delta d_{t+1}, \Delta c_{t+1})$	Pro- Const.	Counter- Const.	Counter- Const.	0	Counter- (⊗)	Counter- (⊗)	0
(e). $\frac{Cov_t(\Delta d_{t+1}, \Delta c_{t+1})}{Var_t(\Delta c_{t+1})}$	Pro- Const.	Const. Const.	Pro- (*) ✓ (*)	0	Const.	Const.	0
(f). $Var_t(r_{t+1}^m - \Delta d_{t+1})$	Counter- ✓	Counter- ✓	Counter- ✓	Counter- (⊗) ✓ (⊗)	Counter- (⊗) ✓ (⊗)	Counter- (⊗) ✓ (⊗)	Counter- (⊗) ✓ (⊗)
(g). $Var_t(r_{t+1}^m)$	Counter- ✓	Counter- ✓	Counter- ✓	Counter- (⊗) ✓ (⊗)	Counter- (⊗) ✓ (⊗)	Counter- (⊗) ✓ (⊗)	Counter- (⊗) ✓ (⊗)
(h). $Cov_t(r_{t+1}^m - \Delta d_{t+1}, \Delta c_{t+1})$	Counter- ✓	Counter- (>0) ✓	Counter- (>0) ✓	0	0	0	Counter- (>0, ⊗) ✓ (⊗)
(i). $Cov_t(r_{t+1}^m, \Delta c_{t+1})$	Pro- Counter-	Counter- Counter-	Counter- Counter-	0	Counter- (⊗)	Counter- (⊗)	Counter- (⊗) Counter- (⊗)
(j). $\frac{Cov_t(\Delta d_{t+1}, \Delta c_{t+1})}{Cov_t(r_{t+1}^m, \Delta c_{t+1})}$	Pro- ✓	Const. (**) ✓	Pro- ✓	-	1	1	0

(*) procyclical when the scale parameter of bad uncertainty shock in the total consumption shock (σ_{cn}) is greater than the scale parameter of bad uncertainty in dividend (σ_{dn}) in BE2017.

(**) constant when the linear approximation of the price dividend ratio in Equation (19) of Bekaert, Engstrom, and Xing (2009) is used.

(⊗) countercyclical when the time-varying consumption volatility is modeled to be countercyclical; note that the time-varying volatility is a crucial feature of the LRR models; however, the LRR models do not imply countercyclical volatility because the volatility shock and the consumption shock are assumed uncorrelated.

□ Boxed moments are mismatched by all representative models.

Table 2.5: The New DGP for the Joint Consumption-Dividend Dynamics.

In the new DGP, consumption and dividend growth have the following joint dynamics:

$$\begin{aligned}\Delta c_{t+1} &= \bar{c} + \sigma_c \tilde{\omega}_{c,t+1} + \sigma_n \tilde{\omega}_{n,t+1}, \\ n_{t+1} &= (1 - \phi_n) \bar{n} + \phi_n n_t + \sigma_{nn} \tilde{\omega}_{n,t+1}, \\ \Delta d_{t+1} &= \bar{d} + \phi_d (V_{c,t} - \bar{V}_c) + b_t \sigma_c \tilde{\omega}_{c,t+1} + \sigma_d \tilde{\omega}_{d,t+1}, \\ b_{t+1} &= (1 - \phi_b) \bar{b} + \phi_b b_t + \lambda_b \sigma_c \tilde{\omega}_{c,t+1}, \\ V_{c,t} &= \sigma_c^2 + \sigma_n^2 n_t, \\ \bar{V}_c &= \sigma_c^2 + \sigma_n^2 \bar{n},\end{aligned}$$

where the consumption fundamental shock, $\tilde{\omega}_{c,t+1}$, is a centered Gaussian shock with unit standard deviation, the consumption event shock, $\tilde{\omega}_{n,t+1}$, follows a centered heteroskedastic gamma distribution with a strictly positive shape parameter equal to n_t and a unit scale parameter, and the dividend-specific shock, $\tilde{\omega}_{d,t+1}$, follows a centered homoskedastic gamma distribution with a strictly positive shape parameter equal to V_d and a unit scale parameter. Or,

$$\tilde{\omega}_{c,t+1} \sim i.i.d.N(0, 1); \tilde{\omega}_{n,t+1} \sim \Gamma(n_t, 1) - n_t; \tilde{\omega}_{d,t+1} \sim \Gamma(V_d, 1) - V_d.$$

Data As in the empirical part of the paper, I use the AR(3)-de-measured consumption growth and the original dividend growth as Δc_{t+1} and Δd_{t+1} in the DGP estimation. **Panels** Panels A and B present the estimation results, where ‘‘ADF Test’’ denotes the augmented Dickey-Fuller tests with the null that the two latent processes, n_{t+1} and b_{t+1} , follow unit root processes. Panel C presents the monthly unconditional moments of the three filtered shocks. Panel D shows the correlations between the business cycle indicators (the NBER indicator and the detrended consumption-wealth ratio, \widehat{cay}^Q , introduced in Lettau and Ludvigson (2001); source: NBER website and Martin Lettau’s website) and the three filtered shocks aggregated to the quarterly frequency. Robust standard errors are shown in parentheses in Panels A, B, and D; bootstrapped standard errors are shown in parentheses in Panel C. Values in bold are statistically significant at a significant level of 5%. N=665 months (1959/02~2014/06).

Panel A. Estimation Results, Consumption				Panel B. Estimation Results, Dividend			
	Δc_{t+1}	n_{t+1}		Δd_{t+1}	b_{t+1}		
\bar{c}	0.0025 (0.0001)	\bar{n}	0.3742 (0.1609)	\bar{d}	0.0025 (0.0003)	\bar{b}	0.4447 (0.1018)
σ_c	0.0029 (0.0001)	ϕ_n	0.9500 (0.0264)	ϕ_d	-568.0871 (139.0511)	ϕ_b	0.8824 (0.0468)
σ_n	-0.0023 (0.0005)	σ_{nn}	0.2772 (0.1027)	σ_d	-0.0008 (0.0000)	λ_b	14.0978 (1.3764)
		ADF Test	-4.298***	V_d	89.9322 (3.4724)	ADF Test	-4.764***
Panel C. Moments, Filtered Shocks				Panel D. Filtered Shocks and Business Cycle			
	$\tilde{\omega}_c$	$\tilde{\omega}_n$	$\tilde{\omega}_d$		$\tilde{\omega}_c^Q$	$\tilde{\omega}_n^Q$	$\tilde{\omega}_d^Q$
Mean	0.0017 (0.0374)	0.0024 (0.0179)	-0.0025 (0.3387)	NBER	-0.2703 (0.0649)	0.2483 (0.0653)	0.1480 (0.0667)
S.D.	0.9680 (0.0348)	0.4441 (0.0554)	8.8643 (0.5913)	\widehat{cay}^Q	-0.2154 (0.0658)	0.0561 (0.0673)	0.0350 (0.0674)
Skew	0.1785 (0.1326)	5.4390 (0.5747)	0.3070 (0.0751)				
xKurt	0.4491 (0.5023)	40.5216 (8.3810)	9.6735 (2.3810)				

Table 2.6: Theoretical Models: Resolving the Exogenous Part of the Duffee Puzzle.

This table evaluates the abilities of three theoretical models to fit Facts (a)~(e) related to the exogenous part of the Duffee Puzzle as established in Section 3.2. To obtain the sample moments under Column “Data”, I calculate the unconditional moments of residuals during recession ($I_{NBER} = 1$) and non-recession ($I_{NBER} = 0$) periods; monthly empirical data cover period 1959/01-2014/06. Bootstrapped standard errors are shown in parentheses under Column “SE”. Similarly, I obtain their theoretical counterparts using the simulated datasets of the theoretical models under Columns M(1), M(2) and M(3). The algorithm for identifying recession periods in an endowment economy is described in Appendix 2.2. **Moment Symbols** σ , volatility; ρ , correlation; C , covariance; $b(x_1, x_2)$, sensitivity of x_1 to x_2 or $\frac{C(x_1, x_2)}{\sigma^2(x_2)}$; % of Amount of Risk by $C(\Delta d, \Delta c)$, $\frac{C(\Delta d, \Delta c)}{C(r^m, \Delta c)} \times 100\%$. **Data symbol** Δc , consumption growth; Δd , dividend growth. **Models** The three theoretical models are described in Section 3.4 or Appendix 2.3. M(1) is an adapted Campbell and Cochrane (1999) model with the surplus consumption ratio (s) as the only state variable. M(2) is adapted from Bekaert and Engstrom (2017) with heteroskedastic macroeconomic uncertainty (n). M(3) is the full model in this paper with procyclical consumption-dividend comovement (b) as the third state variable. **Numerical Solution** The models are solved numerically using the “series method” introduced in Wachter (2005), and simulated for 100,000 months; see details on calibration in Section 2.4.3.1. All model-implied moments in this paper are calculated using the second half of the simulated dataset, i.e., 50,001-100,000. Bold values indicate that the simulation moment point estimates are within a 95% confidence interval of the empirical moments.

		Data	SE	M(1) Adapted Campbell& Cochrane,1999	M(2) Adapted Bekaert& Engstrom,2017	M(3) This Paper
	s as State Variable	-	-	Yes	Yes	Yes
	n as State Variable	-	-	No	Yes	Yes
	b as State Variable	-	-	No	No	Yes
(a).	$\sigma(\Delta c)$ ($I_{recc.} = 0$)	0.0031***	(0.0001)	0.0032	0.0031	0.0031
	$\sigma(\Delta c)$ ($I_{recc.} = 1$)	0.0036	(0.0002)	0.0032	0.0036	0.0036
(b).	$\sigma(\Delta d)$ ($I_{recc.} = 0$)	0.0069*	(0.0005)	0.00741	0.00741	0.00742
	$\sigma(\Delta d)$ ($I_{recc.} = 1$)	0.0060	(0.0006)	0.00741	0.00741	0.00492
(c).	$\rho(\Delta d, \Delta c)$ ($I_{recc.} = 0$)	0.1823***	(0.0565)	0.1577	0.1622	0.1627
	$\rho(\Delta d, \Delta c)$ ($I_{recc.} = 1$)	0.0148	(0.0591)	0.1571	0.1399	0.0639
(d).	$C(\Delta d, \Delta c)$ ($I_{recc.} = 0$) ($\times 10^{-5}$)	0.3916**	(0.1523)	0.3703	0.3703	0.3720
	$C(\Delta d, \Delta c)$ ($I_{recc.} = 1$) ($\times 10^{-5}$)	0.0317	(0.1609)	0.3703	0.3703	0.1122
(e).	$b(\Delta d, \Delta c)$ ($I_{recc.} = 0$)	0.4075***	(0.1419)	0.3686	0.3902	0.3920
	$b(\Delta d, \Delta c)$ ($I_{recc.} = 1$)	0.0251	(0.1277)	0.3659	0.2900	0.0879

Note: the significance levels for testing the equality of non-recession ($I_{recc.} = 0$) and recession ($I_{recc.} = 1$) moments (Wald Test given the covariance-variance matrix from the GMM estimations) are denoted as follow: *** $p < 0.01$, ** $p < 0.05$, * $p < 0.1$.

Table 2.7: Theoretical Models: Unconditional Moments of the Duffee Puzzle Components.

This table presents 18 unconditional moments from simulated and empirical datasets. **Moment Symbols** E , mean; σ , volatility; $Skew$, scaled skewness; $xKurt$, excess kurtosis; ρ , correlation; C , covariance; $b(x_1, x_2)$, sensitivity of x_1 to x_2 or $\frac{C(x_1, x_2)}{\sigma^2(x_2)}$; % of Amount of Risk by $C(\Delta d, \Delta c)$, $\frac{C(\Delta d, \Delta c)}{C(r^m, \Delta c)}$ %. **Data** r^m , log real change in CRSP market index including dividends. Other details on data, models, model solutions, and simulations are described in Table 2.6. Bold values indicate that the simulation moment point estimates are within a 95% confidence interval of the empirical moments.

		Data	SE	M(1) Adapted Campbell& Cochrane,1999	M(2) Adapted Bekaert& Engstrom,2017	M(3) This Paper
	s as State Variable	-	-	Yes	Yes	Yes
	n as State Variable	-	-	No	Yes	Yes
	b as State Variable	-	-	No	No	Yes
(1)	$E(\Delta c)$	0.0025	(0.0001)	0.0025	0.0025	0.0025
(2)	$\sigma(\Delta c)$	0.0032	(0.0001)	0.0032	0.0032	0.0032
(3)	$Skew(\Delta c)$	-0.1292	(0.1419)	-0.2740	-0.2039	-0.2039
(4)	$xKurt(\Delta c)$	0.7779	(0.3553)	0.5880	0.4137	0.4137
(5)	Heteroskedastic Δc Innovations	Yes		No	Yes	Yes
(6)	$E(\Delta d)$	0.0026	(0.0003)	0.0025	0.0025	0.0025
(7)	$\sigma(\Delta d)$	0.0068	(0.0005)	0.00741	0.00741	0.00738
(8)	$Skew(\Delta d)$	-1.2271	(0.5145)	-0.2015	-0.2015	-0.2012
(9)	$xKurt(\Delta d)$	7.5599	(3.5260)	0.0628	0.0628	0.0626
(10)	Heteroskedastic Δd Innovations	Yes		No	No	Yes
(11)	$\rho(\Delta d, \Delta c)$	0.1587	(0.0514)	0.1558	0.1557	0.1503
(12)	$C(\Delta d, \Delta c) (\times 10^{-5})$	0.3419	(0.1286)	0.3703	0.3703	0.3574
(13)	$b(\Delta d, \Delta c)$	0.3414	(0.1248)	0.3600	0.3598	0.3441
(14)	$\sigma(r^m - \Delta d)$	0.0375	(0.0017)	0.0259	0.0388	0.0362
(15)	$\sigma(r^m)$	0.0374	(0.0016)	0.0252	0.0377	0.0351
(16)	$C(r^m - \Delta d, \Delta c) (\times 10^{-5})$	2.0978	(0.2371)	2.3799	2.3583	2.5284
(17)	$C(r^m, \Delta c) (\times 10^{-5})$	2.4398	(0.1817)	2.7501	2.7286	2.8858
(18)	% of Amount of Risk by $C(\Delta d, \Delta c)$	14.014%	(4.063%)	13.463%	13.570%	12.385%

Table 2.8: Non-DGP Model Parameter Choices (*=annualized).

This table presents the non-DGP parameter choices and the derived parameter values. Following Campbell and Cochrane (1999), the AR(1) coefficient of the s_t process (ϕ_s) equals the AR(1) coefficient of the monthly log price dividend ratio. rf_{CC} is the constant benchmark risk free rate and is chosen to match the average real 90-day Treasury bill rate, which is proxied by changes in log nominal 90-day Treasury index constructed by CRSP minus inflation rate continuously compounded; the nominal index is constructed by CRSP and the inflation rate is obtained from the Federal Reserve Bank of St. Louis. β is the time discount parameter derived from the rf_{CC} equation. Monthly data covers the period 1959/01-2014/06.

Non-DGP parameters:	Notation	Value
Curvature parameter	γ	2
s_t persistence	ϕ_s	0.9499*
Risk free rate (%)	rf_{CC}	1.4854*
Derived parameters:		
Time discount parameter	β	0.9952*
Steady-state surplus consumption ratio, M(1)	\bar{S}	0.0694
Maximum log surplus consumption ratio, M(1)	s_{max}	-2.1701

Table 2.9: Theoretical Models: Unconditional Asset Price Statistics (*=annualized).

This table presents 10 unconditional moments of financial variables from simulated and empirical datasets. **Moment Symbols** E , mean; σ , volatility; ac , first-order autocorrelation coefficient. Other details on data, models, model solutions, and simulations are described in Tables 2.6~ 2.8. Bold values indicate that the simulation moment point estimates are within a 95% confidence interval of the empirical moments.

	Data	SE	M(1) Adapted Campbell& Cochrane,1999	M(2) Adapted Bekaert& Engstrom,2017	M(3) This Paper
s as State Variable	-	-	Yes	Yes	Yes
n as State Variable	-	-	No	Yes	Yes
b as State Variable	-	-	No	No	Yes
(19) *	$E(r^m - rf), \%$	4.8780 (1.9914)	4.4520	5.9374	5.3537
(20) *	$\sigma(r^m - rf), \%$	14.8816 (0.6109)	8.7437	15.2393	14.5441
(21)	$\exp[E(pd)]$	35.552 (0.5225)	31.3039	20.9597	20.9983
(22)	$\sigma(pd)$	0.3946 (0.0922)	0.1535	0.2882	0.3037
(23) *	$ac(pd)$	0.9499 (0.0411)	0.9438	0.9416	0.9416
(24)	Sharpe Ratio	0.3278 (0.1408)	0.5092	0.3896	0.3681
(25)	Skewness	-0.6815 (0.2526)	0.1874	-0.1205	-0.1078
(26)	Kurtosis	5.5288 (1.2222)	3.5231	3.7325	3.7156
(27) *	$E(rf), \%$	1.4209 (0.1525)	1.3663	1.4239	1.4239
(28) *	$\sigma(rf), \%$	1.1229 (0.0503)	0.0219	0.0490	0.0490

Table 2.10: Theoretical Models: Resolving the Endogenous Part of the Duffee Puzzle.

This table evaluates the abilities of three theoretical models to fit Facts (f)~(j) related to the endogenous part of the Duffee Puzzle as established in Section 3.2. Other details on data, models, model solutions, and simulations are described in Tables 2.6~2.8. Bold values indicate that the simulation moment point estimates are within a 95% confidence interval of the empirical moments.

		Data	SE	M(1) Adapted Campbell& Cochrane,1999	M(2) Adapted Bekaert& Engstrom,2017	M(3) This Paper
	<i>s</i> as State Variable	-	-	Yes	Yes	Yes
	<i>n</i> as State Variable	-	-	No	Yes	Yes
	<i>b</i> as State Variable	-	-	No	No	Yes
(f).	$\sigma(r^m - \Delta d) (I_{recc.} = 0)$	0.0321***	(0.0014)	0.0257	0.0288	0.0317
	$\sigma(r^m - \Delta d) (I_{recc.} = 1)$	0.0497	(0.0056)	0.0264	0.0537	0.0502
(g).	$\sigma(r^m) (I_{recc.} = 0)$	0.0321***	(0.0013)	0.0251	0.0279	0.0308
	$\sigma(r^m) (I_{recc.} = 1)$	0.0496	(0.0054)	0.0246	0.0530	0.0497
(h).	$C(r^m - \Delta d, \Delta c) (I_{recc.} = 0) (\times 10^{-5})$	2.0588*	(0.1726)	2.2489	2.2284	2.3952
	$C(r^m - \Delta d, \Delta c) (I_{recc.} = 1) (\times 10^{-5})$	2.3637	(0.2354)	2.4519	2.5414	2.5621
(i).	$C(r^m, \Delta c) (I_{recc.} = 0) (\times 10^{-5})$	2.4504	(0.1687)	2.6192	2.5986	2.7672
	$C(r^m, \Delta c) (I_{recc.} = 1) (\times 10^{-5})$	2.3954	(0.1833)	2.8222	2.9116	2.6743
(j).	% of Amount of Risk by $C(\Delta d, \Delta c) (I_{recc.} = 0)$	15.980%***	(5.253%)	14.136%	14.248%	13.443%
	% of Amount of Risk by $C(\Delta d, \Delta c) (I_{recc.} = 1)$	1.322%	(3.297%)	13.120%	12.717%	4.196%

Note: the significance levels for testing the equality of non-recession ($I_{recc.} = 0$) and recession ($I_{recc.} = 1$) moments (Wald Test given the covariance-variance matrix from the GMM estimations) are denoted as follow: *** $p < 0.01$, ** $p < 0.05$, * $p < 0.1$.

Table 2.11: Price Dividend Ratio Variance Decomposition.

This table presents 6 moments on the approximate variance decomposition results of the log price dividend ratio using the empirical dataset and three simulated datasets of the three theoretical models. The log price dividend ratio is estimated by univariate and multivariate regression models. **Moment Symbols** $b(x_t)$, linear regression coefficient estimate of state variable x_t in a univariate or multivariate pd regression, where the linear regression framework is denoted as $pd_t = f(\dots, x_t, \dots)$. The variance decomposition in a multivariate framework, VARC, is $\frac{\hat{b}(x)Cov(x, \hat{f})}{Var(\hat{f})}$ where $\hat{b}(x)$ is the coefficient estimate and \hat{f} is the fitted dependent variable; the sum of VARCs across all variables is 100%; VARCs are shown in curly brackets. Bold (italics) values indicate that the simulation moment point estimates are within a 95% (99%) confidence interval of the empirical moments.

	Data	SE	M(1) Adapted Campbell& Cochrane,1999	M(2) Adapted Bekaert& Engstrom,2017	M(3) This Paper
s as State Variable	-	-	Yes	Yes	Yes
n as State Variable	-	-	No	Yes	Yes
b as State Variable	-	-	No	No	Yes
(29) $b(b_t): pd_t = f(b_t)$	1.2807	(0.1292)	-	-	1.1146
$R^2: pd_t = f(b_t)$	12.900%	(3.608%)	-	-	7.797%
(30) $b(s_t): pd_t = f(s_t, n_t, b_t, b_t^2)$	0.5815	(0.0384)	0.6693	0.5564	0.5368
VARC,%	{72.779%}		{100%}	{69.091%}	{64.317%}
(31) $b(n_t): pd_t = f(s_t, n_t, b_t, b_t^2)$	-0.1407	(0.0322)	-	0.3222	0.3121
VARC,%	{14.102%}		-	{30.909%}	{28.998%}
(32) $b(b_t): pd_t = f(s_t, n_t, b_t, b_t^2)$	0.5480	(0.1486)	-	-	<i>0.8951</i>
VARC,%	{13.386%}		-	-	{6.657%}
(33) $b(b_t^2): pd_t = f(s_t, n_t, b_t, b_t^2)$	2.3024	(0.9112)	-	-	0.9157
VARC,%	{-0.268%}		-	-	{0.029%}
(34) $R^2: pd_t = f(s_t, n_t, b_t, b_t^2)$	49.587%	(4.654%)	96.933%	62.012%	65.255%

Table 2.12: The Pricing of b_t in Cross Section: Factor Loadings and Prices of Risk.

This table reports the summary statistics of the cross-sectional Fama and MacBeth (1973) regressions for the 25 size- and book-to-market-sorted portfolios of Fama and French (1993) (source: Kenneth R. French website). In the first stage, Panels A to D report multivariate factor loadings from regressions of each portfolio excess return on the market excess return (“ Mkt ”), the log surplus consumption ratio innovations (“ $sinnov$ ”), the macroeconomic uncertainty innovations (“ $ninnov$ ”) and the procyclical consumption-dividend comovement innovations.

$$R_{i,t} - R_{f,t} = \beta_{i,0} + \beta_{i,Mkt}(R_{Mkt,t} - R_{f,t}) + \beta_{i,sinnov}sinnov_t + \beta_{i,ninnov}ninnov_t + \beta_{i,binnov}binnov_t + \epsilon_{i,t}.$$

“5-1” denotes the difference between Portfolio 5 (highest in B/M or largest in size) and Portfolio 1 (lowest in B/M or smallest in size). “***” denotes 1% significance level, “**” 5% significance level and “*” 10% significance level. In the second stage, portfolio returns are regressed on the loadings, giving an estimate of the price of risk for each factor:

$$E[R_i] - R_f = \lambda_0 + \lambda_{Mkt}\hat{\beta}_{i,Mkt} + \lambda_{sinnov}\hat{\beta}_{i,sinnov} + \lambda_{ninnov}\hat{\beta}_{i,ninnov} + \lambda_{binnov}\hat{\beta}_{i,binnov}.$$

“VARC” reports the variance decomposition (see Table 2.11 for details). Robust standard errors are shown in parentheses. Bold (italics) estimates have significance at the 5% (10%) level. N=556 months (1968/03~2014/06).

Panel A. Multivariate Loadings on Market Excess Returns, $\beta_{i,Mkt}$						
	GROWTH	B/M 2	B/M 3	B/M 4	VALUE	5-1
SMALL	1.4187***	1.2162***	1.0906***	1.0059***	1.0507***	-0.3680***
Size 2	1.3965***	1.1631***	1.0401***	0.9943***	1.1079***	-0.2886***
Size 3	1.3271***	1.1191***	1.0011***	0.9421***	1.0503***	-0.2768***
Size 4	1.2319***	1.0846***	1.0093***	0.9466***	1.0766***	-0.1553***
LARGE	0.9761***	0.9384***	0.8480***	0.8826***	0.9471***	-0.0290
5-1	-0.4426***	-0.2778***	-0.2425***	-0.1233***	-0.1036***	
Panel B. Multivariate Loadings on Surplus Consumption Ratio (s) Innovations, $\beta_{i,sinnov}$						
	GROWTH	B/M 2	B/M 3	B/M 4	VALUE	5-1
SMALL	15.2272	11.8785	12.4366*	10.5175	14.0103*	-1.2169
Size 2	10.9073	8.1214	10.9637*	10.2815	9.4299	-1.4774
Size 3	8.3100	6.1493	5.0391	5.0484	9.5382	1.2282
Size 4	8.1334	9.0119	6.8525	5.8844	14.0090 **	5.8757
LARGE	9.2765	9.1898*	9.6577*	5.9991	16.1341***	6.8576
5-1	-5.9506	-2.6887	-2.7790	-4.5184	2.1238	
Panel C. Multivariate Loadings on Macroeconomic Uncertainty (n) Innovations, $\beta_{i,ninnov}$						
	GROWTH	B/M 2	B/M 3	B/M 4	VALUE	5-1
SMALL	-0.0485 **	-0.0489***	-0.0499***	-0.0653***	-0.0684***	-0.0199
Size 2	-0.0446 **	-0.0415 **	-0.0444 **	-0.0666***	-0.0640***	-0.0193
Size 3	-0.0314	-0.0419***	-0.0458***	-0.0572***	-0.0648***	-0.0333 **
Size 4	-0.0342*	-0.0384 **	-0.0354*	-0.0405 **	-0.0634***	-0.0292 **
LARGE	0.0038	-0.0306*	-0.0371***	-0.0427***	-0.0508***	-0.0546***
5-1	0.0523***	0.0183	0.0127	0.0226	0.0177	
Panel D. Multivariate Loadings on Div.-Cons. Comovement (b) Innovations, $\beta_{i,binnov}$						
	GROWTH	B/M 2	B/M 3	B/M 4	VALUE	5-1
SMALL	11.0184	7.0150	11.5856 **	7.3966	17.1760***	6.1575
Size 2	5.4487	6.8722	4.2486	1.9321	10.3278*	4.8792
Size 3	1.9982	1.4142	3.2624	5.8093	4.5245	2.5263
Size 4	-1.3867	4.3967	5.1377	5.5067	7.1502	8.5369*
LARGE	-4.9418*	0.2228	-1.3690	5.4284	14.7410***	19.6829***
5-1	-15.9603***	-6.7922	-12.9546***	-1.9682	-2.4349	
Panel E. Price of Risk (Second-Stage Fama-MacBeth)						
	λ_{Mkt}	λ_{sinnov}	λ_{ninnov}	λ_{binnov}		
Est.	-0.5577	-0.0144	<i>-0.0697</i>	0.0474		
SE	(0.2682)	(0.0155)	(0.0413)	(0.0216)		
VARC	38.55%	3.29%	41.75%	16.41%		
R^2	41.40%					

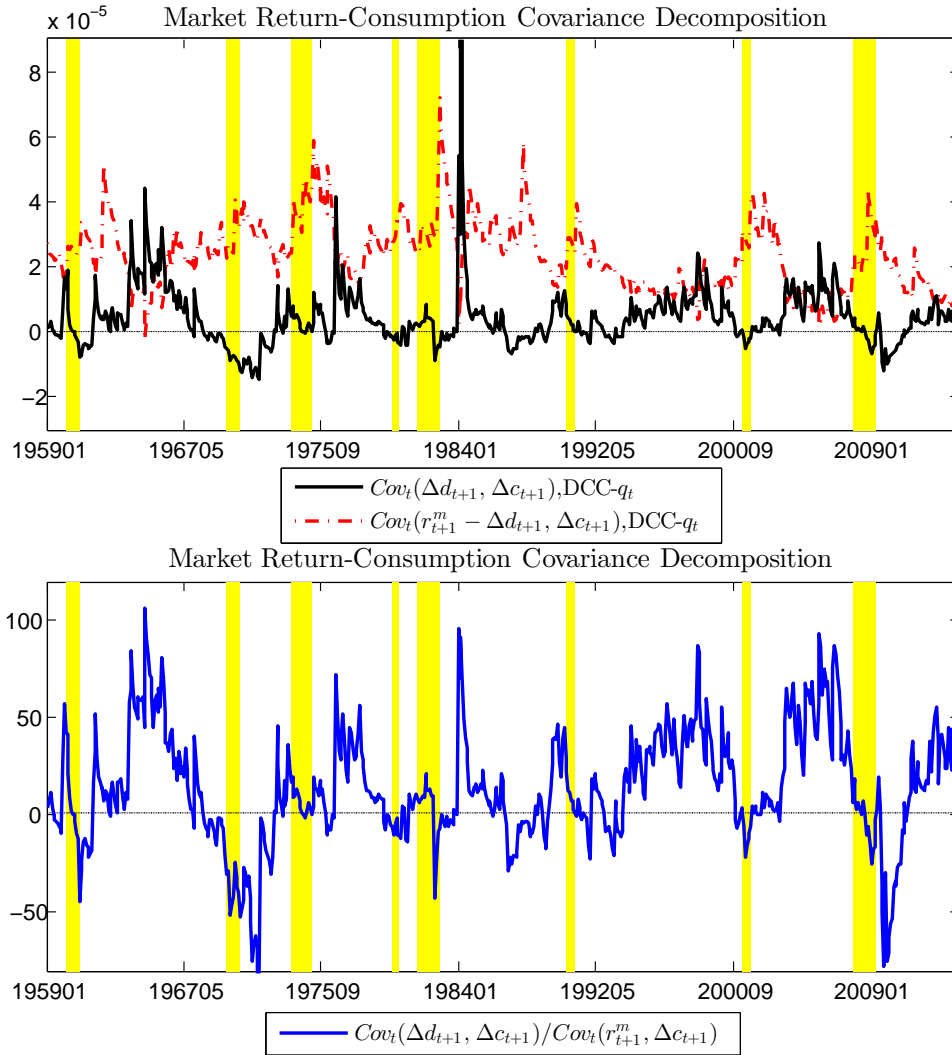


Figure 2.1: The Decomposition of the Duffee Puzzle from the Empirical Analyses.

The top panel depicts the empirical estimates of the two components of amount of risk in the Duffee Puzzle. The solid black line depicts the dynamic conditional covariance of dividend growth and consumption growth (with instrument); the dashed red line depicts the dynamic conditional covariance of the non-dividend part of the market return and consumption growth (with instrument). The bottom panel depicts the time variation in the share of the consumption-dividend conditional covariance in the market return-consumption conditional covariance (namely, the amount of risk). The conditional covariance estimates in the two plots are obtained from the “DCC- q_t ” model estimation results as reported in Table 2.3. The shaded regions are the NBER recession months from the NBER website.

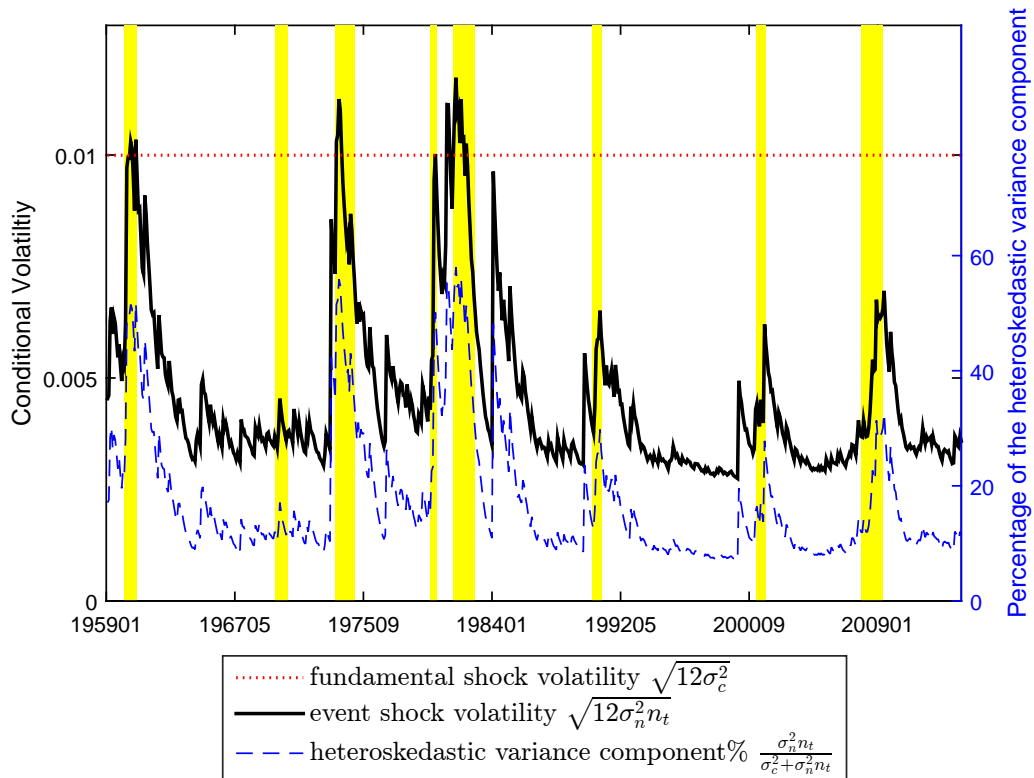


Figure 2.2: Annualized Conditional Volatility of the Two Consumption Shocks from the DGP Estimation.

The plot illustrates the magnitudes and dynamics of the two components of consumption growth volatility. The solid black line depicts the annualized conditional volatility contributed by the heteroskedastic event shock $\tilde{\omega}_{n,t+1}$, or $\sqrt{12\sigma_n^2 n_t}$. The dotted red line depicts the annualized volatility contributed by the homoskedastic fundamental shock $\tilde{\omega}_{c,t+1}$, or $\sqrt{12\sigma_c^2}$. The dashed blue line depicts the percentage of the total consumption variance explained by the heteroskedastic component, or $\frac{\sigma_n^2 n_t}{\sigma_c^2 + \sigma_n^2 n_t}$. The shaded regions are the NBER recession months from the NBER website.

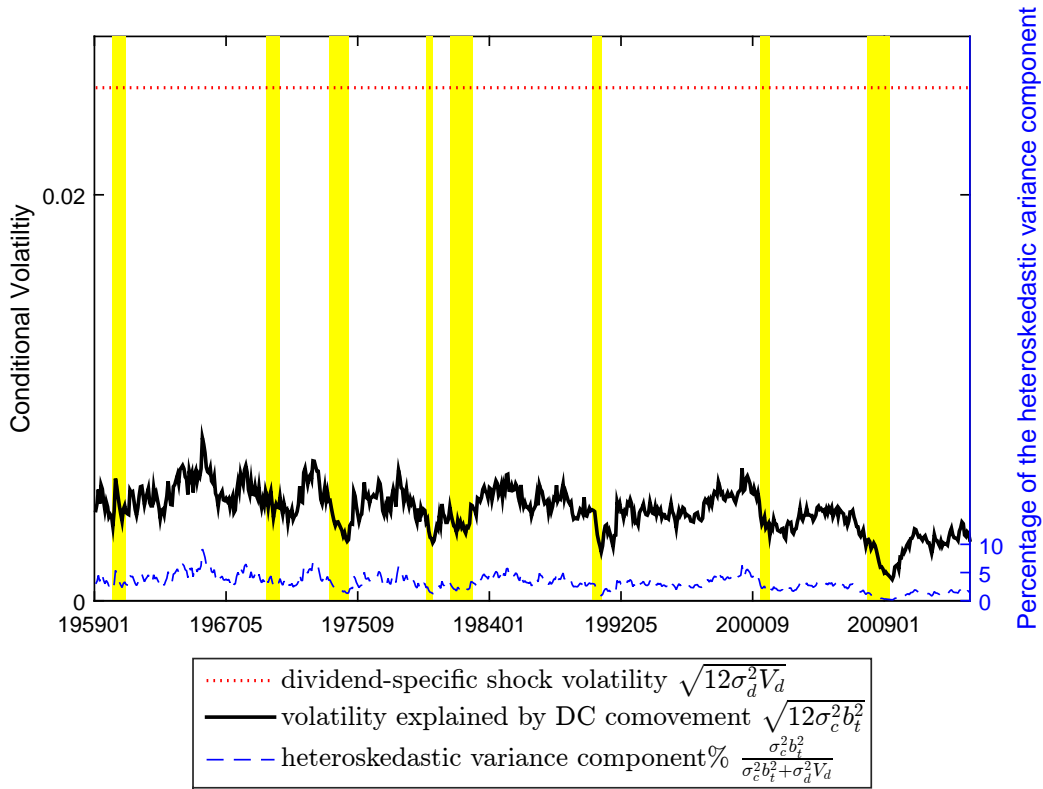


Figure 2.3: Annualized Conditional Volatility of the Two Dividend Shock Components from the DGP Estimation.

The plot illustrates the magnitudes and dynamics of the two components of the dividend growth volatility. The solid black line depicts the annualized conditional volatility contributed by the consumption fundamental shock $\tilde{\omega}_{c,t+1}$, or $\sqrt{12\sigma_c^2 b_t^2}$. The dotted red line depicts the annualized volatility contributed by the dividend-specific shock $\tilde{\omega}_{d,t+1}$, or $\sqrt{12\sigma_d^2 V_d}$. The dashed blue line depicts the percentage of the total dividend variance explained by the heteroskedastic component, or $\frac{\sigma_c^2 b_t^2}{\sigma_c^2 b_t^2 + \sigma_d^2 V_d}$. The shaded regions are the NBER recession months from the NBER website.

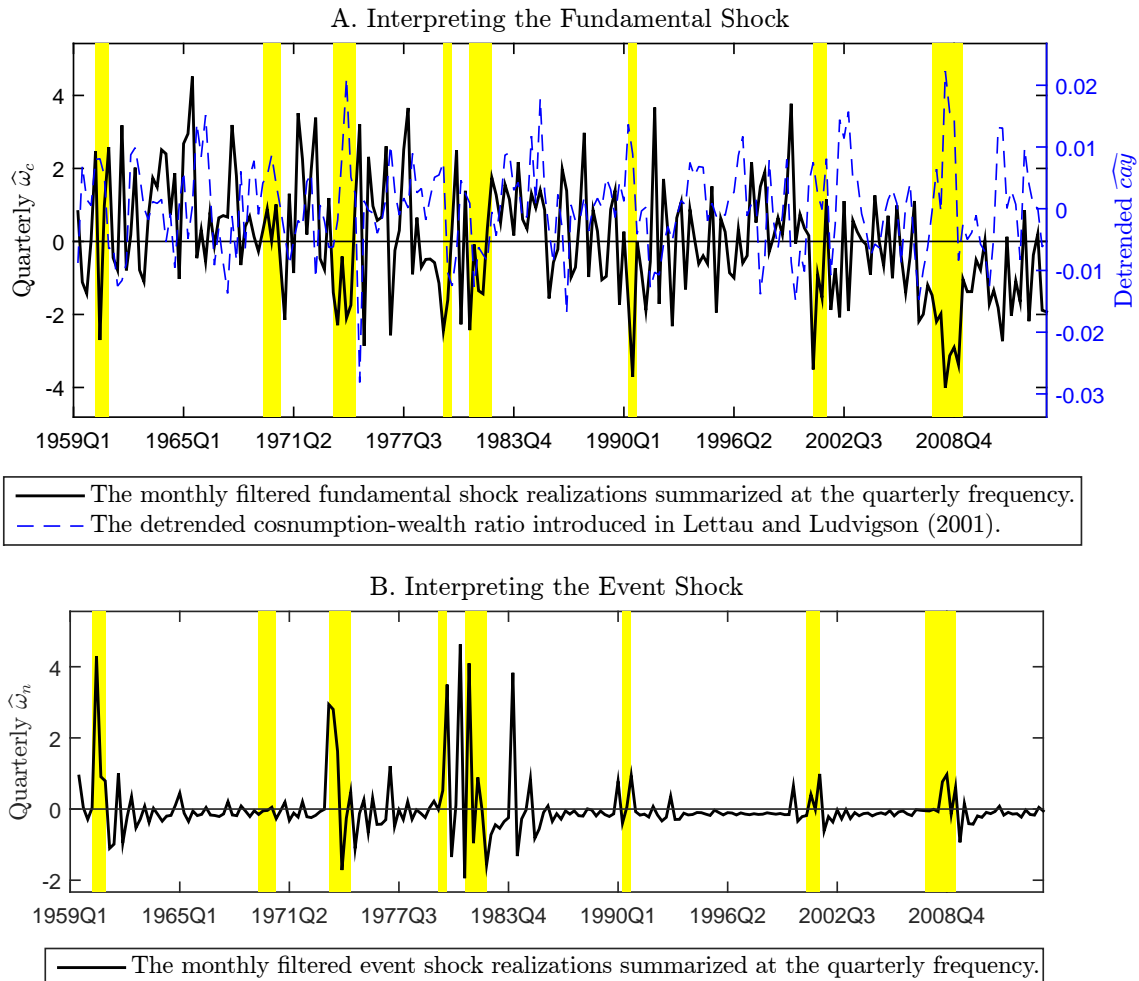


Figure 2.4: Economic Interpretations for the Fundamental Shock and the Event Shock.

The plot provides direct graphical evidence on the economic interpretations of the fundamental shock and the event shock in the new DGP (Equation (2.T10)). The two shocks are estimated using a filtration-based maximum likelihood estimation methodology developed by Bates (2006); the estimation results are shown in Table 2.5. In this figure, the monthly filtered shock realizations—the fundamental shock $\hat{\omega}_c$ and the event shock $\hat{\omega}_n$ —are summarized at the quarterly frequency and plotted against two business condition indicators. Plot A depicts the quarterly fundamental shock against the detrended consumption-wealth ratio introduced in Lettau and Ludvigson (2001). The magnitudes of the quarterly $\hat{\omega}_c$ (detrended \widehat{cay}^Q) are shown in the left (right) axis. Plot B depicts the quarterly event shock realizations. The shaded regions are the NBER recession quarters from the NBER website.

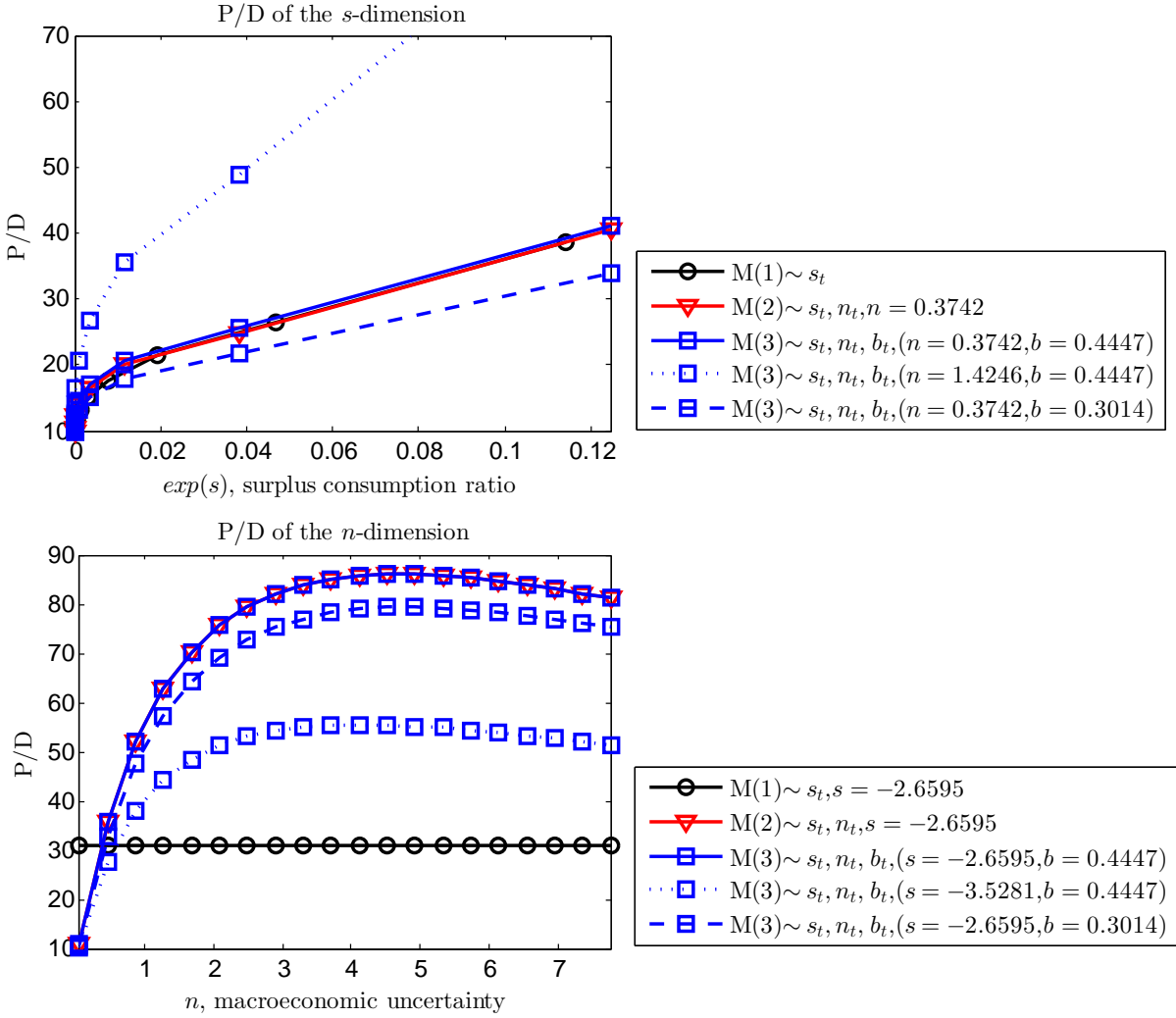


Figure 2.5: Dependence of the Price Dividend Ratio on the State Variables s and n .

The top figure depicts the relationship between PD and $exp(s)$, and the bottom figure depicts the relationship between PD and n . For $M(1)$, price dividend ratio depends on s only; $M(1)$ is depicted in solid black lines with circles. For $M(2)$, price dividend ratio is sensitive to s and n ; to explore the dependence of PD on s (n), I fix n (s) at its mean from the simulation, 0.3742 (-2.6595); $M(2)$ is depicted in solid red lines with triangles. For $M(3)$, price dividend ratio is sensitive to s , n and b . The dimension is reduced by fixing the other state variables at their mean and critical values (i.e., the 95% quantile value in the n_t simulation, 1.4246, the 5% quantile value in the s_t simulation, -3.5281, and the 5% quantile value in the b_t simulation, 0.3014); $M(3)$ is depicted in blue lines with squares. Note that, as suggested by theory, the three solid lines in the top plot coincide; the two solids lines with triangles and squares in the bottom plot also coincide.

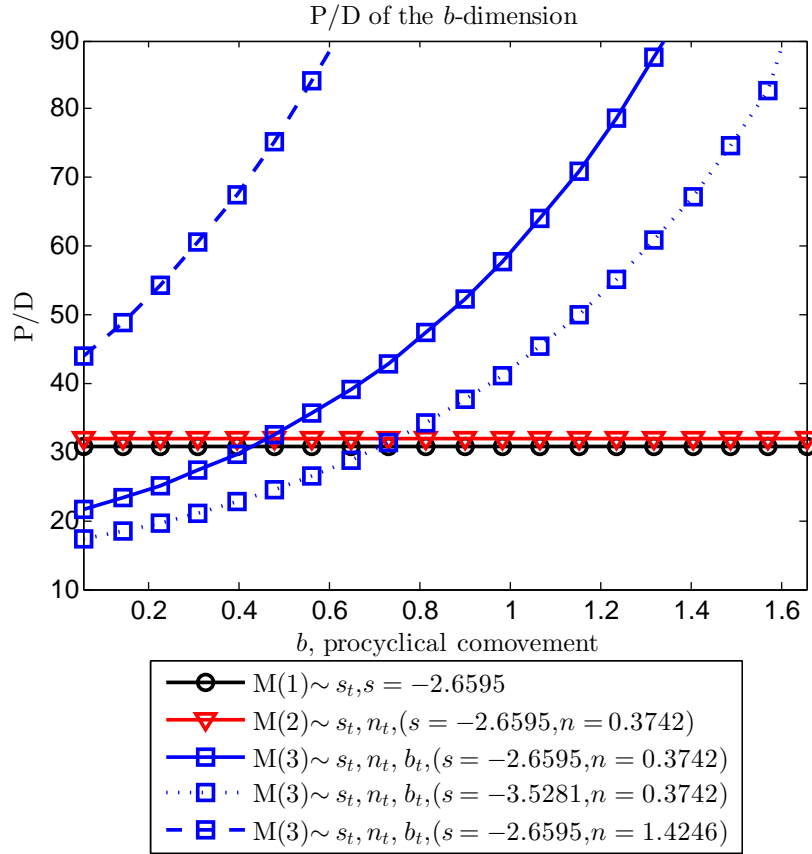


Figure 2.6: Dependence of the Price Dividend Ratio on the State Variable b .

The figure depicts the relationship between PD and b conditional on (s, n) . M(1) and M(2) are invariant of the new state variable b . For M(3), price dividend ratio is sensitive to s , n and b . The multi-dimensional relationship is reduced by fixing the other state variables at their mean and critical values (i.e., the 95% quantile value in the n_t simulation, 1.4246 and the 5% quantile value in the s_t simulation, -3.5281); M(3) is depicted in blue lines with squares.

3

THE TIME VARIATION IN RISK APPETITE AND UNCERTAINTY

We develop new measures of time-varying risk aversion and economic uncertainty that can be calculated from observable financial information at high frequencies. Our approach has four important elements. First, we formulate a dynamic no-arbitrage asset pricing model that consistently prices all assets under assumptions regarding the joint dynamics among asset-specific cash flow dynamics, macroeconomic fundamentals and risk aversion. Second, both the fundamentals and cash flow dynamics feature time-varying heteroskedasticity and non-Gaussianity to accommodate dynamics observed in the data, which we document. This allows us to distinguish time variation in economic uncertainty (the amount of risk) from time variation in risk aversion (the price of risk). Third, despite featuring non-Gaussian dynamics, the model retains closed-form solutions for asset prices. Fourth, our approach exploits information on realized volatility and option prices for the two main risky asset classes, equities and corporate bonds, to help identify and differentiate economic uncertainty from risk aversion. We find that equity variance risk premiums are very informative about risk aversion, whereas credit spreads and corporate bond volatility are highly correlated with economic uncertainty. Model-implied risk premiums beat standard instrument sets predicting excess returns on equity and corporate bonds. A financial proxy to our economic uncertainty predicts output growth negatively and significantly, even in the presence of the VIX.

3.1 Introduction

It has become increasingly commonplace to assume that changes in risk appetites are an important determinant of asset price dynamics. For instance, the behavioral finance literature (see, e.g., Lemmon and Portnaiguina (2006) and Baker and Wurgler (2006) for a discussion) has developed “sentiment indices,” and there are now a wide variety of “risk aversion” or “sentiment” indicators available, created by financial institutions (see Coudert and Gex (2008) for a survey). The “structural” dynamic asset pricing literature has meanwhile proposed time-varying risk aversion as a potential explanation for salient asset price features (see Campbell and Cochrane (1999) and a large number of related articles), whereas reduced-form asset pricing models, aiming to simultaneously explaining stock return dynamics and option prices, have also concluded that time-varying prices of risk are important drivers of stock return and option price dynamics (see Bakshi and Wu, 2010; Bollerslev, Gibson, and Zhou, 2011; Broadie, Chernov, and Johannes, 2007). Risk aversion has also featured prominently in recent monetary economics papers that suggest a potential link between loose monetary policy and the risk appetite of market participants, spurring a literature on what structural economic factors would drive risk aversion changes (see, e.g., Rajan, 2006; Adrian and Shin, 2009; Bekaert, Hoerova, and Lo Duca, 2013). In international finance, Miranda-Agrippino and Rey (2015) and Rey (2015) suggest that global risk aversion is a key transmission mechanism for US monetary policy to be exported to countries worldwide and is a major source of asset return comovements across countries (see also Xu, 2017). Finally, several papers on sovereign bonds (e.g. Bernoth and Erdogan, 2012) have stressed the importance of global risk aversion in explaining their dynamics and contagion across countries.

Our goal is to develop a measure of time-varying risk aversion that is relatively easy to estimate and compute, so that it can be compared to other indices and tracked over time. However, the measure should also correct for deficiencies plaguing many of the current measures. First, it must control for macro-economic uncertainty; we want to separately identify both the aversion to risk (the price of risk) and the amount of risk. To do so, we build on dynamic asset pricing theory. Essentially, our risk aversion measure constitutes a second factor in the pricing kernel

that is not driven by macroeconomic fundamentals. The modeling framework therefore is related, but not identical, to the habit models of Campbell and Cochrane (1999), Menzly, Santos and Veronesi (2004) and Wachter (2006). As in Bekaert, Engstrom and Xing (2009) and Bekaert, Engstrom and Grenadier (2010), we allow for a stochastic risk aversion component that is not perfectly correlated with fundamentals. As an important *byproduct*, we also derive a measure of economic uncertainty, which constitutes an alternative to recent measures (e.g. Juardo, Ludwigson, and Ng, 2015). In the model, asset prices are linked to cash flow dynamics and preferences in an internally consistent fashion. In contrast, a number of articles develop time-varying risk aversion measures motivated by models that really assume “constant” prices of risk and hence are inherently inconsistent (see, for example, Bollerslev, Gibson, and Zhou, 2011), or fail to fully model the link between fundamentals and asset prices (see e.g. Bekaert and Hoerova, 2016). Third, as is well-known, asset prices and returns display dynamics with highly non-Gaussian distributions that are time varying. In fact, a number of articles (see Bollerslev and Todorov, 2011; Liu, Pan, and Wang, 2004; Santa-Clara and Yan, 2010) suggest that compensation for rare events (“jumps”) accounts for a large fraction of equity risk premiums. To accommodate these non-linearities in a tractable fashion, we use the Bad Environment-Good Environment (BEGE, henceforth) framework developed in Bekaert and Engstrom (2017). Shocks are modeled as the sum of two variables with de-meaned gamma distributions, whose shape parameters vary through time. The model delivers conditional non-Gaussian shocks, with changes in “good” or “bad” volatility also changing the conditional distribution of the process. Finally, our data include macroeconomic fundamentals, asset prices, and options prices. The dynamic asset pricing and options literatures indirectly reveal the difficulty in interpreting many existing risk aversion indicators. Often they use information such as the VIX or return risk premiums that are obviously driven by both the amount of risk and risk aversion. Disentangling the two is not straightforward. Articles such as Drechsler and Yaron (2008), Bollerslev et al. (2009) and Bekaert and Hoerova (2016) point towards the use of the VIX in combination with the (conditional) expected variance as particularly informative about risk preferences. Therefore, this paper is also related to the literature on extracting information about risk and risk preferences from option prices (for a survey,

see Gai and Vause, 2006).

The use of different asset classes in deriving a single measure of risk aversion imposes the important assumption that different markets are priced in an integrated setting. This may not (always) be the case. During the 2007-2009 global crisis, it was widely recognized that arbitrage opportunities surfaced between asset classes and sometimes within an asset class (for instance, between Treasury bonds of different maturities, see e.g. Hu, Pan, and Wang, 2013). There may well be a link between risk aversion and the existence of arbitrage opportunities. That is, in uncertain, risk averse times, there is insufficient risky capital available, which causes different asset classes to be priced incorrectly (see, for example, Gilchrist, Yankov, and Zakrajsek, 2009). While consistent pricing across risky asset classes is a maintained assumption in our benchmark model, we can easily test for consistent pricing by examining risk aversion measures implied by different asset classes. We provide an example by comparing risk aversions filtered from risky assets only and from both risky assets and Treasury bonds.

The remainder of the paper is organized as follows. Sections 3.2 and 3.3 presents the model and estimation strategy in detail. Section 3.4 briefly outlines the data we use. Section 3.5 extracts risk aversion and uncertainty from asset prices and discusses the links between the risk aversion estimates and various financial variables. We also examine the behavior of the indices around the Bear Stearns and Lehman Brothers bankruptcies. In Section 3.6, we link our measures of risk appetite and uncertainty to alternative indices including ones produced by practitioners. In Section 3.7, we discuss the case of risk aversion involving Treasury bonds. Concluding remarks are in Section 3.8.

3.2 Modeling Risk Appetite and Uncertainty

In this section, we first define our concept of risk aversion in general terms in Section 3.2.1. We then build a dynamic model with stochastic risk aversion and macro-economic factors affecting the cash flows processes of two main risky asset classes, corporate bonds and equity. The state variables are described in Section 3.2.2 and the pricing kernel in Section 3.2.3.

3.2.1 General Strategy

An ideal measure of risk aversion would be model free and not confound time variation in economic uncertainty with time variation in risk aversion. There are many attempts in the literature to approximate this ideal, but invariably various modeling and statistical assumptions are necessary to tie down risk aversion. For example, in the options literature, a number of articles (Ait-Sahalia and Lo, 2000; Engle and Rosenberg, 2002; Jackwerth, 2000; Bakshi, Kapadia and Madan, 2003; Britten-Jones and Neuberger, 2000) appear at first glance to infer risk aversion from equity options prices in a general fashion, but it is generally the case that the utility function is assumed to be of a particular form and/or to depend only on stock prices.

Another strand of the literature relies on general properties of pricing kernels. Using a strictly positive pricing kernel or stochastic discount factor, M_{t+1} , no-arbitrage conditions imply that for all gross returns, R ,

$$E_t [M_{t+1}R_{t+1}] = 1 \quad (3.T1)$$

It is then straightforward to derive that any asset's expected excess return can be written as an asset specific risk exposure ("beta", or β_t) times a price of risk (or λ_t), which applies to all assets (see also Coudert and Gex, 2008):

$$E_t [R_{t+1}] - R_t^f = \beta_t \lambda_t \quad (3.T2)$$

where R_t^f is the risk free rate, $\beta_t = -\frac{Cov_t(R_{t+1}, M_{t+1})}{Var_t(M_{t+1})}$, and $\lambda_t = \frac{Var_t(M_{t+1})}{E_t(M_{t+1})}$.

Unfortunately, this price of risk is not equal to time-varying risk aversion, and in particular may confound economic uncertainty with risk aversion. In a simple power utility framework, it is easy to show that the price of risk is linked to both the coefficient of relative risk aversion and the volatility of consumption growth, the latter being a reasonable measure of economic uncertainty.

Our approach is to start from a fairly general utility function defined over both fundamentals and non-fundamentals. Our measure of risk aversion simply is then the coefficient of relative

risk aversion implied by the utility function. We specify a fairly general consumption process accommodating time variation in economic uncertainty and use the utility framework to price assets, given general processes for the cash flows of assets. Therefore, while certainly not model free, our risk aversion process is consistent with a wide set of economic models that respect no-arbitrage conditions. Moreover, we can use any risky asset for which we can model cash flows to help identify risk aversion. The identification of the risk aversion process takes into account that economic uncertainty varies through time and controls for non-Gaussianities in cash flow processes.

Consider a period utility function in the HARA class:

$$U\left(\frac{C}{Q}\right) = \frac{\left(\frac{C}{Q}\right)^{1-\gamma}}{1-\gamma} \quad (3.T3)$$

where C is consumption and Q is a process that will be shown to drive time-variation in risk aversion. Essentially, when Q is high, consumption delivers less utility and marginal utility increases. For the general HARA class of utility functions,

$$Q = \left(\frac{a}{\gamma} - \frac{b}{C}\right)^{-1} = f(C) \quad (3.T4)$$

where a and γ are positive parameters, and b is an exogenous benchmark parameter or process. Note that γ (the curvature parameter) is not equal to risk aversion in this framework. In principle, all parameters (a , γ , b) could have time subscripts, but we only allow time-variation in b . Note that the Q process depends on consumption, but we do not allow b to depend on consumption. This excludes internal habit models, for example.

The coefficient of relative risk aversion for this class of models is given by

$$RRA = -\frac{CU''(C)}{U'(C)} = aQ \quad (3.T5)$$

and is thus proportional to Q . Note that $\frac{dQ}{dC} = -b\left(\frac{a}{\gamma}C - b\right)^{-2} < 0$; in good times when consumption increases, risk aversion decreases.

For pricing assets, we need to derive the log pricing kernel which is the intertemporal marginal rate of substitution in a dynamic economy. We assume an infinitely lived agent, facing a constant discount factor of β , and the HARA period utility function given above. The pricing kernel is then given by

$$m_{t+1} = \ln(\beta) + \ln \left[\frac{U'(C_{t+1})}{U'(C_t)} \right] = \ln(\beta) - \gamma \Delta c_{t+1} + \gamma \Delta q_{t+1} \quad (3.T6)$$

where we use t to indicate time, lower case letters to indicate logs of uppercase variables, and Δ to indicate log changes.

To get more intuition for this framework, note that the Campbell and Cochrane (1999) (CC henceforth) utility function is a special case. CC use an external habit model, with utility being a power function over $C_t - H_t$, where H_t is the habit stock. Of course, we can also write

$$C_t - H_t = \frac{C_t}{Q_t} \quad (3.T7)$$

with $Q_t = \frac{C_t}{C_t - H_t}$. So the CC utility function is a special case of our framework with $a = \gamma$ and $b = H$. As C_t gets closer to the habit stock, risk aversion increases. Q_t is thus the inverse of the surplus ratio in the CC article. CC also model q_t exogenously but restrict the correlation between q_t and Δc_t to be perfect. The “moody investor” economy in Bekaert, Engstrom, and Grenadier (2010) is also a special case. In that model, q_t is also exogenously modeled, but has its own shock; that is, there are preference shocks not correlated with fundamentals. In our general quest to identify risk aversion, we surely must allow for such shocks to hit q as well. The model in Brandt and Wang (2003) is also a special case but the risk aversion process specifically depends on inflation in addition to consumption growth. In fact, DSGE models in macro-economics routinely feature preference shocks (see e.g. Besley and Coate, 2003).

In sum, our approach specifies a stochastic process for q (risk aversion), which constitutes a second factor in the pricing kernel that is not fully driven by fundamentals (consumption growth).

3.2.2 Economic Environment: State Variables

3.2.2.1 Macroeconomic Factors

In canonical asset pricing models agents have utility over consumption, but it is well known that consumption growth and asset returns show very little correlation. Moreover, consumption data are only available at the quarterly frequency. Because the use of options data is key to our identification strategy and these data are only available since 1986, it is important to use macroeconomic data that are available at the monthly frequency. We therefore chose to use industrial production, which is available at the monthly frequency, as our main macroeconomic factor. In the macro-economic literature, much attention has been devoted recently to the measurement of “real” uncertainty (see e.g. Jurado, Ludvigson and Ng, 2015) and its effects on the real economy (see e.g. Bloom, 2009). We add to this literature by using a novel econometric framework to extract two macro risk factors from industrial production: “good” uncertainty, denoted by p_t , and “bad” uncertainty, denoted by n_t .

Specifically, the change in log industrial production index, θ_t , has time-varying conditional moments governed by two state variables: p_t and n_t . The conditional mean is modeled as a persistent process to accommodate a time-varying long-run mean of output growth:

$$\theta_{t+1} = \bar{\theta} + \rho_{\theta}(\theta_t - \bar{\theta}) + m_p(p_t - \bar{p}) + m_n(n_t - \bar{n}) + u_{t+1}^{\theta}, \quad (3.T8)$$

where the growth shock is decomposed into two independent centered gamma shocks,

$$u_{t+1}^{\theta} = \sigma_{\theta p} \omega_{p,t+1} - \sigma_{\theta n} \omega_{n,t+1}. \quad (3.T9)$$

The shocks follow centered gamma distributions with time-varying shape parameters,

$$\omega_{p,t+1} \sim \tilde{\Gamma}(p_t, 1) \quad (3.T10)$$

$$\omega_{n,t+1} \sim \tilde{\Gamma}(n_t, 1), \quad (3.T11)$$

where $\tilde{\Gamma}(x, 1)$ denotes a centered gamma distribution with shape parameter x and a unit scale parameter. The shape factors, p_t and n_t , follow autoregressive processes,

$$p_{t+1} = \bar{p} + \rho_p(p_t - \bar{p}) + \sigma_{pp}\omega_{p,t+1} \quad (3.T12)$$

$$n_{t+1} = \bar{n} + \rho_n(n_t - \bar{n}) + \sigma_{nn}\omega_{n,t+1}, \quad (3.T13)$$

where ρ_x denotes the autoregressive term of process x_{t+1} , σ_{xx} the sensitivity to shock $\omega_{x,t+1}$, and \bar{x} the long-run mean. We denote the macroeconomic state variables as, $\mathbf{Y}_t^{mac} = \begin{bmatrix} \theta_t & p_t & n_t \end{bmatrix}'$, and the set of unknown parameters are $\bar{\theta}, \rho_\theta, m_p, m_n, \bar{n}, \sigma_{\theta p}, \sigma_{\theta n}, \rho_p, \sigma_{pp}, \rho_n$, and σ_{nn} .

In this model, the conditional mean has an autoregressive component, but macro risks can also affect expected growth. This can both accommodate cyclical effects (lower conditional means in bad times), or the uncertainty effect described in Bloom (2009). The shocks reflect the BEGE framework of Bekaert and Engstrom (2017), implying that the conditional higher moments of output growth are linear functions of the bad and good uncertainties. For example, the conditional variance and the conditional unscaled skewness are as follows,

$$\begin{aligned} \text{Conditional Variance:} \quad E_t \left[(u_{t+1}^\theta)^2 \right] &= \sigma_{\theta p}^2 p_t + \sigma_{\theta n}^2 n_t, \\ \text{Conditional Unscaled Skewness:} \quad E_t \left[(u_{t+1}^\theta)^3 \right] &= 2\sigma_{\theta p}^3 p_t - 2\sigma_{\theta n}^3 n_t. \end{aligned}$$

This reveals the sense in which p_t represents “good” and n_t “bad” volatility: p_t (n_t) increases (decreases) the skewness of industrial production growth.

The industrial production process is a key determinant of the consumption growth process, but we model consumption growth jointly with the cash flow processes for equities imposing the economic restriction that those processes are cointegrated.

3.2.2.2 Cash Flows and Cash Flow Uncertainty

To model the cash flows for equities and corporate bonds, we focus attention on two variables that exhibit strong cyclical movements, namely earnings (see e.g. Longstaff and Piazzesi, 2004) and corporate defaults (see e.g. Gilchrist and Zakrajšek, 2012).

3.2.2.2.1 Corporate Bond Loss Rate

To model corporate bonds, we use data on default rates. Suppose a portfolio of one-period nominal bonds has a promised payoff of $exp(c)$ at $(t + 1)$, but will in fact only pay an unknown fraction $F_{t+1} \leq 1$ of that amount. Let $l_t = \ln(1/F_t) \geq 0$ be the log loss function. Then the actual nominal payment will be $exp(c - l_{t+1})$. We use default data on corporate bonds to measure this loss rate and provide more detail on the pricing of defaultable bonds in the pricing section (Section 3.2.3).

The log loss rate, l_t , is defined as the logarithm of the current aggregate default rate multiplied by the loss-given-default rate. The dynamic system of the corporate bond loss rate is modeled as follows:

$$l_{t+1} = l_0 + \rho_{ll}l_t + \rho_{lp}p_t + \rho_{ln}n_t + \sigma_{lp}\omega_{p,t+1} + \sigma_{ln}\omega_{n,t+1} + u_{t+1}^l \quad (3.T14)$$

$$u_{t+1}^l = \sigma_{ll}\omega_{l,t+1} \quad (3.T15)$$

$$\omega_{l,t+1} \sim \tilde{\Gamma}(v_t, 1), \quad (3.T16)$$

where

$$v_{t+1} = v_0 + \rho_{vv}v_t + \sigma_{vl}\omega_{l,t+1}. \quad (3.T17)$$

The conditional mean depends on an autoregressive term and the good and bad uncertainty state variables p_t and n_t . The loss rate total disturbance is governed by three independent heteroskedastic centered gamma shocks: the good and bad environment macro shocks $\{\omega_{p,t+1}, \omega_{n,t+1}\}$ and the (orthogonal) loss rate shock $\omega_{l,t+1}$. The loss rate shock follows a centered gamma distribution where the shape parameter v_t varies through time.

This dynamic system allows macro-economic uncertainty to affect both the conditional mean and conditional variance of the loss rate process. However, it also allows the loss rate to have an autonomous autoregressive component in its conditional mean (making l_t a state variable) and accommodates heteroskedasticity not spanned by macro-economic uncertainty. There-

fore, v_t can be viewed as “financial” cash flow uncertainty. Note that the shock to v_t is the same as the shock for the loss process itself. If σ_{ll} and σ_{vl} are positive, as we would expect, the loss rate and its volatility are positively correlated; that is, in bad times with a high incidence of defaults, there is also more uncertainty about the loss rate, and because the gamma distribution is positively skewed, the (unscaled) skewness of the process increases. We would also expect the sensitivities to the good (bad) environment shocks, σ_{lp} (σ_{ln}) to be negative (positive): defaults should decrease (increase) in relatively good (bad) times.

The conditional variance of the loss rate is $\sigma_{lp}^2 p_t + \sigma_{ln}^2 n_t + \sigma_{ll}^2 v_t$, and its conditional unscaled skewness is $2 \left(\sigma_{lp}^3 p_t + \sigma_{ln}^3 n_t + \sigma_{ll}^3 v_t \right)$. The set of unknown parameters are $l_0, \rho_{ll}, \rho_{lp}, \rho_{ln}, \sigma_{lp}, \sigma_{ln}, \sigma_{ll}, v_0, \rho_{vv}$, and σ_{vl} .

3.2.2.2.2 Log Earnings Growth

Log earnings growth, g_t , is defined as the change in log real earnings of the aggregate stock market. It is modeled as follows:

$$g_{t+1} = g_0 + \rho_{gg} g_t + \boldsymbol{\rho}'_{gy} \mathbf{Y}_t^{mac} + \sigma_{gp} \omega_{p,t+1} + \sigma_{gn} \omega_{n,t+1} + \sigma_{gl} \omega_{l,t+1} + u_{t+1}^g \quad (3.T18)$$

$$u_{t+1}^g = \sigma_{gg} \omega_{g,t+1} \quad (3.T19)$$

$$\omega_{g,t+1} \sim N(0, 1). \quad (3.T20)$$

The conditional mean is governed by an autoregressive component and the three macro factors; the time variation in the conditional variance comes from the good and bad uncertainty factors, and the loss rate uncertainty factor. The earnings shock is assumed to be Gaussian and homoskedastic, which cannot be rejected by the data in our sample.¹ A key implicit assumption is that the conditional variance of earnings growth is spanned by macro-economic uncertainty and the financial uncertainty present in default rates. The set of unknown parameters is $\{g_0, \rho_{gg}, \boldsymbol{\rho}'_{gy}, \sigma_{gp}, \sigma_{gn}, \sigma_{gl}, \sigma_{gg}\}$.

¹More specifically, we conduct the Kolmogorov-Smirnov test for Gaussianity and the Engle test for heteroscedasticity using the residuals of log earnings growth u^g (this section), log consumption-earnings ratio u^c (later), and log dividend-earnings ratio u^d (later). We fail to reject the null that the residuals series, after controlling for heteroskedastic fundamental shocks, are Gaussian and homoskedastic.

3.2.2.2.3 Log Consumption-Earnings Ratio

We model consumption as stochastically cointegrated with earnings so that the consumption-earnings ratio becomes a relevant state variable. Define $\kappa_t \equiv \ln \left(\frac{C_t}{E_t} \right)$ which is assumed to follow:

$$\kappa_{t+1} = \kappa_0 + \rho_{\kappa\kappa}\kappa_t + \boldsymbol{\rho}'_{\kappa\mathbf{y}}\mathbf{Y}_t^{mac} + \sigma_{\kappa p}\omega_{p,t+1} + \sigma_{\kappa n}\omega_{n,t+1} + \sigma_{\kappa l}\omega_{l,t+1} + u_{t+1}^\kappa \quad (3.T21)$$

$$u_{t+1}^\kappa = \sigma_{\kappa\kappa}\omega_{\kappa,t+1} \quad (3.T22)$$

$$\omega_{\kappa,t+1} \sim N(0, 1). \quad (3.T23)$$

Similarly to earnings growth, there is an autonomous conditional mean component but the heteroskedasticity of κ_t is spanned by other state variables. The set of unknown parameters is

$$\{\kappa_0, \rho_{\kappa\kappa}, \boldsymbol{\rho}'_{\kappa\mathbf{y}}, \sigma_{\kappa p}, \sigma_{\kappa n}, \sigma_{\kappa l}, \sigma_{\kappa\kappa}\}.$$

3.2.2.2.4 Log Dividend Payout Ratio

The log dividend payout ratio, η_t , is expressed as the log ratio of dividends to earnings. Recent evidence in Kostakis, Magdalinos, and Stamatogiannis (2015) shows that the monthly dividend payout ratio is stationary. We model η_t analogously to κ_t and g_t :

$$\eta_{t+1} = \eta_0 + \rho_{\eta\eta}\eta_t + \boldsymbol{\rho}'_{\eta\mathbf{y}}\mathbf{Y}_t^{mac} + \sigma_{\eta p}\omega_{p,t+1} + \sigma_{\eta n}\omega_{n,t+1} + \sigma_{\eta l}\omega_{l,t+1} + u_{t+1}^\eta \quad (3.T24)$$

$$u_{t+1}^\eta = \sigma_{\eta\eta}\omega_{\eta,t+1} \quad (3.T25)$$

$$\omega_{\eta,t+1} \sim N(0, 1). \quad (3.T26)$$

The set of unknown parameters is $\{\eta_0, \rho_{\eta\eta}, \boldsymbol{\rho}'_{\eta\mathbf{y}}, \sigma_{\eta p}, \sigma_{\eta n}, \sigma_{\eta l}, \sigma_{\eta\eta}\}$.

3.2.2.3 Pricing Kernel State Variables

In the model we introduced above, the real pricing kernel depends on consumption growth and changes in risk aversion. To price nominal cash flows (or to price default free nominal bonds), we also need an inflation process. We discuss the modeling of these variables here.

3.2.2.3.1 Consumption Growth

By definition, log real consumption growth, $\Delta c_{t+1} = \ln\left(\frac{C_{t+1}}{C_t}\right) = g_{t+1} + \Delta\kappa_{t+1}$. Therefore, consumption growth is spanned by the previously defined state variables and shocks.

3.2.2.3.2 Risk Aversion

The state variable capturing risk aversion, $q_t \equiv \ln\left(\frac{C_t}{C_t - H_t}\right)$ is, by definition, nonnegative. We impose the following structure,

$$q_{t+1} = q_0 + \rho_{qq}q_t + \rho_{qp}p_t + \rho_{qn}n_t + \sigma_{qp}\omega_{p,t+1} + \sigma_{qn}\omega_{n,t+1} + u_{t+1}^q \quad (3.T27)$$

$$u_{t+1}^q = \sigma_{qq}\omega_{q,t+1} \quad (3.T28)$$

$$\omega_{q,t+1} \sim \tilde{\Gamma}(q_t, 1). \quad (3.T29)$$

The risk aversion disturbance is comprised of three parts, exposure to the good uncertainty shock, exposure to the bad uncertainty shock, and an orthogonal preference shock. Thus, given the distributional assumptions on these shocks, the model-implied conditional variance is $\sigma_{pp}^2 p_t + \sigma_{qn}^2 n_t + \sigma_{qq}^2 q_t$, and the conditional unscaled skewness $2(\sigma_{qp}^3 p_t + \sigma_{qn}^3 n_t + \sigma_{qq}^3 q_t)$. We model the pure preference shock also with a demeaned gamma distributed shock, so that its variance and (unscaled) skewness are proportional to its own level. Controlling for current business conditions, when risk aversion is high, so is its conditional variability and unscaled skewness. The higher moments of risk aversion are perfectly spanned by macroeconomic uncertainty on the one hand and pure sentiment (q_t) on the other hand. Note that our identifying assumption is that q_t itself does not affect the macro variables and $u_{q,t+1}$ represents a pure preference shock. The conditional mean is modeled as before: an autonomous autoregressive component and dependence on p_t and n_t . The set of unknown parameters describing the risk aversion process is $\{q_0, \rho_{qq}, \rho_{qp}, \rho_{qn}, \sigma_{qp}, \sigma_{qn}, \sigma_{qq}\}$.

3.2.2.3.3 Inflation

To price nominal cash flows and nominal bonds, we must specify an inflation process. The conditional mean of inflation depends on an autoregressive term and the three macro factors \mathbf{Y}_t^{mac} . The conditional variance and higher moments of inflation are proportional to the good and bad uncertainty factors $\{p_t, n_t\}$. The inflation innovation u_{t+1}^π is assumed to be Gaussian and homoskedastic. There is no feedback from inflation to the macro variables:

$$\pi_{t+1} = \pi_0 + \rho_{\pi\pi}\pi_t + \boldsymbol{\rho}'_{\pi\mathbf{y}} \mathbf{Y}_t^{mac} + \sigma_{\pi p}\omega_{p,t+1} + \sigma_{\pi n}\omega_{n,t+1} + u_{t+1}^\pi \quad (3.T30)$$

$$u_{t+1}^\pi = \sigma_{\pi\pi}\omega_{\pi,t+1} \quad (3.T31)$$

$$\omega_{\pi,t+1} \sim N(0, 1). \quad (3.T32)$$

The set of unknown parameters is $\{\pi_0, \rho_{\pi\pi}, \boldsymbol{\rho}'_{\pi\mathbf{y}}, \sigma_{\pi p}, \sigma_{\pi n}, \sigma_{\pi\pi}\}$.

3.2.2.4 Matrix Representation

The dynamics of all state variables introduced above can be written compactly in matrix notation. We define the macro factors $\mathbf{Y}_t^{mac} = \begin{bmatrix} \theta_t & p_t & n_t \end{bmatrix}'$ and other state variables $\mathbf{Y}_t^{other} = \begin{bmatrix} \pi_t & l_t & g_t & \kappa_t & \eta_t & v_t & q_t \end{bmatrix}'$. Among the ten state variables, the industrial production growth θ_t , the inflation rate π_t , the loss rate l_t , earnings growth g_t , the log consumption-earnings ratio κ_t and the log divided payout ratio η_t are observable, while the other four state variables, $\{p_t, n_t, v_t, q_t\}$ are latent. There are eight independent centered gamma and Gaussian shocks in this economy. The system can be formally described as follows (technical details are relegated to the Appendix):

$$\mathbf{Y}_{t+1} = \boldsymbol{\mu} + \mathbf{A}\mathbf{Y}_t + \boldsymbol{\Sigma}\boldsymbol{\omega}_{t+1}, \quad (3.T33)$$

where constant matrices, $\boldsymbol{\mu}$ (10×1), \mathbf{A} (10×10) and $\boldsymbol{\Sigma}$ (10×8), are implicitly defined, $\mathbf{Y}_t = \begin{bmatrix} \mathbf{Y}_t^{mac'} & \mathbf{Y}_t^{other'} \end{bmatrix}'$ (10×1) is a vector comprised of the state variable levels, and $\boldsymbol{\omega}_{t+1} = \begin{bmatrix} \omega_{p,t+1} & \omega_{n,t+1} & \omega_{\pi,t+1} & \omega_{l,t+1} & \omega_{g,t+1} & \omega_{\kappa,t+1} & \omega_{\eta,t+1} & \omega_{q,t+1} \end{bmatrix}'$ (8×1) is a vector comprised of all the independent shocks in the economy.

Note that, among the eight shocks, four shocks follow the gamma shock dynamics laws—the good uncertainty shock ($\omega_{p,t+1}$), the bad uncertainty shock ($\omega_{n,t+1}$), the loss rate shock ($\omega_{l,t+1}$), and the risk aversion shock ($\omega_{q,t+1}$). The remaining four shocks are standard homoskedastic Gaussian shocks (i.e., $N(0, 1)$). Importantly, given our preference structure, the state variables driving the time variation in the higher order moments of these shocks are the only ones driving the time variation in asset risk premiums and their higher order moments. Economically, we therefore rely on time variation in risk aversion—as in the classic Campbell-Cochrane model and its variants (see e.g. Bekaert, Engstrom and Grenadier, 2010; Wachter, 2006)—and time variation in economic uncertainty—as in the Bansal-Yaron (2004) model—to explain risk premiums. The model implications for conditional asset return variances turn out to be critical in identifying the dynamics of risk aversion (see also Le and Singleton, 2013).

Our specific structure admits conditional non-Gaussianity yet generates affine pricing solutions.² The model is tractable because the moment generating functions of gamma and Gaussian distributed variables can be derived in closed form, delivering exponentiated affine functions of the state variables. In particular,

$$E_t [\exp(\boldsymbol{\nu}'\mathbf{Y}_{t+1})] = \exp \left[\boldsymbol{\nu}'\mathbf{S}_0 + \frac{1}{2}\boldsymbol{\nu}'\mathbf{S}_1\boldsymbol{\Sigma}^{other}\mathbf{S}'_1\boldsymbol{\nu} + \mathbf{f}_S(\boldsymbol{\nu})\mathbf{Y}_t \right], \quad (3.T34)$$

where \mathbf{S}_0 (10×1) is a vector of drifts; \mathbf{S}_1 (10×4) is a selection matrix of 0s and 1s which picks out the Jensen's inequality terms of the four Gaussian shocks; $\boldsymbol{\Sigma}^{other}$ (4×4) represents the covariance of the Gaussian shocks. The matrix $\mathbf{f}_S(\boldsymbol{\nu})$ is a non-linear function of $\boldsymbol{\nu}$, involving the feedback matrix, and the scale parameters of the gamma-distributed variables. See Appendix A.1 for more details.

3.2.3 Asset Pricing

In this section, we present the model solutions. First, we formally define the real and pricing kernel as a function of the previously defined state variables. Assuming complete markets,

²Previous research by Bekaert, Engstrom and Xing (2009) and Bekaert and Engstrom (2017) also combines time variation in economic uncertainty with changes in risk aversion.

this kernel prices any cash flow pattern spanned by our state variable dynamics. Second, asset prices of two risky assets—defaultable corporate bonds and equities—are derived. The solution of the model shows that asset prices are (quasi) affine functions of the state variables, which is crucial in developing the estimation procedure in this paper. In particular, we derive approximate expressions for endogenous returns to use in estimating the model parameters, and a risk appetite index.

We also show how to price nominal bonds, but they do not feature in our main estimation procedure because they often function as flights-to-safety assets and it is conceivable that much more intricate modeling is necessary not to break the implicit assumption of a unique pricing kernel (and one risk aversion process) pricing all risky assets. We test market integration between risky assets and Treasury bonds formally in Section 3.7.

3.2.3.1 The pricing kernel

Taking the ratio of marginal utilities at time $t + 1$ and t , we obtain the intertemporal marginal rate of substitution which constitutes the real pricing kernel denoted by M_{t+1} . As Equation (3.T6) indicates, it has the same form as the pricing kernel in the Campbell and Cochrane model, however, the kernel state variables and kernel shocks are quite different. Unlike the CC model, changes in the log surplus consumption ratio (the inverse of risk aversion) are not perfectly correlated with the consumption growth shock, and consumption growth is heteroskedastic. The real pricing kernel in our model follows an affine process as well:

$$m_{t+1} = m_0 + \mathbf{m}'_2 \mathbf{Y}_t + \mathbf{m}'_1 \boldsymbol{\Sigma} \boldsymbol{\omega}_{t+1}, \quad (3.T35)$$

where m_0 , \mathbf{m}_1 (10×1), \mathbf{m}_2 (10×1) are constant scalar or matrices that are implicitly defined using Equations (18)–(23) and (27)–(29). To price nominal assets, we define the nominal pricing kernel, \tilde{m}_{t+1} , which is a simple transformation of the log real pricing kernel, m_{t+1} ,

$$\tilde{m}_{t+1} = m_{t+1} - \pi_{t+1}, \quad (3.T36)$$

$$= \tilde{m}_0 + \tilde{\mathbf{m}}'_2 \mathbf{Y}_t + \tilde{\mathbf{m}}'_1 \boldsymbol{\Sigma} \boldsymbol{\omega}_{t+1}, \quad (3.T37)$$

where \tilde{m}_0 , $\tilde{\mathbf{m}}_1$ (10×1) and $\tilde{\mathbf{m}}_2$ (10×1) are implicitly defined. The nominal risk free rate, $\tilde{r}f_t$, is defined as $-\ln \{E_t [\exp(\tilde{m}_{t+1})]\}$ which can be expressed as an affine function of the state vector.

3.2.3.2 Asset prices

In this section, we further discuss the pricing of the two risky assets—corporate bonds and equities. The Appendix contains detailed proofs and derivations.

3.2.3.2.1 Defaultable Nominal Bonds

Above, we assume that a one period nominal bond faces a fractional (logarithmic) loss of l_t . Given the structure assumed for l_t and Equation (34), the log price-coupon ratio of the one-period defaultable bond portfolio is

$$pc_t^1 = \ln \{E_t [\exp(\tilde{m}_{t+1} - l_{t+1})]\} \quad (3.T38)$$

$$= b_0^1 + \mathbf{b}_1^{1'} \mathbf{Y}_t, \quad (3.T39)$$

where b_0^1 and $\mathbf{b}_1^{1'}$ are implicitly defined. Consider next a portfolio of multi-period zero-coupon defaultable bonds with a promised terminal payment of C at period $(t + N)$. As for the one-period bond, the actual coupon payment will be less than or equal to the promised payment with the actual coupon, and the ex-post nominal payoff is given by $\exp(c - l_{t+n})$. We ignore the possibility of early default or prepayment. Then, the price-coupon ratio of a one-period defaultable bond at period $(t + N - 1)$, PC_{t+N-1}^1 , is $\exp(b_0^1 + \mathbf{b}_1^{1'} Y_{t+N-1})$. Given the Euler equation and the law of iterated expectations, it then follows by induction that all farther dated zero-coupon nominally defaultable corporate bond prices are similarly affine in the state variables:

$$\begin{aligned} pc_t^N &= \ln \left\{ E_t [\tilde{M}_{t+1} PC_{t+1}^{N-1}] \right\}, \\ &= b_0^N + \mathbf{b}_1^{N'} \mathbf{Y}_t. \end{aligned} \quad (3.T40)$$

The assumed zero-coupon structure of the payments before maturity implies that the unexpected returns to this portfolio are exactly linearly spanned by the shocks to \mathbf{Y}_t .

3.2.3.2.2 Equities

Equity is a claim to the dividend stream; let P_t denote the ex-dividend price of the claim, then, the price-dividend ratio, PD_t , is given by:

$$PD_t = E_t \left[M_{t+1} \frac{(P_{t+1} + D_{t+1})}{D_t} \right] \quad (3.T41)$$

$$= \sum_{n=1}^{\infty} E_t \left[\underbrace{\exp \left(\sum_{j=1}^n m_{t+j} + \Delta d_{t+j} \right)}_{\equiv F_t^n} \right], \quad (3.T42)$$

When $n = 1$, $F_t^1 = E_t[\exp(m_{t+1} + \Delta d_{t+1})]$ can be expressed as an exact exponential affine function of the state vector. Recursively, the n -th summation term yields the following identity:

$$F_t^n = E_t \left[\exp \left(\sum_{j=1}^n m_{t+j} + \Delta d_{t+j} \right) \right] \quad (3.T43)$$

$$= E_t \left[\exp(m_{t+1} + \Delta d_{t+1}) F_{t+1}^{n-1} \right]. \quad (3.T44)$$

Therefore, by induction, any summation term with $n > 1$ can also be expressed as an exponential affine function of the state vector. Therefore, the price-dividend ratio is the sum of an infinite number of exponential affine functions of the state vector.

3.2.3.3 Asset Returns

Given that the log price-coupon ratio of a defaultable nominal corporate bond can be expressed as an exact affine function of the state variables, it immediately implies that the log nominal return (before maturity), $\tilde{r}_{t+1}^{cb} = pc_{t+1} - pc_t$, can be represented in closed-form. For equities, the log nominal equity return is derived as follows, $\tilde{r}_{t+1}^{eq} = \ln \left(\frac{PD_{t+1} + 1}{PD_t} \frac{D_{t+1}}{D_t} \Pi_{t+1} \right)$. It is therefore a non-linear but known function of the state variables. We approximate this function by a linear function (See the Appendix for details). Note that this procedure is very different from the very popular Campbell-Shiller (1988) model to approximate returns with a linear expression. Because they approximate the return expression and then price future cash flows with approximate expected returns, their procedure accumulates pricing errors. We approximate a

known quasi-affine pricing function in deriving a return expression.

To account for the approximation error, we allow for two asset-specific homoskedastic shocks that are orthogonal to the state variable innovations. As a result, the log nominal asset returns have the following dynamic factor expression,

$$\tilde{r}_{t+1}^i = \tilde{\xi}_0^i + \tilde{\xi}_1^{i'} \mathbf{Y}_t + \tilde{\mathbf{r}}^{i'} \Sigma \boldsymbol{\omega}_{t+1} + \varepsilon_{t+1}^i, \quad (3.T45)$$

where \tilde{r}_{t+1}^i is the log nominal asset return i from t to $t+1$, $\forall i = \{eq, cb\}$; $\tilde{\xi}_1^i$ (10×1) is the loading vector on the state vector; $\tilde{\mathbf{r}}^i$ (10×1) is the loading vector on the state variable shocks, and ε_{t+1}^i is a homoskedastic noise term with unconditional volatility σ_i .

Rather than exploiting the pricing restrictions on prices, we exploit the restrictions the economy imposes on asset returns, physical variances and risk-neutral variances. Given Equation (3.T45) and the pricing kernel, the model implies that one period expected log excess returns are given by:

$$\begin{aligned} RP_t^i \equiv E_t(\tilde{r}_{t+1}^i) - \tilde{r}_t^i &= \left\{ \sigma_p(\tilde{\mathbf{r}}^i) + \ln \left[\frac{1 - \sigma_p(\tilde{\mathbf{m}}_1 + \tilde{\mathbf{r}}^i)}{1 - \sigma_p(\tilde{\mathbf{m}}_1)} \right] \right\} p_t \\ &+ \left\{ \sigma_n(\tilde{\mathbf{r}}^i) + \ln \left[\frac{1 - \sigma_n(\tilde{\mathbf{m}}_1 + \tilde{\mathbf{r}}^i)}{1 - \sigma_n(\tilde{\mathbf{m}}_1)} \right] \right\} n_t \\ &+ \left\{ \sigma_v(\tilde{\mathbf{r}}^i) + \ln \left[\frac{1 - \sigma_v(\tilde{\mathbf{m}}_1 + \tilde{\mathbf{r}}^i)}{1 - \sigma_v(\tilde{\mathbf{m}}_1)} \right] \right\} v_t \\ &+ \left\{ \sigma_q(\tilde{\mathbf{r}}^i) + \ln \left[\frac{1 - \sigma_q(\tilde{\mathbf{m}}_1 + \tilde{\mathbf{r}}^i)}{1 - \sigma_q(\tilde{\mathbf{m}}_1)} \right] \right\} q_t \\ &- \mathbf{m}'_1 \mathbf{S}_1 \Sigma^{other} \mathbf{S}'_1 \tilde{\mathbf{r}}^i - \frac{1}{2} \left[\tilde{\mathbf{r}}^{i'} \mathbf{S}_1 \Sigma^{other} \mathbf{S}'_1 \tilde{\mathbf{r}}^i + \sigma_i^2 \right]. \end{aligned} \quad (3.T46)$$

As shown earlier, $\tilde{\mathbf{m}}_1$ and $\tilde{\mathbf{r}}^i$ are vectors containing the sensitivities of the log nominal pricing kernel and the log nominal asset returns to the state variable shocks, respectively. The symbols $\sigma_p(\mathbf{x})$, $\sigma_n(\mathbf{x})$, $\sigma_v(\mathbf{x})$ and $\sigma_q(\mathbf{x})$ represent linear functions of state variables' sensitivities to the good uncertainty shock ($\omega_{p,t+1}$), the bad uncertainty shock ($\omega_{n,t+1}$), the loss rate shock ($\omega_{l,t+1}$) and the risk aversion shock ($\omega_{q,t+1}$). For instance, because $\tilde{\mathbf{m}}_1 = \begin{bmatrix} 0 & 0 & 0 & -1 & 0 & -\gamma & -\gamma & 0 & 0 & \gamma \end{bmatrix}'$

and $\Sigma_{\bullet \mathbf{s}} = \begin{bmatrix} 0 & 0 & 0 & 0 & 0 & 0 & 0 & 0 & 0 & \sigma_{qq} \end{bmatrix}'$,³

$\sigma_q(\tilde{\mathbf{m}}_1) = \tilde{\mathbf{m}}_1' \Sigma_{\bullet \mathbf{s}} = \gamma \sigma_{qq} > 0$, where $\gamma > 0$ follows from concave utility and $\sigma_{qq} > 0$

implies positive skewness of risk aversion in Equation (3.T27). It immediately implies that an asset with a negative sensitivity to the risk aversion shock exhibits a higher risk premium when risk aversion is high. That is, for such an asset, $\sigma_q(\tilde{\mathbf{r}}^i) < 0$; then, it can be easily shown that $\sigma_q(\tilde{\mathbf{r}}^i) + \ln \left[\frac{1 - \sigma_q(\tilde{\mathbf{m}}_1 + \tilde{\mathbf{r}}^i)}{1 - \sigma_q(\tilde{\mathbf{m}}_1)} \right] \approx \sigma_q(\tilde{\mathbf{r}}^i) - \frac{\sigma_q(\tilde{\mathbf{r}}^i)}{1 - \sigma_q(\tilde{\mathbf{m}}_1)} > 0$. Expected excess returns thus vary through time and are affine in p_t, n_t, v_t (macroeconomic and cash flow uncertainties) and q_t (market-specific risk aversion).

The physical conditional return variance is obtained given the return loadings of Equation (3.T45):

$$\begin{aligned} VAR_t^i \equiv VAR_t(\tilde{r}_{t+1}^i) &= \left(\sigma_p(\tilde{\mathbf{r}}^i) \right)^2 p_t + \left(\sigma_n(\tilde{\mathbf{r}}^i) \right)^2 n_t + \left(\sigma_v(\tilde{\mathbf{r}}^i) \right)^2 v_t + \left(\sigma_q(\tilde{\mathbf{r}}^i) \right)^2 q_t \\ &+ \tilde{\mathbf{r}}^{i'} \mathbf{S}_1 \Sigma^{other} \mathbf{S}_1' \tilde{\mathbf{r}}^i + \sigma_i^2, \end{aligned} \quad (3.T47)$$

where \mathbf{S}_1 is defined in Section 2.2.4. See Appendix A.1 for more details. The expected variance under the physical measure is time-varying and affine in p_t, n_t, v_t and q_t .

The one-period risk-neutral conditional return variance is:

$$\begin{aligned} VAR_t^{i,Q} \equiv VAR_t^Q(\tilde{r}_{t+1}^i) &= \left(\frac{\sigma_p(\tilde{\mathbf{r}}^i)}{1 - \sigma_p(\tilde{\mathbf{m}}_1)} \right)^2 p_t + \left(\frac{\sigma_n(\tilde{\mathbf{r}}^i)}{1 - \sigma_n(\tilde{\mathbf{m}}_1)} \right)^2 n_t + \left(\frac{\sigma_v(\tilde{\mathbf{r}}^i)}{1 - \sigma_v(\tilde{\mathbf{m}}_1)} \right)^2 v_t \\ &+ \left(\frac{\sigma_q(\tilde{\mathbf{r}}^i)}{1 - \sigma_q(\tilde{\mathbf{m}}_1)} \right)^2 q_t + \tilde{\mathbf{r}}^{i'} \mathbf{S}_1 \Sigma^{other} \mathbf{S}_1' \tilde{\mathbf{r}}^i + \sigma_i^2. \end{aligned} \quad (3.T48)$$

Note that the functions in Equation (3.T48) are affine transformations from the ones in Equation (3.T47), using the “ $\sigma(m)$ ” functions. Under normal circumstances, we would expect that the relative importance of “bad” uncertainty, the loss rate’s uncertainty and risk aversion increases under the risk neutral measure relative to the importance of “good” uncertainty. In Equation (3.T48), this intuition can potentially be formally established as $\sigma_n(m)$, $\sigma_l(m)$, $\sigma_q(m)$ are positive and $\sigma_p(m)$ is negative. For example, as derived above, $\sigma_q(\tilde{\mathbf{m}}_1) = \gamma \sigma_{qq}$ is strictly positive.

³Matrix $\Sigma_{\bullet j}$ is the j -th column of the shock coefficient matrix in the state variable process, or Σ in Equation (3.T33).

3.3 The Identification and Estimation of Risk Aversion and Uncertainty

In what follows, we describe our general estimation philosophy which is focused on retrieving a risk aversion process that can be traced at high frequencies, and then outline the methodology in detail. The first step is the identification of macro-economic and cash flow uncertainties; the second step is the actual estimation of the remainder of the model parameters and the identification of risk aversion.

3.3.1 General Estimation Philosophy

While there are 10 state variables in the model, there are only four latent state variables that drive risk premiums and conditional physical and risk neutral variances in the model as described in Equations (3.T46)–(3.T48). Three of these state variables, good uncertainty, p_t , bad uncertainty, n_t and cash flow uncertainty, v_t , describe economic uncertainty. We want to ensure that these variables are identified from macro-economic and cash flow information alone and are not contaminated by asset prices. We therefore pre-estimate these variables. This constitutes the first step in the estimation methodology.

Given the dynamics of these variables, there are a variety of ways that we can retrieve risk aversion from the model and data on corporate bonds and equities. However, an important goal of the paper is to make risk aversion observable, even at high frequencies. Under the null of the model, asset prices, risk premiums and variances are an exact function of the state variables, including risk aversion. It thus follows that (market-wide) risk aversion should be spanned by a judiciously chosen set of asset prices and risk variables. Given our desire to generate a high frequency risk aversion index, we select these instruments to be observable at high frequencies and to reflect risk and return information for our two asset classes. In particular, we assume

$$q_t = \chi' z_t, \tag{3.T49}$$

where \mathbf{z}_t is a vector of 6 observed asset prices and ones. The instruments include (1) term spread (the difference between the 10-year and 3-month Treasury bond yield), (2) the credit spread (the difference between Moody’s BAA yield and 10-year Treasury bond yield), (3) a “detrended” dividend yield, (4) the realized equity return variance, (5) the risk-neutral equity return variance, and (6) the realized corporate bond return variance.

The term spread may reflect information about the macro-economy (see e.g. Harvey, 1988) and was also included in the risk appetite index of Bekaert and Hoerova (2016). The credit spread and dividend yield have direct price information from the corporate bond and equity market respectively and thus reflect partially information about risk premiums. Ideally, we would include information on both risk-neutral and physical variances for both equities and corporate bonds, but we do not have data on the risk neutral corporate bond return variance. We use the realized variance for both markets, rather than say an estimate of the physical conditional variance, because realized variances are effectively observed, whereas conditional variances must be estimated. Given a loading vector $\boldsymbol{\chi}$, the risk aversion process can be computed daily from observable data.

So far, the methodology is reminiscent of the FAVAR literature (see Bernanke, Boivin, and Elias, 2005) and Stock and Watson (2002), where unobserved macro-factors are identified using large data sets of observable macro-data using a spanning assumption. However, in contrast to the above literature and all “principle component” type analysis, we exploit the restrictions the economy imposes on risk premiums, and physical and risk neutral variances to estimate the loadings of the time-varying risk aversion process. That is, our risk aversion estimate is forced to have the (dynamic) properties of risk aversion implied by the above model: it is an element of the pricing kernel, which must, in turn, correctly price asset returns and be consistent with observed measures of return volatility under both the physical and risk-neutral measures. To do so, we adopt a GMM procedure detailed in Section 3.3.3. Imposing the model restrictions and no arbitrage through a positive pricing kernel also differentiates the estimation from the approach taken in Bekaert and Hoerova (2016).

3.3.2 Identifying Economic Uncertainty

Given that there is no feedback from risk aversion to the three uncertainty state variables, we can pre-estimate the uncertainty factors without using financial asset prices.

First, we use the monthly log real growth rate of industrial production to measure θ_t . In the system for θ_t , described in Equations (3.T8)–(3.T13), there are three state variables, which we collect in \mathbf{Y}_t^{mac} ,

$$\widehat{\mathbf{Y}}_t^{mac} = \begin{bmatrix} \theta_t & \hat{p}_t & \hat{n}_t \end{bmatrix}' .^4$$

We denote the filtered shocks,

$$\widehat{\boldsymbol{\omega}}_t^{mac} = \begin{bmatrix} \hat{\omega}_{p,t} & \hat{\omega}_{n,t} \end{bmatrix}' .$$

The system is estimated using Bates (2006)'s approximate MLE procedure (see the Appendix for details).

Second, we must determine the latent cash flow uncertainty factor v_t , which represents the conditional variance of the log corporate bond default rate. Recall that we assume loss-given-default is a constant, and thus the log corporate bond default rate is the log loss rate plus a constant. The dynamics of the variables are described in Equations (3.T14)–(3.T17). Note that conditional on the model parameters, the residuals of the v_t process are observed and thus the conditional variance can be estimated recursively as in a GARCH process. Thus, the estimation here is exact maximum likelihood, using the correct de-centered gamma density function for the $\omega_{l,t+1}$ shock. Denote the estimated loss rate shape parameter as \hat{v}_t , and the loss rate shock as $\hat{\omega}_{l,t+1}$.

3.3.3 Identifying Risk Aversion

To identify the risk aversion process and the parameters in the spanning condition (Equation (3.T49) above), we exploit the restrictions the model imposes on return risk premiums (equities and corporate bonds), physical variances (equities and corporate bonds) and risk neutral

⁴In the remainder of the paper, a hat superscript is used to indicate estimated variables or matrices.

variances (for equities only). The estimation is a GMM system in which we use the same instruments as the ones used to span risk aversion (\mathbf{z}_t). Apart from the χ parameters, we must also identify the parameters in the kernel (β , the discount factor, and γ , the curvature parameter), and the scale parameter of the preference shock, σ_{qq} . Note that the level of risk aversion is also driven by the q_t process, so that γ and β are not well identified. We impose $\gamma = 2$ and $\beta = 0.999$. The GMM system thus has 8 unknown parameters,

$$\Theta = [\chi_0, \chi_{tsprd}, \chi_{csprd}, \chi_{DY5yr}, \chi_{rvareq}, \chi_{qwareq}, \chi_{rvarcb}, \sigma_{qq}],$$

where the notation is obvious, and *DY5yr* refers to the detrended dividend yield, described later. Before the moment conditions can be evaluated, we must identify the state variables and their shocks, the pricing kernel, and the return shocks. The estimation is therefore intricate and we now describe the various steps in some detail. For each candidate $\hat{\Theta} = [\hat{\chi}', \hat{\sigma}_{qq}]$ vector:

1. Identify the implied risk aversion series given the loading choices, $\hat{q}_t = \hat{\chi}' \mathbf{z}_t$. We impose a lower boundary of 10^{-8} on q_t during the estimation. This is consistent with the theoretical assumption, as q_t is motivated from a habit formation model ($q_t = \ln(Q_t) = \ln\left(\frac{C_t}{C_t - H_t}\right) > 0$). It is also consistent with the distributional assumption for q_t which is the positive shape parameter of the ω_q shock.⁵
2. Identify the state variable levels (\mathbf{Y}_t) and shocks ($\Sigma \omega_{t+1}$).

The parameters of the following state variable processes, $\{\theta_t, p_t, n_t, l_t, v_t\}$, are pre-determined according to Section 3.3.2. For the remaining cash flow state variables $\{\pi_t, g_t, \kappa_t, \eta_t\}$, we estimate the parameters in each iteration using simple projections. To identify the risk aversion-specific shock in the risk aversion process, we first project \hat{q}_{t+1} on $\hat{q}_t, \hat{p}_t, \hat{n}_t, \hat{\omega}_{p,t+1}$ and $\hat{\omega}_{n,t+1}$ to obtain the residual term \hat{u}_{t+1}^q , and then divide it by $\hat{\sigma}_{qq}$ to obtain the preference shock $\hat{\omega}_{q,t+1}$ (see Equations (27)–(29)). We later exploit the implied residual variance and unscaled skewness calculated using the distributional properties of gamma shocks as two moment conditions. Now, given the choice of $\hat{\chi}$, a full set of state variables levels,

⁵However, for the best model, the minimum q is 0.32 and the boundary is non-binding.

$\widehat{\mathbf{Y}}_t = \left[\widehat{\mathbf{Y}}_t^{mac} \quad \pi_t \quad l_t \quad g_t \quad \kappa_t \quad \eta_t \quad \widehat{v}_t \quad \widehat{q}_t \right]'$, and the eight independent shocks, $\widehat{\boldsymbol{\omega}}_{t+1}$ including $\widehat{\omega}_{t+1}^q$, can be identified.⁶

3. Identify the nominal pricing kernel.

Consumption growth in this model is (endogenously) implied by two state variables, real log earnings growth and (changes in) the log consumption-earnings ratio. Given consumption growth (i.e., $g_t + \Delta\kappa_t$), the risk aversion process \widehat{q}_t , γ and β , the monthly nominal kernel is obtained:

$$\widehat{m}_{t+1} = \ln(\beta) - \gamma\Delta c_{t+1} + \gamma(\widehat{q}_{t+1} - \widehat{q}_t) - \pi_{t+1}.$$

Constant matrices related to the log nominal kernel— $\widetilde{m}_0, \widetilde{m}_1, \widetilde{m}_2$ (as in the affine representation of the kernel; see Equation (3.T37))—are implicitly identified.

4. Estimate the return loadings.

In this step, we obtain the loadings of nominal asset returns on the state variable shocks, controlling for time-varying conditional means. Note that there are 8 state variables $\{\theta_t, p_t, n_t, \pi_t, g_t, \kappa_t, v_t, q_t\}$ affecting the pricing kernel. The remaining state variables, $\{l_t, \eta_t\}$, correspond to cash flow state variables in the corporate bond and equity markets. We estimate the loadings by simple projections, assuming the asset-specific approximation shock is homoskedastic:

$$\widetilde{r}_{t+1}^i = \xi_0^i + \boldsymbol{\xi}_1^{i'} \widehat{\mathbf{Y}}_t + \widetilde{\mathbf{r}}^{i'} \widehat{\boldsymbol{\Sigma}} \widehat{\boldsymbol{\omega}}_{t+1} + \varepsilon_{t+1}^i, \quad (3.T50)$$

where \widetilde{r}_{t+1}^i is the log nominal return for asset i , $\widehat{\boldsymbol{\Sigma}}$ and $\widehat{\boldsymbol{\omega}}_{t+1}$ are identified previously, and ε_{t+1}^i has mean 0 and variance σ_i^2 . To obtain asset moments, $\widetilde{\mathbf{r}}^{i'}$ is the crucial shock loading vector, but we also need $\widehat{\sigma}_i$.

5. Obtain the model-implied endogenous moments.

We derive three moments for the asset returns: 1) the expected excess return implied by the model (using the pricing kernel), RP^i ; 2) the physical (conditional expected) return

⁶The parameters obtained from this substep are $\pi_0, \rho_{\pi\pi}, \rho_{\pi\theta}, \rho_{\pi p}, \rho_{\pi n}, \sigma_{\pi p}, \sigma_{\pi n}, \sigma_{\pi l}, \sigma_{\pi\pi}, l_0, \rho_{ll}, \rho_{lp}, \rho_{ln}, \sigma_{lp}, \sigma_{ln}, \sigma_{ll}, g_0, \rho_{gg}, \rho_{g\theta}, \rho_{gp}, \rho_{gn}, \sigma_{gp}, \sigma_{gn}, \sigma_{gl}, \sigma_{gg}, \kappa_0, \rho_{\kappa\kappa}, \rho_{\kappa\theta}, \rho_{\kappa p}, \rho_{\kappa n}, \sigma_{\kappa p}, \sigma_{\kappa n}, \sigma_{\kappa l}, \sigma_{\kappa\kappa}, \eta_0, \rho_{\eta\eta}, \rho_{\eta\theta}, \rho_{\eta p}, \rho_{\eta n}, \sigma_{\eta p}, \sigma_{\eta n}, \sigma_{\eta l}, \sigma_{\eta\eta}, v_0, \rho_{vv}, \rho_{vl}, q_0, \rho_{qq}, \rho_{qp}, \rho_{qn}, \sigma_{qp}$ and σ_{qn} .

variance, VAR^i , which only depends on the return definition in Equation (3.T50) and 3) the risk neutral conditional variance, $VAR^{i,Q}$, which also uses the pricing kernel. The expressions for these variables are derived in Equations (3.T46)–(3.T48) where p_t , n_t , v_{t,q_t} , \tilde{r}^i , Σ^{other} and σ_i have been estimated in previous steps.

6. Obtain the moment conditions $\varepsilon(\Theta; \Psi_t)$. Given data on asset returns and options, we use the derived moments to define 7 error terms that can be used to create GMM orthogonality conditions. There are three types of errors we use in the system. First, neither risk premiums nor physical conditional variances are observed in the data, but we use the restriction that the observed returns/realized variances minus their expectations under the null of the model ought to have a conditional mean of zero:

$$\varepsilon_1(\Theta; \Psi_t) = \begin{bmatrix} \left(\tilde{r}_{t+1}^{eq} - \tilde{r}f_t \right) - \widehat{RP}_t^{eq} \\ RVAR_{t+1}^{eq} - \widehat{VAR}_t^{eq} \\ \left(\tilde{r}_{t+1}^{cb} - \tilde{r}f_t \right) - \widehat{RP}_t^{cb} \\ RVAR_{t+1}^{cb} - \widehat{VAR}_t^{cb} \end{bmatrix}, \quad (3.T51)$$

where \tilde{r}_{t+1}^i is the realized nominal return from t to $t + 1$, r_{f_t} is the risk free rate, and $RVAR_{t+1}^i$ is the realized nominal variance from t to $t + 1$ defined as the sum of the squares of the log high-frequency returns from t to $t + 1$ (see the Data section for details). Here Ψ_t denotes the information set at time t . The risk neutral variance can be measured from options data (see Bakshi, Kapadia, and Madan, 2003), and so we use the error:

$$\varepsilon_2(\Theta; \Psi_t) = \left[QVAR_t^{eq} - \widehat{VAR}_t^{eq,Q} \right], \quad (3.T52)$$

where $QVAR_t^{eq}$ is the ex-ante risk-neutral variances of r_{t+1}^{eq} calculated from the data. We assume that $\varepsilon_2(\Theta; \Psi_t)$ reflects model and measurement error, orthogonal to Ψ_t . Finally, we also construct two moment conditions to identify σ_{qq} , exploiting the model dynamics for

u_{t+1}^q (i.e., the shock to the risk aversion process as in Equation (3.T27)):

$$\boldsymbol{\varepsilon}_3(\boldsymbol{\Theta}; \Psi_t) = \begin{bmatrix} (\hat{u}_{t+1}^q)^2 - (\hat{\sigma}_{qq})^2 \hat{q}_t \\ (\hat{u}_{t+1}^q)^3 - 2(\hat{\sigma}_{qq})^3 \hat{q}_t \end{bmatrix} \quad (3.T53)$$

Let $\boldsymbol{\varepsilon}_{1,2}(\boldsymbol{\Theta}; \Psi_t) = \begin{bmatrix} \boldsymbol{\varepsilon}_1(\boldsymbol{\Theta}; \Psi_t)' & \boldsymbol{\varepsilon}_2(\boldsymbol{\Theta}; \Psi_t) \end{bmatrix}$. Under our assumptions these errors are mean zero given the information set, Ψ_t . We can therefore use them to create the usual GMM moment conditions. Given our previously defined set of instruments, \mathbf{z}_t (7×1 , including a vector of 1's), we define the moment conditions as:

$$E[\mathbf{g}_t(\boldsymbol{\Theta}; \Psi_t, \mathbf{z}_t)] \equiv E \left[\begin{array}{c} \underbrace{\boldsymbol{\varepsilon}_{1,2}(\boldsymbol{\Theta}; \Psi_t)}_{5 \times 1} \otimes \underbrace{\mathbf{z}_t}_{7 \times 1} \\ \underbrace{\boldsymbol{\varepsilon}_3(\boldsymbol{\Theta}; \Psi_t)}_{2 \times 1} \end{array} \right] = \underbrace{\mathbf{0}}_{37 \times 1}. \quad (3.T54)$$

Note that to keep the set of moment conditions manageable, we only use two moment conditions for the identification of σ_{qq} . Denote $\mathbf{g}_t(\boldsymbol{\Theta}; \Psi_t, \mathbf{z}_t)$ (37×1) as the vector of errors at time t , and $\mathbf{g}_T(\boldsymbol{\Theta}; \Psi, \mathbf{z})$ (37×1) the sample mean of $\mathbf{g}_t(\boldsymbol{\Theta}; \Psi_t, \mathbf{z}_t)$ from $t = 1$ to $t = T$. Then, the GMM objective function is,

$$J(\boldsymbol{\Theta}; \Psi, \mathbf{z}) \equiv T \mathbf{g}'_T(\boldsymbol{\Theta}; \Psi, \mathbf{z}) \mathbf{W} \mathbf{g}_T(\boldsymbol{\Theta}; \Psi, \mathbf{z}),$$

where \mathbf{W} is the weighting matrix. We use the standard GMM procedure, first using an identity weighting matrix, yielding a first stage set of parameters $\hat{\boldsymbol{\Theta}}_1$. We then compute the usual optimal weighting matrix as the inverse of the spectral density at frequency zero of the orthogonality conditions, $\hat{\mathbf{S}}_1$, using 5 Newey-West (1987) lags:

$$\hat{\mathbf{S}}_1 = \sum_{j=-5}^{j=5} \frac{5-|j|}{5} \hat{E}[\mathbf{g}_t(\hat{\boldsymbol{\Theta}}_1; \Psi_t, \mathbf{z}_t) \mathbf{g}_{t-j}(\hat{\boldsymbol{\Theta}}_1; \Psi_{t-1}, \mathbf{z}_{t-1})']. \quad (3.T55)$$

Then, the inverse of $\hat{\mathbf{S}}$ is shrunk towards the identity matrix with a shrinkage parameter of

0.1 in obtaining the second-step weight matrix \mathbf{W}_2 :

$$\mathbf{W}_2 = 0.9\hat{\mathbf{S}}^{-1} + 0.1\mathbf{I}_{37 \times 37}, \quad (3.T56)$$

where $\mathbf{I}_{37 \times 37}$ is a identity matrix of dimension 37×37 . This gives rise to a second-round $\hat{\Theta}_2$ estimator. To ensure that poor first round estimates do not affect the estimation, we conduct one more iteration, compute $\hat{\mathbf{S}}_2(\hat{\Theta}_2)$, and produce a third-round GMM estimator, $\hat{\Theta}_3$. Lastly, the asymptotic distribution for the third-step GMM estimation parameter is, $\sqrt{T}(\hat{\Theta}_3 - \Theta_0) \xrightarrow{d} N(0, \mathbf{Avar}(\hat{\Theta}_3))$, where $\widehat{\mathbf{Avar}}(\hat{\Theta}_3) = (\mathbf{G}'_T(\hat{\Theta}_3)\hat{\mathbf{S}}_2^{-1}\mathbf{G}_T(\hat{\Theta}_3))^{-1}$ and where \mathbf{G}_T denotes the gradient of \mathbf{g}_T .

Because the estimation involves several steps and is quite non-linear in the parameters, we increase the chance of finding the true global optimum by starting from 24,000 different starting values for $\hat{\chi}$ drawn randomly from a large set of possible starting values for each parameter. The global optimum is defined as the parameter estimates generating the lowest minimum objective function value.

3.4 Data

Because we combine macro and cash flow data to estimate the dynamics of the state variables, with financial data in the GMM estimation, we use the longest data available for the various estimations of the state variable dynamics. The estimation of the macroeconomic uncertainty state variables uses the period from January 1947 to February 2015, and the estimation of the loss rate uncertainty state variable uses data from January 1982 to February 2015. For the GMM estimation, the sample spans the period from June 1986 to February 2015 ($T=345$ months). All estimations are conducted at the monthly frequency.

3.4.1 State variables

Our output variable—delivering three state variables (θ_t , p_t and n_t)—is the change in log real industrial production where the monthly real industrial production index is obtained from the Federal Reserve Bank at St. Louis. Inflation (π), is defined as the change in the log of the consumer price index (CPI) obtained from the Bureau of Labor Statistics (BLS).

The fifth state variable, the log corporate bond loss rate (l), is defined as the log of the default rate on all U.S. corporate bonds multiplied with the loss-given-default rate (LGD). As commonly assumed in empirical research, LGD is a constant parameter, and is set to 1 (without loss of generality). Specifically, the monthly default rate is obtained by first dividing the total dollar amount of speculative-grade debt that is in default by the total par amount of speculative-grade debt outstanding (source: Moody’s “Corporate Default and Recovery Rates”). Then, we take the average of these monthly corporate bond default rates from the past six months.

The sixth state variable, real earnings growth (g), is defined as the change in log real earnings per capita. Real earnings is the product of real earnings per share and the number of shares outstanding during the same month. The seventh state variable, the log consumption-earnings ratio (κ), uses real consumption and real earnings. Real monthly consumption is defined as the sum of seasonally-adjusted real personal consumption expenditures on nondurable goods and services; the consumption deflator is different from the CPI. The source for consumption is the U.S. Bureau of Economic Analysis (BEA). The source for earnings is Shiller’s website. To obtain per capita units, we divide real consumption and real earnings by the population numbers provided by the BEA.

The eighth state variable, the log dividend payout ratio (η), uses the log ratio of real dividends and real earnings. Therefore, given g and κ , consumption growth is implicitly defined; given g and η , dividend growth is implicitly defined. Real dividend and earnings per share are available from Shiller’s website. We use the 12-month trailing dividends and earnings, i.e., $E_t^{12} = E_{t-12} + \dots + E_{t-1}$ where E_t denotes the monthly earnings. There are no true monthly earnings data because almost all firms report earnings results only quarterly. According to Shiller’s website, the monthly dividend and earnings data provided are inferred from the S&P four-quarter

totals, which are available since 1926. Calculating 12-month trailing values of earnings and dividends is common practice to control for the strong seasonality in the data. Total market shares are obtained from CRSP.

3.4.2 Financial Variables

Daily equity returns are the continuously compounded value-weighted nominal market returns with dividends from CRSP. The monthly return (r^{eq}) is the sum of daily returns within the same month. To create excess returns, we subtract the one-month Treasury bill rate, also from CRSP. We use the square of the month-end VIX index (divided by 120000) as the one-period risk-neutral conditional variance of equity returns ($QVAR^{eq}$) which is obtained from the Chicago Board Options Exchange (CBOE) and is only available from the end of January 1990. We use the VXO index prior to 1990, also from CBOE. We construct the monthly one-period physical conditional variance of equity returns ($PVAR^{eq}$) in two steps. First, we calculate the monthly realized variance as the sum of the squared daily equity returns within the same month; then, we project the monthly realized variance onto the lagged risk-neutral variance and the lagged realized variance to obtain the monthly $PVAR^{eq}$, as in Bekaert, Hoerova, and Lo Duca (2013).

The daily corporate bond market return is the continuously compounded log change in daily Dow Jones corporate bond total return index (source: Global Financial Data). The monthly return (r^{cb}) is the sum of daily returns within the same month. The conditional variance under the physical measure ($PVAR^{cb}$) is the projection of monthly realized variance onto the lagged realized variance and the lagged credit spread (defined as the difference between the month-end BAA yield and the 10-year zero-coupon Treasury yield).

We also obtain the 10-year log Treasury bond market return (r^{tb}) from DataStream. We calculate the monthly realized variance as the sum of the squared daily bond returns within the same month; then, we project the monthly realized variance onto the lagged risk-neutral variance and the lagged realized variance to obtain the monthly $PVAR^{tb}$. The risk-neutral variance of Treasury bond returns is obtained as follows. Prior to 2003, the monthly risk-neutral conditional

variance of Treasury bond returns ($QVAR^{tb}$) is calculated using the Black-Scholes formula with the 10-year Treasury bond option data with expiration as close as possible to 90 days. After 2003, we use the TYVIX series from CBOE, a 10-year U.S. Treasury Bond Volatility Index which is calculated analogously to CBOE’s VIX. We find that the Black-Scholes risk-neutral variance (our calculation) is 0.98 correlated with the TYVIX for the period after January 2003.

In attempting to span risk aversion, we use some observed financial variables. The term spread is the difference between the 10-year Treasury yield and the 3-month Treasury yield, where the yield data is obtained from the Federal Reserve Bank of St. Louis. The credit spread is the difference between Moody’s BAA yield and the 10-year Treasury bond yield. The de-trended dividend yield is calculated as the difference between the raw dividend yield and an moving average term that takes the 5 year average of monthly dividend yields, starting one year before, or $DY5yr_t = DY_t - \sum_{i=1}^{60} DY_{t-12-i}$ where DY_t denotes the dividend yield level at time t (the ratio of 12-month trailing dividends and the equity market price).

3.5 Estimation Results

In this section, we describe the estimation of the state variable processes, and the actual risk aversion process.

3.5.1 State Variable Dynamics

3.5.1.1 Macro-economic factors

We estimate the model in Equations (3.T8)–(3.T13) over the full sample (January 1947 to February 2015) using the approximate likelihood procedure of Bates (2006) (for more details, see the Appendix). While we entertained a number of alternative model specifications, the current model was best in terms of the standard BIC criterion. The parameter estimates are reported in Table 3.1. Industrial production features slight positive auto-correlation and high realizations of “bad” volatility decrease its conditional mean significantly. The p_t process is extremely persistent (almost a unit root) and quasi Gaussian, forcing us to fix its unconditional mean at 500 (for

such values, skewness and kurtosis are effectively zero). The n_t process has a much lower mean featuring an unconditional skewness coefficient of 0.50 ($\frac{2}{\sqrt{16.14}}$) and excess kurtosis of 0.37 ($\frac{6}{16.14}$). It is also less persistent than the p_t process.

We graph the conditional mean and the p_t and n_t process in Figure 3.1 together with NBER recessions. The strong countercyclicality of the n_t process and the procyclicality of the conditional mean of “technology” or output growth are apparent from the graph. We also confirmed it by running a regression of the three processes (conditional mean, p_t , and n_t) on a constant and a NBER dummy. The NBER dummy obtains a highly statistically significant positive (negative) coefficient for the n_t (conditional mean) equation. The coefficient is in fact positive in the p_t equation as well, but not statistically significant. In fact, the n_t regression features an adjusted R^2 of almost 45%.

In Figure 3.2, we plot the conditional variance of industrial production and its conditional skewness. Clearly, macro-economic uncertainty is highly countercyclical, and thus exposure to such uncertainty may render asset prices countercyclical as well. Interestingly, the scaled skewness coefficient is procyclical. This arises from the fact that, while unscaled skewness is countercyclical, the countercyclicality of the variance in the denominator dominates.

3.5.1.2 Cash flow dynamics

The key variable here is the corporate bond loss rate, of which the dynamics are described by Equations (3.T14)–(3.T17). Estimation here is considerably simpler because the previous estimation delivered filtered estimates of p_t , n_t , $\omega_{p,t}$ and $\omega_{n,t}$. Therefore, we can essentially use a linear projection to retrieve the estimates for Equation (3.T14) and then use regular maximum likelihood to estimate the conditional variance process specified in Equations (3.T15)– (3.T16). The results are recorded in Table 3.2.

The loss rate process is persistent with the autocorrelation coefficient close to 0.88. The p_t -process does not significantly affect the loss rate process, neither through the conditional mean or through shock exposures. However, the $\omega_{n,t}$ shock has a statistically significant effect on the loss rate process; moreover n_t affects the loss rate’s conditional mean with a statistically significant

positive coefficient. The conditional variance is also persistent (with an autoregressive coefficient of 0.91).

In Figure 3.3, we plot the conditional moments of the loss rate process, including the v_t process. Note that v_t is only weakly countercyclical. In fact, a regression of v_t on a constant and a NBER dummy, yields a NBER coefficient of 0.202 (t Stat = 0.941). Not surprisingly, the conditional mean of the loss rate is countercyclical, partly through its positive dependence on the n_t process. The conditional volatility also appears countercyclical, which is the combined result of a weakly countercyclical v_t process and a strongly countercyclical n_t process (σ_{ln} being positive). The loss rate process is naturally positively skewed through the positively skewed u^l -shocks and its positive dependence on ω_n . This is confirmed by Figure 3.3, showing the average conditional skewness to be 0.63. However, the scaled skewness dips in recessions, because the conditional variance is so strongly countercyclical. In Figure 3.4, we decompose the conditional variance of the loss rate in its contributions coming from v_t , p_t and n_t . The dominant source of variation is v_t but its relative importance drops in recessions when the relative importance of n_t increases, reaching almost 40% in the Great Recession. The p_t process has a negligible effect on the loss rate variance. Clearly, the loss rate variance has substantial independent variation not spanned by macro-economic uncertainty.

With the loss rate process estimated, the dynamics of the other cash flow state variables (earnings growth, the consumption earnings ratio and the payout ratio) follow straightforwardly. We can simply use linear projections of the variables onto previously identified state variables and shocks. The results are contained in Table 3.3. Earnings growth is less persistent than the two ratio variables. All variables load positively on industrial production growth but the coefficients are not statistically significant. The n_t state variable has a positive effect on the conditional mean of the consumption-earnings and dividend-earnings ratio, indicating that in recessions these ratios are expected to be larger than in normal times. This makes economic sense as consumption and dividends are likely smoothed over the cycle whereas earnings are particularly cycle sensitive (see also Longstaff and Piazzesi, 2004). The same intuition explains why the ratio variables load positively on ω_n shocks and earnings growth loads negatively on this shock. The

ω_p and ω_l shocks do not have a significant effect on these state variables.

The projections implicitly define the variable specific shocks, which are assumed (and demonstrated, see Footnote 1) to be homoskedastic. Table 3.3 indicates that they still feature substantial and significant variability. We do not impose any correlation structure on these shocks, and Table 3.4 shows that they are quite correlated. Essentially, because earnings growth is quite variable, the ratio variables are positively correlated with one another and negatively correlated with earnings growth. When we do asset pricing with the model, this correlation structure must be accounted for (see below). The correlations with the other state variable shocks and between these state variable shocks ($\omega_p, \omega_n, \omega_l$) ought to be zero in theory and the table shows that they are economically indeed close to zero.

3.5.2 Risk Aversion

Here we report results regarding the estimation process for risk aversion. Recall that we assume risk aversion to be spanned by 6 financial instruments. In Table 3.5, we report some properties of these financial instruments. First, all of them are highly persistent. This is the main reason we use a stochastically detrended dividend yield series ($AR(1)=0.982$) rather than the actual dividend yield series ($AR(1)=0.991$), which shows a secular decline over part of the sample that induces much autocorrelation. This decline is likely due to American tax policy and therefore not likely informative about risk aversion (see e.g. Boudoukh et.al, 2007). Second, the various instruments are positively correlated but the correlations never exceed 85% so that we should not worry about multi-collinearity. Perhaps surprisingly, the term spread is also positively correlated with the 5 other instruments, even though it is generally believed that high term spreads indicate good times, whereas the yield and variance instruments would tend to be high in bad times. Third, 4 of the instruments show significant positive skewness. This is critical as we have assumed that the risk aversion dynamics are positively skewed through its gamma distributed shock (see Equation (3.T29)), and we need the linear spanning model to be consistent with the assumed dynamics for risk aversion.

Table 3.6 reports the reduced form estimates in the spanning relation. The system esti-

mates 8 parameters with 37 moment conditions. The test of the over-identifying restrictions fails to reject but we investigate the fit of the model along various dimensions in more detail later. The significant determinants of the risk aversion process are the dividend yield, realized equity return and corporate bond return variances and the equity return risk neutral variance. The positive coefficient on the risk neutral and the negative coefficient on the physical realized equity return variances is consistent with the idea that the variance risk premium may be quite informative about risk aversion in financial markets (see also Bekaert and Hoerova, 2016). The implied risk aversion process shows a 0.40 correlation with the NBER indicator and is thus highly counter-cyclical.

In Table 3.7, we estimate the dynamic properties of the risk aversion process according to Equation (3.T27). All the parameters are estimated by OLS, except for the σ_{qq} parameter, which is delivered by the GMM estimation (see Section 3.3.3). The process shows moderate persistence (an autocorrelation coefficient of 0.63) but the conditional mean surprisingly shows a significant positive loading on p_t , which accounts for 77% of the variation in the conditional mean. Risk aversion shocks do not load significantly on the macro-economic uncertainty shocks and therefore most of their variation is driven by the risk aversion specific shock. It appears that economic models that impose a very tight link between aggregate fundamentals and risk aversion, such as pure habit models (Campbell and Cochrane, 1999) are missing important variation in actual risk aversion. In addition, risk aversion is much less persistent than the risk aversion implied by these models; the autocorrelation coefficient of the surplus ratio process in the CC model is 0.99 at the monthly level; the first-order autocorrelation coefficient of q_t derived in this paper is 0.63.

While the test of the over-identifying restrictions fails to reject, Table 3.8 examines in more detail how well the estimated dynamic system fits critical asset price moments in the data. The model over-estimates the equity premium but is still within one standard error of the data moment.⁷ In contrast, the corporate bond risk premium is under-estimated by about 2 standard

⁷Bootstrapped standard errors for the five asset price moments (equity risk premium, equity physical variance, equity risk-neutral variance, corporate bond risk premium, and corporate bond physical variance) use different block sizes to accommodate different serial auto-correlations, to ensure that the sampled blocks are approximately i.i.d.. In particular, Politis and Romano (1995) (and later discussed in Politis and White, 2004) suggest looking for the smallest integer after which the correlogram appears negligible, where the significance of the autocorrelation estimates is tested using the Ljung-Box Q Test (Ljung and Box, 1978).

errors relative to the data moment. The model implied variance moments are all quite close to their empirical counterparts. Finally, the table also reports the model-implied variance and unscaled skewness of the risk aversion innovation, $\sigma_{qq}^2 q_t$ and $2\sigma_{qq}^3 q_t$ (respectively).

Of all the asset return moments examined here, the only observed one is the risk neutral variance (the VIX index). Because we have filtered state variables, we can therefore compare how well this process fits the actual observed risk neutral variance at each point in time. Figure 3.5 graphs the empirical and model implied risk neutral variance. While the model fails to match the distinct spikes of the VIX in several crisis periods, the fit is remarkably good, with the correlation between the two series being 87.26%.

3.6 Risk Aversion, Uncertainty and Asset Prices

In this section, we first characterize the link between risk aversion and macroeconomic uncertainty, on the one hand and asset prices, on the other hand. We compare the time variation in risk aversion and macroeconomic uncertainty and document how our measures correlate with extant measures of uncertainty and risk aversion.

3.6.1 Risk Aversion, Macro-Economic Uncertainty and the First and Second Moments of Asset Returns

Figure 3.6 graphs the risk aversion process, which in our model is:

$$ra_t^{BEX} = \gamma \exp(q_t). \quad (3.T57)$$

The weak countercyclicality of the process is immediately apparent with risk aversion spiking in all three recessions, but also showing distinct peaks in other periods. The highest risk aversion of 11.58 is reached at the end of January in 2009, at the height of the Great Recession. But the risk aversion process also peaks in the October 1987 crash, the August 1998 crisis (Russia default and LTCM collapse), after the TMT bull market ended in August 2002 and in August 2011 (Euro

area debt crisis).

How important is risk aversion for asset prices? In this article’s model, the priced state variables for risk premiums and variances are those entering the conditional covariance between asset returns and the pricing kernel and therefore are limited to the risk aversion q_t , the macro-economic uncertainty state variables, p_t and n_t and the loss rate variability v_t . In Table 3.9, we report the loadings of risk premiums and variances on the 4 state variables. To help interpret these coefficients, we scaled the projection coefficients by the standard deviation of the state variables so that they can be interpreted as the response to a one standard deviation move in the state variable. For the equity premium, by far the most important state variable is q_t which has an effect more than 10 times larger than that of n_t . The effects of p_t and v_t are trivially small. The economic effect of a one standard deviation change in q_t is large representing 54 basis points at the monthly level (almost as high as the average equity premium). For the corporate bond premium, n_t and q_t are again the most important state variables, with n_t now generating the largest effect. A one standard deviation increase in n_t increases the corporate bond risk premium by 8 basis points at a monthly basis, about 1/3 of the average monthly premium. The coefficients for variances are somewhat harder to interpret, but n_t and q_t remain the most important state variables with the former (latter) more important for corporate bond (equity) variances. Because the relationship between asset prices and state variables is affine, we also compute a variance decomposition, coefficient $\times \frac{Cov(x_t, Mom_t)}{Var(Mom_t)}$ where $x \in \{p, n, v, q\}$ and Mom represents an asset price moment like the equity risk premium, or corporate bond physical variance. These variance proportions add up to one. In the model, 95% of the equity risk premium’s variance is driven by risk aversion; only 29% of the corporate bond risk premium is driven by risk aversion, while more than 70% is accounted for by “bad” macro-economic uncertainty. Similarly, the physical equity variance is predominantly driven by risk aversion (73%) while 99% of the corporate bond return’s physical variance is driven by bad macroeconomic uncertainty. Nevertheless, macro-economic uncertainty also accounts for 27% of the variance of the physical equity variance. It would be logical that the risk neutral variance would load more on risk aversion and less on macroeconomic uncertainty than the physical variance and this is indeed the case, with risk aversion accounting

for 87% of the variance of the risk neutral variance.

Bekaert, Hoerova and Lo Duca (2013) argue that the variance risk premium houses much information about risk aversion. Is this true in our model? To answer this question, we compute the model-implied variance risk premium as the difference between the risk neutral variance and the physical variance. A projection on the 4 state variables reveals that 97.4% of the variance of the variance risk premium is accounted for by risk aversion. Conversely, regressing risk aversion on the variance premium, the coefficient is 149.83 with a t-stat of 112.41, and the R^2 is 97.3%. Through the lens of our model, the variance premium is clearly a good proxy for risk aversion.

Finally, because the state variables perfectly explain conditional first and second moments of asset returns in the model, they should help predict realized returns and variances in the data. We test this in Table 3.10. We regress realized monthly excess returns and variances in both the equity and corporate bond markets on 1) the 4 state variables, or 2) the model-implied conditional moment (either the conditional risk premium or the conditional variance). Not imposing the model restrictions on how the state variables combine to the model implied conditional moment, only slightly decreases the adjusted R^2 , except for equity returns where the R^2 decreases from 5.6% to 0.1%. In this case, the coefficient on the model implied moment is about 0.67 and not significantly different from 1, but it is borderline significantly different from zero. For corporate bond risk premiums, the coefficient is higher than 1, and not significantly different from one. Not surprisingly, the R^2 s are higher for the realized equity and corporate bond variances hovering around 21–22%. The coefficients on the model-implied conditional moments are too high mostly because we under-estimate the conditional variances. When investigating the coefficients of individual state variables, risk aversion significantly predicts both returns and both realized variances. Bad economic uncertainty predicts the realized variances and equity returns, but not bond returns. The loss rate variance only significantly predicts bond return variances. The last line reports correlations of the implied risk premiums (the fitted values) with the NBER recession indicator, showing all of them to be significantly countercyclical.

Given the vast literature on return predictability, it is informative to contrast the predictive power of our model implied premiums with the predictive power of the usual instruments

used in the literature. We do this exercise out of sample as the literature has shown huge biases due to in sample over-fitting (Goyal and Welch, 2008). Our model premium candidates are either derived from a projection of excess returns on the 4 state variables (Model 2) or the actual model-implied risk premium (Model 1). We consider three empirical models, depending on the instruments used: 1) dividend yield, 2) dividend yield, term spread and credit spread, 3) physical uncertainty and variance risk premium estimate. These instruments are equity market centric and for corporate bond returns, we replace the physical uncertainty by the physical uncertainty derived from corporate bond returns. We then generate out-of-sample predictions for the risk premiums according to the various empirical models by starting the sample after five years of data and then running rolling samples to generate predictions from the five-year point to one month before the end of the sample. For the model implied risk premiums, Model 1 uses whatever the model predicts the premium to be. For Model 2, the projections are also conducted in a rolling fashion, but note that the construction of the state variables uses information from the full sample. With those competing risk premium estimates in hand, we then run simple horse races by estimating:

$$\tilde{r}_{t+1} - rf_t = a \text{ Mod}(t, i) + (1 - a) \text{ Emp Mod}(t, j) + e_{t+1}, \text{ for } i = 1, 2, j = 1, 2, 3. \quad (3.T58)$$

The results are reported in Table 3.11. For the model implied risk premiums (Model 1), the “ a ” coefficients are quite close to 1.0. Only when confronted with the empirical model facing the spread variables, is its coefficient significantly below 1.0 for the corporate bond risk premium. Model 2 fares less well, with the coefficients only being above 0.5 for the equity return regressions when the model is pitted against empirical models 2 and 3. We conclude that our model seems to capture the predictable variation better than the fitted values extracted from standard instruments used in the literature. While the model premium is not strictly out of sample, the model imposes numerous restrictions relative to the empirical models.

3.6.2 An Uncertainty Index

An advantage of the risk aversion process we estimated is that because of its dependence on financial instruments it can be computed at even a daily level. Unfortunately, our filtered macro-economic uncertainty variables were extracted from industrial production which is only available at the monthly level. Here we consider whether we can use the financial instruments to approximate macro uncertainty. First, total macro-economic uncertainty, the conditional variance of industrial production growth, is a function of both p_t and n_t , $\sigma_{\theta p}^2 p_t + \sigma_{\theta n}^2 n_t$ where the coefficient estimates of σ_p and σ_n are provided in Table 3.1. In Table 3.12, we show the coefficients from a regression of uncertainty on the financial instruments used to span risk aversion. The R^2 is almost 48% and uncertainty loads significantly on all instruments except for the realized equity variance. Unlike the risk aversion process, uncertainty loads very strongly on credit spreads and the physical corporate bond variance. The term spread also has a significant negative effect on uncertainty (and no effect on risk aversion). This makes sense as flattening yield curves are associated with future economic downturns. The table also reports regressions from the two components in macro-economic uncertainty, bad and good uncertainty, onto the instruments. Clearly, the variation in macro-economic uncertainty is dominated by the bad component and the coefficients for the bad component projection coefficients are very similar to those of total uncertainty. From this analysis, we create an uncertainty index which represents the part of total uncertainty that is explained by the financial instruments:

$$unc_t^{BEX} = \chi^{unc'} z_t. \quad (3.T59)$$

In Figure 3.7, we graph the financial instrument proxies to uncertainty and risk aversion for comparison. The correlation between actual uncertainty and risk aversion is 49%; when we use the proxy the correlation increases to 68%. Obviously, most of the time crisis periods feature both high uncertainty and high risk aversion. There are exceptions however. For example, the October 1987 crash happened during a time of relatively low economic uncertainty. It also appears that at the end of the 90s, macro-uncertainty seems to secularly increase, consistent with

the Great Moderation ending around that time (see also Baele et al., 2015).

Bloom (2009) has argued that uncertainty precedes bad economic outcomes. We regress future real industrial production growth at various horizons on our uncertainty index—its financial proxy and the actual one—and the risk aversion process. In addition, we use the VIX as suggested in Bloom (2009). The results are in Table 3.13. We use Hodrick (1992) standard errors to accommodate the overlap in the data. Panel A shows univariate results. All indices predict growth with a negative sign at the one month, one quarter and one year horizons. Our financial instrument uncertainty index generates the highest R^2 by far. This suggests that it is indeed macro uncertainty predicting output growth, with the VIX having much lower predictive power in univariate regressions. This result is confirmed in multivariate regressions. In Panel B, we use our risk aversion index (ra^{BEX}), financial uncertainty index (unc^{BEX}), and the VIX simultaneously. The financial uncertainty index comes in statistically significant for all horizons. Risk aversion (with a positive sign) and the VIX squared (with a negative sign) are only significant at the annual horizon. Thus, our uncertainty index dominates the VIX index in terms of its predictive power for real activity. Panel C shows that the financial uncertainty proxy also dominates the actual economic uncertainty (unc^{true}), which is only significant at the quarterly horizon.

3.6.3 Correlations with Extant Measures

In this section, we examine how correlated our risk aversion and uncertainty indices are with existing measures. For risk aversion, we consider three categories: risk aversion indices based on “fundamental” habit models, sentiment indices and commercially available risk aversions indices. For uncertainty, we focus on the recent uncertainty index developed by Jurado, Ludvigson and Ng (2015) and the Baker, Bloom and Davis (2016) political uncertainty measure.

Recall that in an external habit model such as Campbell and Cochrane (1999), the curvature of the utility function is a negative affine function of the log “consumption surplus ratio,” which in turns follows a heteroskedastic autoregressive process with shocks perfectly correlated with consumption growth. We follow Wachter (2006) and create a “fundamental” risk aversion process from consumption data and CC’s parameter estimates, which we denote by RA_{CC} . Ta-

ble 3.14 shows that it is only weakly correlated with our risk aversion measure but the correlation is still significantly different from zero. Clearly, the asset pricing literature should start accepting that risk aversion shows higher frequency movements inconsistent with the focus on low frequency changes tightly linked to consumption growth as in the extant habit models. Work by Bekaert, Engstrom and Grenadier (2010) and Martin (2017) also suggests the existence of more variable risk aversion in financial markets.

The behavioral finance literature suggests that the sentiment of retail investors may drive asset prices and cause non-fundamental price swings. As a well-known representative of this work, we use the sentiment index from Baker and Wurgler (2006). The index is based on the first principal component of six (standardized) sentiment proxies including: the closed-end fund discount, the NYSE share turnover, the number and the average first-day returns of IPOs, the share of equity issues in total equity and debt issues, and the dividend premium (the log-difference of the average market-to-book ratios of payers and nonpayers). We denote their index by $Sent_{BW}$. High values mean positive sentiment so we expect a negative correlation with our risk aversion indicator, and indeed the correlation is significantly negative but still relatively small at -0.16.

Because the Baker-Wurgler index relies on financial data, it may not directly reflect the sentiment of retail investors. Lemmon and Portnaiguina (2006) and Qiu and Welch (2006) therefore suggest using a consumer sentiment index such as the Michigan Consumer Sentiment Index (MCSI). The correlation with this index is also negative, as expected, and larger in absolute magnitude at -0.26; note that we obtain higher correlation with a pure consumer sentiment index than $Sent_{BW}$ derived from financial variables.

Finally, many financial services companies create their own risk appetite indices. As a well-known example, we obtained data on the Credit Suisse First Boston Risk Appetite Index (RAI). The indicator draws on the correlation between risk appetite and the relative performance of safe assets (proxied by seven to ten-year government bonds) and risky assets (equities and emerging market bonds). The underlying assumption is that an increasing risk preference shifts the demand from less risky investments to assets associated with higher risks, thus pushing their prices up relative to low-risk assets (and vice versa). The indicator is based on the cross-sectional

linear regression of excess returns of 64 international stock and bond indices on their risk, approximated by historic volatility. The slope of the regression line represents the risk appetite index. The index shows a -0.48 correlation with our index and is thus highly correlated with our concept of risk aversion.

Our uncertainty measure only uses industrial production data. Jurado, Ludvigson and Ng (2015) use the weighted sum of the conditional volatilities of 132 financial and macroeconomic series, with the bulk of them being macroeconomic. They have three versions of the measure depending on the forecasting horizon, but we focus on the one month horizon, which is most consistent with our model (MUC_{JLN}). The correlation with our uncertainty index is highly significant and substantial at 80%.

Macroeconomic uncertainty may be correlated with political uncertainty, which has recently been proposed as a source of asset market risk premiums (Pastor and Veronesi, 2013). Baker, Bloom and Davis (2016) create a policy uncertainty measure, based on newspaper coverage frequency, which we denote by UC_{BBD} . The index shows a highly significant correlation of 0.34 with our uncertainty index. One advantage of UC_{BBD} relative to the Jurado et al. (2015) measure is that it can also be computed at daily frequency. However, our financial proxy to uncertainty can also be computed at the daily frequency.

Monthly indices may hide important variation within the month in uncertainty and risk aversion. To demonstrate this, Figure 3.8 shows how the indices behaved around two critical events in the recent global financial crisis: the Bear Stearns collapse and bail out and the Lehman Brothers bankruptcy. In general, Bear Stearns' woes generated less effect on our measures than did Lehman Brothers, as expected. To be more specific, Figure 3.8 plots 2-month intervals of daily risk aversion indices (top plots) and daily financial uncertainty indices (bottom plots) around the two events. By the end of February and March 2008, the q_t index reached 0.57 and 0.44, respectively; the difference is small, considering the substantive time variation in the full sample. However, our daily risk aversion index climbed to 1 on March 16th, the day of Bear Stearns bailout. The uncertainty index also kept increasing until that day. Uncertainty and risk aversion drop steeply afterwards. During August and September 2008, both risk aversion

and uncertainty gradually increase, with q_t rising to above 1 on the day of Lehman Brothers' bankruptcy—which is the same value reached during Bear Stearns' collapse. However, as the magnification of the Lehman Brothers bankruptcy became clear to financial market participants, both risk aversion and uncertainty continues to rise, with q_t rising to 3.88 on October 10th which corresponds to the coordinated global action by central banks to lower interest rate.⁸

3.7 The Curious Case of Treasury Bond Markets

We only used risky asset classes to create the risk appetite index. Under the null of the model, the pricing kernel should price all asset returns. A very important asset class is Treasury bond returns. Given a process for inflation, it is straightforward to price Treasury bond returns with our model. It is also the case that for bonds returns we cannot only compute physical return variances, but also have risk neutral variances (see Data section). Therefore, we considered formally whether the different asset classes are “integrated,” meaning priced by the same pricing kernel. Interestingly, the term structure literature has a long tradition with “preferred habitat” theories, suggesting different clienteles and different pricing for different parts of the term structure (see also Guibaud, Nosbusch and Vayanos, 2013). However, for our purposes, the problem with considering Treasuries as determining general risk aversion is that they are often viewed as the benchmark “safe” assets and are subject to occasional flights-to safety (see Baele et al, 2017). This makes it ex-ante unlikely that a simple pricing model such as ours can jointly price the three assets classes.

To formally test this, we conduct two exercises. First, we simply use our pricing kernel derived from equity and corporate bond returns and test whether it can price bond returns and bond variance swaps. To be specific, market integration is tested by evaluating the fit of 3 bond return moments (risk premium, physical and risk-neutral variance) where the model-implied moments are priced by our pricing kernel. According to the test results in Table 3.15, we reject

⁸On October 8th, the Federal Reserve and the central banks of the EU, Canada, UK, Sweden and Switzerland cut their rates by half a point. China's central bank cut its rate by .27 of a point. This was done to lower LIBOR, thus lowering the cost of bank borrowing. Overnight bank lending rates dropped in response, indicating a potential turning point in the crisis. (Source: Guardian, “Global rate cuts helps ease overnight interbank rates,” October 8, 2008)

the market integration hypothesis because none of the Treasury bond market moments is within the 95% confidence intervals of the empirical point estimates.

Second, we created an “integrated” risk aversion process using asset moments from both risky (equity and corporate bond) and “safe” (Treasury bond) asset markets. To be more specific, we include two more instruments from the Treasury bond market to span the integrated risk aversion process: realized and risk-neutral Treasury bond return variances. In addition, we filter this risk aversion index using moments from risky and safe assets; thus, three asset moments are added to the GMM system: the risk premium, physical variance and risk-neutral variance of Treasury bonds. The resulting risk aversion index is negatively correlated with our risk aversion index (with a -0.157 correlation) and procyclical instead of countercyclical (with a -0.267 correlation with the NBER indicator).⁹ We conclude that the current model is inadequate to price Treasury bonds and their role in asset markets deserves more scrutiny.

3.8 Conclusion

We formulate a no arbitrage model where fundamentals such as industrial production, consumption earnings ratios, corporate loss rates, etc. follow dynamic processes that admit time-variation in both conditional variances and the shape of the shock distribution. The agent in the economy takes this time-varying uncertainty into account when pricing equity and corporate bonds, but also faces preference shocks imperfectly correlated with fundamentals. The state variables in the economy that drive risk premiums and higher order moments of asset prices involve risk aversion, good and bad economic uncertainty and the conditional variance of loss rates on corporate bonds. We use equity and corporate bond returns, physical equity and corporate bond return variances and the risk neutral equity variance to estimate the model parameters and simultaneously derive a risk aversion spanning process . Risk aversion is a function of 6 financial instruments, namely the term spread, credit spread, a detrended dividend yield, realized and risk-neutral equity return variance, and realized corporate bond return variance.

We find that risk aversion loads significantly and positively on the risk neutral equity vari-

⁹Detailed estimation results and time series are available upon requests.

ance and the realized corporate bond variance, and negatively on the realized equity return variance. Risk aversion is much less persistent than the risk aversion process implied by standard habit models. It is the main driver of the equity premium and the equity return risk neutral variance. It also accounts for 73% of the conditional variance of equity returns with the remainder accounted for by bad macro uncertainty. These proportions are reversed for the corporate bond risk premium and the corporate bond physical variance is almost entirely driven by bad macro uncertainty. Hence, different asset markets reflect differential information about risk appetite versus economic uncertainty. Our model-implied risk premiums beat standard predictors of equity and corporate bond returns in an out-of-sample horse race.

While our risk aversion measure is correlated with some existing risk appetite and sentiment indices, the simplest approximation may be the variance risk premium in equity markets which is 98.7% correlated with our risk appetite index.

Because the spanning instruments are financial data, we can track the risk aversion index at higher frequencies. Similarly, we obtain a financial proxy to economic uncertainty (the conditional variance of industrial production growth) which can be obtained at the daily frequency as well. This measure is 80% correlated with the well-known Jurado, Ludvigson and Ng (2015) measure, extracted from macro data. The financial proxy to economic uncertainty predicts output growth negatively and significantly and is a much stronger predictor of output growth than is the VIX. We plan to make both our risk aversion and uncertainty indices available on our websites and update them regularly, which could potentially be useful for both academic researchers and practitioners.

Appendices

3.A The state variables

3.A.1 Matrix representation of the state variables

In this section, we show the matrix representation of the system of ten state variables in this economy. The ten state variables, as introduced in Section 3, are as follows,

$$\mathbf{Y}_t = [\theta_t, p_t, n_t, \pi_t, l_t, g_t, \kappa_t, \eta_t, v_t, q_t]',$$

where $\{p_t, n_t\}$ denote the upside uncertainty factor and the downside uncertainty factor, as latent variables extracted from the system of output growth (i.e., change in log real industrial production index); π_t represents the inflation rate; l_t represents the log of corporate loss rate; g_t represents the log change in real earnings; κ_t represents the log consumption-earnings ratio; η_t represents the log dividend payout ratio; v_t represents the cash flow uncertainty factor, as the latent variable extracted from the system of corporate loss rate l_t ; q_t represents the latent risk aversion of the economy. The state variables have the following matrix representation:

$$\mathbf{Y}_{t+1} = \boldsymbol{\mu} + \mathbf{A}\mathbf{Y}_t + \boldsymbol{\Sigma}\boldsymbol{\omega}_{t+1}, \quad (3.T60)$$

where $\boldsymbol{\omega}_{t+1} = [\omega_{p,t+1}, \omega_{n,t+1}, \omega_{\pi,t+1}, \omega_{l,t+1}, \omega_{g,t+1}, \omega_{\kappa,t+1}, \omega_{\eta,t+1}, \omega_{q,t+1}]$ (8×1) is a vector comprised of eight independent shocks in the economy. Among the eight shocks, the conditional variance, skewness and higher-order moments of the following four centered gamma shocks— $\omega_{p,t+1}$, $\omega_{n,t+1}$, $\omega_{l,t+1}$, and $\omega_{q,t+1}$ —are assumed to be proportional to p_t , n_t , v_t , and q_t respectively. The underlying distributions for the rest four shocks are assumed to be Gaussian with unit standard deviation.

The constant matrices are defined implicitly,

$$\boldsymbol{\mu} = \begin{bmatrix} (1 - \rho_\theta)\bar{\theta} - m_p\bar{p} - m_n\bar{n} \equiv \theta_0 \\ (1 - \rho_p)\bar{p} \equiv p_0 \\ (1 - \rho_n)\bar{n} \equiv n_0 \\ \pi_0 \\ l_0 \\ g_0 \\ \kappa_0 \\ \eta_0 \\ v_0 \\ q_0 \end{bmatrix}, \quad (3.T61)$$

$$\mathbf{A} = \begin{bmatrix} \rho_\theta & m_p & m_n & 0 & 0 & 0 & 0 & 0 & 0 & 0 \\ 0 & \rho_p & 0 & 0 & 0 & 0 & 0 & 0 & 0 & 0 \\ 0 & 0 & \rho_n & 0 & 0 & 0 & 0 & 0 & 0 & 0 \\ \rho_{\pi\theta} & \rho_{\pi p} & \rho_{\pi n} & \rho_{\pi\pi} & 0 & 0 & 0 & 0 & 0 & 0 \\ 0 & \rho_{lp} & \rho_{ln} & 0 & \rho_{ll} & 0 & 0 & 0 & 0 & 0 \\ \rho_{g\theta} & \rho_{gp} & \rho_{gn} & 0 & 0 & \rho_{gg} & 0 & 0 & 0 & 0 \\ \rho_{\kappa\theta} & \rho_{\kappa p} & \rho_{\kappa n} & 0 & 0 & 0 & \rho_{\kappa\kappa} & 0 & 0 & 0 \\ \rho_{\eta\theta} & \rho_{\eta p} & \rho_{\eta n} & 0 & 0 & 0 & 0 & \rho_{\eta\eta} & 0 & 0 \\ 0 & 0 & 0 & 0 & 0 & 0 & 0 & 0 & \rho_{vv} & 0 \\ 0 & \rho_{qp} & \rho_{qn} & 0 & 0 & 0 & 0 & 0 & 0 & \rho_{qq} \end{bmatrix}, \quad (3.T62)$$

$$\boldsymbol{\Sigma} = \begin{bmatrix} \sigma_{\theta p} & -\sigma_{\theta n} & 0 & 0 & 0 & 0 & 0 & 0 & 0 \\ \sigma_{pp} & 0 & 0 & 0 & 0 & 0 & 0 & 0 & 0 \\ 0 & \sigma_{nn} & 0 & 0 & 0 & 0 & 0 & 0 & 0 \\ \sigma_{\pi p} & \sigma_{\pi n} & \sigma_{\pi\pi} & 0 & 0 & 0 & 0 & 0 & 0 \\ \sigma_{lp} & \sigma_{ln} & 0 & \sigma_{ll} & 0 & 0 & 0 & 0 & 0 \\ \sigma_{gp} & \sigma_{gn} & 0 & \sigma_{gl} & \sigma_{gg} & 0 & 0 & 0 & 0 \\ \sigma_{\kappa p} & \sigma_{\kappa n} & 0 & \sigma_{\kappa l} & 0 & \sigma_{\kappa\kappa} & 0 & 0 & 0 \\ \sigma_{\eta p} & \sigma_{\eta n} & 0 & \sigma_{\eta l} & 0 & 0 & \sigma_{\eta\eta} & 0 & 0 \\ 0 & 0 & 0 & \sigma_{vl} & 0 & 0 & 0 & 0 & 0 \\ \sigma_{qp} & \sigma_{qn} & 0 & 0 & 0 & 0 & 0 & 0 & \sigma_{qq} \end{bmatrix}. \quad (3.T63)$$

Given the moment generating functions (mgf) of gamma and Gaussian distributions, we show that the model is affine, $\forall \boldsymbol{\nu} \in \mathbb{R}^{10}$,

$$\begin{aligned} M_Y(\boldsymbol{\nu}) &:= E_t [\exp(\boldsymbol{\nu}'\mathbf{Y}_{t+1})] = \exp(\boldsymbol{\nu}'\boldsymbol{\mu} + \boldsymbol{\nu}'\mathbf{A}\mathbf{Y}_t) E_t [\exp(\boldsymbol{\nu}'\boldsymbol{\Sigma}\boldsymbol{\omega}_{t+1})] \\ &= \exp \left[\boldsymbol{\nu}'\mathbf{S}_0 + \frac{1}{2}\boldsymbol{\nu}'\mathbf{S}_1\boldsymbol{\Sigma}^{other}\mathbf{S}'_1\boldsymbol{\nu} + \mathbf{f}_S(\boldsymbol{\nu})\mathbf{Y}_t \right], \end{aligned} \quad (3.T64)$$

where $\mathbf{S}_0 = \boldsymbol{\mu}$ (10×1),

$$\mathbf{S}_1 = \begin{bmatrix} 0 & 0 & 0 & 0 \\ 0 & 0 & 0 & 0 \\ 0 & 0 & 0 & 0 \\ 1 & 0 & 0 & 0 \\ 0 & 0 & 0 & 0 \\ 0 & 1 & 0 & 0 \\ 0 & 0 & 1 & 0 \\ 0 & 0 & 0 & 1 \\ 0 & 0 & 0 & 0 \\ 0 & 0 & 0 & 0 \end{bmatrix}, \quad (3.T65)$$

$$\boldsymbol{\Sigma}^{other} = \begin{bmatrix} \sigma_{\pi\pi}^2 & \sigma_{\pi g} & \sigma_{\pi\kappa} & \sigma_{\pi\eta} \\ \sigma_{g\pi} & \sigma_{gg}^2 & \sigma_{g\kappa} & \sigma_{g\eta} \\ \sigma_{\kappa\pi} & \sigma_{\kappa g} & \sigma_{\kappa\kappa}^2 & \sigma_{\kappa\eta} \\ \sigma_{\eta\pi} & \sigma_{\eta g} & \sigma_{\eta\kappa} & \sigma_{\eta\eta}^2 \end{bmatrix} \quad (\text{cov-var matrix of } \{\omega_\pi, \omega_g, \omega_\kappa, \omega_\eta\}), \quad (3.T66)$$

$$\mathbf{f}_S(\boldsymbol{\nu}) = \boldsymbol{\nu}' \mathbf{A} + \begin{bmatrix} 0 \\ -\sigma_p(\boldsymbol{\nu}) - \ln(1 - \sigma_p(\boldsymbol{\nu})) \\ -\sigma_n(\boldsymbol{\nu}) - \ln(1 - \sigma_n(\boldsymbol{\nu})) \\ 0 \\ 0 \\ 0 \\ 0 \\ -\sigma_v(\boldsymbol{\nu}) - \ln(1 - \sigma_v(\boldsymbol{\nu})) \\ -\sigma_q(\boldsymbol{\nu}) - \ln(1 - \sigma_q(\boldsymbol{\nu})) \end{bmatrix}', \quad (3.T67)$$

$$\sigma_p(\boldsymbol{\nu}) = \boldsymbol{\nu}' \boldsymbol{\Sigma}_{\bullet 1}, \quad (3.T68)$$

$$\sigma_n(\boldsymbol{\nu}) = \boldsymbol{\nu}' \boldsymbol{\Sigma}_{\bullet 2}, \quad (3.T69)$$

$$\sigma_v(\boldsymbol{\nu}) = \boldsymbol{\nu}' \boldsymbol{\Sigma}_{\bullet 4}, \quad (3.T70)$$

$$\sigma_q(\boldsymbol{\nu}) = \boldsymbol{\nu}' \boldsymbol{\Sigma}_{\bullet 8}, \quad (3.T71)$$

where $\mathbf{M}_{\bullet j}$ denotes the j -th column of the matrix \mathbf{M} .

3.A.2 Consumption growth

Consumption growth in this economy is endogenous defined and can be expressed in an affine function:

$$\Delta c_{t+1} = g_{t+1} + \Delta \kappa_{t+1} \quad (3.T72)$$

$$= c_0 + \mathbf{c}'_2 \mathbf{Y}_t + \mathbf{c}'_1 \boldsymbol{\Sigma} \boldsymbol{\omega}_{t+1}, \quad (3.T73)$$

$$(3.T74)$$

where $c_0 = g_0 + \kappa_0$, $\mathbf{c}_1 = [0 \ 0 \ 0 \ 0 \ 0 \ 1 \ 1 \ 0 \ 0 \ 0]'$, and

$$\mathbf{c}_2 = \begin{bmatrix} \rho_{g\theta} + \rho_{\kappa\theta} \\ \rho_{gp} + \rho_{\kappa p} \\ \rho_{gn} + \rho_{\kappa n} \\ 0 \\ 0 \\ \rho_{gg} \\ \rho_{\kappa\kappa} - 1 \\ 0 \\ 0 \\ 0 \end{bmatrix}. \quad (3.T75)$$

3.B Asset Pricing

In this section, we solve the model analytically. First, given consumption growth and changes in risk aversion, the log of real pricing kernel of the economy is derived as an affine function of the state variables. Next, we show that asset prices of claims on cash flows from three different asset markets can be expressed in (quasi) affine equations. The model is solved using the non-arbitrage condition. The goal of this section is to derive the analytical solutions for the expected excess returns, the physical variance of asset returns and the risk-neutral variance of asset returns in closed forms. The implied moments are crucial for the estimation procedure.

3.B.1 The real pricing kernel

The log real pricing kernel for this economy is given by,

$$m_{t+1} = \ln(\beta) - \gamma\Delta c_{t+1} + \gamma\Delta q_{t+1} \quad (3.T76)$$

$$= m_0 + \mathbf{m}'_2 \mathbf{Y}_t + \mathbf{m}'_1 \boldsymbol{\Sigma} \boldsymbol{\omega}_{t+1}, \quad (3.T77)$$

where $m_0 = \ln(\beta) + \gamma(q_0 - g_0 - \kappa_0)$, $\mathbf{m}_1 = [0 \ 0 \ 0 \ 0 \ 0 \ -\gamma \ -\gamma \ 0 \ 0 \ \gamma]'$, and

$$\mathbf{m}_2 = \begin{bmatrix} \gamma(-\rho_{g\theta} - \rho_{\kappa\theta}) \\ \gamma(\rho_{qp} - \rho_{gp} - \rho_{\kappa p}) \\ \gamma(\rho_{qn} - \rho_{gn} - \rho_{\kappa n}) \\ 0 \\ 0 \\ -\gamma\rho_{gg} \\ -\gamma(\rho_{\kappa\kappa} - 1) \\ 0 \\ 0 \\ \gamma(\rho_{qq} - 1) \end{bmatrix}. \quad (3.T78)$$

As a result, the moment generating function of the real pricing kernel is, $\forall \nu \in \mathbb{R}$,

$$\begin{aligned}
E_t[\exp(\nu m_{t+1})] &= \exp[\nu m_0 + \nu \mathbf{m}'_2 \mathbf{Y}_t] \\
&\cdot \exp\{[-\nu \sigma_p(\mathbf{m}_1) - \ln(1 - \nu \sigma_p(\mathbf{m}_1))] p_t + [-\nu \sigma_n(\mathbf{m}_1) - \ln(1 - \nu \sigma_n(\mathbf{m}_1))] n_t\} \\
&\cdot \exp\{[-\nu \sigma_v(\mathbf{m}_1) - \ln(1 - \nu \sigma_v(\mathbf{m}_1))] v_t + [-\nu \sigma_q(\mathbf{m}_1) - \ln(1 - \nu \sigma_q(\mathbf{m}_1))] q_t\} \\
&\cdot \exp\left\{\frac{1}{2} \nu^2 \left[\mathbf{m}'_1 \mathbf{S}_1 \Sigma^{other} \mathbf{S}'_1 \mathbf{m}_1 \right]\right\}, \tag{3.T79}
\end{aligned}$$

where m_0 , \mathbf{m}_1 , \mathbf{m}_2 , \mathbf{S}_1 , and Σ^{other} are constant matrices defined earlier, and

$$\sigma_p(\mathbf{m}_1) = \mathbf{m}'_1 \Sigma_{\bullet 1}, \tag{3.T80}$$

$$\sigma_n(\mathbf{m}_1) = \mathbf{m}'_1 \Sigma_{\bullet 2}, \tag{3.T81}$$

$$\sigma_v(\mathbf{m}_1) = \mathbf{m}'_1 \Sigma_{\bullet 4}, \tag{3.T82}$$

$$\sigma_q(\mathbf{m}_1) = \mathbf{m}'_1 \Sigma_{\bullet 8}. \tag{3.T83}$$

Accordingly, the model-implied short rate $r f_t$ is,

$$r f_t = -\ln\{E_t[\exp(m_{t+1})]\} \tag{3.T84}$$

$$= -m_0 - \mathbf{m}'_2 \mathbf{Y}_t \tag{3.T85}$$

$$+ [\sigma_p(\mathbf{m}_1) + \ln(1 - \sigma_p(\mathbf{m}_1))] p_t + [\sigma_n(\mathbf{m}_1) + \ln(1 - \sigma_n(\mathbf{m}_1))] n_t \tag{3.T86}$$

$$+ [\sigma_v(\mathbf{m}_1) + \ln(1 - \sigma_v(\mathbf{m}_1))] v_t + [\sigma_q(\mathbf{m}_1) + \ln(1 - \sigma_q(\mathbf{m}_1))] q_t \tag{3.T87}$$

$$- \frac{1}{2} \left[\mathbf{m}'_1 \mathbf{S}_1 \Sigma^{other} \mathbf{S}'_1 \mathbf{m}_1 \right], \tag{3.T88}$$

$$= r f_0 + \mathbf{r} \mathbf{f}'_2 \mathbf{Y}_t. \tag{3.T89}$$

To price nominal assets, we define the nominal pricing kernel, \tilde{m}_{t+1} , which is a simple transformation of the log real pricing kernel, m_{t+1} ,

$$\tilde{m}_{t+1} = m_{t+1} - \pi_{t+1}, \tag{3.T90}$$

$$= \tilde{m}_0 + \tilde{\mathbf{m}}'_2 \mathbf{Y}_t + \tilde{\mathbf{m}}'_1 \Sigma \omega_{t+1}, \tag{3.T91}$$

where $\tilde{m}_0 = m_0 - \pi_0$, $\tilde{\mathbf{m}}_1 = \mathbf{m}_1 - [0 \ 0 \ 0 \ 1 \ 0 \ 0 \ 0 \ 0 \ 0 \ 0]'$, and

$$\tilde{\mathbf{m}}_2 = \mathbf{m}_2 - \begin{bmatrix} \rho_{\pi\theta} \\ \rho_{\pi p} \\ \rho_{\pi n} \\ \rho_{\pi\pi} \\ 0 \\ 0 \\ 0 \\ 0 \\ 0 \\ 0 \end{bmatrix}. \tag{3.T92}$$

The nominal risk free rate $\tilde{r} f_t$ is defined as $-\ln\{E_t[\exp(\tilde{m}_{t+1})]\}$.

3.B.2 Valuation ratio

It is a crucial step in this paper to show that asset prices are (quasi) affine functions of the state variables. It is especially not obvious for equity price-dividend ratio, of which we provide proofs below. First, we rewrite the real dividend growth in a general matrix expression:

$$\begin{aligned}\Delta d_{t+1} &= g_{t+1} + \Delta \eta_{t+1} \\ &= h_0 + \mathbf{h}'_2 \mathbf{Y}_t + \mathbf{h}'_1 \Sigma \boldsymbol{\omega}_{t+1},\end{aligned}\tag{3.T93}$$

where $h_0 = g_0 + \eta_0$, $\mathbf{h}_1 = [0 \ 0 \ 0 \ 0 \ 0 \ 1 \ 0 \ 1 \ 0 \ 0]'$, and

$$\mathbf{h}_2 = \begin{bmatrix} \rho_{g\theta} + \rho_{\eta\theta} \\ \rho_{gp} + \rho_{\eta p} \\ \rho_{gm} + \rho_{\eta m} \\ 0 \\ 0 \\ \rho_{gg} \\ 0 \\ \rho_{\eta\eta} - 1 \\ 0 \\ 0 \end{bmatrix}.\tag{3.T94}$$

The price-dividend ratio, $PD_t = E_t \left[M_{t+1} \left(\frac{P_{t+1} + D_{t+1}}{D_t} \right) \right]$, can be rewritten as,

$$PD_t = \sum_{n=1}^{\infty} E_t \left[\exp \left(\sum_{j=1}^n m_{t+j} + \Delta d_{t+j} \right) \right].\tag{3.T95}$$

Let F_t^n denote the n -th term in the summation:

$$F_t^n = E_t \left[\exp \left(\sum_{j=1}^n m_{t+j} + \Delta d_{t+j} \right) \right],\tag{3.T96}$$

and $F_t^n D_t$ is the price of zero-coupon equity that matures in n periods.

To show that equity price is an approximate affine function of the state variables, we first prove that $F_t^n (\forall n \geq 1)$ is exactly affine using induction. First, when $n = 1$,

$$\begin{aligned}F_t^1 &= E_t [\exp (m_{t+1} + \Delta d_{t+1})] \\ &= E_t \{ \exp [(m_0 + h_0) + (\mathbf{m}'_2 + \mathbf{h}'_2) \mathbf{Y}_t + (\mathbf{m}'_1 + \mathbf{h}'_1) \Sigma \boldsymbol{\omega}_{t+1}] \} \\ &= \exp [(m_0 + h_0) + (\mathbf{m}'_2 + \mathbf{h}'_2) \mathbf{Y}_t] \\ &\quad \cdot \exp \{ [-\sigma_p(\mathbf{m}_1 + \mathbf{h}_1) - \ln(1 - \sigma_p(\mathbf{m}_1 + \mathbf{h}_1))] p_t + [-\sigma_n(\mathbf{m}_1 + \mathbf{h}_1) - \ln(1 - \sigma_n(\mathbf{m}_1 + \mathbf{h}_1))] n_t \} \\ &\quad \cdot \exp \{ [-\sigma_v(\mathbf{m}_1 + \mathbf{h}_1) - \ln(1 - \sigma_v(\mathbf{m}_1 + \mathbf{h}_1))] v_t + [-\sigma_q(\mathbf{m}_1 + \mathbf{h}_1) - \ln(1 - \sigma_q(\mathbf{m}_1 + \mathbf{h}_1))] q_t \} \\ &\quad \cdot \exp \left\{ \frac{1}{2} [(\mathbf{m}'_1 + \mathbf{h}'_1) \mathbf{S}_1 \Sigma^{other} \mathbf{S}'_1 (\mathbf{m}_1 + \mathbf{h}_1)] \right\} \\ &= \exp (e_0^1 + \mathbf{e}_1^1 \mathbf{Y}_t),\end{aligned}\tag{3.T97}$$

where m_0 , \mathbf{m}_1 , \mathbf{m}_2 , h_0 , \mathbf{h}_1 , \mathbf{h}_2 , \mathbf{S}_1 , and Σ^{other} are constant matrices defined earlier, and

$$\sigma_p(\mathbf{m}_1 + \mathbf{h}_1) = (\mathbf{m}'_1 + \mathbf{h}'_1)\Sigma_{\bullet 1}, \quad (3.T98)$$

$$\sigma_n(\mathbf{m}_1 + \mathbf{h}_1) = (\mathbf{m}'_1 + \mathbf{h}'_1)\Sigma_{\bullet 2}, \quad (3.T99)$$

$$\sigma_v(\mathbf{m}_1 + \mathbf{h}_1) = (\mathbf{m}'_1 + \mathbf{h}'_1)\Sigma_{\bullet 4}, \quad (3.T100)$$

$$\sigma_q(\mathbf{m}_1 + \mathbf{h}_1) = (\mathbf{m}'_1 + \mathbf{h}'_1)\Sigma_{\bullet 8}, \quad (3.T101)$$

and $e_0^1 = m_0 + h_0 + \frac{1}{2} [(\mathbf{m}'_1 + \mathbf{h}'_1)\mathbf{S}_1\Sigma^{other}\mathbf{S}'_1(\mathbf{m}_1 + \mathbf{h}_1)]$, and

$$e_1^1 = \mathbf{m}_2 + \mathbf{h}_2 + \begin{bmatrix} 0 \\ -\sigma_p(\mathbf{m}_1 + \mathbf{h}_1) - \ln(1 - \sigma_p(\mathbf{m}_1 + \mathbf{h}_1)) \\ -\sigma_n(\mathbf{m}_1 + \mathbf{h}_1) - \ln(1 - \sigma_n(\mathbf{m}_1 + \mathbf{h}_1)) \\ 0 \\ 0 \\ 0 \\ 0 \\ 0 \\ -\sigma_v(\mathbf{m}_1 + \mathbf{h}_1) - \ln(1 - \sigma_v(\mathbf{m}_1 + \mathbf{h}_1)) \\ -\sigma_q(\mathbf{m}_1 + \mathbf{h}_1) - \ln(1 - \sigma_q(\mathbf{m}_1 + \mathbf{h}_1)) \end{bmatrix}. \quad (3.T102)$$

Now, suppose that the $(n-1)$ -th term $F_t^{n-1} = \exp(e_0^{n-1} + \mathbf{e}_1^{n-1'}\mathbf{Y}_t)$, then

$$\begin{aligned} F_t^n &= E_t \left[\exp \left(\sum_{j=1}^n m_{t+j} + \Delta d_{t+j} \right) \right] \\ &= E_t \left\{ E_{t+1} \left[\exp(m_{t+1} + \Delta d_{t+1}) \exp \left(\sum_{j=1}^{n-1} m_{t+j+1} + \Delta d_{t+j+1} \right) \right] \right\} \\ &= E_t \left\{ \exp(m_{t+1} + \Delta d_{t+1}) \underbrace{E_{t+1} \left[\exp \left(\sum_{j=1}^{n-1} m_{t+j+1} + \Delta d_{t+j+1} \right) \right]}_{F_{t+1}^{n-1}} \right\} \\ &= E_t \left[\exp(m_{t+1} + \Delta d_{t+1}) \exp(e_0^{n-1} + \mathbf{e}_1^{n-1'}\mathbf{Y}_{t+1}) \right] \\ &= \exp(e_0^n + \mathbf{e}_1^{n'}\mathbf{Y}_t), \end{aligned} \quad (3.T103)$$

where e_0^n and $\mathbf{e}_1^{n'}$ are defined implicitly.

Hence, the price-dividend ratio is approximately affine:

$$\begin{aligned}
PD_t &= \sum_{n=1}^{\infty} E_t \left[\exp \left(\sum_{j=1}^n m_{t+j} + \Delta d_{t+j} \right) \right] \\
&= \sum_{n=1}^{\infty} F_t^n \\
&= \sum_{n=1}^{\infty} \exp (e_0^n + \mathbf{e}_1^{n'} \mathbf{Y}_t). \tag{3.T104}
\end{aligned}$$

■

3.B.3 Log nominal equity return

We apply first-order Taylor approximations to the log nominal equity return, and obtain a linear system,

$$\begin{aligned}
\tilde{r}_{t+1}^{eq} &= \ln \left(\frac{P_{t+1} + D_{t+1}}{P_t} \Pi_{t+1} \right) \\
&= \ln \left(\frac{PD_{t+1} + 1}{PD_t} \right) \ln \left(\frac{D_{t+1}}{D_t} \right) \ln (\Pi_{t+1}) \\
&= \Delta d_{t+1} + \pi_{t+1} + \ln \left[\frac{1 + \sum_{n=1}^{\infty} \exp (e_0^n + \mathbf{e}_1^{n'} \mathbf{Y}_{t+1})}{\sum_{n=1}^{\infty} \exp (e_0^n + \mathbf{e}_1^{n'} \mathbf{Y}_t)} \right] \\
&\approx \Delta d_{t+1} + \pi_{t+1} + \text{const.} + \frac{\sum_{n=1}^{\infty} \exp (e_0^n + \mathbf{e}_1^{n'} \bar{\mathbf{Y}}) \mathbf{e}_1^{n'}}{1 + \sum_{n=1}^{\infty} \exp (e_0^n + \mathbf{e}_1^{n'} \bar{\mathbf{Y}})} \mathbf{Y}_{t+1} - \frac{\sum_{n=1}^{\infty} \exp (e_0^n + \mathbf{e}_1^{n'} \bar{\mathbf{Y}}) \mathbf{e}_1^{n'}}{\sum_{n=1}^{\infty} \exp (e_0^n + \mathbf{e}_1^{n'} \bar{\mathbf{Y}})} \mathbf{Y}_t \\
&= \tilde{\xi}_0^{eq} + \tilde{\xi}_1^{eq'} \mathbf{Y}_t + \tilde{\mathbf{r}}^{eq'} \boldsymbol{\Sigma} \boldsymbol{\omega}_{t+1}, \tag{3.T105}
\end{aligned}$$

where \tilde{r}_{t+1}^{eq} is the log *nominal* return of asset i from t to $t + 1$, $\tilde{\xi}_0^{eq}$ is constant, $\tilde{\xi}_1^{eq}$ is a vector of state vector coefficients, and $\tilde{\mathbf{r}}^{eq}$ is a vector of shock coefficients. Thus, this step involves linear approximation.

More generally, to acknowledge the errors that are potentially caused by the linear approximations (the Taylor approximation in log price-dividend ratio in the return equation), we write down the return innovations for asset i with an idiosyncratic shock:

$$\tilde{r}_{t+1}^i - E_t (\tilde{r}_{t+1}^i) = \tilde{\mathbf{r}}^{i'} \boldsymbol{\Sigma} \boldsymbol{\omega}_{t+1} + \varepsilon_{t+1}^i, \tag{3.T106}$$

where $E_t (\tilde{r}_{t+1}^i)$ is the expected return, $\tilde{\mathbf{r}}^i$ (10×1) is the asset i return loadings on selected state variable innovations (the choice of which depends on the asset classes), and ε_{t+1}^i is the Gaussian noise uncorrelated with the state variable shocks but may be cross-correlated (with other asset-specific shocks). The Gaussian shock ε_{t+1}^i has an unconditional variance σ_i^2 .

3.B.4 Model-implied moments

In this section, we derive three model-implied asset conditional moments— expected excess returns, physical and risk-neutral conditional variances of nominal asset returns. The moments

are crucial in creating the moment conditions during the third step of model estimation.

3.B.4.1 One-period expected excess return

We impose the no-arbitrage condition, $1 = E_t[\exp(\tilde{m}_{t+1} + \tilde{r}_{t+1}^i)]$ ($\forall i \in \{\text{equity, treasury bond, corporate bond}\}$), and obtain the expected excess returns. Expand the law of one price (LOOP) equation:

$$\begin{aligned}
1 &= E_t[\exp(\tilde{m}_{t+1} + \tilde{r}_{t+1}^i)] \\
&= \exp \left[E_t(\tilde{m}_{t+1}) + E_t(\tilde{r}_{t+1}^i) \right] \\
&\cdot \exp \left\{ \left[-\sigma_p(\tilde{\mathbf{m}}_1 + \tilde{\mathbf{r}}^i) - \ln \left(1 - \sigma_p(\tilde{\mathbf{m}}_1 + \tilde{\mathbf{r}}^i) \right) \right] p_t + \left[-\sigma_n(\tilde{\mathbf{m}}_1 + \tilde{\mathbf{r}}^i) - \ln \left(1 - \sigma_n(\tilde{\mathbf{m}}_1 + \tilde{\mathbf{r}}^i) \right) \right] n_t \right\} \\
&\cdot \exp \left\{ \left[-\sigma_v(\tilde{\mathbf{m}}_1 + \tilde{\mathbf{r}}^i) - \ln \left(1 - \sigma_v(\tilde{\mathbf{m}}_1 + \tilde{\mathbf{r}}^i) \right) \right] v_t + \left[-\sigma_q(\tilde{\mathbf{m}}_1 + \tilde{\mathbf{r}}^i) - \ln \left(1 - \sigma_q(\tilde{\mathbf{m}}_1 + \tilde{\mathbf{r}}^i) \right) \right] q_t \right\} \\
&\cdot \exp \left\{ \frac{1}{2} \left[(\tilde{\mathbf{m}}_1' + \tilde{\mathbf{r}}^{i'}) \mathbf{S}_1 \boldsymbol{\Sigma}^{other} \mathbf{S}_1' (\tilde{\mathbf{m}}_1 + \tilde{\mathbf{r}}^i) + \sigma_i^2 \right] \right\}, \tag{3.T107}
\end{aligned}$$

where $\tilde{\mathbf{m}}_1$, $\tilde{\mathbf{r}}^i$, σ_i , \mathbf{S}_1 , and $\boldsymbol{\Sigma}^{other}$ are constant matrices defined earlier, and

$$\begin{aligned}
\sigma_p(\tilde{\mathbf{m}}_1 + \tilde{\mathbf{r}}^i) &= (\tilde{\mathbf{m}}_1' + \tilde{\mathbf{r}}^{i'}) \boldsymbol{\Sigma}_{\bullet 1}, \\
\sigma_n(\tilde{\mathbf{m}}_1 + \tilde{\mathbf{r}}^i) &= (\tilde{\mathbf{m}}_1' + \tilde{\mathbf{r}}^{i'}) \boldsymbol{\Sigma}_{\bullet 2}, \\
\sigma_v(\tilde{\mathbf{m}}_1 + \tilde{\mathbf{r}}^i) &= (\tilde{\mathbf{m}}_1' + \tilde{\mathbf{r}}^{i'}) \boldsymbol{\Sigma}_{\bullet 4}, \\
\sigma_q(\tilde{\mathbf{m}}_1 + \tilde{\mathbf{r}}^i) &= (\tilde{\mathbf{m}}_1' + \tilde{\mathbf{r}}^{i'}) \boldsymbol{\Sigma}_{\bullet 8}. \tag{3.T108}
\end{aligned}$$

Given the nominal risk free rate derived earlier using real pricing kernel and inflation, the nominal excess return is,

$$\begin{aligned}
E_t(\tilde{r}_{t+1}^i) - \tilde{r}f_t &= \left\{ \sigma_p(\tilde{\mathbf{r}}^i) + \ln \left[\frac{1 - \sigma_p(\tilde{\mathbf{m}}_1 + \tilde{\mathbf{r}}^i)}{1 - \sigma_p(\tilde{\mathbf{m}}_1)} \right] \right\} p_t \\
&+ \left\{ \sigma_n(\tilde{\mathbf{r}}^i) + \ln \left[\frac{1 - \sigma_n(\tilde{\mathbf{m}}_1 + \tilde{\mathbf{r}}^i)}{1 - \sigma_n(\tilde{\mathbf{m}}_1)} \right] \right\} n_t \\
&+ \left\{ \sigma_v(\tilde{\mathbf{r}}^i) + \ln \left[\frac{1 - \sigma_v(\tilde{\mathbf{m}}_1 + \tilde{\mathbf{r}}^i)}{1 - \sigma_v(\tilde{\mathbf{m}}_1)} \right] \right\} v_t \\
&+ \left\{ \sigma_q(\tilde{\mathbf{r}}^i) + \ln \left[\frac{1 - \sigma_q(\tilde{\mathbf{m}}_1 + \tilde{\mathbf{r}}^i)}{1 - \sigma_q(\tilde{\mathbf{m}}_1)} \right] \right\} q_t \\
&- \tilde{\mathbf{m}}_1' \mathbf{S}_1 \boldsymbol{\Sigma}^{other} \mathbf{S}_1' \tilde{\mathbf{r}}^i - \frac{1}{2} \left[\tilde{\mathbf{r}}^{i'} \mathbf{S}_1 \boldsymbol{\Sigma}^{other} \mathbf{S}_1' \tilde{\mathbf{r}}^i + \sigma_i^2 \right] \tag{3.T109}
\end{aligned}$$

where

$$\sigma_p(\tilde{\mathbf{r}}^i) = \tilde{\mathbf{r}}^{i'} \boldsymbol{\Sigma}_{\bullet 1}, \quad (3.T110)$$

$$\sigma_n(\tilde{\mathbf{r}}^i) = \tilde{\mathbf{r}}^{i'} \boldsymbol{\Sigma}_{\bullet 2}, \quad (3.T111)$$

$$\sigma_v(\tilde{\mathbf{r}}^i) = \tilde{\mathbf{r}}^{i'} \boldsymbol{\Sigma}_{\bullet 4}, \quad (3.T112)$$

$$\sigma_q(\tilde{\mathbf{r}}^i) = \tilde{\mathbf{r}}^{i'} \boldsymbol{\Sigma}_{\bullet 8}, \quad (3.T113)$$

$$\sigma_p(\tilde{\mathbf{m}}_1 + \tilde{\mathbf{r}}^i) = (\tilde{\mathbf{m}}_1' + \tilde{\mathbf{r}}^{i'}) \boldsymbol{\Sigma}_{\bullet 1}, \quad (3.T114)$$

$$\sigma_n(\tilde{\mathbf{m}}_1 + \tilde{\mathbf{r}}^i) = (\tilde{\mathbf{m}}_1' + \tilde{\mathbf{r}}^{i'}) \boldsymbol{\Sigma}_{\bullet 2}, \quad (3.T115)$$

$$\sigma_v(\tilde{\mathbf{m}}_1 + \tilde{\mathbf{r}}^i) = (\tilde{\mathbf{m}}_1' + \tilde{\mathbf{r}}^{i'}) \boldsymbol{\Sigma}_{\bullet 4}, \quad (3.T116)$$

$$\sigma_q(\tilde{\mathbf{m}}_1 + \tilde{\mathbf{r}}^i) = (\tilde{\mathbf{m}}_1' + \tilde{\mathbf{r}}^{i'}) \boldsymbol{\Sigma}_{\bullet 8}. \quad (3.T117)$$

3.B.4.2 One-period physical conditional return variance

The physical variance is easily obtained given the loadings:

$$\begin{aligned} VAR_t(\tilde{\mathbf{r}}_{t+1}^i) &= \left(\sigma_p(\tilde{\mathbf{r}}^i)\right)^2 p_t + \left(\sigma_n(\tilde{\mathbf{r}}^i)\right)^2 n_t + \left(\sigma_v(\tilde{\mathbf{r}}^i)\right)^2 v_t + \left(\sigma_q(\tilde{\mathbf{r}}^i)\right)^2 q_t \\ &+ \tilde{\mathbf{r}}^{i'} \mathbf{S}_1 \boldsymbol{\Sigma}^{other} \mathbf{S}_1' \tilde{\mathbf{r}}^i + \sigma_i^2. \end{aligned} \quad (3.T118)$$

3.B.4.3 One-period risk-neutral conditional return variance

To obtain the risk-neutral variance of the asset returns, we use the moment generating function under the risk-neutral measure:

$$\begin{aligned}
mgf_t^Q(\tilde{r}_{t+1}^i; \nu) &= \frac{E_t[\exp(\tilde{m}_{t+1} + \nu\tilde{r}_{t+1}^i)]}{E_t[\exp(\tilde{m}_{t+1})]} \\
&= \exp\{E_t(\tilde{m}_{t+1}) + \nu E_t(\tilde{r}_{t+1}^i)\} \\
&\cdot \exp\left\{\left[-\sigma_p(\tilde{\mathbf{m}}_1 + \nu\tilde{\mathbf{r}}^i) - \ln(1 - \sigma_p(\tilde{\mathbf{m}}_1 + \nu\tilde{\mathbf{r}}^i))\right] p_t\right\} \\
&\cdot \exp\left\{\left[-\sigma_n(\tilde{\mathbf{m}}_1 + \nu\tilde{\mathbf{r}}^i) - \ln(1 - \sigma_n(\tilde{\mathbf{m}}_1 + \nu\tilde{\mathbf{r}}^i))\right] n_t\right\} \\
&\cdot \exp\left\{\left[-\sigma_v(\tilde{\mathbf{m}}_1 + \nu\tilde{\mathbf{r}}^i) - \ln(1 - \sigma_v(\tilde{\mathbf{m}}_1 + \nu\tilde{\mathbf{r}}^i))\right] v_t\right\} \\
&\cdot \exp\left\{\left[-\sigma_q(\tilde{\mathbf{m}}_1 + \nu\tilde{\mathbf{r}}^i) - \ln(1 - \sigma_q(\tilde{\mathbf{m}}_1 + \nu\tilde{\mathbf{r}}^i))\right] q_t\right\} \\
&\cdot \exp\left\{\frac{1}{2}\left[(\tilde{\mathbf{m}}_1' + \nu\tilde{\mathbf{r}}^{i'})\mathbf{S}_1\Sigma^{other}\mathbf{S}_1'(\tilde{\mathbf{m}}_1 + \nu\tilde{\mathbf{r}}^i) + \nu^2\sigma_i^2\right]\right\} \\
&/ \exp\{E_t(\tilde{m}_{t+1})\} \\
&/ \exp\{[-\sigma_p(\tilde{\mathbf{m}}_1) - \ln(1 - \sigma_p(\tilde{\mathbf{m}}_1))] p_t + [-\sigma_n(\tilde{\mathbf{m}}_1) - \ln(1 - \sigma_n(\tilde{\mathbf{m}}_1))] n_t\} \\
&/ \exp\{[-\sigma_v(\tilde{\mathbf{m}}_1) - \ln(1 - \sigma_v(\tilde{\mathbf{m}}_1))] v_t + [-\sigma_q(\tilde{\mathbf{m}}_1) - \ln(1 - \sigma_q(\tilde{\mathbf{m}}_1))] q_t\} \\
&/ \exp\left\{\frac{1}{2}\left[\tilde{\mathbf{m}}_1'\mathbf{S}_1\Sigma^{other}\mathbf{S}_1'\tilde{\mathbf{m}}_1\right]\right\} \\
&= \exp\{\nu E_t(\tilde{r}_{t+1}^i)\} \\
&\cdot \exp\left\{\left[-\sigma_p(\nu\tilde{\mathbf{r}}^i) - \ln\left(\frac{1 - \sigma_p(\tilde{\mathbf{m}}_1 + \nu\tilde{\mathbf{r}}^i)}{1 - \sigma_p(\tilde{\mathbf{m}}_1)}\right)\right] p_t\right\} \\
&\cdot \exp\left\{\left[-\sigma_n(\nu\tilde{\mathbf{r}}^i) - \ln\left(\frac{1 - \sigma_n(\tilde{\mathbf{m}}_1 + \nu\tilde{\mathbf{r}}^i)}{1 - \sigma_n(\tilde{\mathbf{m}}_1)}\right)\right] n_t\right\} \\
&\cdot \exp\left\{\left[-\sigma_v(\nu\tilde{\mathbf{r}}^i) - \ln\left(\frac{1 - \sigma_v(\tilde{\mathbf{m}}_1 + \nu\tilde{\mathbf{r}}^i)}{1 - \sigma_v(\tilde{\mathbf{m}}_1)}\right)\right] v_t\right\} \\
&\cdot \exp\left\{\left[-\sigma_q(\nu\tilde{\mathbf{r}}^i) - \ln\left(\frac{1 - \sigma_q(\tilde{\mathbf{m}}_1 + \nu\tilde{\mathbf{r}}^i)}{1 - \sigma_q(\tilde{\mathbf{m}}_1)}\right)\right] q_t\right\} \\
&\cdot A(\nu), \tag{3.T119}
\end{aligned}$$

where $A(\nu) = \exp\left\{\frac{1}{2}\left[(\tilde{\mathbf{m}}_1' + \nu\tilde{\mathbf{r}}^{i'})\mathbf{S}_1\Sigma^{other}\mathbf{S}_1'(\tilde{\mathbf{m}}_1 + \nu\tilde{\mathbf{r}}^i) - \tilde{\mathbf{m}}_1'\mathbf{S}_1\Sigma^{other}\mathbf{S}_1'\tilde{\mathbf{m}}_1 + \nu^2\sigma_i^2\right]\right\}$, and

$$\sigma_p(\tilde{\mathbf{m}}_1' + \nu\tilde{\mathbf{r}}^{i'}) = (\tilde{\mathbf{m}}_1' + \nu\tilde{\mathbf{r}}^{i'})\Sigma_{\bullet 1}, \tag{3.T120}$$

$$\sigma_n(\tilde{\mathbf{m}}_1' + \nu\tilde{\mathbf{r}}^{i'}) = (\tilde{\mathbf{m}}_1' + \nu\tilde{\mathbf{r}}^{i'})\Sigma_{\bullet 2}, \tag{3.T121}$$

$$\sigma_v(\tilde{\mathbf{m}}_1' + \nu\tilde{\mathbf{r}}^{i'}) = (\tilde{\mathbf{m}}_1' + \nu\tilde{\mathbf{r}}^{i'})\Sigma_{\bullet 4}, \tag{3.T122}$$

$$\sigma_q(\tilde{\mathbf{m}}_1' + \nu\tilde{\mathbf{r}}^{i'}) = (\tilde{\mathbf{m}}_1' + \nu\tilde{\mathbf{r}}^{i'})\Sigma_{\bullet 8}. \tag{3.T123}$$

The first-order moment is the first-order derivate at $\nu = 0$:

$$\begin{aligned}
E_t^Q(\tilde{r}_{t+1}^i) &= \frac{\partial mgf_t^Q(\tilde{r}_{t+1}^i; \nu)}{\partial \nu} \Big|_{\nu=0} \\
&= E_t(\tilde{r}_{t+1}^i) + \frac{\sigma_p(\tilde{\mathbf{m}}_1)\sigma_p(\tilde{\mathbf{r}}^i)}{1 - \sigma_p(\tilde{\mathbf{m}}_1)} p_t + \frac{\sigma_n(\tilde{\mathbf{m}}_1)\sigma_n(\tilde{\mathbf{r}}^i)}{1 - \sigma_n(\tilde{\mathbf{m}}_1)} n_t + \frac{\sigma_v(\tilde{\mathbf{m}}_1)\sigma_v(\tilde{\mathbf{r}}^i)}{1 - \sigma_v(\tilde{\mathbf{m}}_1)} v_t + \frac{\sigma_q(\tilde{\mathbf{m}}_1)\sigma_q(\tilde{\mathbf{r}}^i)}{1 - \sigma_q(\tilde{\mathbf{m}}_1)} q_t \\
&\quad + \tilde{\mathbf{m}}_1' \mathbf{S}_1 \Sigma^{other} \mathbf{S}_1' \tilde{\mathbf{r}}^i.
\end{aligned} \tag{3.T124}$$

Note the similarity between $E_t(\tilde{r}_{t+1}^i) - E_t^Q(\tilde{r}_{t+1}^i)$ from this equation and the equity premium derived before using the no-arbitrage condition. The second-order moment is derived,

$$\begin{aligned}
VAR_t^Q(\tilde{r}_{t+1}^i) &= E_t^Q((\tilde{r}_{t+1}^i)^2) - \left(E_t^Q(\tilde{r}_{t+1}^i)\right)^2 \\
&= \frac{\partial^2 mgf_t^Q(\tilde{r}_{t+1}^i; \nu)}{\partial \nu^2} \Big|_{\nu=0} - \left(\frac{\partial mgf_t^Q(\tilde{r}_{t+1}^i; \nu)}{\partial \nu} \Big|_{\nu=0}\right)^2 \\
&= \left(\frac{\sigma_p(\tilde{\mathbf{r}}^i)}{1 - \sigma_p(\tilde{\mathbf{m}}_1)}\right)^2 p_t + \left(\frac{\sigma_n(\tilde{\mathbf{r}}^i)}{1 - \sigma_n(\tilde{\mathbf{m}}_1)}\right)^2 n_t + \left(\frac{\sigma_v(\tilde{\mathbf{r}}^i)}{1 - \sigma_v(\tilde{\mathbf{m}}_1)}\right)^2 v_t + \left(\frac{\sigma_q(\tilde{\mathbf{r}}^i)}{1 - \sigma_q(\tilde{\mathbf{m}}_1)}\right)^2 q_t \\
&\quad + \tilde{\mathbf{r}}^{i'} \mathbf{S}_1 \Sigma^{other} \mathbf{S}_1' \tilde{\mathbf{r}}^i + \sigma_i^2.
\end{aligned} \tag{3.T125}$$

3.C Variables and parameters

Symbol	
θ_t	change in log real industrial production index or growth
p_t	positive uncertainty factor
n_t	negative uncertainty factor
$\omega_{p,t}$	“good environment” shock
$\omega_{n,t}$	“bad environment” shock
\mathbf{Y}_t^{mac}	technology factors consisting of $\{\theta_t, p_t, n_t\}$
ω_t^{mac}	technology shocks consisting of $\{\omega_{p,t}, \omega_{n,t}\}$
π_t	change in log historical consumer price index
u_t^π	independent state variable shock of π
$\omega_{\pi,t}$	inflation shock
l_t	log corporate bond loss rate
u_t^l	independent state variable shock of l
$\omega_{l,t}$	loss rate shock
g_t	change in log earnings
u_t^g	independent state variable shock of e
$\omega_{g,t}$	earnings shock
κ_t	log consumption-earnings ratio
u_t^κ	independent state variable shock of κ
$\omega_{\kappa,t}$	log consumption-earnings ratio shock
η_t	log dividend payout ratio
u_t^η	independent state variable shock of η

$\omega_{\eta,t}$	log dividend payout ratio shock
v_t	loss rate shock shape parameter
q_t	risk aversion
u_t^q	independent state variable shock of q
$\omega_{q,t}$	risk aversion shock
Y_t	a vector of 10 state variables
ω_t	a vector of 8 independent shocks
Δc_t	change in log consumption
m_t	log real pricing kernel
\tilde{m}_t	log nominal pricing kernel
y_t^1	nominal short rate
PC_t	price-to-coupon ratio of one period defaultable bond
PD_t	price-dividend ratio
r_t^i	log asset return for assets i
$E_{t-1}(r_t^i)$	expected return for assets i
u_t^i	asset-specific shock of assets i
VAR_{t-1}^i	model-implied one-period physical conditional return variance of assets i
$VAR_{t-1}^{i,Q}$	model-implied one-period risk-neutral conditional return variance of assets i
z_t	a vector of observable asset prices / instruments
$PVAR_t^i$	empirical one-period physical conditional return variance of assets i for $t+1$
$QVAR_t^i$	empirical one-period risk-neutral conditional return variance of assets i for $t+1$

Symbol	
θ	unconditional mean of growth
m_p	sensitivity of output growth on lagged upside uncertainty
m_n	sensitivity of output growth on lagged downside uncertainty
\bar{p}	unconditional mean of positive uncertainty factor
\bar{n}	unconditional mean of negative uncertainty factor
ρ_p	autocorrelation coefficient of positive uncertainty factor
ρ_n	autocorrelation coefficient of negative uncertainty factor
$\sigma_{\theta p}$	scale parameter of growth to “good environment” shock
$\sigma_{\theta n}$	scale parameter of growth to “bad environment” shock
σ_{pp}	scale parameter of positive uncertainty factor to “good environment” shock
σ_{nn}	scale parameter of negative uncertainty factor to “bad environment” shock
j_0^*	constant in Variable j process
ρ_{jj}^*	autocorrelation coefficient of Variable j
ρ_{jyp}^*	sensitivity coefficient of Variable j to positive uncertainty factor
ρ_{jyn}^*	sensitivity coefficient of Variable j to negative uncertainty factor
$\rho_{jy\theta}^*$	sensitivity coefficient of Variable j to output growth factor
ρ_{jy}^*	$[\rho_{jp}, \rho_{jn}, \rho_{jx}]$
σ_{jp}^*	scale parameter of Variable j to “good environment” shock
σ_{jn}^*	scale parameter of Variable j to “bad environment” shock
σ_{jj}^{**}	unconditional volatility of u_t^j

σ_{jj} ***	scale parameter of the state variable gamma shock u_t^j
σ_{vl}	scale parameter of the v_t to the loss shock
μ	constant vector in the state variable system (10×1)
A	autocorrelation vector in the state variable system (10×10)
Σ	scale / volatility parameter matrix of the 8 shocks (10×8)
c_0	constant in the consumption growth process
c_1	sensitivity vector of consumption growth to state variable shocks
c_2	sensitivity vector of consumption growth to state variable levels
m_0	constant in the real pricing kernel process
m_1	sensitivity vector of real pricing kernel to state variable shocks
m_2	sensitivity vector of real pricing kernel to state variable levels
r^i	return loadings on state variable shocks
σ_i	unconditional volatility of u_t^i
χ	risk aversion loadings on observed asset prices

* for all $j \in \{\pi, l, g, \kappa, \eta, v, q\}$:
** for all $j \in \{\pi, g, \kappa, \eta\}$:
*** for all $j \in \{l, q\}$:

3.0

Table 3.1: The Dynamics of the Macro Factors

This table reports parameter estimates from the model below using the monthly log growth rate of U.S. industrial production from January 1947 to February 2015. This system involves latent processes (good shape parameter governing positive skewness p_t and bad shape parameter governing negative skewness n_t) and is estimated using the MLE-filtration methodology described in Bates (2006).

$$\begin{aligned}\theta_{t+1} &= \bar{\theta} + \rho_{\theta}(\theta_t - \bar{\theta}) + m_p(p_t - 500) + m_n(n_t - \bar{n}) + u_{t+1}^{\theta} \\ p_{t+1} &= 500 + \rho_p(p_t - 500) + \sigma_{pp}\omega_{p,t+1} \\ n_{t+1} &= \bar{n} + \rho_n(n_t - \bar{n}) + \sigma_{nn}\omega_{n,t+1}\end{aligned}$$

, where

$$\begin{aligned}u_{t+1}^{\theta} &= \sigma_{\theta p}\omega_{p,t+1} - \sigma_{\theta n}\omega_{n,t+1} \\ \omega_{p,t+1} &\sim \tilde{\gamma}(p_t, 1) \\ \omega_{n,t+1} &\sim \tilde{\gamma}(n_t, 1) \\ \sigma_{pp} &> 0 \\ \sigma_{nn} &> 0.\end{aligned}$$

Standard errors are in parentheses. Note that “ $\omega_{n,t}$ loading” in Column “ θ_t ” is $-\sigma_{\theta n}$; “ $\omega_{n,t}$ loading” in Column “ p_t ” (“ n_t ”) is $+\sigma_{pp}$ ($+\sigma_{nn}$).

	θ_t	p_t	n_t
mean	0.00002 (0.00045)	500 (fix)	16.14206 (2.14529)
AR	0.13100 (0.03094)	0.99968 (0.01918)	0.91081 (0.01350)
m_p	0.00001 (0.00034)		
m_n	-0.00020 (0.00002)		
$\omega_{p,t}$ loading	0.00011 (0.00001)	0.55277 (0.07073)	
$\omega_{n,t}$ loading	-0.00174 (0.00014)		2.17755 (0.15027)
LL	2861.30797		
BIC	-5648.85	AIC	-5700.62

Table 3.2: The Dynamics of the Corporate Loss Rate

This table reports parameter estimates for the corporate loss rate model using monthly data from January 1982 to February 2015. The mean equation of the loss rate is as follows,

$$\begin{aligned} l_{t+1} &= l_0 + \rho_{ll}l_t + \rho_{lp}p_t + \rho_{ln}n_t + \sigma_{lp}\omega_{p,t+1} + \sigma_{ln}\omega_{n,t+1} + u_{t+1}^l \\ u_{t+1}^l &= \sigma_{ll}\omega_{l,t+1} \\ \omega_{l,t+1} &\sim \tilde{\gamma}(v_t, 1), \end{aligned}$$

where the variance equation is,

$$v_{t+1} = v_0 + \rho_{vv}v_t + \sigma_{vl}\omega_{l,t+1}.$$

The mean equation is estimated by projection, the variance equation by MLE. Standard errors are in parentheses.

Mean Equation					
l_0	ρ_{ll}	ρ_{lyp}	ρ_{lyn}	σ_{lp}	σ_{ln}
-0.3463	0.8779	0.0001	0.0047	-0.0004	0.0177
(0.0911)	(0.0209)	(0.0002)	(0.0010)	(0.0004)	(0.0039)
Variance Equation					
σ_{ll}	v_0	ρ_{vv}	σ_{vl}		
0.0599	0.8544	0.9051	0.1820		
(0.0008)	(0.1867)	(0.0205)	(0.0203)		

Table 3.3: Cash Flow Dynamics

Parameters of cash flow processes are shown in Equation (3.T18) for the log earnings growth, Equation (3.T21) for the log consumption-earnings ratio, Equation (3.T24) for the log dividend-earnings ratio, and Equation (3.T30) for the inflation rate. Estimation is by simple linear projection. Bold (italic) coefficients have <5% (10%) p-values. Robust errors are shown in parentheses. The sample period is 1986/06 to 2015/02 (345 months).

	earnings growth	log CE	log DE	inflation
	g_{t+1}	κ_{t+1}	η_{t+1}	π_{t+1}
drift	0.0285 (0.0273)	0.1101 (0.0453)	-0.1005 (0.0337)	0.0031 (0.0014)
AR	0.6619 (0.0432)	0.9400 (0.0088)	0.9188 (0.0103)	0.3973 (0.0500)
θ_t	0.7932 (0.6214)	0.8494 (0.8104)	1.2237 (0.8420)	-0.0718 (0.0315)
p_t	-5.29E-05 (5.66E-05)	4.42E-05 (7.10E-05)	-2.55E-05 (7.48E-05)	-2.07E-06 (2.84E-06)
n_t	-0.0006 (0.0004)	0.0049 (0.0005)	0.0053 (0.0006)	-7.04E-05 (1.94E-05)
$\omega_{p,t+1}$ loading	-8.63E-05 (1.16E-04)	4.94E-05 (1.42E-04)	5.34E-05 (1.46E-04)	-4.83E-06 (5.87E-06)
$\omega_{n,t+1}$ loading	-0.0029 (0.0011)	0.0061 (0.0014)	0.0063 (0.0014)	8.27E-05 (5.60E-05)
$\omega_{l,t+1}$ loading	0.0010 (0.0009)	-0.0014 (0.0011)	-0.0014 (0.0011)	
Gaussian shock volatility	0.0465 (0.0018)	0.0568 (0.0021)	0.0582 (0.0022)	0.0023 (0.0001)
Adjusted R^2 (conditional mean)	55.58%	98.19%	97.89%	20.58%

Table 3.4: Shock Correlations

$\omega_{p,t+1}$:	good uncertainty shock	$\tilde{\Gamma}(p_t, 1)$;
$\omega_{n,t+1}$:	bad uncertainty shock	$\tilde{\Gamma}(n_t, 1)$;
$\omega_{l,t+1}$:	loss rate-specific shock	$\tilde{\Gamma}(v_t, 1)$;
$\omega_{g,t+1}$:	log earnings growth-specific shock	$N(0,1)$;
$\omega_{\kappa,t+1}$:	log C/E-specific shock	$N(0,1)$;
$\omega_{\eta,t+1}$:	log D/E-specific shock	$N(0,1)$;
$\omega_{q,t+1}$:	risk aversion-specific shock	$\tilde{\Gamma}(q_t, 1)$.

Bold (italic) coefficients have <5% (10%) p-values. The sample period is 1986/06 to 2015/02 (345 months).

	ω_p	ω_n	ω_π	ω_l	ω_g	ω_κ	ω_η	ω_q
ω_p	1	-0.1129	0.0000	-0.0316	0.0000	0.0000	0.0000	0.0000
ω_n		1	0.0000	0.0246	0.0000	0.0000	0.0000	0.0000
ω_π			1	<i>0.0937</i>	0.1083	-0.0215	-0.0604	0.0175
ω_l				1	0.0000	0.0000	0.0000	0.0788
ω_g					1	-0.6989	-0.6798	0.0684
ω_κ						1	0.9882	-0.0283
ω_η							1	-0.0265
ω_q								1

Table 3.5: Financial Instruments Spanning Risk Aversion

This table presents summary statistics of the 6 financial instruments that are used to span our risk aversion measure: “tsprd” is the difference between 10-year treasury yield and 3-month Treasury yield; “csprd” is the difference between Moody’s BAA yield and the 10-year zero-coupon Treasury yield; “DY5yr” is the detrended dividend yield where the moving average takes the 5 year average of monthly dividend yields, starting one year before; “rvareq” and “rvarcb” are realized variances of log equity returns and log corporate bond returns, calculated from daily returns; “qvareq” is the risk-neutral conditional variance of log equity returns; for the early years (before 1990), we use VXO and authors’ calculations. Bold (italic) coefficients have <5% (10%) p-values. Block bootstrapped errors are shown in parentheses. The sample period is from 1986/06 to 2015/02 (345 months).

	tsprd	csprd	DY5yr	rvareq	qvareq	rvarcb
Correlation Matrix						
tsprd	1	0.3524	0.2583	0.1266	0.1240	0.2949
csprd		1	0.5063	0.4793	0.5999	0.5340
DY5yr			1	0.1675	0.1641	0.3101
rvareq				1	0.8430	0.5942
qvareq					1	0.5374
rvarcb						1
Summary Statistics						
Mean	0.0179	0.0231	-0.0030	0.0029	0.0040	0.0002
Boot.SE	(0.0006)	(0.0004)	(0.0003)	(0.0003)	(0.0002)	(1.45E-05)
S.D.	0.0116	0.0075	0.0061	0.0059	0.0037	0.0003
Boot.SE	(0.0003)	(0.0005)	(0.0003)	(0.0014)	(0.0005)	(3.86E-05)
Skewness	-0.2322	1.7891	0.0959	8.1198	3.7225	4.2227
Boot.SE	(0.0810)	(0.2515)	(0.1882)	(1.5951)	(0.5123)	(0.6872)
AR(1)	0.9669	0.9642	0.9822	0.4311	0.7461	0.5775
SE	(0.0137)	(0.0143)	(0.0083)	(0.0489)	(0.0360)	(0.0442)

Table 3.6: Reduced-Form Risk Aversion Parameters

This table presents the two-step GMM estimation results for risk aversion, $q_t = \chi'z_t$, estimated using equity market and corporate bond market asset prices. The utility function curvature γ is fixed at 2. The first-step weight matrix is an identity matrix; the second-step weight matrix builds on the Newey-West spectral density function with 5-month lags, and then is shrunk towards an identity matrix where the shrinkage parameter is 0.1. The GMM system also consistently estimates σ_{qq} . Therefore, the system has 8 unknown parameters. The p-value of Hansen's overidentification test (J test) is calculated from the asymptotic χ^2 distribution with the degree of freedom being 29 (37-8). Bold (italic) coefficients have <5% (10%) p-values. Efficient standard errors are shown in parentheses. The sample period is 1986/06 to 2015/02 (345 months).

q_t	
Efficient GMM Estimators	
constant	0.264 (0.510)
χ_{tsprd}	-0.442 (4.507)
χ_{csprd}	-7.599 (7.186)
χ_{dy5yr}	6.550 (8.158)
χ_{rvareq}	-43.232 (1.879)
χ_{qvareq}	104.599 (8.288)
$\chi_{rvarecb}$	239.663 (114.473)
Correlation with the NBER Indicator	
$\rho(q_t, NBER_t)$	0.397 (0.045)
Model Specifications	
Hansen's J	27.919
p-value	0.5222

Table 3.7: Structural Risk Aversion Parameters.

This table presents the model-implied risk aversion process parameters. “Projection”: coefficient estimates are obtained from simple projection. “GMM”: the scale parameter of the risk aversion innovation which is estimated in the GMM framework (Table 3.6). The second and third panels report the variance decomposition results of the conditional mean and shock structure of \hat{q}_{t+1} , denoted with “VARC”. In the second panel, $VARC = \beta_x \frac{cov(\hat{y}, x)}{var(\hat{y})}$ where $\hat{y} = \hat{E}_t(\hat{q}_{t+1})$. VARC in the third panel is calculated using the residual, $\hat{q}_{t+1} - \hat{E}_t(\hat{q}_{t+1})$. Bold (italic) coefficients have <5% (10%) p-values. Robust and efficient standard errors are shown in parentheses. The sample period is 1986/06 to 2015/02 (345 months).

$$\begin{aligned}\hat{q}_{t+1} &= q_0 + \rho_{qq}\hat{q}_t + \rho_{qp}\hat{p}_t + \rho_{qn}\hat{n}_t + \sigma_{qp}\hat{\omega}_{p,t+1} + \sigma_{qn}\hat{\omega}_{n,t+1} + u_{t+1}^q, \\ u_{t+1}^q &= \sigma_{qq}\omega_{q,t+1}, \\ \omega_{q,t+1} &= \tilde{\Gamma}(q_t, 1).\end{aligned}$$

Structural Risk Aversion Parameters, q_{t+1}							
	◦ Projection						◦ GMM
	Constant	p_t	n_t	q_t	$\omega_{p,t+1}$	$\omega_{n,t+1}$	$\omega_{q,t+1}$
Est	-0.1040	0.0006	0.0056	0.6293	0.0004	-0.0009	0.1211
(SE)	(0.0835)	(0.0002)	(0.0010)	(0.0412)	(0.0004)	(0.0034)	(0.0067)
Conditional Mean Variance Decomposition (60.70% of Total Variance)							
		p_t	n_t	q_t			
VARC		77.15%	1.68%	21.17%			
Shock Structure Variance Decomposition (39.30% of Total Variance)							
					$\omega_{p,t+1}$	$\omega_{n,t+1}$	$\omega_{q,t+1}$
VARC					0.35%	0.30%	99.35%

Table 3.8: Fit of Moments.

This table evaluates the fit of conditional moments of equity and corporate bond returns. That is, Column “Model” reports the averages of the relevant model-implied conditional moments. The “Empirical Averages” represent the sample averages of the excess returns (for “Mom 1” and “Mom 4”), the sample average of empirical conditional variances (for “Mom 2”, “Mom 3”, and “Mom 5”). In “Mom 6” and “Mom 7”, “Risk Aversion Innovation” is u_{t+1}^q in Equation (3.T27). The variance and unscaled skewness rows compare the average model-implied conditional moments with the unconditional moments. Bolded number(s) denote a distance of less than 1.645 standard errors from the corresponding point estimate, and italicized number(s) a distance of more than 1.645 but less than 1.96 standard errors. Block bootstrapped standard errors are shown in parentheses; we allow the block size to vary for different moments, block sizes=[0 6 15 1 10] for Mom 1 to Mom 5, respectively. Asymptotic standard errors (standard deviation divided by square root of the number of observations) are reported for Mom 6 and Mom 7. The sample period is 1986/06 to 2015/02 (345 months).

	Moment	Model	Empirical Average	Boot.SE/SE
Mom 1	Equity Risk Premium	0.00749	0.00530	(0.00246)
Mom 2	Equity Physical Variance	0.00310	0.00286	(0.00051)
Mom 3	Equity Risk-neutral Variance	0.00369	0.00397	(0.00049)
Mom 4	Corporate Bond Risk Premium	<i>0.00289</i>	0.00388	(0.00050)
Mom 5	Corporate Bond Physical Variance	0.00027	0.00024	(0.00003)
Mom 6	Risk Aversion Innovation Variance	0.00823	0.00906	(0.00215)
Mom 7	Risk Aversion Innovation Unscaled Skewness	0.00246	0.00246	(0.00134)

Table 3.9: Asset Prices and the State Variables.

The asset conditional moments are explained by $\{p_t, n_t, v_t, q_t\}$. The coefficients are scaled by the standard deviation of the state variable in the same column, and then multiplied by 10000 for reporting purposes. VARC is coefficient $\ast \frac{Cov(x_t, Mom_t)}{Var(Mom_t)}$ where $x \in \{p, n, v, q\}$ and Mom is from Mom 1 to Mom 5. The variance decomposition is reported in a bold italic font.

Model-implied coefficients of moments on state variables $\{p_t, n_t, v_t, q_t\}$					
	Moment	p_t	n_t	v_t	q_t
Mom 1	Equity Risk Premium	0.1286	4.6231	0.0039	54.0505
	VARC	0.014%	4.449%	0.000%	95.537%
Mom 2	Equity Physical Variance	0.0651	2.5845	0.0006	5.5008
	VARC	-0.031%	26.640%	0.000%	73.391%
Mom 3	Equity Risk-neutral Variance	0.0652	2.5454	0.0006	11.2064
	VARC	0.011%	12.646%	0.000%	87.343%
Mom 4	Corporate Bond Risk Premium	0.0752	7.6016	-0.0200	3.8662
	VARC	-0.143%	71.227%	-0.001%	28.918%
Mom 5	Corporate Bond Physical Variance	0.0009	0.3137	0.0007	0.0015
	VARC	-0.090%	99.865%	-0.001%	0.226%

Table 3.10: Predicting Realized Excess Returns and Variances.

This table reports the regression coefficients of realized excess returns and realized variances of equity and corporate bond. The coefficients are scaled by the standard deviation of the state variable in the same row, and then multiplied by 100 for reporting purposes. “Model-Implied Moments” are risk premiums (for realized excess returns) and physical variances (for realized variances). Bold (italic) coefficients have <5% (10%) p-values. The R^2 is adjusted. Standard errors are shown in parentheses. The sample period is 1986/06 to 2015/02 (345 months).

	$\tilde{r}_{t+1}^{eq} - rf_t$	$RVAR_{t+1}^{eq}$	$\tilde{r}_{t+1}^{cb} - rf_t$	$RVAR_{t+1}^{cb}$
p_t	-0.1648 (0.2584)	0.0190 (0.0312)	-0.1098 (0.0922)	-0.0003 (0.0014)
n_t	-1.2623 (0.2928)	0.1695 (0.0354)	0.0044 (0.1045)	0.0093 (0.0016)
v_t	-0.3478 (0.2359)	0.0410 (0.0285)	-0.1089 (0.0842)	-0.0029 (0.0013)
q_t	0.6562 (0.1866)	0.1047 (0.0226)	<i>0.1262</i> (0.0666)	0.0036 (0.0010)
Model-Implied Moments	<i>0.6671</i> (0.4018)	3.8517 (0.4017)	1.6610 (0.8376)	3.8195 (0.4250)
Corr w/ NBER	0.45	0.54	0.61	0.65
R^2	5.6%	0.1%	21.8%	21.0%
			1.2%	0.8%
				22.0%
				18.9%

Table 3.11: Out-Of-Sample Exercise.

This table analyzes in-sample (see Section 3.3.3) and out-of-sample risk premium estimates of equity returns and corporate bond returns. “Realized” indicates the realized excess returns. “Mod (1)” indicates the in-sample (full-sample) estimates of model-implied risk premiums, the dynamics of which are determined by $\{p_t, n_t, v_t, q_t\}$. “Mod (2)” indicates the out-of-sample estimates of model-implied risk premiums. Define a 60-month rolling window from $t - 60$ to $t - 1$, then project one-period ahead excess returns on the 4 state variables, use the coefficient estimates to obtain $E_t(\tilde{r}_{t+1} - rf_t)$, repeat. We also consider three out-of-sample empirical models that use three instruments sets (subsets of \mathbf{z}_t), respectively: (1) dividend yield, (2) dividend yield + term spread + credit spread, (3) physical uncertainty plus variance risk premium estimate. The table then reports the optimal combination of Mod and Emp Mod estimate. Least Square standard errors are shown in parentheses. Bold (italic) coefficients have <5% (10%) p-values. R^2 is adjusted. The (full) sample period is 1986/06 to 2015/02 (345 months).

Least-Square Estimate of a in				
$\tilde{r}_{t+1} - rf_t = a \times \text{Mod}(t, i) + (1 - a) \times \text{Emp Mod}(t, j) + e_{t+1}$				
$i = 1, 2; j = 1, 2, 3$				
	◦ <i>Equity</i> :		◦ <i>Corporate Bond</i> :	
	Mod (1)	Mod (2)	Mod (1)	Mod (2)
Emp Mod (1)	0.8262	0.4843	1.0155	0.2553
	(0.1095)	(0.0995)	(0.1365)	(0.1161)
Emp Mod (2)	0.9613	0.6618	0.8236	0.4748
	(0.0934)	(0.0870)	(0.0841)	(0.0903)
Emp Mod (3)	0.8305	0.6216	0.9238	0.4719
	(0.0810)	(0.0801)	(0.1090)	(0.0903)

Table 3.12: Uncertainty Index.

This table presents regression results of the filtered macroeconomic uncertainty (from industrial production growth) on the set of instruments used to determine risk aversion. “Total” is the total industrial production growth variance, which is a function of p_t and n_t , $\sigma_{\theta p}^2 p_t + \sigma_{\theta n}^2 n_t$. “ $\times 10^3$ ” in the header means that the coefficients and their SEs reported are multiplied by 1000 for reporting convenience. Bold (italic) coefficients have <5% (10%) p-values. Robust and efficient standard errors are shown in parentheses. The R^2 is adjusted. The sample period is 1986/06 to 2015/02 (345 months).

	($\times 10^3$)		($\times 10^3$)		($\times 10^3$)	
	Total	VARC	Upside	VARC	Downside	VARC
constant	-0.006		0.006		-0.012	
	(0.005)		(0.000)		(0.005)	
χ_{tsprd}	-0.573	-2.38%	-0.005	5.21%	-0.568	-2.54%
	(0.112)		(0.002)		(0.113)	
χ_{csprd}	1.919	61.33%	-0.006	4.05%	1.925	60.98%
	(0.246)		(0.005)		(0.247)	
χ_{DY5yr}	1.083	19.83%	-0.063	84.69%	1.146	21.21%
	(0.234)		(0.005)		(0.235)	
χ_{rvareq}	-0.318	-4.81%	-0.022	-0.41%	-0.296	-4.39%
	(0.399)		(0.008)		(0.401)	
χ_{qvareq}	<i>1.243</i>	14.28%	0.066	8.08%	<i>1.177</i>	13.24%
	(0.673)		(0.014)		(0.676)	
χ_{rvarcb}	14.829	11.76%	0.158	-1.61%	14.671	11.49%
	(5.910)		(0.124)		(5.933)	
R^2	47.72%		44.35%		47.95%	

Table 3.13: On the Predictive Power of Risk Aversion Index and Uncertainty Index on Future Output Growth.

This table reports the coefficient estimates of the following predictive regression,

$$\theta_{t+k} = a + \mathbf{b}' \mathbf{x}_t + res_{t+k}, \quad (3.T126)$$

where θ_{t+k} represents future industrial production growth during period $t + 1$ and $t + k$ ($\sum_{\tau=1}^k \theta_{t+\tau}$) and \mathbf{x}_t represents a vector of current predictors. We consider (1) our risk aversion index ra^{BEX} , (2) our uncertainty index unc^{BEX} (financial proxy), (3) the risk-neutral conditional variance (the square of the month-end VIX (after 1990) / VXO (prior to 1990) index divided by 120000), $QVAR$, and (4) the true total macroeconomic uncertainty filtered from industrial production index unc^{true} . The coefficients are scaled by the standard deviation of the predictor in the same column for reporting purposes. Hodrick (1992) standard errors are reported in parentheses, and adjusted R^2 s are in %. Bold (italic) coefficients have <5% (10%) p-values.

	ra^{BEX}	unc^{BEX}	$QVAR$	unc^{true}	
A. Univariate					
1m	-0.002 (0.001) 7.9%	-0.003 (0.000) 19.2%	-0.002 (0.001) 6.5%	-0.002 (0.001) 12.9%	
1q	-0.005 (0.001) 13.9%	-0.008 (0.001) 34.9%	-0.005 (0.002) 15.3%	-0.007 (0.001) 26.3%	
4q	-0.006 (0.003) 2.0%	-0.016 (0.004) 15.2%	-0.008 (0.003) 3.7%	-0.010 (0.004) 6.2%	
B. Multivariate (1)					R^2
1m	0.000 (0.001)	-0.003 (0.001)	0.001 (0.000)		19.4%
1q	0.002 (0.001)	-0.008 (0.001)	-0.001 (0.001)		35.3%
4q	0.013 (0.002)	-0.021 (0.005)	-0.005 (0.002)		18.4%
C. Multivariate (2)					R^2
1m	0.000 (0.001)	-0.002 (0.000)	0.001 (0.000)	-0.001 (0.001)	19.1%
1q	0.002 (0.001)	-0.006 (0.001)	-0.001 (0.001)	-0.003 (0.001)	36.7%
4q	0.013 (0.002)	-0.022 (0.005)	<i>-0.005</i> (0.002)	0.001 (0.003)	17.4%

Table 3.14: Alternative Risk Aversion and Uncertainty Measures.

This table report the correlation between our risk aversion and economic uncertainty indices and existing measures. For risk aversion (Panel A), we consider three categories. A.1) We follow Wachter (2006) to create a fundamental risk aversion process from inflation-adjusted (real) quarterly consumption growth ($\sum_{j=0}^4 0_j \Delta c_{t-j}$); A.2) we consider the well-known sentiment index by Baker and Wurgler (2006) from the behavior finance literature, and the Michigan Consumer Sentiment Index (that directly measures the consumer sentiment); A.3) we also consider an industry index, the Credit Suisse First Boston Risk Appetite Index. For economic uncertainty (Panel B), we consider B.1) the macroeconomic uncertainty index created by Jurado, Ludvigson, and Ng (2015), and B.2) the Economic Policy Uncertainty Index created by Baker, Bloom, and Davis (2016). Correlations are calculated using overlapping samples at the monthly frequency. Standard errors are shown in parentheses. Bold correlation coefficients have <5% p-values.

A. Correlations with Extant Risk Aversion Indices	
<i>A.1) "Fundamental" Habit Model:</i>	
Wachter (2006) / Campbell and Cochrane (1999)	0.1228 (0.0536)
<i>A.2) Sentiment Index:</i>	
Baker and Wurgler (2006)	-0.1554 (0.0533)
Michigan Consumer Sentiment Index	-0.2603 (0.0521)
<i>A.3) Industry Index</i>	
Credit Suisse First Boston Risk Appetite Index	-0.4770 (0.0475)
B. Correlations with Extant Uncertainty Indices	
<i>B.1) Macroeconomic Uncertainty:</i>	
Jurado, Ludvigson, and Ng (2015)	0.8003 (0.0324)
<i>B.2) Political Uncertainty:</i>	
Baker, Bloom, and Davis (2016)	0.3438 (0.0507)

Table 3.15: Market Integration Test.

This table tests market integration by evaluating the fit of Treasury bond return moments priced using the pricing kernel extracted from risky assets. Column "Model" reports the averages of the relevant model-implied conditional moments. The "Empirical Averages" represent the sample averages of the excess returns ("Mom 1"), the sample average of empirical conditional variances ("Mom 2", "Mom 3"). Bolded number(s) denote a distance of less than 1.645 standard errors from the corresponding point estimate, and italicized number(s) a distance of more than 1.645 but less than 1.96 standard errors. Block bootstrapped standard errors are shown in parentheses; we allow the block size to vary for different moments, block sizes=[0 14 13] for Mom 1 to Mom 3, respectively. The sample period is 1986/06 to 2015/02 (345 months).

	Moment	Model	Empirical Average	Boot.SE
Mom 1	Treasury Bond Risk Premium	-0.00366	0.00285	(0.00117)
Mom 2	Treasury Bond Physical Variance	0.00111	0.00035	(0.00004)
Mom 3	Treasury Bond Risk-neutral Variance	0.00113	0.00043	(0.00003)

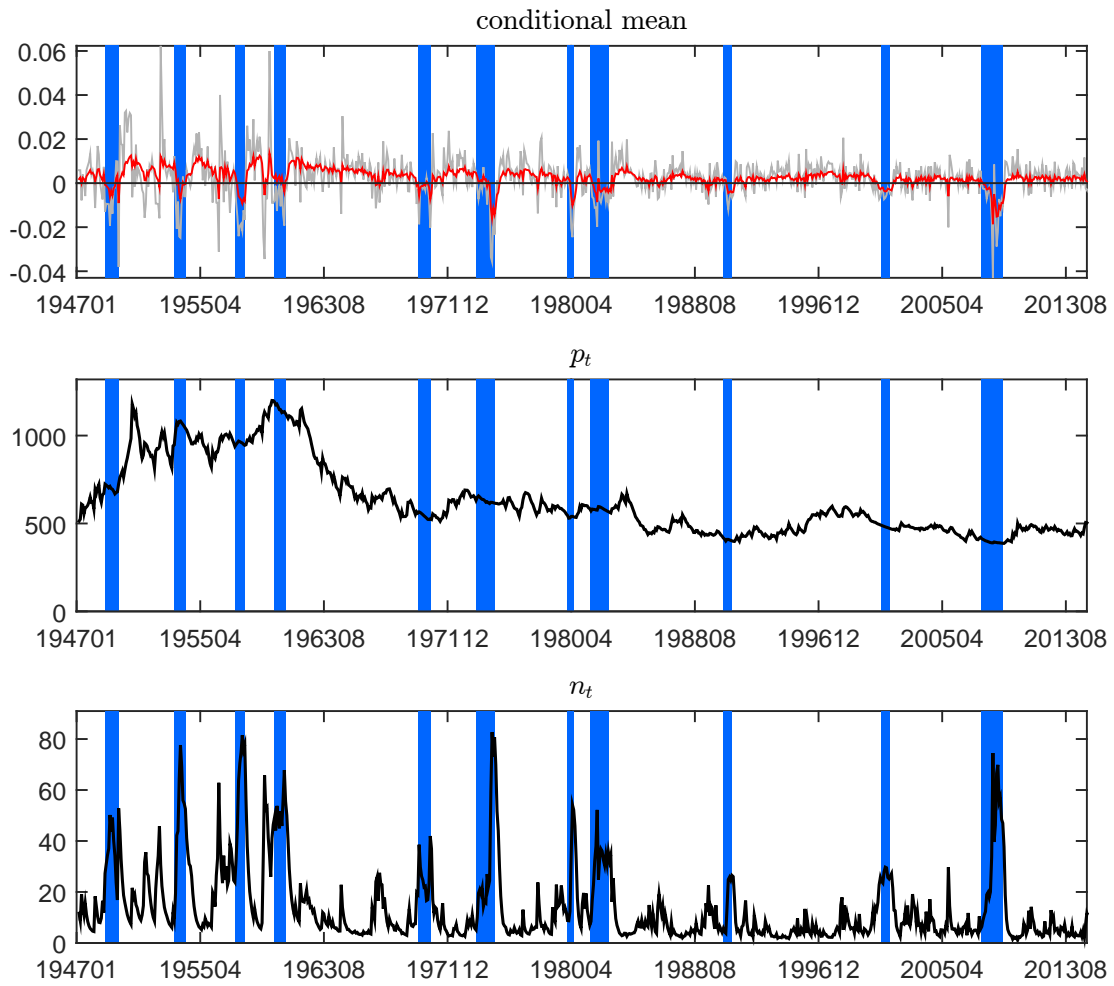


Figure 3.1: Filtered state variables extracted from industrial production growth.

The shaded regions are NBER recession months from the NBER website.

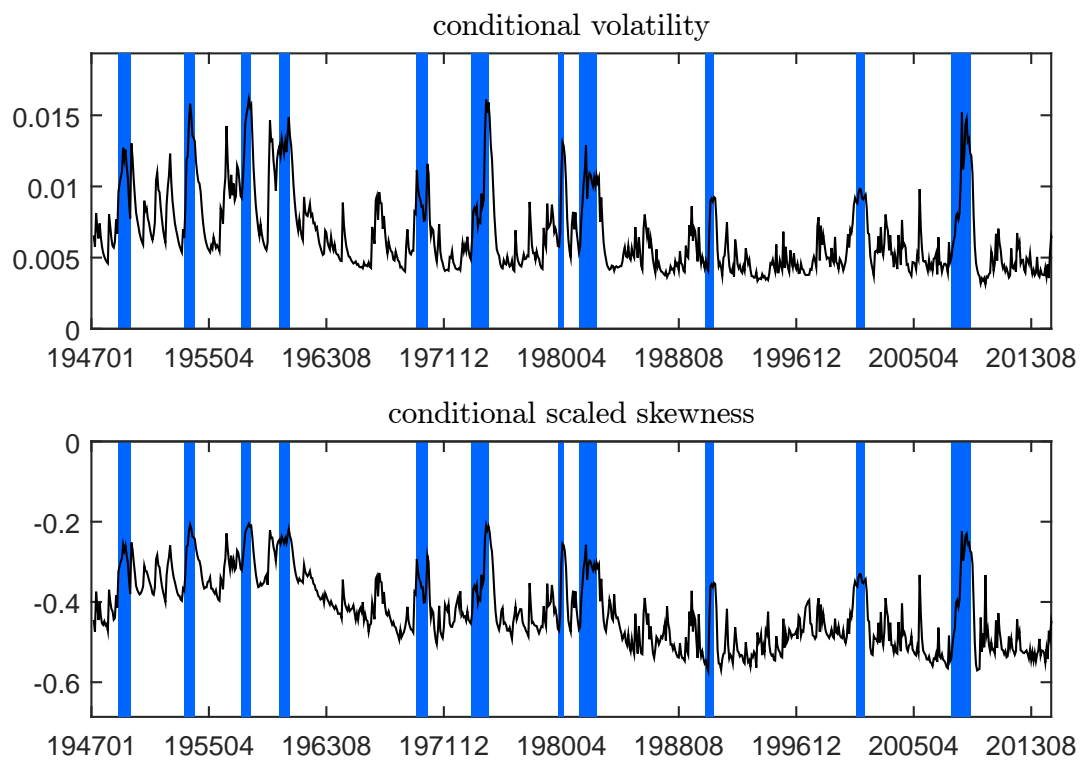


Figure 3.2: Model-implied conditional moments for industrial production growth.

The shaded regions are NBER recession months from the NBER website.

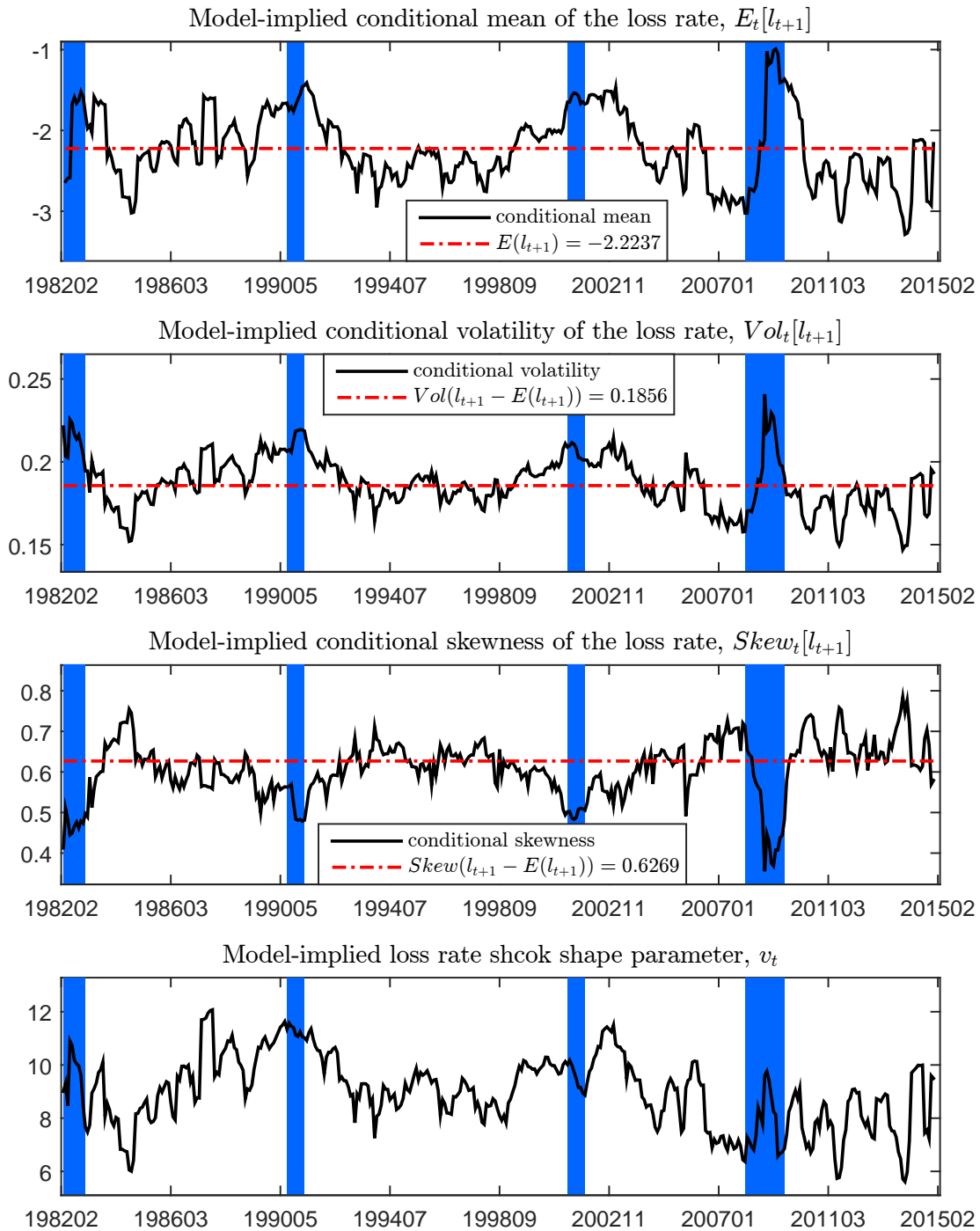


Figure 3.3: Conditional moments of the loss rate.

The shaded regions are NBER recession months from the NBER website.

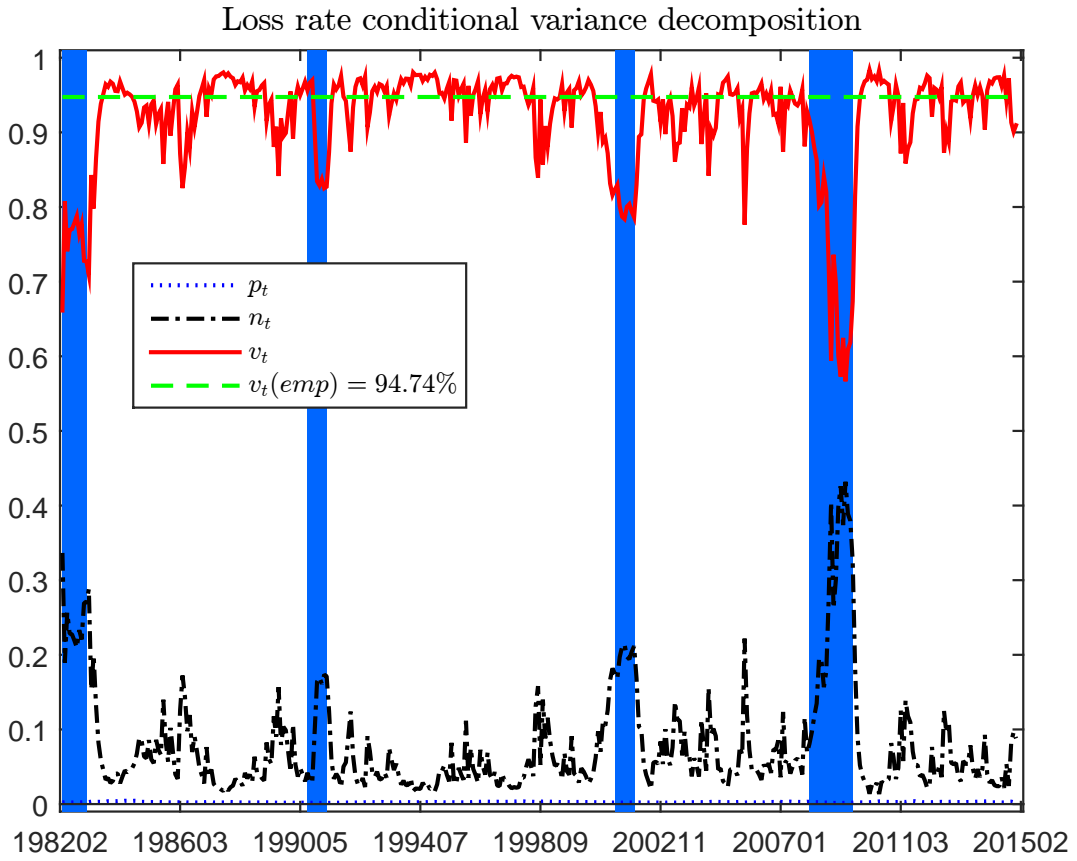


Figure 3.4: Decomposition of the conditional variance of the loss rate.

The shaded regions are NBER recession months from the NBER website. The green dashed line depicts the ratio of the unconditional variance of u_{t+1}^l to the unconditional variance of the total loss rate disturbance, or $1-R^2$ from the projection.

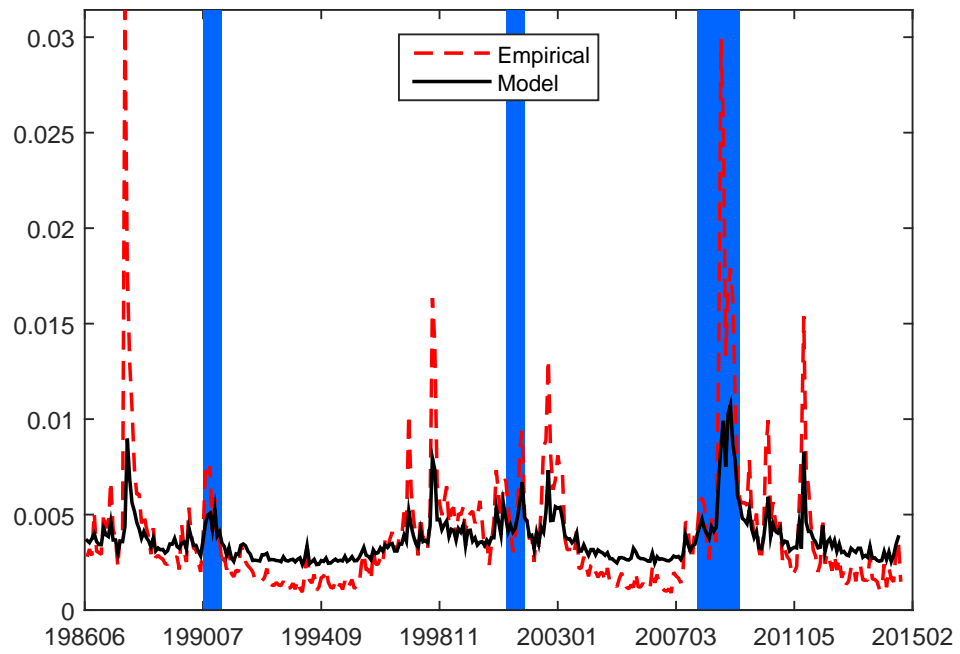


Figure 3.5: Model-implied and empirical risk-neutral conditional variances of equity market returns.

The shaded regions are NBER recession months from the NBER website.

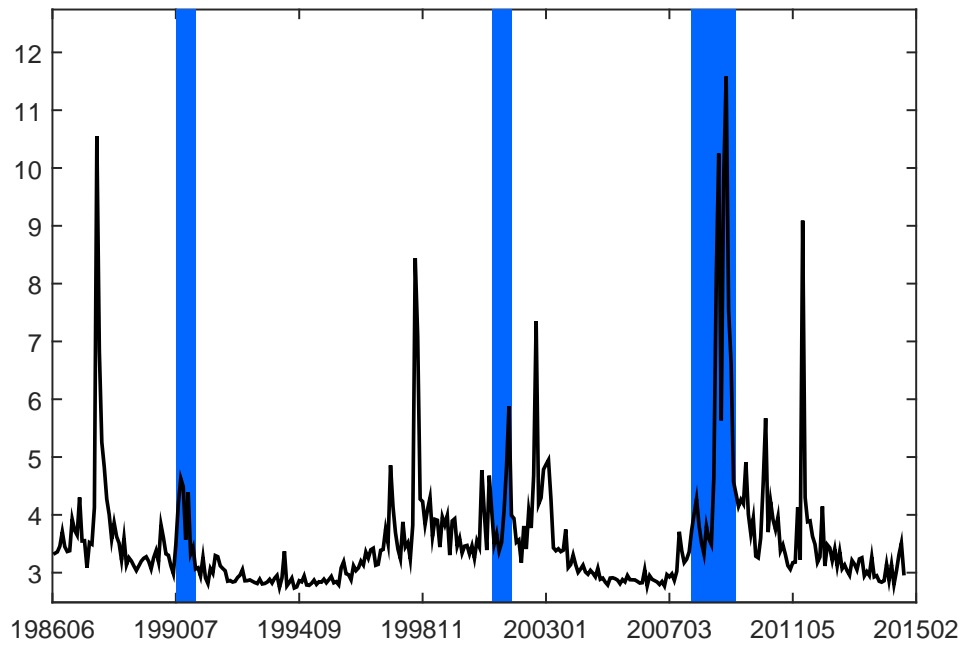


Figure 3.6: The Time Variation in the Risk Aversion. Risk aversion is $\gamma \exp(q_t)$.

The shaded regions are the NBER recession months from the NBER website.

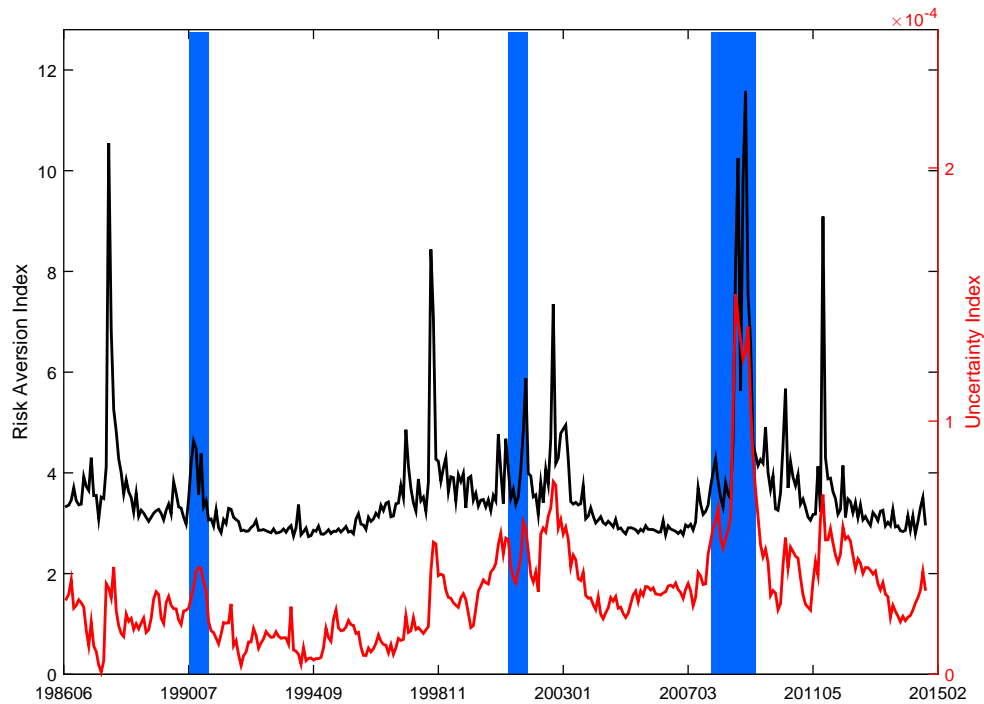


Figure 3.7: Risk aversion index (solid blue/left y-axis) and Uncertainty index (dashed red/right y-axis).

According to Section 3.4, both the risk aversion index denoted as $ra^{BEX} = \gamma \exp(q_t)$ and the uncertainty index denoted as unc^{BEX} are functions of a set of financial instruments. See Equations (3.T49) and (3.T59). Correlation between the two series is 67.94%. The shaded regions are NBER recession months from the NBER website.

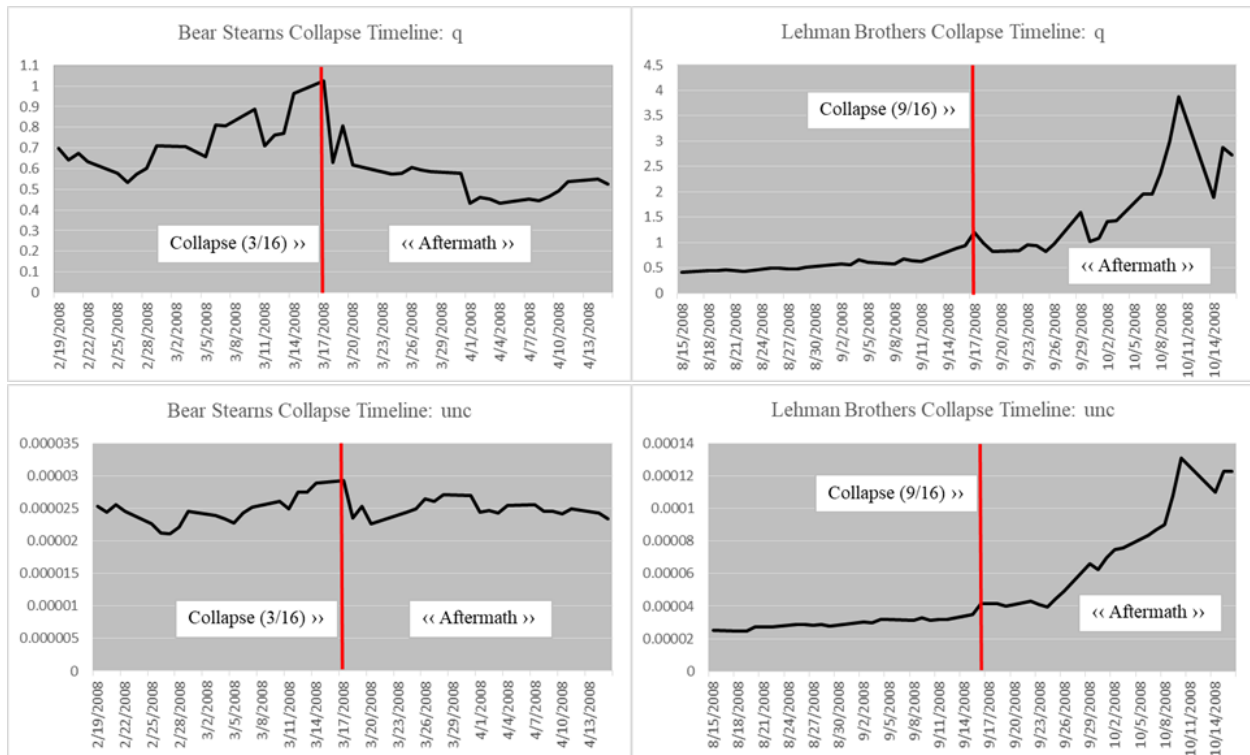


Figure 3.8: q_t and Uncertainty Index at Daily Frequency Around the Bear Stearns and Lehman Brothers Collapses in 2008.

We calculate and plot our daily indices one month before and after the collapses.

REFERENCES

- [1] ADRIAN, T., AND SHIN, H. S. Money, liquidity and monetary policy. *American Economic Review* (2009).
- [2] AIELLI, G. P. Dynamic conditional correlation: on properties and estimation. *Journal of Business & Economic Statistics* 31, 3 (2013), 282–299.
- [3] AIT-SAHALIA, Y., AND LO, A. W. Nonparametric risk management and implied risk aversion. *Journal of Econometrics* 94, 1 (2000), 9–51.
- [4] ALLEN, F., BERNARDO, A. E., AND WELCH, I. A theory of dividends based on tax clienteles. *The Journal of Finance* 55, 6 (2000), 2499–2536.
- [5] ANDERSEN, T. G., BOLLERSLEV, T., DIEBOLD, F. X., AND VEGA, C. Real-time price discovery in global stock, bond and foreign exchange markets. *Journal of international Economics* 73, 2 (2007), 251–277.
- [6] ANG, A., AND BEKAERT, G. International asset allocation with regime shifts. *The Review of Financial Studies* 15, 4 (2002), 1137–1187.
- [7] ANG, A., BEKAERT, G., AND WEI, M. The term structure of real rates and expected inflation. *The Journal of Finance* 63, 2 (2008), 797–849.

- [8] ANG, A., AND CHEN, J. Asymmetric correlations of equity portfolios. *Journal of financial Economics* 63, 3 (2002), 443–494.
- [9] BACKUS, D. K., FORESI, S., AND TELMER, C. I. Affine term structure models and the forward premium anomaly. *The Journal of Finance* 56, 1 (2001), 279–304.
- [10] BAELE, L., BEKAERT, G., CHO, S., INGHELBRECHT, K., AND MORENO, A. Macroeconomic regimes. *Journal of Monetary Economics* 70 (2015), 51–71.
- [11] BAELE, L., BEKAERT, G., INGHELBRECHT, K., AND WEI, M. Flights to safety. *Working Paper* (2013).
- [12] BAELE, L., BEKAERT, G., INGHELBRECHT, K., AND WEI, M. Flights to safety. *Working Paper* (2017).
- [13] BAKER, M., AND WURGLER, J. Investor sentiment and the cross-section of stock returns. *The Journal of Finance* 61, 4 (2006), 1645–1680.
- [14] BAKER, S. R., BLOOM, N., AND DAVIS, S. J. Measuring economic policy uncertainty. *The Quarterly Journal of Economics* 131, 4 (2016), 1593–1636.
- [15] BAKSHI, G., KAPADIA, N., AND MADAN, D. Stock return characteristics, skew laws, and the differential pricing of individual equity options. *The Review of Financial Studies* 16, 1 (2003), 101–143.
- [16] BAKSHI, G., AND WU, L. The behavior of risk and market prices of risk over the nasdaq bubble period. *Management Science* 56, 12 (2010), 2251–2264.
- [17] BALI, T. G., BROWN, S. J., AND TANG, Y. Is economic uncertainty priced in the cross-section of stock returns? *Journal of Financial Economics* (2017).

- [18] BALL, L. Why does high inflation raise inflation uncertainty? *Journal of Monetary Economics* 29, 3 (1992), 371–388.
- [19] BANSAL, N., CONNOLLY, R. A., AND STIVERS, C. Regime-switching in stock index and treasury futures returns and measures of stock market stress. *Journal of Futures Markets* 30, 8 (2010), 753–779.
- [20] BANSAL, R., DITTMAR, R. F., AND LUNDBLAD, C. T. Consumption, dividends, and the cross section of equity returns. *The Journal of Finance* 60, 4 (2005), 1639–1672.
- [21] BANSAL, R., KIKU, D., AND YARON, A. An empirical evaluation of the long-run risks model for asset prices. *Critical Finance Review* 1, 1 (2012), 183–221.
- [22] BANSAL, R., AND SHALIASTOVICH, I. A long-run risks explanation of predictability puzzles in bond and currency markets. *The Review of Financial Studies* 26, 1 (2012), 1–33.
- [23] BANSAL, R., SHALIASTOVICH, I., ET AL. Confidence risk and asset prices. *American Economic Review* 100, 2 (2010), 537–541.
- [24] BANSAL, R., AND YARON, A. Risks for the long run: A potential resolution of asset pricing puzzles. *The Journal of Finance* 59, 4 (2004), 1481–1509.
- [25] BATES, D. S. Maximum likelihood estimation of latent affine processes. *The Review of Financial Studies* 19, 3 (2006), 909–965.
- [26] BAUR, D. G., AND LUCEY, B. M. Flights and contagion: an empirical analysis of stock–bond correlations. *Journal of Financial Stability* 5, 4 (2009), 339–352.
- [27] BEKAERT, G., CHO, S., AND MORENO, A. New keynesian macroeconomics and the term structure. *Journal of Money, Credit and Banking* 42, 1 (2010), 33–62.

- [28] BEKAERT, G., AND ENGSTROM, E. Asset return dynamics under habits and bad environment–good environment fundamentals. *Journal of Political Economy* 125, 3 (2017), 713–760.
- [29] BEKAERT, G., AND ENGSTROM, E. Asset return dynamics under habits and bad-environment good-environment fundamentals. *Journal of Political Economy* 125, 3 (2017), 713–760.
- [30] BEKAERT, G., ENGSTROM, E., AND ERMOLOV, A. Bad environments, good environments: A non-gaussian asymmetric volatility model. *Journal of Econometrics* 186, 1 (2015), 258–275.
- [31] BEKAERT, G., ENGSTROM, E., AND GRENADIER, S. R. Stock and bond returns with moody investors. *Journal of Empirical Finance* 17, 5 (2010), 867–894.
- [32] BEKAERT, G., ENGSTROM, E., AND XING, Y. Risk, uncertainty, and asset prices. *Journal of Financial Economics* 91, 1 (2009), 59–82.
- [33] BEKAERT, G., ENGSTROM, E., AND XU, N. R. The time variation in risk appetite and uncertainty. *Working Paper* (2017).
- [34] BEKAERT, G., AND HARVEY, C. R. Time-varying world market integration. *The Journal of Finance* 50, 2 (1995), 403–444.
- [35] BEKAERT, G., HODRICK, R. J., AND ZHANG, X. International stock return comovements. *The Journal of Finance* 64, 6 (2009), 2591–2626.
- [36] BEKAERT, G., AND HOEROVA, M. The vix, the variance premium and stock market volatility. *Journal of Econometrics* 183, 2 (2014), 181–192.

- [37] BEKAERT, G., AND HOEROVA, M. What do asset prices have to say about risk appetite and uncertainty? *Journal of Banking & Finance* 67 (2016), 103–118.
- [38] BEKAERT, G., HOEROVA, M., AND DUCA, M. L. Risk, uncertainty and monetary policy. *Journal of Monetary Economics* 60, 7 (2013), 771–788.
- [39] BERNANKE, B. S., BOIVIN, J., AND ELIASZ, P. Measuring the effects of monetary policy: a factor-augmented vector autoregressive (favar) approach. *The Quarterly journal of economics* 120, 1 (2005), 387–422.
- [40] BERNOTH, K., AND ERDOGAN, B. Sovereign bond yield spreads: A time-varying coefficient approach. *Journal of International Money and Finance* 31, 3 (2012), 639–656.
- [41] BESLEY, T., AND COATE, S. Centralized versus decentralized provision of local public goods: a political economy approach. *Journal of public economics* 87, 12 (2003), 2611–2637.
- [42] BLOOM, N. The impact of uncertainty shocks. *Econometrica* 77, 3 (2009), 623–685.
- [43] BOLLERSLEV, T. Generalized autoregressive conditional heteroskedasticity. *Journal of econometrics* 31, 3 (1986), 307–327.
- [44] BOLLERSLEV, T. A conditionally heteroskedastic time series model for speculative prices and rates of return. *The Review of Economics and Statistics* (1987), 542–547.
- [45] BOLLERSLEV, T., ENGLE, R. F., AND WOOLDRIDGE, J. M. A capital asset pricing model with time-varying covariances. *Journal of Political Economy* 96, 1 (1988), 116–131.
- [46] BOLLERSLEV, T., GIBSON, M., AND ZHOU, H. Dynamic estimation of volatility risk premia and investor risk aversion from option-implied and realized volatilities. *Journal of Econometrics* 160, 1 (2011), 235–245.

- [47] BOLLERSLEV, T., TAUCHEN, G., AND ZHOU, H. Expected stock returns and variance risk premia. *The Review of Financial Studies* 22, 11 (2009), 4463–4492.
- [48] BOLLERSLEV, T., AND TODOROV, V. Tails, fears, and risk premia. *The Journal of Finance* 66, 6 (2011), 2165–2211.
- [49] BOLLERSLEV, T., AND WOOLDRIDGE, J. M. Quasi-maximum likelihood estimation and inference in dynamic models with time-varying covariances. *Econometric Reviews* 11, 2 (1992), 143–172.
- [50] BOUDOUKH, J., MICHAELY, R., RICHARDSON, M., AND ROBERTS, M. R. On the importance of measuring payout yield: Implications for empirical asset pricing. *The Journal of Finance* 62, 2 (2007), 877–915.
- [51] BRAV, A., GRAHAM, J. R., HARVEY, C. R., AND MICHAELY, R. Payout policy in the 21st century. *Journal of Financial Economics* 77, 3 (2005), 483–527.
- [52] BRENNAN, M. J., AND THAKOR, A. V. Shareholder preferences and dividend policy. *The Journal of Finance* 45, 4 (1990), 993–1018.
- [53] BRITTEN-JONES, M., AND NEUBERGER, A. Option prices, implied price processes, and stochastic volatility. *The Journal of Finance* 55, 2 (2000), 839–866.
- [54] BROADIE, M., CHERNOV, M., AND JOHANNES, M. Model specification and risk premia: Evidence from futures options. *The Journal of Finance* 62, 3 (2007), 1453–1490.
- [55] BRUNNERMEIER, M. K., NAGEL, S., AND PEDERSEN, L. H. Carry trades and currency crashes. *NBER Macroeconomics Annual* 23, 1 (2008), 313–348.

- [56] CAMPBELL, J. Y. Stock returns and the term structure. *Journal of Financial Economics* 18, 2 (1987), 373–399.
- [57] CAMPBELL, J. Y., AND COCHRANE, J. H. By force of habit: A consumption based explanation of aggregate stock market behavior. *Journal of Political Economy* 107, 2 (1999), 205–251.
- [58] CAMPBELL, J. Y., AND COCHRANE, J. H. By force of habit: A consumption-based explanation of aggregate stock market behavior. *Journal of Political Economy* 107, 2 (1999), 205–251.
- [59] CAMPBELL, R. A., FORBES, C. S., KOEDIJK, K. G., AND KOFMAN, P. Increasing correlations or just fat tails? *Journal of Empirical Finance* 15, 2 (2008), 287–309.
- [60] CAPPIELLO, L., ENGLE, R. F., AND SHEPPARD, K. Asymmetric dynamics in the correlations of global equity and bond returns. *Journal of Financial econometrics* 4, 4 (2006), 537–572.
- [61] CECCHETTI, S. G., AND KRAUSE, S. Financial structure, macroeconomic stability and monetary policy. Tech. rep., National Bureau of Economic Research, 2001.
- [62] CHEN, R.-R., AND SCOTT, L. Maximum likelihood estimation for a multifactor equilibrium model of the term structure of interest rates. *The Journal of Fixed Income* 3, 3 (1993), 14–31.
- [63] CHRISTOFFERSEN, P., ERRUNZA, V., JACOBS, K., AND LANGLOIS, H. Is the potential for international diversification disappearing? a dynamic copula approach. *The Review of Financial Studies* 25, 12 (2012), 3711–3751.

- [64] COEURDACIER, N., AND REY, H. Home bias in open economy financial macroeconomics. *Journal of Economic Literature* 51, 1 (2013), 63–115.
- [65] COLACITO, R., ENGLE, R. F., AND GHYSELS, E. A component model for dynamic correlations. *Journal of Econometrics* 164, 1 (2011), 45–59.
- [66] CONNOLLY, R., STIVERS, C., AND SUN, L. Stock market uncertainty and the stock-bond return relation. *Journal of Financial and Quantitative Analysis* 40, 1 (2005), 161–194.
- [67] COUDERT, V., AND GEX, M. Does risk aversion drive financial crises? testing the predictive power of empirical indicators. *Journal of Empirical Finance* 15, 2 (2008), 167–184.
- [68] DAVID, A., AND VERONESI, P. What ties return volatilities to price valuations and fundamentals? *Journal of Political Economy* 121, 4 (2013), 682–746.
- [69] DE SANTIS, G., AND GERARD, B. International asset pricing and portfolio diversification with time-varying risk. *The Journal of Finance* 52, 5 (1997), 1881–1912.
- [70] DEANGELO, H., AND DEANGELO, L. Capital structure, payout policy, and financial flexibility. *Working Paper* (2007).
- [71] DEMARZO, P., AND SANNIKOV, Y. Learning in dynamic incentive contracts. *Working Paper* (2008).
- [72] DRECHSLER, I., AND YARON, A. What’s vol got to do with it. *The Review of Financial Studies* 24, 1 (2010), 1–45.
- [73] DUFFEE, G. R. Time variation in the covariance between stock returns and consumption growth. *The Journal of Finance* 60, 4 (2005), 1673–1712.

- [74] ENGLE, R. Dynamic conditional correlation: A simple class of multivariate generalized autoregressive conditional heteroskedasticity models. *Journal of Business & Economic Statistics* 20, 3 (2002), 339–350.
- [75] ENGLE, R., AND KELLY, B. Dynamic equicorrelation. *Journal of Business & Economic Statistics* 30, 2 (2012), 212–228.
- [76] ENGLE, R. F., AND SHEPPARD, K. Theoretical and empirical properties of dynamic conditional correlation multivariate garch. Tech. rep., National Bureau of Economic Research, 2001.
- [77] EPSTEIN, L. G., AND ZIN, S. E. Substitution, risk aversion, and the temporal behavior of consumption and asset returns: A theoretical framework. *Econometrica: Journal of the Econometric Society* (1989), 937–969.
- [78] ERMOLOV, A. Time-varying risk of nominal bonds: How important are macroeconomic shocks? *working paper* (2015).
- [79] FAGIOLO, G., NAPOLETANO, M., AND ROVENTINI, A. Are output growth-rate distributions fat-tailed? some evidence from oecd countries. *Journal of Applied Econometrics* 23, 5 (2008), 639–669.
- [80] FAMA, E. F., AND FRENCH, K. R. Common risk factors in the returns on stocks and bonds. *Journal of Financial Economics* 33, 1 (1993), 3–56.
- [81] FAMA, E. F., AND MACBETH, J. D. Risk, return, and equilibrium: Empirical tests. *Journal of Political Economy* 81, 3 (1973), 607–636.

- [82] FORBES, K. J., AND RIGOBON, R. No contagion, only interdependence: measuring stock market comovements. *The journal of Finance* 57, 5 (2002), 2223–2261.
- [83] FORBES, K. J., AND WARNOCK, F. E. Capital flow waves: Surges, stops, flight, and retrenchment. *Journal of International Economics* 88, 2 (2012), 235–251.
- [84] FRENCH, K. R., SCHWERT, G. W., AND STAMBAUGH, R. F. Expected stock returns and volatility. *Journal of financial Economics* 19, 1 (1987), 3–29.
- [85] FUDENBERG, D., AND TIROLE, J. A theory of income and dividend smoothing based on incumbency rents. *Journal of Political Economy* (1995), 75–93.
- [86] GAI, P., AND VAUSE, N. Measuring investors risk appetite. *International Journal of Central Banking* (2006).
- [87] GAMBETTI, L., PAPPA, E., AND CANOVA, F. The structural dynamics of us output and inflation: what explains the changes? *Journal of Money, Credit and Banking* 40, 2-3 (2008), 369–388.
- [88] GENZ, A., AND BRETZ, F. *Computation of multivariate normal and t probabilities*, vol. 195. Springer Science & Business Media, 2009.
- [89] GILCHRIST, S., AND ZAKRAJŠEK, E. Credit spreads and business cycle fluctuations. *The American Economic Review* 102, 4 (2012), 1692–1720.
- [90] GLOSTEN, L. R., JAGANNATHAN, R., AND RUNKLE, D. E. On the relation between the expected value and the volatility of the nominal excess return on stocks. *The journal of finance* 48, 5 (1993), 1779–1801.
- [91] GREENE, W. H. *Econometric analysis*. Pearson Education India, 2003.

- [92] GUIBAUD, S., NOSBUSCH, Y., AND VAYANOS, D. Bond market clienteles, the yield curve, and the optimal maturity structure of government debt. *The Review of Financial Studies* 26, 8 (2013), 1914–1961.
- [93] GUTTMAN, I., KADAN, O., AND KANDEL, E. Dividend stickiness and strategic pooling. *Review of Financial Studies* 23, 12 (2010), 4455–4495.
- [94] HAMILTON, J. D., AND LIN, G. Stock market volatility and the business cycle. *Journal of Applied Econometrics* 11, 5 (1996), 573–593.
- [95] HARVEY, C. R. The real term structure and consumption growth. *Journal of Financial Economics* 22, 2 (1988), 305–333.
- [96] HENTSCHEL, L. All in the family nesting symmetric and asymmetric garch models. *Journal of Financial Economics* 39, 1 (1995), 71–104.
- [97] HU, G. X., PAN, J., AND WANG, J. Noise as information for illiquidity. *The Journal of Finance* 68, 6 (2013), 2341–2382.
- [98] JACKWERTH, J. C. Recovering risk aversion from option prices and realized returns. *The Review of Financial Studies* 13, 2 (2000), 433–451.
- [99] JENNRICH, R. I. An asymptotic χ^2 test for the equality of two correlation matrices. *Journal of the American Statistical Association* 65, 330 (1970), 904–912.
- [100] JOTIKASTHIRA, C., LE, A., AND LUNDBLAD, C. Why do term structures in different currencies co-move? *Journal of Financial Economics* 115, 1 (2015), 58–83.
- [101] JURADO, K., LUDVIGSON, S. C., AND NG, S. Measuring uncertainty. *The American Economic Review* 105, 3 (2015), 1177–1216.

- [102] KANDEL, S., AND STAMBAUGH, R. F. Expectations and volatility of consumption and asset returns. *Review of Financial Studies* 3, 2 (1990), 207–232.
- [103] KENOURGIOS, D., SAMITAS, A., AND PALTALIDIS, N. Financial crises and stock market contagion in a multivariate time-varying asymmetric framework. *Journal of International Financial Markets, Institutions and Money* 21, 1 (2011), 92–106.
- [104] KOSTAKIS, A., MAGDALINOS, T., AND STAMATOIANNIS, M. P. Robust econometric inference for stock return predictability. *The Review of Financial Studies* 28, 5 (2015), 1506–1553.
- [105] KOTZ, S., AND NADARAJAH, S. *Multivariate t-distributions and their applications*. Cambridge University Press, 2004.
- [106] KUMAR, P. Shareholder-manager conflict and the information content of dividends. *Review of Financial Studies* 1, 2 (1988), 111–136.
- [107] LAMBRECHT, B. M., AND MYERS, S. C. A lintner model of payout and managerial rents. *The Journal of Finance* 67, 5 (2012), 1761–1810.
- [108] LE, A., AND SINGLETON, K. J. The structure of risks in equilibrium affine models of bond yields. Tech. rep., Working Paper, UNC, 2013.
- [109] LEMMON, M., AND PORTNIAGUINA, E. Consumer confidence and asset prices: Some empirical evidence. *The Review of Financial Studies* 19, 4 (2006), 1499–1529.
- [110] LETTAU, M., AND LUDVIGSON, S. Consumption, aggregate wealth, and expected stock returns. *the Journal of Finance* 56, 3 (2001), 815–849.

- [111] LETTAU, M., LUDVIGSON, S. C., AND WACHTER, J. A. The declining equity premium: What role does macroeconomic risk play? *Review of Financial Studies* 21, 4 (2008), 1653–1687.
- [112] LI, Q., YANG, J., HSIAO, C., AND CHANG, Y.-J. The relationship between stock returns and volatility in international stock markets. *Journal of Empirical Finance* 12, 5 (2005), 650–665.
- [113] LINTNER, J. Distribution of incomes of corporations among dividends, retained earnings, and taxes. *The American Economic Review* (1956), 97–113.
- [114] LIU, J., PAN, J., AND WANG, T. An equilibrium model of rare-event premia and its implication for option smirks. *The Review of Financial Studies* 18, 1 (2004), 131–164.
- [115] LJUNG, G. M., AND BOX, G. E. On a measure of lack of fit in time series models. *Biometrika* 65, 2 (1978), 297–303.
- [116] LONGIN, F., AND SOLNIK, B. Is the correlation in international equity returns constant: 1960–1990? *Journal of international money and finance* 14, 1 (1995), 3–26.
- [117] LONGIN, F., AND SOLNIK, B. Extreme correlation of international equity markets. *The journal of finance* 56, 2 (2001), 649–676.
- [118] LONGSTAFF, F. A., AND PIAZZESI, M. Corporate earnings and the equity premium. *Journal of Financial Economics* 74, 3 (2004), 401–421.
- [119] LONGSTAFFA, F. A., AND PIAZZESIB, M. Corporate earnings and the equity premium. *Journal of Financial Economics* 74 (2004), 401–421.

- [120] LUCAS JR, R. E. Asset prices in an exchange economy. *Econometrica: Journal of the Econometric Society* (1978), 1429–1445.
- [121] MAIO, P., AND SANTA-CLARA, P. Dividend yields, dividend growth, and return predictability in the cross section of stocks. *Journal of Financial and Quantitative Analysis* 50, 1-2 (2015), 33–60.
- [122] MARTIN, I. What is the expected return on the market? *The Quarterly Journal of Economics* 132, 1 (2017), 367–433.
- [123] MENZLY, L., SANTOS, T., AND VERONESI, P. Understanding predictability. *Journal of Political Economy* 112, 1 (2004), 1–47.
- [124] MIRANDA-AGRIPPINO, S., AND REY, H. World asset markets and the global financial cycle. Tech. rep., National Bureau of Economic Research, 2015.
- [125] NELSON, D. B. Conditional heteroskedasticity in asset returns: A new approach. *Econometrica: Journal of the Econometric Society* (1991), 347–370.
- [126] PÁSTOR, L., AND VERONESI, P. Political uncertainty and risk premia. *Journal of Financial Economics* 110, 3 (2013), 520–545.
- [127] POLITIS, D. N., AND ROMANO, J. P. Bias-corrected nonparametric spectral estimation. *Journal of time series analysis* 16, 1 (1995), 67–103.
- [128] POLITIS, D. N., AND WHITE, H. Automatic block-length selection for the dependent bootstrap. *Econometric Reviews* 23, 1 (2004), 53–70.
- [129] QIU, L., AND WELCH, I. Investor sentiment measures. Tech. rep., 2006.

- [130] RAJAN, R. G. Has finance made the world riskier? *European Financial Management* 12, 4 (2006), 499–533.
- [131] REY, H. Dilemma not trilemma: the global financial cycle and monetary policy independence. Tech. rep., 2015.
- [132] RIBEIRO, R., AND VERONESI, P. Excess comovement of international stock markets in bad times: a rational expectations equilibrium model. In *II Encontro Brasileiro de Finanças* (2002).
- [133] ROSENBERG, J. V., AND ENGLE, R. F. Empirical pricing kernels. *Journal of Financial Economics* 64, 3 (2002), 341–372.
- [134] RUIZ, E. Quasi-maximum likelihood estimation of stochastic volatility models. *Journal of Econometrics* 63, 1 (1994), 289–306.
- [135] SANTA-CLARA, P., AND YAN, S. Crashes, volatility, and the equity premium: Lessons from s&p 500 options. *The Review of Economics and Statistics* 92, 2 (2010), 435–451.
- [136] SCHWERT, G. W. Why does stock market volatility change over time? *The Journal of Finance* 44, 5 (1989), 1115–1153.
- [137] SEGAL, G., SHALIASTOVICH, I., AND YARON, A. Good and bad uncertainty: Macroeconomic and financial market implications. *Journal of Financial Economics* 117, 2 (2015), 369–397.
- [138] SHANKEN, J. Intertemporal asset pricing: An empirical investigation. *Journal of Econometrics* 45, 1-2 (1990), 99–120.
- [139] SHILLER, R. *Market Volatility*. The MIT Press, Cambridge, 1989.

- [140] STOCK, J. H., AND WATSON, M. W. Forecasting using principal components from a large number of predictors. *Journal of the American statistical association* 97, 460 (2002), 1167–1179.
- [141] TAYLOR, J. B. The inflation/output trade-off revisited. *Goals, Guidelines and Constraints Facing Monetary Policymakers, Federal Reserve Bank of Boston, Boston, Massachusetts* (1994), 21–38.
- [142] NBER RECESSION DATING COMMITTEE. United states business cycle expansions and contractions <http://www.nber.org/cycles.html>.
- [143] VICEIRA, L. M., WANG, Z. K., AND ZHOU, J. Global portfolio diversification for long-horizon investors.
- [144] WACHTER, J. A. Solving models with external habit. *Finance Research Letters* 2, 4 (2005), 210–226.
- [145] WACHTER, J. A. A consumption-based model of the term structure of interest rates. *Journal of Financial Economics* 79, 2 (2006), 365–399.
- [146] WELCH, I., AND GOYAL, A. A comprehensive look at the empirical performance of equity premium prediction. *Review of Financial Studies* 21, 4 (2008), 1455–1508.
- [147] WORKING, H. Note on the correlation of first differences of averages in a random chain. *Econometrica: Journal of the Econometric Society* (1960), 916–918.
- [148] WU, G. The determinants of asymmetric volatility. *The Review of Financial Studies* 14, 3 (2001), 837–859.

- [149] XU, N. R. Global risk aversion and international return comovements. *Working Paper* (2017).
- [150] XU, N. R. Procyclicality of the comovement between dividend growth and consumption growth. *Working Paper* (2017).
- [151] ZAKOIAN, J.-M. Threshold heteroskedastic models. *Journal of Economic Dynamics and control* 18, 5 (1994), 931–955.
- [152] ZELLNER, A. An efficient method of estimating seemingly unrelated regressions and tests for aggregation bias. *Journal of the American statistical Association* 57, 298 (1962), 348–368.
- [153] ZELLNER, A., AND HUANG, D. S. Further properties of efficient estimators for seemingly unrelated regression equations. *International Economic Review* 3, 3 (1962), 300–313.